Design and Synthesis of Optimal Power System Architectures considering Reliability Specifications for a More Electric Aircraft Application

Angel Andres Recalde Lino (M. Sc. Eng.)

Thesis submitted to the University of Nottingham

for the degree of Doctor of Philosophy

November 2021

Abstract

This research deals with the investigation of formal mathematical methods to synthesize an electric power system architecture for a future generation of electrified aircraft. Since construction of a power system is driven by weight, reliability, efficiency, and cost, which are known to be conflicting objectives, the synthesis task considers optimization at its core to reduce energy waste and pollution while increasing efficiency and safety. The architecture synthesis is defined as an automatic process where a set of design specifications drives a series of mathematical operations formulated as an optimization problem and produces an outcome that comprises a mapping of components and connections, i.e., a topology, so that reliable power distribution between power sources and electrical loads can be established. Because the design space is vast, high abstraction is required to characterize components' functionalities that can be verified against the specifications. For this reason, a Platform Based Design approach has been selected for the design framework proposed. In this case, an architecture is an abstract representation of the system's topology that complies with the functional and reliability specifications. In some cases, specifications are directly transformed into mathematical constraints, and in other cases, some preselection is required based on the design application. There are two platforms within the electric power system design, the generation system required to supply load demand, and the distribution system. The former is a platform that specifies the number and size of generators and power sources, while the latter constructs a distribution network containing alternative paths in case of failures. Given the complex nature of the design problem, the non-linear optimization formulations are transformed into Mixed Integer Linear Programming problems that can be solved with powerful and efficient commercial solvers. To illustrate the potential of this approach, a case study is presented for the synthesis of an onboard electric power system. An experimental small-scale testbed has been built to prove the key findings of this study, as well as to analyze and to evaluate the achieved performances.

Claims and Novelty

In this thesis:

- A method for synthesizing a power system architecture from scratch is proposed. Optimization formulations that satisfy a set of initial design functional and safety requirements are used in the synthesis method.
- Unlike other methodologies that combine several mathematical languages and computational tools, the proposed approach can synthesize an architecture by sequentially solving two optimization subproblems that determine the generation and the distribution system.
- Reliability performance is included in the design specifications. The synthesized power system architecture is ensured to comply with a set of reliability requirements by introducing reliability performance constraints in the optimization formulations.
- Complex and non-linear optimization formulations in the proposed electric power system design method are transformed into Mixed Integer Linear Programming problems. Hence the approach can benefit from using powerful and efficient commercially available solvers thus focusing on the design problem exploration rather upon the solution approaches.

Table of Contents

Abstract i
Claims and Novelty ii
Table of Contents iii
List of Tables viii
List of Figures ix
List of Acronyms xii
List of Optimization Problems xiii
Nomenclature xiv
1. Introduction 20
1.1. Background 20
1.2. Electrical Power System 21
1.3. EPS Architecture 24
Example of EPS architecture 24
Outlining an EPS architecture 26
1.4. Aims and Objectives of Thesis 29
1.5. Structure of Thesis 30
1.6. Publications 32
2. Literature Review 35
2.1. Introduction 35
2.2. Preliminaries 35
2.3. Safety in power system design 37
Reliability of a small EPS (example) 40
2.4. Design Approaches 40
2.4.1. System Design 41
Platform Based Design approaches 42
Integrated Design by Optimization 46
Reliability-based Design Optimization 47
2.4.2. Network Design 47
2.4.3. Other Design Methodologies 50
2.4.4. Summary 51

2.5. Linearization and MILP 53
2.6. Discussion 59
2.7. Conclusion 61
3. Framework for a reliability-based design 63
3.1. Introduction 63
3.2. Aircraft Design 64
Previous steps in EPS design 64
Performance optimization and controllers. 66
Designs are unique 67
3.3. Design Framework proposal 68
3.3.1. Preliminaries 69
Levels of abstraction 70
Examples of abstractions 71
3.3.2. Platform Based Design 72
Key concepts in PBD 73
Industry's observations for the EPS design 74
Abstractions in the EPS design 76
3.3.3. A Framework for designing the EPS 77
Subproblems for the EPS design 77
Original EPS design problem 78
EPS design and the proposed design framework 80
3.3.4. Optimization and Reliability in the Design Framework 82
General optimization formulation 82
Types of optimization problems 83
3.4. General Mathematical Formulations 85
3.4.1. Generator Selection and Generator-Load Pairing 87
Functional specifications for power sources (generators) 89
Example of synthesis of a generation system 90
General formulation of GS&GLP subproblem 92
Optimization objective of GS&GLP 92
Reliability constraint 94
GS&GLP general optimization 96
3.4.2. Power Distribution Design 96

Functional specifications for distribution components 98
Example of synthesis of a power distribution system 99
General formulation of the PDD subproblem 103
Optimization objective of PDD 103
Power flow relations in PDD components 105
Reliability constraint 107
PDD general optimization 110
3.5. Recap 111
3.6. Conclusion 111
4. A reliability-based optimization design 114
4.1. Introduction 114
4.2. Linear transformations in the EPS design 115
4.2.1. Generator selection and generator-load pairing 115
Design variables 115
Linearized objective for GS&GLP 119
General constraints for GS&GLP 121
Reliability constraints for GS&GLP 122
GS&GLP Linear Formulation 124
4.2.2. Power Distribution Design 125
Design variables 126
Linearized objective for PDD 127
General constraints for PDD 127
Reliability constraints for PDD 130
Series system or single distribution path 131
Series-parallel system or multiple distribution paths 131
PDD with single distribution paths (series-system) 132
PDD as a Resilient Design for a set of Failure Scenarios 134
PDD as a Resilient Design with two-disjoint paths 137
Simpler calculation for the reliability of two-disjoint path 140
Linearization of two-disjoint path reliability constraint 141
4.3. Recap 143
4.3.1. PDD Linear Formulations 144
4.4. Conclusion 145

5. Performance Optimization in EPS Designs 148
5.1. Introduction 148
5.2. Optimal Voltage Selection 150
5.2.1. Physics of Power System Voltage 152
5.2.2. Calculation of a Safe Operating Voltage 155
5.2.3. Safe Operating Voltage Optimization 158
5.2.4. General formulation for optimal voltage 160
5.3. Component location and cable selection 163
5.4. Load Flow in EPS architecture 169
5.4.1. The EPS load flow problem 170
5.4.2. Linearization of the DC Load Flow 172
5.5. Performance Optimization 177
5.5.1. Operation after EPS design 178
5.5.2. Types of performance optimization problems 181
5.5.3. A performance optimization problem 183
Topology reconfiguration 186
Loss minimization problem in DC system 189
5.6. Recap 192
5.7. Conclusion 195
6. Case study in the EPS design 197
6.1. Introduction 197
6.2. Design of an EPS architecture 198
6.2.1. Design Specifications and Requirements 200
6.2.2. Optimal voltage for an EPS 208
6.2.3. Generator Selection and Generator-Load Pairing 212
6.2.4. Power Distribution Design 216
6.2.5. Discussion of the design results 229
6.3. Conclusion 232
7. Experimental Testbed 233
7.1. Introduction 233
7.2. The EPS testbed 234
7.2.1. EPS architecture design 235
7.2.2. EPS controller 242

7.2.2.1. Main controller 244
7.2.2.2. Failure simulation board 244
7.2.3. Experimental setup 246
7.2.4. Operation 247
7.2.5. Reconfiguration implementation 250
7.3. Performance evaluation 253
7.4. Conclusion 258
8. Conclusion 260
8.1. Summary 260
8.2. Future Work 264
References 267
Appendix I Load Flow 285

List of Tables

Table 2.1 Design and optimization methodologies for aircraft and MEA. 52
Table 3.1 Types of Reliability-based formulations. 84
Table 6.1 Design requirements for electrical loads. 202
Table 6.2 Power generation platform abstraction. 204
Table 6.3 Power distribution platform abstraction. 205
Table 6.4 Proposed resilient design scenarios for the same EPS design application. 207
Table 6.5 Design specification example for optimal voltage selection. 209
Table 6.6 Standard wire gauge set $\mathcal{C}$ example for optimal voltage selection, ΔT = 70°C, wire in free air, sea level. 210
Table 6.7 Maximum power transfer and density with corresponding wire gauges for a set $\mathcal{N}$ of SOV values. 210
Table 6.8 GS&GLP optimal solution for a MEA EPS design example. 215
Table 6.9 Reliability targets for distribution paths (per load) from optimal GS&GLP solution. 218
Table 6.10 PDD optimal result for Scenario 1 in Table 6.4. 221
Table 6.11 PDD optimal results for Scenarios 2 to 7 in Table 6.4. 224
Table 6.12 PDD optimal results for Scenarios 8 to 14 in Table 6.4. 227
Table 6.13 EPS architecture optimal results summary for scenarios in Table 6.4. 230
Table 7.1 Load sizing for DC EPS testbed. 235
Table 7.2 Testbed generation platform abstraction (example). 239
Table 7.3 Testbed power distribution platform abstraction (example). 239
Table 7.4 Extract of the combinatorial table for reconfiguration task. 252

List of Figures

Figure 1.1 Example of EPS architecture for MEA 25
Figure 1.2 Example of architecture for an EPS supplying two non-essential loads 26
Figure 1.3 New EPS architecture candidates in case L2 is essential, a) additional converter, b) battery bank supply 27
Figure 1.4 New EPS architecture candidates in case L2 is essential and an additional generator is allowed, a) main converter only, b) additional converter 27
Figure 1.5 New EPS architecture in case L1 and L2 are essential 28
Figure 2.1 Conventional Design Flow 36
Figure 2.2 Conceptual map of safety attributes (source: author) 39
Figure 2.3 Power system example 40
Figure 2.4 Design approaches for the EPS design exercise 41
Figure 2.5 Contract based Design flow for EPS design 44
Figure 2.6 Conceptual map of design approaches in network flow and network design 50
Figure 2.7 Various linearization techniques (graphical examples). 58
Figure 3.1 EPS architecture design within aircraft design (diagram flow). 66
Figure 3.2 Original problem for the design of an EPS 79
Figure 3.3 Design Framework Proposal (conceptual) 80
Figure 3.4 An example of a GS&GLP template for the design of a generation system for a 3-load EPS 88
Figure 3.5 Functional abstraction for a generator candidate in the GS&GLP platform 90
Figure 3.6 GS&GLP process; inputs at the left, optimization-based formulation in the middle, and outcome at the right 91
Figure 3.7 Series- and parallel-system in the context of GS&GLP 95
Figure 3.8 An example of a PDD template for the design of a distribution system for a 3-load EPS 97
Figure 3.9 PDD process; inputs at the left, optimization-based formulation in the middle, and outcome at the right 101
Figure 3.10 Assigned pairs corresponding to the PDD example 101
Figure 3.11 Example of EPS detailing power flow relationship for component i in PDD. 105
Figure 3.12 Series system and series-parallel system in the context of PDD. 109

Figure 3.13 Generator Selection and Generator-Load Pairing and Power Distribution Design summary. 112
Figure 4.1 Example of power flow balance for a component i. 129
Figure 4.2 Graphical summary of the MILP reliability-based formulations for the EPS design framework proposal. 146
Figure 5.1 Flow diagram for performance optimization of EPS architecture. 149
Figure 5.2 Paschen's curve for Air at a pressure of 10kPa, temperature of 15°C. 154
Figure 5.3 Basic cable arrangement for a power conducting cable. 156
Figure 5.4 Vd and SOV curves for a cable with $i = 0.09mm$, $\varepsilon r = 4.4$, at an air pressure of 10 kPa and T = 15°C. 157
Figure 5.5 Plan and side view of a B737-400 aircraft. 164
Figure 5.6 Bilinear term $ViVj$ in the feasible operating range, in p.u. (left), in real values around 540 VDC (right). 174
Figure 5.7 Performance evaluation within EPS architecture design. 176
Figure 5.8 Example of EPS architecture in normal operation. 178
Figure 5.9 Example of EPS reconfiguration after performance optimization with load flow. 180
Figure 5.10 Relation between topology reconfiguration and optimization for maximum efficiency. 182
Figure 5.11 Performance optimization including steady-state and dynamic. 185
Figure 5.12 Example of simple Finite State Machine. 189
Figure 5.13 Performance optimization in the context of architecture design (all methods). 194
Figure 6.1 Standard view of CPLEX Studio 12.9.0 for programming and solving optimization problems. 199
Figure 6.2 Zoomed view of optimization program file in CPLEX Studio 12.9.0. 199
Figure 6.3 Zoomed view of data file in CPLEX Studio 12.9.0. 200
Figure 6.4 Example of source matrix contactor bus (HV bus bar). 201
Figure 6.5 GS&GLP template for the EPS design example. 204
Figure 6.6 PDD template for the EPS design example. 206
Figure 6.7 Maximum power transfer (left) and power density (right) for optimal voltage selection example. 211
Figure 6.8 GS&GLP programmed in OPL in CPLEX Studio 12.9.0 (excerpt). 213
Figure 6.9 GS&GLP outcome in CPLEX Studio 12.9.0 (script excerpt). 214
Figure 6.10 GS&GLP optimal solution for the EPS design example (graphical). 215

Figure 6.11 PDD programmed in OPL in CPLEX Studio 12.9.0 (excerpt). 219
Figure 6.12 PDD outcome in CPLEX Studio 12.9.0 (script excerpt, outcome for formulation O.P. 6). 220
Figure 6.13 MEA EPS for scenario 1 of Table 6.4 (distribution paths of Table 6.8 in bold). 221
Figure 6.14 Example of failure in converter 1; all connections ij in red are considered as failed. 222
Figure 6.15 MEA EPS optimal architectures for failure-resistant resilient requirements in Table 6.4. 223
Figure 6.16 EPS architecture for scenario 8 (two-disjoint path); each disjoint path is in bold. 225
Figure 6.17 MEA EPS optimal architectures for two disjoint path resilient requirements in Table 6.4. 226
Figure 6.18 Weight, cost, and reliability for the 14 resilient scenarios in Table 6.4. 228
Figure 7.1 Electronic components available for the DC EPS testbed. 237
Figure 7.2 Line diagram of the DC EPS testbed. 240
Figure 7.3 Control and data acquisition signal layout for the DC EPS testbed. 243
Figure 7.4 Experimental setup of the DC EPS testbed. 246
Figure 7.5 Configuration for normal operation (normal mode) in DC EPS testbed. 247
Figure 7.6 System reconfiguration in case of failures in Source 1 (a), and Xa (b). 249
Figure 7.7 Results from DC EPS testbed, (a) power [W], (b) reconfiguration time [ms]. 254
Figure 7.8 Reconfiguration options in case of simultaneous failure in Aux 1, Aux 2, Xa, and Xb. 255
Figure 7.9 Voltage response and transients in HVDC and LVDC buses (zone A) for failure in Xa. 256
Figure 7.10 Voltage response and transients in HVDC and LVDC buses (zone A) for a failure in Source 1. 257

List of Acronyms

MEA	More Electric Aircraft
EPS	Electrical Power System
PBD	Platform Based Design
CbC	Correct by Construction
CbD	Contract based Design
IDO	Integrated Design by Optimization
RBDO	Reliability-based Design Optimization
MILP	Mixed Integer Linear Programming
LTL	Linear Temporal Logic
STL	Signal Temporal Logic
AC	Alternating Current
DC	Direct Current
FSM	Finite State Machine
CAD	Computer Aided Design
ECS	Environmental Control System
PD	Partial Discharge

List of Optimization Problems

O.P. *1* General formulation of optimization problem

O.P. 2 General formulation for EPS design

O.P. 3 General formulation of GS&GLP problem

O.P. 4 General formulation of PDD problem

O.P. 5 Linearized formulation of GS&GLP problem

O.P. 6 Linearized formulation of PDD problem, path as a series-system

O.P. 7 Linearized formulation of PDD problem, resilient design for failure scenarios

O.P. 8 Linearized formulation of PDD problem, resilient design with two-disjoint paths

O.P. 9 Voltage Selection

O.P. 11 Linearized formulation of voltage selection

O.P. 10 Component location and cable selection

O.P. 12 Linearized formulation of load flow for DC systems

O.P. 13 Loss minimization problem

Nomenclature

GENERAL VARIABLES

c	cost
w	weight
η	efficiency
r	reliability
P	power
I	current
V	voltage

GENERAL INDEXES

s	power source (generator)
l	electrical load
k	**assigned pair** between generator s and load l
i or j	any component from the power distribution system
$\not{f}$	any failure case, it is a vector of Boolean (0 or 1) values with all $\not{f}_{ij}$
q	any path of the two-disjoint path formulation

GENERAL DESIGN PARAMETERS

L_l	load demand (kW) of load l
$r_{\text{TARGET, } l}$	reliability target for load l

SETS {ELEMENTS}

From the design specifications and requirements:

$\mathcal{L}$ $\{L\}$ or $\mathcal{B}$ $\{L\}$	set of loads l (design specifications and requirements)
$\mathcal{H}$ $\{h\}$	set of commercial generators
$P^G_{\mathcal{H}}$ $\{P^G_h\}$	set of power ratings for generators in set $\mathcal{H}$

$z_{\mathcal{B}}^{G}$ $\{z_b^G\}$	set of accumulative load values in set $\mathcal{B}$
$\beta_{\mathcal{B}}^{G}$ $\{\beta_b^G\}$	set of accumulative load normalized values in set $\mathcal{B}$ (loading values)
$\eta_{h,\mathcal{B}}^{\mathrm{LOSS}}$ $\{\eta_{h,b}^{\mathrm{LOSS}}\}$	set of loss values for rating of generator h and loading b
$r_{s,O}^{E}$ $\{r_{s,o}^{E}\}$	set of logarithmic values for combined reliability of assigned pair k
F $\{f\}$	set of failure cases

For the GS&GLP problem:

$\mathcal{G}$ $\{G\}$	set of power sources s (template) (G is also superindex)
$\mathcal{E}$ $\{G$ to $L\}$	set of generator-load pairs (template)
K $\{k\}$	set of all assigned pairs k (s to l) from virtual power distribution, $K \subseteq \mathcal{E}$

For the PDD problem:

$\mathcal{N}$ $\{B, X, D\}$	set of power distribution components {HV box, converter, LV bus}
$\mathcal{A}$ $\{B$ to $\{X, \dots\}, \dots\}$	set of connections between power distribution components

GS&GLP VARIABLES

w_s	power source's weight (kg)
η_s	power source's efficiency (-)
g_s	Boolean (0 or 1) selection for power source
y_{sl}	Boolean (0 or 1) selection for assigned pair s, l
P_s^G	power rating of power source s
β_s	loading of power source s
r_{PD}	reliability of virtual power distribution system
r_{sl}	reliability of assigned pair s, l (virtual power distribution system)

After-linearization variables:

η_s^{LOSS}	power source's losses (in kW or %)
$u_{s,h}$	Boolean (0 or 1) selection of rating h for power source s
$z_{s,h,b}$	Boolean (0 or 1) selection of rating h and loading b for power source s
$r_{s,l,o}^{S}$	Boolean (0 or 1) selection of log reliability value o for assigned pair s, l

GS&GLP PARAMETERS (from specifications or pre-calculated)

r_s	reliability of power source s
$\eta_s(\beta_s)$	approximation of efficiency as a function of loading
$w_s(P_s^G)$	approximation of weight as a function of power rating
P_h^G	power ratings from the set $P_{\mathcal{H}}^G$
β_b^G	loading (normalized load value) from the set $\beta_{\mathcal{B}}^G$
$\hat{P}_{hb}^G$	generator's supply power, $\hat{P}_{h,b}^G = P_h^G \beta_b^G$
$\eta_{h,b}^{\mathrm{LOSS}}$	generator's loss for rating h and loading b
$r_{s,o}^E$	logarithmic value for combined reliability, $r_{s,o}^E = \ln(1 - r_{sl} r_s)$

PDD VARIABLES

For connection i, j:

$x_{i,j}$	Boolean (0 or 1) selection
P_{ij}	power that flows through connection
$P_{ij,k}$	power that flows through connection for assigned pair k
$\eta_{i,j}$	efficiency
$P_{ji,k}^{\not f}$	power flowing through connection in failure case $\not f$, assigned pair k
$P_{ij,k}^q$	power flowing through connection in path q, assigned pair k

For component i:

v_i	Boolean (0 or 1) selection
P_i	power flowing through component
$P_{i,k}$	power flowing through component for assigned pair k
η_i	efficiency

Reliability:

$z_{i,k}$	Boolean (0 or 1) that reserves component i to assigned pair k
$z_{ij,k}$	Boolean (0 or 1) that reserves connection i, j to assigned pair k
$u_{i,k}$	Boolean (0 or 1) that reserves component i to pair k (two-disjoint path)
$u_{ij,k}$	Boolean (0 or 1) that reserves connection i, j to pair k (two-disjoint path)

r_k^q	reliability of the disjoint path q
$\mathcal{s}_{i,k}^q$	probability of successfully reaching component i in path q for assigned pair k
$\mathcal{s}_{LOAD,k}^q$	reliability of the disjoint path q for assigned pair k
$\mathcal{o}_{ab,k}$	Boolean (0 or 1) selection for q paths' reliability product

PDD PARAMETERS (from specifications or pre-calculated)

For connection i, j:

$c_{i,j}$	fixed cost
c_{ij}^{kW}	variable cost
$r_{i,j}$	reliability of connection i, j
P_{ij}^{MAX}	maximum power (upper boundary)

For component i:

m_i	fixed cost
m_i^{kW}	variable cost
r_i	reliability of component i
P_i^{MAX}	maximum power (upper boundary)

Other parameters:

d_k^{LOAD}	load demand of load l for assigned pair k (generator s to load l)
d_k^{GEN}	power supplied by generator s in assigned pair k
d_k	power flowing through assigned pair k, $d_k = \left\lvert d_k^{LOAD} \right\rvert$

Reliability:

$\mathcal{f}_{ij}$	Boolean (0 or 1) value that represents failure in connection i, j
α, β	vector of disjoint path (1 and 2) reliability values
α_a, β_b	elements of the vectors α, β respectively
Γ	matrix of two-disjoint path reliability values
$\gamma_{a,b}$	element of the matrix Γ

OPTIMAL VOLTAGE SELECTION

d	gap of length d
V_d	voltage field (in V or %) in the gap of length d
i	insulation thickness (in mm) of a cable
ε_r	relative permittivity of insulation material
c	conductor's diameter
D	distance between conductor's centre and ground
e	clearance distance (insulation to ground)
$V_{PASCHEN}$	minimum voltage from the Paschen's curve
$\mathcal{C}$ $\{c\}$	set of available (commercial) standardized conductors
$\mathcal{N}$ $\{n\}$	set of SOV (safe operating voltage) values
$\mathcal{P}$	power transfer capability (in kW)
ρ	linear power density for cable (power per unit of weight and length)
ρ_c	linear power density for conductor c
ρ_i	linear power density for insulation i
$\alpha_{n,c}$	Boolean (0 or 1) that selects a conductor c at a SOV of n
$i_{n,d}$	insulation for a conductor c at a SOV of n
$\mathcal{P}_{\mathcal{N},\mathcal{C}}$	power transfer capability for conductors in $\mathcal{C}$ at SOV values in $\mathcal{N}$
$\rho_{\mathcal{N},\mathcal{C}}$	linear power density for conductors in $\mathcal{C}$ at SOV values in $\mathcal{N}$

COMPONENT LOCATION AND CABLE SELECTION

m_i	abscissa location variable for component i
n_i	ordinate location variable for component i
$m_i^{\mathrm{MIN}}, m_i^{\mathrm{MAX}}$	permissible minimum and maximum abscissa location
$n_i^{\mathrm{MIN}}, n_i^{\mathrm{MAX}}$	permissible minimum and maximum ordinate location
l_{ij}	length of connection between components i and j
ϵ	tolerance gap
$\mathcal{O}$ $\{o\}$	set of standardized wire gauges for conductors

$c_{ij,o}^{\mathrm{AWG}}$	Boolean (0 or 1) that selects a wire gauge o for connection i, j
I_o^{AWG}	ampacity coefficient for conductor with wire gauge o
r_o^{AWG}	ohmic resistance per unit of length for wire gauge o
w_o^{AWG}	weight per unit of length for wire gauge o
V_{ij}^{SOV}	SOV voltage of connection i, j (predetermined)
V_{MAX}^{DROP}	maximum voltage's drop permissible in the system

LOAD FLOW PROBLEM (DC systems)

i	bus number
$N\ \{n\}$	set of buses
G_{ij}	conductance between bus i and other bus j
V_i	voltage at bus i
g_i^0	self-conductance of bus i
p_i^0	power consumed or supplied at bus i
i_i^0	current consumed or supplied at bus i
w_{ij}	replacing variable for the bilinear term $V_i V_j$
v_i	replacing variable for the quadratic term V_i^2
V_{MIN}, V_{MAX}	minimum and maximum permissible voltage
M	big and positive value
$I_{i,j}$	current flowing through connection i, j
R_{ij}	resistance (ohmic) of connection i, j

1. Introduction

1.1. Background

The aerospace industry is certainly being transformed at an accelerated pace to cope with stringent sustainability targets that demand preparedness for 2050 [1]. Aviation emissions have risen due to the vertiginous increase in air traffic and will continue to do so with aviation expansion in emerging economies. The long-term goal is to halve the net CO_2 emissions by 2050 compared to what they were in 2005 to reduce pollution impact [2]. Among the most important measures to turn aircraft more efficient, the reduction in fossil fuel consumption is at the core. A drastic deceleration in the amount of emission and air pollution is expected even when the number of flights per year is increasing vertiginously due to a growing economy and air traffic. Joint ventures worldwide have already started to work on new technologies for the next generation of aircraft; public and private sectors are intensely cooperating in more electric aircraft (MEA) projects and portfolios. For instance, Clean Aviation [3] (built on Clean Sky Joint Undertaking) is one of the leading research and innovation programme for transforming aviation towards sustainable and climate neutral future [4].

Reducing fossil fuel can be achieved either through a series of transformations in current aircraft systems or via an integral redesign of the aircraft. The former has been practiced for a long time in airlines, mainly via the upgrade of gas turbine engines for more efficient units [5]. On the other side, several companies have developed world class research and cutting-edge technology to produce flying prototypes [6] and demonstrated the feasibility of disruptive all-electric and hybrid airplanes for commercial purposes. In addition, in the last three decades there has been a steep ascent in replacing several hydraulic and pneumatic subsystems with electro-driven systems which has been baptized with a concept known as more electric aircraft (MEA) [7], [8].

There are several levels of electrification possible in MEA. The objective of increasing the amount of electrically driven systems is that electricity transmission and distribution is more efficient than its hydraulic and pneumatic counterparts [9]. Besides, it could be less prone to damage and degradation during the system's lifetime, so that higher reliability can be achieved. In the current state-of-the-art it could be said that there are two main visions for the future of the aircraft industry, one where hybrid aircraft still use fossil fuel but distribute power electrically for most of the subsystems, and the other where no fossil fuel is being carried or consumed on-board, but is replaced with other forms of energy storage, including batteries and fuel cells [10]. The latter demands materials and devices with very high power-densities, capable of storing huge amounts of energy, however these devices have not yet been completely synthesized and are still under intense research [11].

Beyond the level of electrification, it is a certainty that an electrical system must be placed at the center of the future MEA. This system transmits and distributes all the power onboard and constitutes the network in charge of transporting generated power and delivering it to the loads, at a high availability. The construction of such a system demands a deep understanding of power consumption in all aircraft subsystems for a specific aerospace vehicle. In addition, building such a network must observe the relationship between the main industry drivers: weight, reliability, efficiency, and cost. These drivers are conflicting, so the system's selection is a compromise between having identified the available budget and resources.

1.2. Electrical Power System

The aircraft EPS is a microgrid capable of operating autonomously during taxiing, take-off, cruise, and landing. In an existing EPS, the jet engine is the primary source of power. Most of this power is used for aircraft propulsion (primary power) while the rest is distributed into electrical, hydraulic, pneumatic, and mechanical power (secondary power) required by the rest of the aircraft subsystems, such as flight

actuation systems, fuel and oil pumping, wing de-icing, cabin pressurization, and Environmental Control System (ECS). Electrical power is generated in electrical generators driven by gearbox connections coupled to the engine shaft. In conventional aircraft, electrical power is used to power loads such as avionics systems, lighting, and in-flight entertainment systems.

In addition to electrical generators and loads, the EPS consists of a series of distribution components for power transmission and conversion. Among the main types of components, there are:

- Power sources: apart from engine driven generators, there are also energy storage systems based on batteries and other non-fossil fuels, and renewable power sources. Current state-of-the-art air vehicles are mainly based on rechargeable Li-Ion, Li-Po, batteries, which is the same technology used in electric cars. Increased interest has been paid to hydrogen due to its significant energy density although its storage and distribution has not reached commercial viability yet [12]. On the other hand, solar energy has been implemented in flying prototypes although the low power conversion efficiency (sun irradiation to electricity) demands large surfaces for solar panel deployment while necessarily limiting maneuver and payload.
- Buses: allow multiple incoming or outgoing power connections. Load buses typically supply multiple loads, while generation buses are reserved for one generator-at-a-time supply. It is usually represented as a node energized at a specific voltage established by the supplying or consuming devices connected to it.
- Converters: power electronics-based converters transform input power, at a specific voltage and current format, into a different voltage and current output as required by load buses or other subsystems. In some cases, power flow can be bidirectional, allowing power waste reduction. There are a significant number of converter types including AC/AC (cyclo-converters, mainly implemented on military aircraft), AC/DC (rectifiers, for converting AC to DC voltage and current),

DC/AC (inverters, for supplying AC loads from a DC bus or source), and DC/DC (from a high/low voltage to a low/high voltage, e.g., buck and boost converters).

- Transformers: these are magnetic devices (non-power electronic) with two- or more windings (coils producing electromagnetic fields) that step up- or down AC voltage as required by the load buses or subsystems. They offer galvanic isolation but there are smaller, lighter, and cheaper autotransformer units (ATRU) that contain a single winding, although no galvanic isolation is then possible. It is common to find a transformer connected to a rectifier (TRU) in a compact unit.
- Switching devices: these devices allow connections and disconnections between their terminals. They can be manual or signal-controlled, e.g., interruptors, disconnectors, breakers, contactors, and other solid-state (semiconductor) devices. Protective devices such as breakers and overload relays automatically disconnect two components or subsystems whenever the conditions for safe power flow are not met, otherwise, they remain closed. On the other hand, controllable switches (e.g., contactors, solid state switch) are commanded on demand and interrupts power flow between their terminals at any time as requested by an external user or control system.
- Cabling system: this consists of all connections between components (power sources, buses, converters, transformers, etc.) that are located throughout the aircraft. The connections between subsystems within the microgrid are commonly referred as interconnections, but they are basically connections too. In typical aircraft, connections are cables made of copper or aluminum conductors coated with special insulation material (PVC, XLPE, etc.).

With the expected increase of electrically driven loads and electric propulsion, power requirements could step up from hundreds of kilowatts (current aircraft) to dozens of megawatts, thus demanding a significantly heavier cabling system. A radically different analysis has proposed superconducting systems as an alternative to supply large propulsion loads [13], although no flying prototype has been released yet. In superconductivity, a very thin conductor made of a special alloy material is kept at very low

temperature (close to 0 K) and allows a huge amount of current flow, which is ideal for megawatt power transmission. Copper replacement with superconductor could reduce cabling weight, however, auxiliary systems to maintain low temperatures and dissipate losses must be also considered in the total cabling weight.

Determining the cabling system requires knowledge of the components to connect. Components to be included in the EPS depend on the loads considered in the aircraft vehicle. Thus, defining an EPS architecture, i.e., the connection arrangement of power sources, loads, and distribution components, mainly requires satisfaction of load requirements and specifications.

1.3. EPS Architecture

Power loads are located throughout the aircraft and their power consumption follows specific requirements for voltage level (high voltage HV, low voltage LV) and type of current (alternate, direct, i.e., AC, DC). Each load's criticality determines if loads are essential, i.e., supply must never be interrupted for more than a specific period, or non-essential, i.e., loads can be permanently shed if required, e.g., in-flight entertainment systems. Hence, the EPS architecture must consider all these requirements to provide a system that effectively generates and distributes electrical power to the loads. A comprehensive review of conventional EPS for existing aircraft can be found in [14], including detailed explanation for both commercial and military vehicles. These architectures satisfy current aircraft requirements, but future aircraft will need to be designed for different considerations and specifications.

Example of EPS architecture

An example of a new architecture for MEA is shown in **Figure *1.1*** [15]. There are ATRUs, TRUs, AC/AC and DC/AC converters, and a battery bank to support avionics loads (flight controls) uninterruptedly. There are 4 types of loads, including avionics, and each type demands power in a different format, thus the need

for several converters. The Auxiliary Power Unit (APU) replaces any generator, G1 or G2, in case of generation failure.

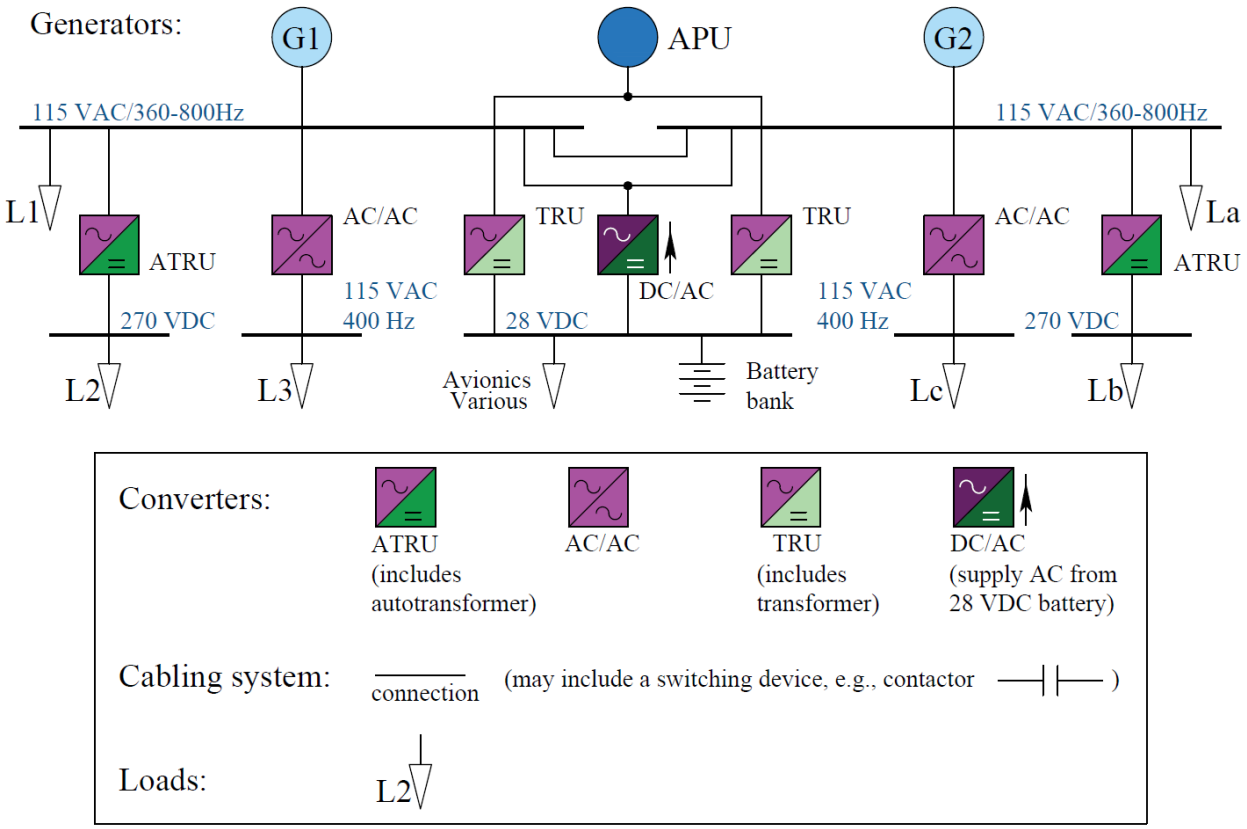

Figure 1.1 Example of EPS architecture for MEA

The architecture in **Figure *1.1*** considers the removal of the constant speed driver (for keeping AC frequency constant) from the electrical generator so that it can be directly coupled to the engine gearbox, therefore, the 115 VAC buses now have a frequency between 360 and 800 Hz. However, there could be a different EPS architecture to supply the same loads in **Figure *1.1***. Assuming that all requirements and specifications are available to the designer, there must be a way to synthesize such an architecture. In fact, there could be one way that provides several options, or many ways that provide even more options.

Outlining an EPS architecture

To exemplify the process of sketching several architectures for the same set of requirements and specifications, consider two loads. Also, assume the following conditions:

- Loads L1 and L2 are non-essential, i.e., they can be shed.
- L1 is low-voltage AC (LVAC) and L2 is low-voltage DC (LVDC)
- Both loads must be supplied from one generator only.

The EPS for supplying these loads could have the architecture shown in **Figure *1.2***. There is an AC/DC converter to supply the LVDC load, while the LVAC could be directly supplied from the generator bus.

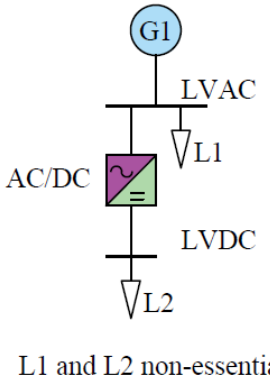

Figure 1.2 Example of architecture for an EPS supplying two non-essential loads

G1's output in **Figure *1.2*** is assumed to be 115 VAC which is considered LVAC in power distribution (in most cases). The EPS in **Figure *1.2*** satisfies the specifications above. Loads are non-essential, so that a failure in the generator or converter interrupts power flow and loads could be shed permanently without unsatisfying the requirements. Now, assume that there is a new specification:

- L2 is essential, that is, power must be always available in L2

The new architecture must be different from **Figure *1.2*** because L2 is essential. Assuming the converter could fail (but for the moment assume that the generator cannot), the architecture could be as shown in

Figure *1.3* (a) where there is an additional converter (supplied from the only generator available) in case the main converter fails. Another option is to supply L2 from a different power source. Having restricted the system to have only one generator, one alternative is to add a battery bank with its corresponding DC/DC converter as shown in **Figure *1.3*** (b), which would cover the case of generator failure as well. This converter manages power charging and discharging for the battery.

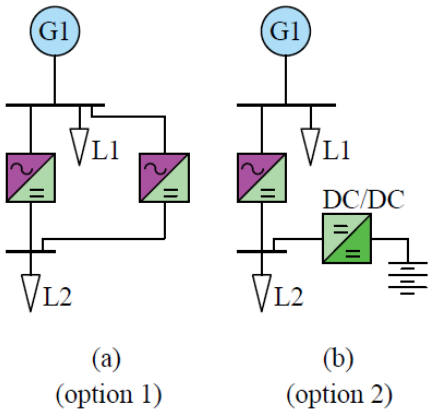

Figure 1.3 New EPS architecture candidates in case L2 is essential, a) additional converter, b) battery bank supply

Now, the condition of having only one generator could be relaxed to include another generator, sized accordingly (i.e., to supply only L2) in case G1 fails. This additional generator could supply L2 through the same converter as shown in **Figure *1.4*** (a) or using an additional converter (see **Figure *1.4*** (b)).

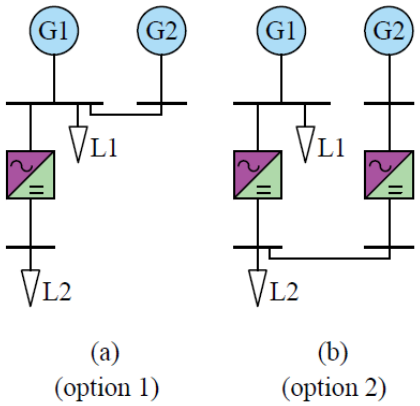

Figure 1.4 New EPS architecture candidates in case L2 is essential and an additional generator is allowed, a) main converter only, b) additional converter

The EPS architecture in **Figure *1.4*** (a) is also a feasible candidate in case L1 is essential and L2 is non-essential (L1 could be supplied either from G1 or G2). If both loads were essential, the EPS architecture could be as shown in **Figure *1.5***. There are two generators and two converters in case of failure in either of them. In this architecture candidate, a battery bank could also be included at the LVDC level.

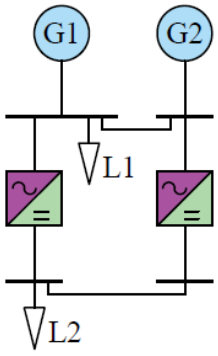

Figure 1.5 New EPS architecture in case L1 and L2 are essential

Then, a question that pops is which architecture from **Figure *1.3***, **Figure *1.4***, or **Figure *1.5*** is more convenient. Another question could be if they are feasible. In fact, it can be said that each architecture covers different requirements. In the previous specifications the only restriction relaxed was the initial number of generators. Besides, there were no limitations on adding a battery bank or a second converter. There are multiple options to choose from, and there are many others not explained here.

Going back to **Figure *1.1***, one could wonder if that EPS architecture is appropriate in case ATRU fails and L2 were essential. If left as it is, does it mean that other essential loads must be connected to 28 VDC bus only? Certainly, several questions arise when deciding upon an EPS architecture. However, the main decisions for selecting an architecture are always constrained by conflicting resources, i.e., weight, reliability, efficiency, and cost. The loads in the EPS in **Figure *1.5*** have a very-high power availability if compared to **Figure *1.2***, but at the cost of increasing weight and cost. There must be a way to search among feasible candidates and select the most appropriate (or group of most appropriate) candidates and perform a trade-off between conflicting resources. That is the reason why optimization of weight,

reliability, efficiency, and cost is crucial in the architecture synthesis. Optimization in this context is the automatic procedure that aims in finding an optimal solution to an objective function or functions (minimize weight, and cost, maximize reliability and efficiency) under a set of constraints (e.g., limited volume, etc.). Optimization performs a search among the design space and selects a candidate that complies to the specifications. This candidate is optimal because its cost and weight were reduced as much as possible, and its efficiency and reliability were increased as much as possible. Hence, an optimization-based design framework is required to synthesize an EPS architecture. A framework is regarded as a structure (organized group of methods or algorithms) intended to support or guide the design process.

This thesis is about how to synthesize EPS architectures (such as the ones illustrated in **Figure *1.1*** to **Figure *1.5***) in order to comply with specifications and optimize resources, that is, to maximize reliability and efficiency and minimize weight and cost. The EPS construction starts with the definition of functional and reliability requirements specific to the appointed application. In this context, the 'application' is the purpose of the aircraft vehicle, e.g., 9 passenger commercial short-haul aircraft. These specifications are then translated into mathematical constraints that are used to formulate an optimization problem whose outcome represents an EPS architecture. In the pursuit of synthesizing an EPS from scratch, several mathematical and optimization tools are used.

1.4. Aims and Objectives of Thesis

The main aim of this thesis is to develop formal optimization methods to formulate an architecture design problem that is capable of synthesizing from scratch an EPS architecture that satisfies a set of functional and safety requirements.

The specific objectives are as follows:

- Propose a design framework inspired by a Platform Based Design methodology that allows an efficient search for an optimal architecture among a vast design space. Further extension on previous work in the synthesis of EPS architectures [16] is performed to increase the use of formal mathematical tools into design problems.
- Produce Mixed Integer Linear Programming (MILP) formulations that allow utilization of powerful commercial solvers to find a global optimum. In contrast to other approaches that combine several mathematical languages and tools, the proposed design framework uses optimization as the only tool to produce an architecture that satisfies the design requirements directly.
- Synthesize an optimal direct current (DC) architecture that satisfies a set of functional and safety requirements proposed by the author as a case study for the illustration of the use of the proposed design framework. DC systems have immense potential in future more electric aircraft applications [17], hence the case study focuses on a DC power system.
- Evaluate a DC architecture implemented as a small-scale experimental test rig for a specific aircraft application and unique set of functional and reliability requirements. This evaluation is provided to demonstrate the concept of a DC distribution system, validate a topology reconfiguration technique, and provide a platform for testing power transfer and interconnections.

1.5. Structure of Thesis

This thesis is structured as follows:

Chapter 2 starts with a review of the state-of-the-art methodologies found in the literature for the construction and synthesis of aircraft EPS. A large percentage of the existing research is dedicated to the proposal of power and energy management techniques for AC and AC/DC hybrid systems and the design of a specific aircraft subsystem, e.g., traction drivetrain, engine driven generation train system, flight

control electro-mechanical actuators, etc. A small percentage of research considers the manual evaluation of pre-selected potential architectures to propose an optimal architecture among a few candidates. Only a few exceptions are dedicated to the exploration of formal methods to synthesize an EPS architecture from scratch given a set of initial specifications.

Chapter 3 presents the proposed design framework in a conceptual manner considering design requirements, i.e., weight, reliability, efficiency, and cost optimization, which are denominated as industry drivers. Reliability is the primary design requirement (driver) to produce a safe system. The Platform Based Design inspired framework divides the original design problem into two subproblems: generation system design, and power distribution design. These subproblems are sequentially solved and the outcome is an EPS architecture that complies with the initial design specifications written as a set of functional and safety requirements. The outcome of each subproblem is considered a platform and the success of the synthesis relies on the accurate translation of the design specifications and the functional abstractions of components.

Chapter 4 produces the optimization formulations for the generation system and power distribution system design subproblems. Because the aim is to find a global optimum solution, these non-linear formulations are linearized with several linearization techniques. The level of accuracy in such transformations is decided upon by the tightness that additional constraints hold on the problem's variables. These formulations are Mixed Integer Linear Programming problems that can be solved with a powerful and efficient commercial solver. This allows the designer to focus on the exploration of the mathematical formulations while the solver engines perform the optimal search efficiently.

Chapter 5 introduces performance evaluation into the EPS architecture design problem. Having synthesized an architecture that is optimal, the following task is to operate it according to the different conditions experienced during operation. This task is equivalent to a power management system that

changes the system's state based on an initial condition to achieve an optimal performance for that specific condition. Since the load flow is vital for determining the system's state and evaluating the system's performance, a feasible approximation of the load flow is presented. Because load flow is solved with the knowledge of the system's voltage and the electrical characteristics of components and connections, methods for determining the system's voltage and component location and cable selection are introduced. Having formulated a load flow, performance optimization problems can be formulated.

Chapter 6 reports a case study for the design of a direct current EPS for a small more electric aircraft application. Design requirements for aircraft EPS are highly uncommon in the literature, besides, electrical load sizing for more electric aircraft requires deep understanding of the way in which power and energy is used onboard during all flight stages. Therefore, a set of functional and safety specifications as well as a group of electrical loads have been proposed by the author to illustrate the potential of the design framework for a particular case.

Chapter 7 reports some experimental validation of the theoretical results from previous chapters. A small-scale experimental test rig has been built with electronic devices to model a DC power system. The aim is to demonstrate the concept of a DC power distribution, validate a topology reconfiguration technique, and propose an experimental platform to test power transferences and interconnections.

Finally, Chapter 8 concludes the thesis with the overall outcome of the research performed. Possible future research work is also discussed in this chapter.

1.6. Publications

The scientific publications related to the work in this thesis are below.

Journals

- A. Recalde, J. Atkin, S. Bozhko, “Optimal Design and Synthesis of MEA Power System Architectures considering Reliability Specifications”, *Transportation Electrification IEEE Transactions on*, vol. 6, no. 4, pp. 1801 – 1818, 2020
- A. Recalde, M. Lukic, A. Hebala, P. Giangrande, C. Klumpner, S. Nuzzo, P. Connor, J. Atkin, S. Bozhko, M. Galea, “Energy Storage System Selection for Optimal Fuel Consumption of Aircraft Hybrid Electric Taxiing Systems”, *Transportation Electrification IEEE Transactions on*, vol. 7, no. 3, pp. 1870 – 1887, 2020

Conference papers

- A. Recalde, S. Bozhko, J. Atkin, “Methodologies for the Synthesis of Reliable MEA Electrical Power System Architectures”, *2020 IEEE Vehicle Power and Propulsion Conference (VPPC)*, 2020
- A. Recalde, S. Bozhko, J. Atkin, C. Hill, “A Reliability Approach for the MEA Power System Architecture Design Optimization Problem”, *2018 IEEE International Conference on Electrical Systems for Aircraft, Railway, Ship Propulsion and Road Vehicles & International Transportation Electrification Conference (ESARS-ITEC)*, 2019
- A. Recalde, S. Bozhko, J. Atkin, S. Sumsurroah, “Optimal Voltage for More Electric Aircraft direct current Cabling System”, *2021 IEEE Transportation Electrification Conference and Exposition (ITEC)*, 2021
- A. Recalde, S. Bozhko, J. Atkin, “Linear Power Flow Characterization of DC Power Distribution System for MEA Optimization”, *2020 IEEE Transportation Electrification Conference and Expo (ITEC)*, 2020

- A. Recalde, S. Bozhko, J. Atkin, S. Sumsurroah, “A Direct Current Power System Testbed for a More Electric Aircraft Application”, *2021 AIAA Propulsion and Energy Forum and IEEE Electric Aircraft Technologies Symposium (EATS)*, 2021.
- A. Recalde, S. Bozhko, J. Atkin, “Design of More Electric Aircraft DC Power Distribution Architectures considering Reliability Performance”, *2019 AIAA/IEEE Electric Aircraft Technologies Symposium (EATS)*, 2019
- A. Recalde, S. Bozhko, J. Atkin, “Optimal Weight Power System Design and Synthesis for More Electric Aircraft”, *2020 AIAA/IEEE Electric Aircraft Technologies Symposium (EATS)*, 2020

2. Literature Review

2.1. Introduction

In this chapter, state-of-the-art academic research into power system design for MEA applications is explored and detailed. A large percentage of the literature is dedicated to the proposal of power and energy management techniques for MEA systems and the design of a specific aircraft subsystems for traction, engine driven integrated generation, and flight control actuators. A smaller percentage explores in detail the manual evaluation of pre-selected innovative architecture candidates available in the literature. Only a few exceptions focus on the formulation of a formal design problem whose outcome represents a power system architecture that satisfies initial design specifications. The deviation from the conventional and traditional design flow is imperative to manage the challenges in constructing an EPS for future MEA.

Several techniques such as Platform Based Design [18], Integrated Design by Optimization [19], Reliability Based Design Optimization [20], and Network Design [21] have been used in other engineering fields to solve design problems but are still uncommon in the synthesis of an electrical system that integrates the rest of the aircraft subsystems. The aim is to find a method to design an electrical network from scratch that complies to certain requirements and specifications. Most of the design techniques are based on optimization formulations that are converted to Mixed Integer Linear Programming (MILP) problems to use full potential of powerful commercial solvers. A section on MILP and linearization is also provided.

2.2. Preliminaries

The aviation industry has traditionally used conventional design flow [22]. This process has a cyclic flow triggered by new specifications encountered in the performance evaluation stage [23], as shown in **Figure *2.1***. The conventional design flow iterates until it reaches a certain performance target. During this

iterative process, design decisions could be changed without establishing certainty on future performance. The most common application of the conventional design flow is the design of a subsystem or device, e.g., integrated generation subsystem, electromechanical actuator, traction electrical machine, etc. Very high levels of reliability can be achieved with this approach, but it has some drawbacks. One major disadvantage is that it is time consuming due to the large number of iterations required for systems with large number of components, especially if there were changes in design specifications while in the design loop. As the complexity increases, the quality of the solution could be compromised, causing unpredictable outcomes eventually. Besides, this approach limits the investigation of disruptive solutions because the performance evaluation drives the design loop and when introducing new technologies, structures, and concepts, there is an inherent uncertainty due to lack of complete information, e.g., failure modes, unexpected behavior, etc.

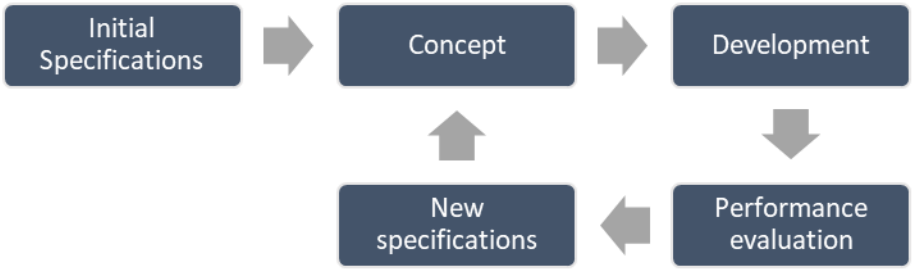

Figure 2.1 Conventional Design Flow

The exploration of EPS architectures for MEA demands an effective design flow that integrates design and performance evaluation so that both the uncertainty and the number of design iterations can be reduced as much as possible. Hence, the drawbacks of conventional design flow in generating disruption from known solutions can be mitigated. The design problem can be specified either as a system design problem or a network design problem. Network design focuses on the transmission of any flow (e.g., water, data packages, electricity, etc.) through a network of components and the performance of such transmission to optimize the utilization of network resources [24]. On the other hand, system design can cover a

broader aspect of the design process, that is, from the definition of an architecture to the product development, hence, it is more oriented to the manufacturing industry. Referring to the EPS context, network design could specifically construct a network of components (an EPS architecture) to allow electrical power flow transmission from generators to loads considering optimization of certain performance parameters. With system design, not only is the EPS architecture obtained, but also the control system and physical design (final implementation). The integration of architecture, control system, and physical design is commonly known as a cyber-physical system [25] which combines both hardware and software.

The design problem for an EPS can be formulated by combining techniques from the system and network design fields. In this context, the EPS is a network that distributes electrical power from generators to loads, and also a system that efficiently balances generation and distribution through its power and energy management systems. Being the aircraft industry a safety driven industry, EPS design for future MEA must comply with the strictest safety and reliability specifications [26]. Conventional aircraft EPS design has to comply with standards and guidelines for military and aerospace vehicles. Standards such as MIL-STD-217, MIL-STD-1553, SAE-ARP-4761, SAE-ARP-4754, some of them also observed in commercial aviation, are mandatory for the operation and reliability in current aircraft electrical systems. However, the next generation of MEA must comply with and exceed current standards, and it is expected that new standards will reflect future operational requirements from disruptive and innovative designs [17].

2.3. Safety in power system design

Safety is the condition of being secured from danger or prevented from causing danger [27]. Assessing the degree of safety requires compliance with a certain level of reliability. Reliability in safety-critical systems can be considered as a measurable safety performance indicator in a scale in which 0 is not safe

at all, and 1 is 100% safe. In addition to reliability, safety can also be measured by other related attributes such as robustness, resiliency, and survivability. All these attributes are considered as below.

- Reliability is the ability to perform a function within specific conditions for a given period. The main EPS function is to deliver power from power sources to loads. Failure to deliver electrical power can compromise aircraft function, which is unsafe for operators and passengers. As mentioned before, reliability can be expressed as a quantity that measures, in a scale from 0 to 1, the level of safety.
- Robustness is the ability to continue functioning despite variations in the operating conditions of components or subsystems. Faults are included within these operating conditions in some engineering fields, but faults are excluded here and included in survivability.
- Survivability is the capability to complete a mission in the presence of failures, attacks, or accidents. This not only applies to hardware malfunction or failure, but also to software malfunction, failure, or attacks.
- Resiliency is the ability to respond to predicted and unpredicted disruptions and catastrophic events. A failure event could lead to a catastrophic event such as the permanent loss of a main generator, and the system must overcome such event and continue operation. Survivability and resiliency are often applied indistinctively, although resiliency has a broader meaning.

The four attributes are depicted in **Figure *2.2*** using two qualifiers, failure recurrence and failure impact. **Figure *2.2*** has been developed by the author considering the concepts of survivability, resiliency, reliability, and robustness presented in the literature. All attributes can be specified through a set of literary requirements and belong to the initial design specifications. Aerospace engineering design has consistently focused on reliability, which includes survivability, resiliency, and robustness indistinctly. However, in addition to compliance to these attributes, a safer and more reliable system also relies on

economic feasibility. The dynamic between the main industry drivers, i.e., weight, reliability, efficiency, and cost are conflicting, which is the reason for which solutions to design problems are often based on optimization [28], [29].

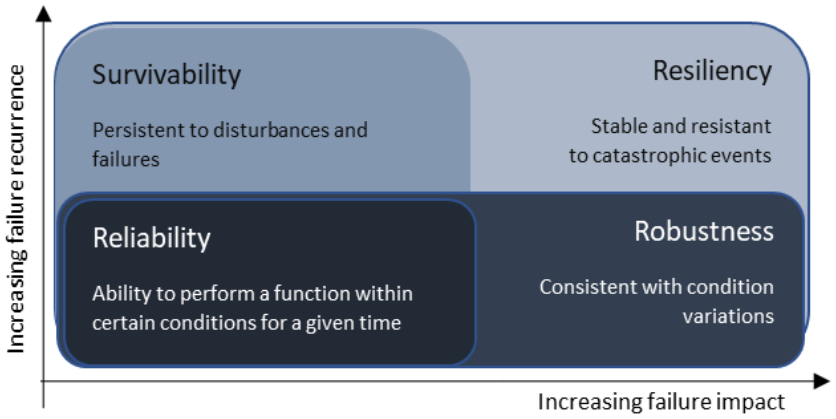

Figure 2.2 Conceptual map of safety attributes (source: author)

At this stage it can be said that the resulting EPS design must consider optimization of available resources (expressed in terms of weight and cost) while providing maximum safety, i.e., the system must be resilient. Observe that the resiliency envelope accounts also for survivability, robustness, and reliability according to **Figure *2.2***. Also note that safety can be quantified and hence can be maximized, in other words, optimization is also involved in the reliability and safety performance of the system. In this case, the design problem is said to be reliability-based because safety is top priority, and optimization-based because resources and safety are optimized. Of course, the design must observe a certain level of reliability to be considered safe; anything beyond that is even better. A reliability- and optimization- based problem to design a system is a complex formulation combining a large number of variables and non-linear constraints. In fact, this is a main difficulty: the system's reliability calculation is a hard problem to solve [30] even for small-sized systems.

Reliability of a small EPS (example)

Let k be the number of paths that power can flow from power sources to loads (i.e., all possible ways to supply loads), and L be the total number of loads. The reliability evaluation of the EPS depends on the values of k (paths) and L (loads). For example, consider the EPS shown in **Figure *2.3***. If both loads were critical, a reliability evaluation technique such as the path-tracing method [31] would deal with $k^L = 16$ possible ways to supply the loads. For the case of $k = 6$ and $L = 8$, which is not even a medium sized system yet, the reliability evaluation requires calculation of more than 1.5 million combinations. This is known as *combinatorial explosion* [32] due to the exponential growth of the number of paths available to deliver power. To avoid combinatorial explosion, a convenient method to increase reliability is required.

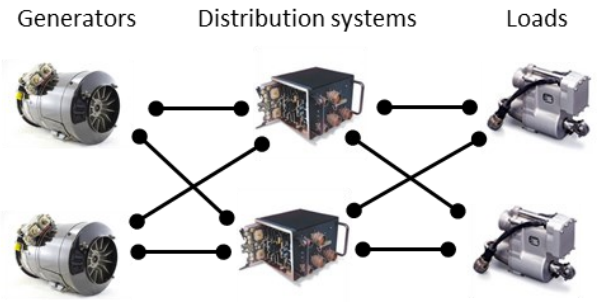

Figure 2.3 Power system example

The design approaches found in the literature can be broadly classified into system design, network design, and other design methodologies comprising combination of system and network design.

2.4. Design Approaches

Based on the available literature for the EPS design for MEA, the design approaches can be classified into three main groups, as depicted in **Figure *2.4***: system design, network design, and other reliability- and optimization-based methods including various types of formulations. System and network design have been mentioned earlier, while the rest of formulations are independent optimization formulations to solve specific problems related to design or performance improvements but are unable to support a

complete EPS design. System design is further divided into design frameworks based on Platform Based Design (PBD) or Integrated Design by Optimization (IDO) approaches, and Reliability-based design optimization (RBDO). The RBDO is almost exclusively reserved for structural and mechanical engineering, while PBD and IDO (both design frameworks), and network design have been used in the MEA EPS design context. All of these approaches are explained in detail below.

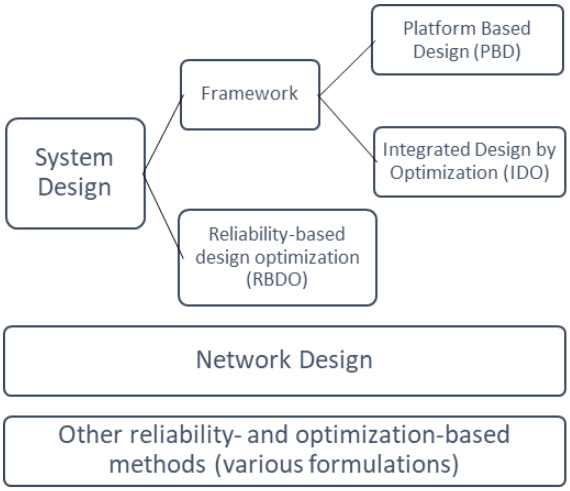

Figure 2.4 Design approaches for the EPS design exercise

2.4.1. System Design

In recent decades, the synthesis of EPS architectures for MEA has been assessed either with design frameworks or with other techniques based on reliability- and optimization- based design, both considered here as system design approaches. Recall that a framework is an interrelated group of methods and algorithms to guide the design process. One of the most relevant design framework methodologies used in EPS design is Platform Based Design (PBD) [33]. PBD was originally generated in the microelectronic device industry as a disruptive way to handle complexity in large-scale integration devices and produce new designs more efficiently [34]. The application of PBD in the EPS design includes the adoption of performance verification tools and specification languages not commonly considered in the design loop [35]. PBD has been formulated as Correct by Construction (CbC) [16] and Contract based

Design (CbD) [36] methodologies. However, both methods have implemented optimization problems for topology synthesis, specifically Mixed Integer Linear Programming (MILP) problems [37]. Optimization is used as a tool to minimize weight or cost while constraining to the candidate solution to achieve a certain level of reliability.

Platform Based Design approaches

Correct by Construction (CbC) and Contract Based Designs (CbD) are wide concepts used in the design of systems. CbC checks and guarantee correctness in the construction of the design problem, so that the final solution is guaranteed to be correct even without testing it. In CbD, contracts are formally specified, and these contracts must be met. CbC and CbD are not disjoint concepts, e.g., a system can be defined formally using contracts (for inputs and outputs), but its synthesis guarantees compliance, so that the system is correct by construction, then CbC and CbD have been used for the same design problem. The MEA EPS design attempts found in the literature can be considered as examples of how CbC and CbD can be implemented. Naturally, there are many other ways to implementing CbC and CbD. PBD (both CbC and CbD) uses a series of abstractions to divide the original design problem into several subproblems (more details in Chapter 3).

Correct by Construction CbC. CbC has been used in the design of an EPS architecture for MEA. In the CbC implementation of [16], the authors develop optimization formulations for the design of an aircraft power system, considering a PBD approach in four steps,

1. Generation selection and generator-load pairing
2. Power distribution design
3. Control system synthesis, and
4. Embedded system design

Each step has its own platform that contains a group of abstractions modelling the components or devices. These components are later selected, sized, and connected between them according to an arrangement provided by an optimization formulation, that is, a system that strictly complies to the initial design specifications is synthesized. However, only a few results have been reported for the first two steps, and the last two steps are still under research. These steps have been decided upon the existing relationship between weight, reliability, efficiency, and cost. The optimization performs a trade-off between conflicting objectives, i.e., weight and cost minimization, and efficiency and reliability maximization. The CbC guarantees the absence of error in the design process, reason for which its outcome is said to be *correct*. Hence, clear specifications with no contradictions or empty characteristics are expected to be able to construct a correct system.

EPS design with CbC (example). To illustrate CbC in the design of an EPS for an unmanned air vehicle (UAV), consider the following example. The UAV is required to autonomously fly 1.5h with a reserve of 30 min in case of route deviations. Assume that the aerodynamic design and electric propulsion design has been already done. Now, for the EPS design with CbC, the batteries (power generation) to support the payload (including the electrical propulsion, batteries, and EPS) within the maximum flight range are designed first, i.e., number and size. Preliminary estimation on some unknown characteristics (e.g., losses) are required for the determination of batteries. Then, the battery-based power source system is used as an input to determine the power distribution to supply all loads, i.e., cabling, electronic speed controllers, etc. Later, the power source system and power distribution are considered in the synthesis of a control system, i.e., power management and flight control. Finally, the embedded system design integrates batteries, power distribution, and control system into a flying unit.

Contract based design CbD. On the other hand, CbD uses *contracts* [38] to translate high-level functional specifications into detailed performance descriptions, that is, exact propositions that are satisfiable and verifiable [39], [40]. An example of its application in EPS design has the design flow depicted in **Figure *2.5***.

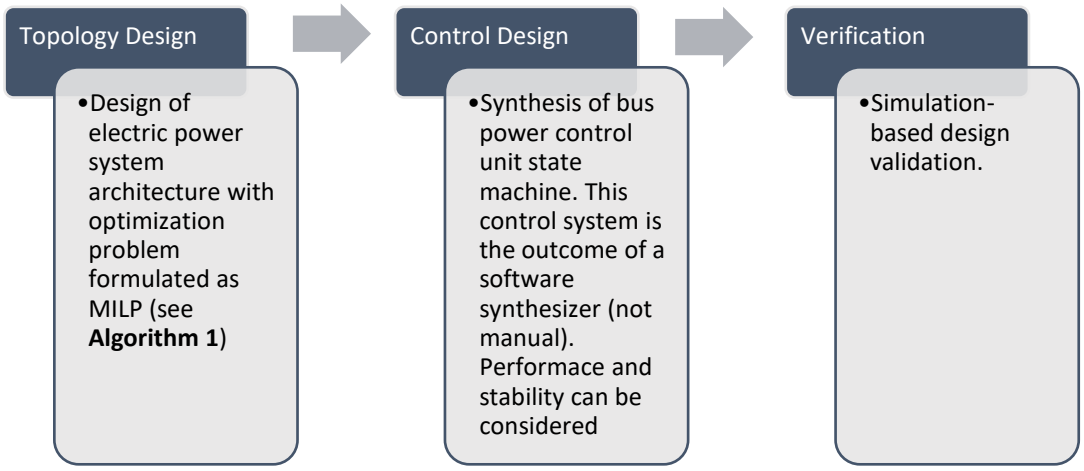

Figure 2.5 Contract based Design flow for EPS design

CbD has been applied in the synthesis of power system architecture for MEA and its corresponding control system [36]. The cost of integrating performance evaluation with the design has been the introduction of new computational tools and mathematical languages explicitly adapted from the computer science field into the aerospace design area. In [36], linear- and signal- temporal logic languages (LTL/STL) are used as formal languages to describe in detail functional specifications which are processed later in an iterative MILP optimization design and reliability modulo evaluation as shown in **Algorithm 1**. A system's reliability can be measured as a probability of failure (not being able to supply critical loads), which is evaluated with an Integer Programming modulo approach [41]. LTL requires the use of advanced computational synthesis tools, such as the reactive protocols synthesizer SR(1) [39] for the synthesis of the power control system, modeled as a finite state machine (FSM). Following this research line, applications of CbD for design of aircraft EPS have been reported in [40], [42], [43]. Experimental demonstration of these EPSs included synthesis of controllers with TULIP (Temporal Logic Planning Toolbox [44]) [45]–[47] and JTLV (Java

Temporal Logic Verification algorithm [48]) verification scripting environment [49]. Further plans to investigate automatic generation of contracts and contract language definitions are expected [50].

Algorithm 1 Pseudocode for topology design in Contract Based Design.

1. **MILP**
   Formulate and solve MILP with: pool of components, and parameters
2. **Reliability Modulo**
   Evaluate reliability of the candidate architecture
   Is candidate's reliability ≥ reliability target?
   If not, ***add reliability constraints***, go to 1
   Else, ***candidate satisfies reliability criteria***, return EPS architecture

EPS design with CbD (example). Illustrating CbD might be cumbersome due to the significant number of computer languages required for abstraction, modelling, and processing. To give a hint on CbD, let an electrical generator be included in an EPS design. Using the language proposed in [50], the model for the generator's contract (contract for input and output) might be as written below.

Component Generator {
  View Electrical {
    Parameters R, v_0 : real;
    Var v, i : real;
    Assume $\{ v_0 i \leq 200 \times 10^3 \}$;
    Guarantee $\{ v = v_0 - Ri \};\}$
}

Component refers to the name of the device, **view** is the layer in which the component is operating (could also be mechanical, thermal, etc.) so there could be other views of the same component, **parameters** list all the characteristics and its numerical type (float number, real number, etc.), and then **assume** and **guarantee** are specific fields in the contract. In this case, no more than 200kW are assumed to be supplied by this generator, and an operation based on the voltage-drop model for the generator is guaranteed. Similarly, other components are modelled as well as other contract models for the operation between components. These models are used in other synthesis stages based on other computer languages.

CbD and CbC have been part of a larger Cyber Physical System design initiative for MEA designs [51]–[55]. The aim is to produce an integrated device (or system) that combines hardware and software in an intelligent mechanism (cyber) based in algorithms, that interacts with its environment (physically). There have been some conceptual descriptions and proposals for the design and integration of aviation systems as cyber physical systems that include real time performance assessment [25], but no reports on actual implementations or formal developments have been observed. This review continues with IDO and RBDO.

Integrated Design by Optimization

Integrated Design by Optimization (IDO) serves as a design framework that focuses on the utilization of model-based design methodologies with advanced simulation tools [56], [57]. IDO consists in a group of techniques, algorithms, and optimization tools that enables integrated performance evaluation in the design of complex systems via advanced model-based description of components and devices. IDO's design process consists of linking the system's model to an optimization algorithm with multiple decision criteria such as geometry, efficiency, and dynamic performance. These criteria are used for optimization in order to accomplish high power quality, static and dynamic stability, and efficient coupling between electrical, thermal, magnetic, and other mechanical subsystems. In [19], there are several IDO-based methods to manage multi-level and multi-criteria optimal designs for electrical energy systems. The formal analysis, synthesis, and management methods used in IDO are presented as systemic design methodologies in [58]. Reports on the utilization of IDO in MEA EPS generation system optimization efforts and other electromechanical actuator sub-system designs can be found in [57].

The representation of complex systems (aircraft wing, fuel system, taxiing system, etc.) involves a high number of interfaces and interconnections between components and field domains (disciplines), e.g., electrical, mechanical, thermal, communication, etc. Hence, the design extends outside the normal boundaries for each discipline, that is, the design becomes multidisciplinary and a multidisciplinary design

optimization is required [59]. In traditional design, specifications were passed between engineering fields and optimization was performed independently on every field. Later, all products were assembled into a larger system. In contrast, multidisciplinary design involves simultaneous synthesis of components or subsystems across several disciplines, considering the interactions between them. For instance, aerodynamics, structures, and controls are strongly coupled disciplines in wing design.

Reliability-based Design Optimization

In addition to IDO, Reliability-based Design Optimization (RBDO) is a system design approach that has been extensively applied for design in civil and structural engineering, albeit seldom in power system design; there are scarce attempts in using RBDO in the design of aircraft EPS. The main purpose of RBDO is to consider aleatory (random) uncertainty in design optimization. In most cases, reliability requirements are stated as hard constraints in an optimization problem, each constraint being related to a given failure mode and its probability of failure. A few applications of RBDO in electrical engineering have included probabilistic constraints in the optimization-based design of an EPS [60], [61], while a piezoelectric energy harvester has been designed in [62]. However, beyond these applications no other approach in the design of a power system has been reported. Although this methodology could aim for developing a reliable design, it lacks the flexibility to integrate the rest of the functional specifications explicitly.

Still, there is an enormous potential to explore power system design with novel frameworks considering the integration of computational resources, communication, and control, combined into an integrated system.

2.4.2. Network Design

Network flows and network design methods have been extensively used for network synthesis and optimum network designs of several kinds of systems in a broad number of engineering fields including telecommunication, transportation, computers and teleprocessing, energy transport systems, water

distribution networks, etc., [63]. In the current stage of early development of MEA, interest in network techniques and graph theory has increased dramatically. In the context of electrical engineering, several power and energy balance constraints are amenable to network design formulations. Besides, the existence of multiple power flows between generators and loads allows the utilization of multiple constraints that are forced to be satisfied simultaneously. In the network design field, this formulation is referred to as a multicommodity capacitated network design [64], in other words, multiple (multi-) power flows (this is the commodity being transported or transmitted) subject to capacity limitations (capacitated).

Not only is the EPS a network whose purpose is to route electrical energy from generators (sources) to loads (sinks), but it must deliver power in a reliable manner, e.g., some loads that are critical must always be supplied. Besides, failures must not compromise the EPS so that critical operations are not permanently interrupted, e.g., the system survives a failure, or it is resilient. In the network design field, resiliency can be introduced in the network design and these types of formulations are known as resilient network design problems [65]–[67]. In these problems, network design is synthesized to provide an EPS with high reliability, i.e., high power availability at load terminals even in the case of failure in some components or subsystems. Hence, network design formulations enable the synthesis of new EPS because it can formulate an optimization-based network construction problem [68] considering reliability.

Network design methods have been extensively used in planning and operation of transmission and distribution in power systems [69]. The following are some applications in EPS design and operation,

- Network expansion problem for long-term planning [69]
- Optimal transmission switching for finding optimal topology in existing network [70]
- Optimal power flow [71] and security constrained optimal power flow [72]
- Optimal power allocation [73] and load management [74], [75]

It is relevant to highlight the fact that reliability (resiliency) constraints can be seamlessly added into a network design problem without the necessity of assessing reliability in a separate performance analysis task, e.g., unlike the approach followed by [36] and shown in **Algorithm *1***. This provides an efficient way to integrate reliability performance evaluation into the design problem. For instance, system's survivability to any single-component failure event, can be modelled as a design constraint in which given a set of possible failure cases, the EPS provides sufficient alternatives to continue supplying critical loads.

Network design formulations can be categorized into four main types as described below.

- Depending on the number of commodities transmitted. Single or simultaneous power flows between power sources and loads can be established in the EPS. Because there is more than one load (or load bus) in any EPS, multicommodity is the rule.
- Depending on how components and connections between source and load are selected. The network formulation may identify and build a path between a source and a load, using this to determine the number of components and interconnections. Alternatively, independent selection of connections and components can be performed without determining paths.
- Depending on how the cost of building the network or transmitting the commodity is calculated. The cost of selecting a component could be fixed regardless of power flow, or variables costs for power flows could be included in the total cost calculation. In the latter case, cost refers to the performance parameter used to build the network. Traditionally, financial cost is the main driver, but weight could also be the main design driver and could replace monetary cost.
- Depending on the level of reliability desired in the network. The network is required to be survivable or resilient, that is, resistant to failures.

These types of network flow design are organized in **Figure *2.6***.

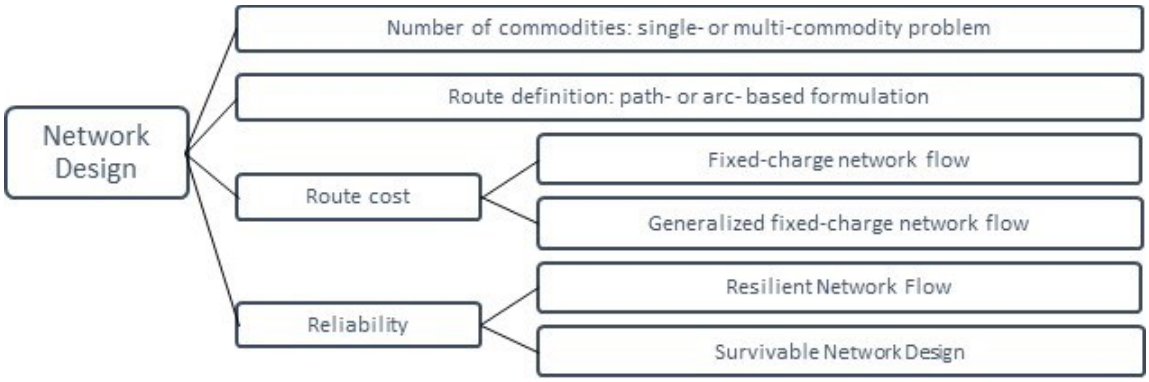

Figure 2.6 Conceptual map of design approaches in network flow and network design

Survivable network design has been extensively used in the telecommunication industry to produce a minimum cost network that continues to support flow under any of a given set of failure scenarios [65]. Failure scenarios are pre-selected, but correctly selecting critical failure scenarios can be a challenging task. Then, resilient network flow aims in ensuring sufficient excess capacity on the surviving sections of the system. Resilient network flow has been often used in power systems and microgrids applications [76].

2.4.3. Other Design Methodologies

Apart from the system design and network design approaches, there are other methodologies that solve specific design problems using mathematical techniques such as optimization. Reliability has also been considered either as a main design objective or as a hard constraint within the optimization formulation. These unclassified methodologies have had contributions such as optimization of existing EPS architectures in order to improve specific attributes, that is, optimizing (sometimes not automatically) the performance of certain parameters. For instance, [77], [78] performed research to optimize current AC three-phase infrastructure for weight saving and load rebalancing independently, but comparative exploration on HVDC configurations for efficient cabin power supply on future more electric aircraft has also been done [79]. Although not adopting rigorous frameworks such as PBD or RBDO, these methodologies are still reliability oriented. Other efforts have been directed towards the investigation of:

- MEA pre-defined architecture analysis and manual selection [15]
- Adaptability of an unmanned air vehicle power system under different operational scenarios [80]
- Candidate architecture analysis and instability prediction via small signal stability of real AC/DC hybrid systems [81]
- Other research exploring several forms of efficient technology adoptions and methods to handle complexity management [28].

From the design approaches detailed above, the design frameworks based on PBD have been specifically used to synthesize an EPS for MEA. While the CbC approach in [16] has proposed formal mathematical methods to produce an EPS architecture comprising generation system and power distribution, the CbD in [36] has reached a synthesized control system on top the EPS architecture. However, comprehensive knowledge of several computer science tools and algorithms are required to replicate this approach.

2.4.4. Summary

A summary of optimization and design methodologies previously examined is presented in **Table *2.1***. The main classification tree (for EPS design approaches) has been depicted in **Figure *2.4***. It can be observed that most of research has been devoted to the design of a particular subsystem, while only a limited number of publications in the literature has focused on the design problem for the synthesis of an EPS from scratch, that is, considering no initial pre-selected or architecture candidate. Although network flow techniques and network design has been extensively used in other engineering fields, limited applications of EPS design have been reported. In almost all cases, optimization is at the heart of the problem formulation, while reliability has been considered as a hard constraint within the optimization to comply with strict safety requirements. It can be said that the aircraft EPS design is a multidisciplinary problem (combining several engineering fields), the aerodynamic design itself being the most important. Having captured the power requirements to supply the aircraft systems, the EPS can be designed. Often, design

starts with a preliminary load sizing assessment based on approximation methods considering maximum power required (conservative estimation) as a starting design point. Later, total load can be updated with a more accurate sizing approach.

Table 2.1 Design and optimization methodologies for aircraft and MEA.

Methodology	Approaches	Applications in aircraft design or optimization
Conventional Design Flow (CDF) *Traditional approach in aerospace industry*		All standards and guidelines of aerospace sector are observed [82]. Some of the reliability tools for the design process are: Failure Mode Effects (FMEA, FMES), Monte Carlo Simulation, and Fault Tree Analysis (FTA) [83],[84]. Some of the probabilistic modelling and life testing technologies are the following: Highly Accelerated Life Tests (HALT), Highly Accelerated Stress Screening (HASS), Accelerated Life Test (ALT), etc. [83]
Platform Based Design (PBD) [33], [34], [85]	Plain PBD	Platform-Based Design for Aircraft Electric Power Systems [35] Synthesis of reliable cyber-physical architectures [41],[54]
	Contract based Design (CbD) [38], [52], [55]	Contract-based methodology for aircraft power system design [36] Architecture synthesis for aircraft power systems [86]
	Correct by Construction (CbC)	Correct-by-Construction Design of Aircraft Electric Power Systems [16] Managing complexity in aerospace systems [87]
Integrated Design by Optimization (IDO) *Mostly applied to electric energy systems*		Opportunities on coupling new architectures and technologies to optimize integrated power sub-systems [57] Several design objectives involving numerous areas of progress in terms of power integration at both the component and device level [88] Summary of design methodology based on a systemic viewpoint [19] A system level integrated design by optimization is explored on MEA [56] Multidisciplinary design optimization (MDO) [59][89]
Reliability Based Design Optimization (RBDO) *Most applications are for civil and structural engineering*		Most of the applications are for civil and structural engineering [90], with rare attempts in electrical networks [60]. The probabilistic reliability analysis provides tools to compute the probability of failure corresponding to a given failure mode or to the entire system. Formulations and methodologies can be found in [91]. The most common analysis are the first-order- and second-order reliability methods (FORM & SORM) [92]. Some of the applications are: • Probabilistic design approaches: comparison from numerical perspectives [93], probabilistic structural design optimization [94] • Topology optimization: reliable low weight structures [95] • Component design: reliable power generation from piezoelectric energy harvester [62]
Network Design *Most applications are for ground power systems, water grid, and telecommunication*		In the power system context, [69] presents an optimization-based method to locate and size transformers and establish secondary feeder routes in a low-voltage distribution network. For a comprehensive analysis on network problems, please refer to [63] Examples for the telecommunication network planning can be found in [64], [66]
Other optimization-based methods *Multi-objective optimization, higher complexity methods with reliability, multidisciplinary optimization*		Architecture evaluation or design: • MEA topology options [96],[79], system architecture for adaptability [80], power conversion modelling based on building blocks models [97], design simplification based on high level of abstraction simulation models [98] Improvement on current electrical performance: • Reconfiguration and balancing problem in aircraft AC networks (*Airbus operations*) [77], weight saving optimized distribution system with modern concepts (*Airbus operations*) [78],

Methodology	Approaches	Applications in aircraft design or optimization
		optimization of energy-supply-structure of modern aircraft utilizing conventional power system technologies [99] Exploration of new architectures: • exploration of several HVDC-architectures for aircraft applications (*Airbus operations*) [79], Ptolemy II-Metropolis/Metro II tools for architectural explorations (*IBM, UT, Bosch, NI, Toyota*) [100], analysis of HVDC parallel electric power system for MEA [101] Higher complexity methods with reliability: • Multiple objective and multi-state design problems [102], [103], RBDO with sequential optimization and reliability assessment SORA [104], simulation-based method with design variables as random variables [105]

The methods reviewed in **Table *2.1*** have been used in the design of aerospace systems, the design of an aerospace electrical power system, or the re-design of current aerospace power systems. MEA requires the design of new aircraft for satisfying requirements of new markets, this being the reason for which re-design of current aircraft systems has not attracted major attention, with the exception of taxiing systems that have been successfully installed in landing power trains on current aircraft [106]. However, new designs for MEA are attracting deployment of new technologies, and new EPS designs are required.

Most of the design approaches in **Table *2.1*** are based on the formulation of optimization problems. These problems explore the design space such that a solution is optimal when the objective of the search (optimization objective) cannot not improve its value towards a higher maximum or a lower minimum (e.g., minimum weight, maximum efficiency, etc.). There is a significant number of solvers for many types of optimization problems, but there has been a significant demand for approximating design problems to a Mixed Integer Linear Programming (MILP). MILP has advantages that are detailed in the following section.

2.5. Linearization and MILP

The design approaches analysed up to this point (Section 2.4) utilize optimization formulations in the form of MILP (Mixed Integer Linear Programming) problems. In this section, linearization and MILP are explained in the context of transforming an original problem and solve it as a MILP.

Most design problems in real applications are non-linear because the representation of the system (to be designed) is highly non-linear due to the dynamics (physical behaviour, electromagnetics, etc.) and the relationships between variables, e.g., voltages and currents in a power system. There is rarely a proportional or linear relationship between variables, inputs, and outputs. One way to solve non-linear equations is by approximation to linear equations, which is known as *linearization*. Linearization works appropriately up to some accuracy and some range for the input variables. Hence, linearization methods must perform a sufficiently accurate approximation of non-linear functions, such that the search for an optimum gets as close as possible to the global optimum, i.e., the solution cannot be improved because there is no *better* set of variables' values that provides a higher (maximization) or lower (minimization) objective value. Having performed linearization on a non-linear optimization problem, Mixed Integer Linear Programming (MILP) [107] methods can be used to solve it. Therefore, there are two steps to solve the original problem: 1) convert the problem to an approximated linear version with linearization techniques, and 2) solve this linearized version of the problem as a MILP.

MILP formulations are advantageous due to the following reasons [32], [108], [109],

- Convergence to a global optimum. If the problem is feasible, the convergence is guaranteed, i.e., there are no constraint conflicts or contradictions, and the objective is not unbounded. Feasible means that there are no conflicts or contradictions between constraints, and that the objective is not unbounded (i.e., an optimal solution lies between a certain range of values). The convergence of the original problem can be slow (even taking millions of years); linearization can help in approximating the problem to a linearized form that converges very close to the global optimum.
- Availability of efficient commercial solvers. MILP problems can be tackled by (relatively) extremely fast and effective commercial solvers such as CPLEX [110] and GUROBI [111], FICO Xpress, MATLAB [112], among others. Solving a MILP could take shorter time compared to solving

the original problem. Also, the use of commercial solvers lets the user concentrate on the investigation of efficient problem formulations of the application under research, rather than focusing on producing efficient solving methods after formulating the problem.

- Linearization techniques are available. A comprehensive body of linearization techniques released in recent decades has made it possible to approximate (original) non-linear problems with mixed continuous and integer variables into MILP equivalents. Some problems can have a very large search space, e.g., combination of values in the variables is huge. An alternative to overcome this issue is a Disjunctive Programming [113] which is a problem modelling alternative whose advantage remains in the retainment and exploitation of the problem's logic structure to reduce the combinatorics and improve relaxations (modifications in constraints).

If the MILP formulation is feasible, it can be solved and an optimal solution can be found [108]. In fact, this solution is a global optimum among all the local optima (optimal values in a specific region of the search space). Based on the nature of its variables, the family of MILP problems can be classified into Linear Programming (LP), Integer Programming (IP), and MILP. All types of MILP problems have linear expressions (functions) in the optimization objective and the constraints [32].

Linear Programming (LP). When all variables are continuous, the problem is said to be a *linear programming* (LP) problem. The optimal solution (if any) is exactly the global solution (not an approximation). Algorithms such as the simplex method or its variations [114], [115], and the interior point method (and all variations of Karmarkar's algorithm [116]), can be used to solve it.

Integer Programming (IP). In contrast to LP, when all variables are discrete, i.e., they can only take integer values, the problem is said to be an *integer programming* (IP) problem. The introduction of integer variables raises the complexity because integrality (variables with integer values only) breaks the convexity of the problem, i.e., continuity is broken. This can be seen as an interruption in the 'smoothness'

of a function that the solver is supposed to walk on to find the optimum; several 'smoothness' properties allow faster and more efficient optimum location. Most resource allocation problems are formulated as IP problems where the assignment or selection variables are represented by binary (zero-one or 0-1) or Boolean variables [109]. IP problems are known to be NP-complete [117], [118] (nondeterministic polynomial-time[1] complete) and no efficient solution algorithm has been found to solve them. When an NP-complete problem must be solved, one approach is to use a polynomial-time algorithm to approximate the solution; the solution is not necessarily optimal (global optimum), but the aim is that it is reasonably close to it (depending on the approximation). Several exact algorithms have been proposed to solve IP [119],

- Branch and bound, relaxes the problem to a LP to obtain upper or lower boundaries.
- Cutting planes, adds other linear inequalities to the original problem.
- Implicit enumeration, often used to solve binary (0-1) problems (usually yes/no decisions).

Some of the above algorithms are used within a MILP solver.

Mixed Integer Linear Programming (MILP). MILP problems can have optimization objectives that are convex (several linear sections). A MILP can contain both continuous and discrete (integer) variables. The convexity is broken due to the presence of integer variables. In some cases, MILP can be solved as an LP problem (relaxing the integrality of the integer variables), and performing a search based on branching (trees) or cutting (limiting portions of the search space). There are options such as:

- Branch and price, uses a reformulation of the problem (problem decomposition)
- branch and cut, combines cutting planes with branch and bound.

[1] Polynomial time refers to the length of time that is considered fast for a deterministic algorithm to check a single solution. Given a particular input, a deterministic algorithm always produces the same output (or solution).

- branch and price and cut.

In other cases, MILP can be solved with heuristics, heuristic-based algorithms, approximation algorithms, and exact algorithms to branch along the integer variables that, depending on the problem formulation, could end in an undesirable combinatorial explosion. Hence, MILP can use advanced heuristics to reduce the solving time and converge as fast as possible to a solution. Commercial solvers can co-ordinately use LP, IP methods, and heuristics to converge to a global optimum (or rely as close as possible to it).

Linear approximations. The objective and constraints of the original (non-linear) problem are linearized to be able to utilize powerful commercial solvers. The following linearization techniques can used [120]:

- Special Ordered Sets (SOS). – a variable is part of a set, and it is ordered (e.g., from lower to higher values). It facilitates the performance of IP solvers such as the branch and bound algorithm. By defining a set of variables as a Special Ordered Set of type k (SOSk), a number of k variables can take a non-zero value (imposed condition). Also, these k variables must be adjacent.
- PieceWise Linear functions (PWL). – is a set of linear functions defined on an interval of real numbers each, that approximates a non-linear function (curve) by linearly interpolating a selected number of points known as *breakpoints*.
- Function discretization. – Instead of linearly interpolating a non-linear function with PWL, the function is represented by a finite set of values (not necessarily integers) and an additional condition to pick only one value from this set is imposed. It can add a significant number of auxiliary variables if the original variable's range is large.
- Piecewise Linear approximation of two variables (2-PWL). – Based on the principle of PWL, non-linear functions of two variables (two dimensional curves or surfaces) can be approximated by a set of variables that interpolates the surface to several planes. There can be one-dimensional (strips), triangle, and rectangle methods.

- McCormick Relaxations. – In the case of bilinear terms (multiplication of two continuous variables), four sets of inequality constraints (per term) are added, and the bilinear term is replaced by a new variable. In order to increase the quality of the relaxation, Disjunctive Programming methods can be used to improve the bivariate (two-variable) partition.

The PWL, function discretization, McCormick envelope, and 2-PWL methods are depicted in **Figure *2.7***. In all the figures, the blue line represents the non-linear function to be linearized. In the PWL, it can be observed that line segments approximate a quadratic function. Similarly, discretization approximates the same function with a set of values (bold black dots). On the other side, McCormick envelope and 2-PWL approximates functions of two variables. In **Figure *2.7***, the McCormick envelope approximates a section of a two-variable function by 'enclosing' it inside an envelope (parallelogram shown on the floor) while the 2-PWL tries to perform two simultaneous PWL, one for the first variable, and another for the second variable.

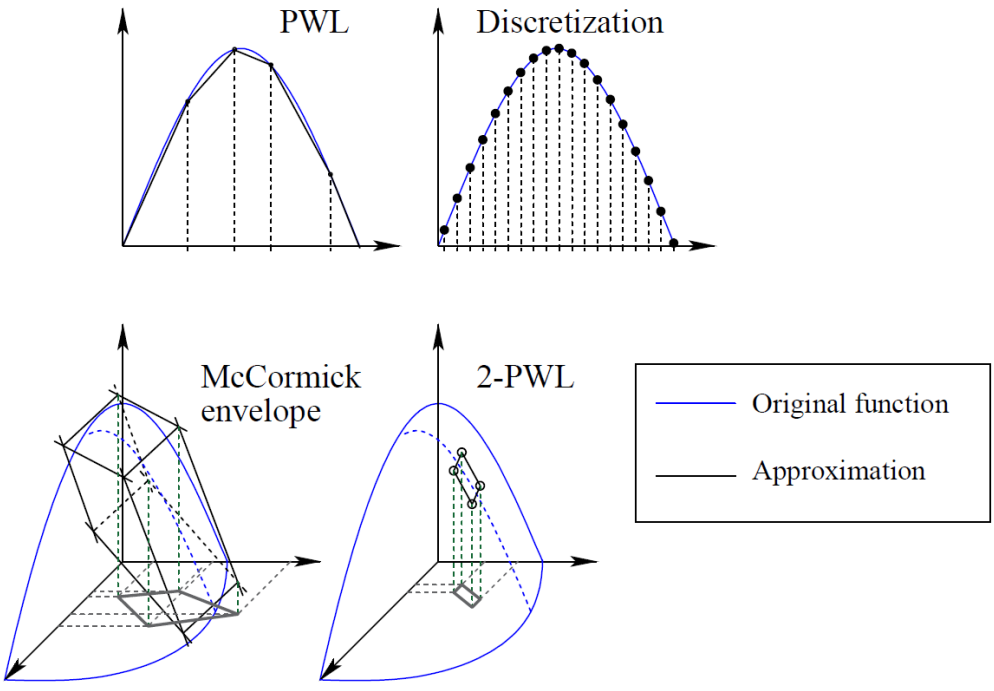

Figure 2.7 Various linearization techniques (graphical examples).

Higher accuracy in the approximation requires a larger number of variables and tighter bounds (improvements in capturing non-linear shapes). If tight bounds are used, MILP solution is much closer to a global optimum. The process of handling huge number of variables and tight bounds is effectively performed by commercial solvers. Depending on the problem's structure and the level of approximation required, several linearization techniques (tight upper or lower boundaries, variable sets, etc.) may be required in the formulation.

2.6. Discussion

In the MEA context, the power system is a *system of systems* because it has the task to supply power to all of the systems in charge of making the aircraft fly, this being the reason for which its design is a very complex task where reliability is at the core of the synthesis problem. The aircraft EPS being a complex system consisting of several subsystems made of hardware, software, and communication interacting with other aircraft systems, the design of an architecture has been explored considering Cyber Physical System design concepts, specifically with a Platform Based Design (PBD) methodology that has been implemented utilizing optimization problems formulated as Mixed Integer Linear Programming. PBD has attracted attention from other fields due to its capacity to reduce design complexity by dividing the original problem into a hierarchical set of subproblems determined by a series of abstractions, starting from an architectural level, and progressing until it reaches physical implementation. There have been two main PBD approaches in the synthesis of power system architectures from scratch considering a set of specifications, Correct by Construction in [16] and Contract based Design in [36], both focusing on ensuring reliability performance throughout the design process. The former work has reported no results but proposed conceptual formulations for the design problem while the latter work has reported theoretical results that have been later implemented in a small-scale testbed for the purpose only of evaluating the performance of the control synthesis.

Beyond these formal approaches, some attempts have explored several types of optimizations in the design of the EPS without proposing a formal framework for the synthesis of the power system itself, but for other purposes such as performance improvement of potential pre-defined architectures or existing power systems. This can be explained from the point of view that MEA is an initiative that aims to transform the aircraft sector gradually. In fact, research has focused more on the optimization of particular aircraft subsystems that demand attention due to their higher inefficiency and for which improvements could have large impact in reducing waste and successfully promote the more- and full-electric aircraft concept. However, the next stage in the development of the aircraft industry is the production of a new generation of aircraft that would have been re-designed and integrally re-engineered with the latest technology advancements that can achieve far more pollution reduction and energy efficiency than current aircraft which have been improved with control adjustments and limited subsystem replacements.

Reliability is certainly a design driver. However, the traditional RBDO used in civil and structural engineering are amenable for problems where the structures must remain undeformed during operation, and their parameters' uncertainty around a nominal value must not affect the combined resistance to an external deforming force. Having a failure occur, the failed section is still part of the whole structure and could lead to further failures. On the other hand, the definition of failures on electrical systems are completely different because, unlike mechanical structures, the system can isolate the failed section or reconfigure itself to continue providing power flow where needed. Within the optimization- and reliability- based formulations found in the literature, two features have also been attractive for MEA,

- Implementation of DC power systems. DC has gained significant interest due to reduction of losses and the possibility of weight improvement when compared to AC. However, this feature heavily depends on the aircraft design and must not be taken as appropriate in all cases.

- The obtention of an optimal architecture with MILP. Advantages and linearization techniques has been explained in Section 2.5.

Finally, besides MILP utilization in power system design, research has turned its attention to direct current electrical systems for future more electric aircraft. Among the main reasons there are:

- Integration of DC power electronics in the EPS can provide high power density and efficiency [121]
- Absence of frequency synchronization unlike AC systems [122]
- No reactive power flow, hence important weight savings in sizing components and more freedom in power flows and power management [123]
- DC microgrids can be more robust to voltage sags [122]

With the current expectation on batteries and fuel cells as potential power sources for MEA, it is convenient to distribute power as DC because the electrochemical power production of such sources is in DC, and there could be important savings due to fewer power conversion stages compared to AC. Having a nominal voltage level for the EPS, only voltage level adoption is required, assuming the rest of the EPS devices absorb or consume energy in a DC format. On the other hand, AC systems demand several power-conversion stages and control systems to match frequency, phase, magnitude, and balance active and reactive powers to maintain stability in voltage and frequency. Hence, DC systems are the target candidates in the exploration of new power systems.

2.7. Conclusion

The design of power systems for more electric aircraft is a complex task. A power system is a system of systems that becomes the heart of power and energy distribution in future aircraft and its design involves the integration of several disciplines, this being the reason for which its construction has borrowed several concepts from the cyber physical system design initiative. There have been limited framework proposals

for the integral design of an optimal architecture which considers the main industry drivers, reliability being the most important one. On the other hand, there are extensive applications of optimization and reliability-based design in other power system related problems such as performance improvement in existing systems, efficiency and stability enhancement, subsystem replacements for improving fuel reduction, etc. Although these applications aim for optimizing power systems, they avoid presenting a formal method to synthesize a power system from scratch. Hence, there is still an unexplored research gap for the design of MEA EPS. Three features will be at the centre of the design process: performance evaluation; the exploitation of network design techniques; and the use of MILP techniques for finding an optimum architecture. The availability of commercial solvers allows for focusing on the efficiency problem formulation rather than the solution methods themselves.

3. Framework for a reliability-based design

3.1. Introduction

A design framework for the synthesis of an EPS architecture is presented in this chapter, which considers the main aerospace industry drivers. The main drivers for the synthesis of MEA EPS are weight, reliability, efficiency, and cost. The design framework is provided with a set of design specifications that details the functional and behavioral requirements as well as a template (pool) of components and connections based on a pre-defined selection of technical aspects that are application dependent. The aim is to optimally select components (deciding upon their number and sizes) and connections to form a power grid the complies with the design specifications. The pool aims to provide a set of feasible components with unique characteristics that may be or may not be included in the final design. The set of specifications and requirements must separately be completely satisfied. The expected outcome is an optimal EPS architecture that provides high availability of power at loads' terminals, in other words, the result is an EPS architecture constructed by synthesis using formal mathematical optimization. The proposed framework divides the synthesis process into two steps: the selection and sizing of the generation system (power sources), and the selection and sizing of the power distribution components.

The EPS is the enabler system in MEA for increasing the use of electric power onboard. However, its design depends on the power and energy requirements of an aircraft that must have been (aerodynamically) designed for a particular application (i.e., the air transportation market). Nevertheless, this chapter is focused on the EPS architecture synthesis, which follows the steps of aircraft design, preliminary load sizing, and determination of design requirements and specifications (manufacturers). To close the gap between the EPS architecture (theoretical) and the real EPS (aircraft implementation), basic methods used in performance optimization during EPS operation are detailed in Chapter 5.

3.2. Aircraft Design

The design of an EPS architecture is not isolated from the overall aircraft design. In fact, the design of the aircraft precedes the EPS design [124]. The mission of any aircraft is to fly between two locations, transporting a specific payload, hence, the preliminary aircraft design identifies an aircraft configuration suitable to accomplish this mission (aerodynamics, flight mechanics, flight control, etc.). The systems (including electrical system) installed within the aircraft enable the completion of the flight mission. In future aircraft, it is expected that electrical energy consumption will be increased (most of the systems will be electrically driven), then, the EPS design will be increasingly important because it will enable major power distribution onboard.

Previous steps in EPS design

Aircraft design allows preliminary sizing of the loads (e.g., flight controls, propulsion, wing anti-icing, avionics, ECS), i.e., the electrically driven systems are the loads that the EPS will supply [125]. Along the preliminary load sizing, design specifications and requirements for the EPS architecture design are also determined. In the case of MEA and other future aircraft designs, the design task is unable to start from a known configuration from current aircraft because the aircraft design is radically different from current solutions, then, the EPS architecture also starts from scratch.

In summary, the design (from scratch) of an aircraft EPS architecture commences with the following,

1. Aircraft conceptual design. The MEA initiative relies on the transportation electrification task and the envisioning of a sustainable future for aviation and aerospace. Although electrification of particular subsystems on existing aircraft has successfully reduced waste and pollution, an integral exercise to boost savings requires larger re-definitions, replacements, and adjustments, which existing systems cannot support. It is necessary to develop new designs from scratch, think outside the current box (diverging from current solutions) to achieve improved usage of energy

resources, novel materials, and efficient operation, that is, new designs for air transportation are mainly possible with new constructions [125]. After aircraft conceptual design has been released, a deep understanding of the power usage on electrical loads is obtained.

2. Preliminary sizing of loads. In most cases, the loads are estimated based on their power and energy consumption (load profile is highly desirable), so that a detailed definition is not necessary at the stage of the EPS architecture design [126], [127].
3. Initial EPS design specifications. These specifications comprise a detailed description of how the EPS is supposed to generate and transmit (distribute) the power to the different loads. There are sets of rules of how an EPS can perform load shedding, what to do in case of contingencies, sufficient adequacy requirements to reconfigure the system in case of failures, power sharing between generators and other power sources, etc. The specification list can be extensive and demand knowledge of how the loads are going to be supplied, i.e., AC or DC, voltage level, frequency, voltage controlled by battery, injection of regeneration's power when possible, etc.

These 3 steps must be performed before attempting the design framework proposed in this chapter. Detailed research or contributions of each one is out of the scope of this work.

It can be observed that, unless the electrical loads have been sized and the design specifications are set for a specific aircraft application, the EPS design task cannot be independently performed, and, in fact, it needs at least an aircraft preliminary design. There is an inherent connection between how electrical power is being generated (in the EPS) and consumed (in the rest of electrically driven aircraft systems), so that the EPS architecture satisfies the requirements predefined during aircraft design. The EPS design requirements definitely include performance specifications, so that the system is designed to withstand a set of conditions and it is prepared to respond to these conditions during operation. The response is executed by a control system (controller) that continuously monitors the system's conditions (e.g.,

unexpected failures, state of charge of battery, overload in generators, etc.) and sets the appropriate response to any events.

EPS architecture design in the context of aircraft design is depicted in **Figure *3.1***. This figure condenses the abovementioned design sequence in overall aircraft design.

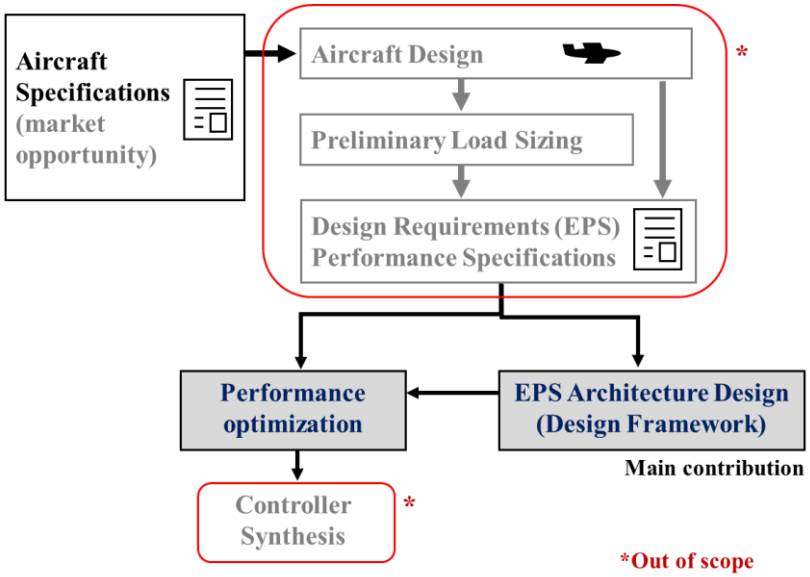

Figure 3.1 EPS architecture design within aircraft design (diagram flow).

In **Figure *3.1***, a business opportunity starts the aircraft aerodynamic and mechanical design. Having determined the aircraft design, preliminary load sizing can be done. This sizing is part of the design requirements and specifications. Then, these specifications are used in the design framework proposed in this chapter. Performance optimization is analyzed in Chapter 5 and main methods are proposed to close the gap between the synthesized EPS architecture (theoretical) and a real aircraft EPS.

Performance optimization and controllers.

According to **Figure *3.1***, performance optimization leads to a problem of controller synthesis (out of the scope of this work). The controller monitors and commands EPS components and connections to bring the system to an appropriate operation point (state). The controller must react to non-failure changes

(e.g., load changes, overloads, etc.) and unexpected events due to failures. In the former, the system that is initially unperturbed (normal state) is brought by the controller to a new state that achieves a performance target or a state that has optimized performance for those conditions. For example, the controller increases generation output when load is increased, but power distribution among generators can be such that generation efficiency is maximized. This is known as a power allocation problem [75], and it belongs to a family of performance optimization problems that seeks for maximum efficiency (minimum losses) during operation. In the latter, the system has lost a component or connection due to failure, and the controller reconfigures the system to form alternative paths to avoid supply interruption in critical loads. Formation of alternative paths is known as topology reconfiguration. For example, the system has spare generation capacity to always supply critical loads in case of loss of some generation power, then the controller activates this spare capacity and redispatch generators (distribute power among generators) in case of failure in one generator.

In both examples above, the system must have been designed with some spare capacity so the controller can use this capacity and react accordingly. Hence, there must be a close relationship between the optimization-based design formulations (used during the design time) and the optimization-based formulations used within the controller (formulations at runtime). The optimization formulations used in the design can be adapted to create a new optimization formulation that can be used in the controller at runtime (during operation). Thus, new runtime optimization formulations, based on design optimization formulations, can be used to optimally manage the EPS resources and spare capacity; the EPS has obtained these resources during its architecture design.

Designs are unique

There is no *one-size-fits-all* EPS architecture and controller for MEA and future aircraft. Thus, the purpose of the proposed framework (this chapter) is to provide effective formulations for finding a global optimal

solution (or approximate to it as much as possible) that is tailored to the designer needs in a relatively short time. The design exercise is a one-time assignment that is not constrained by time (it is reasonable to wait a few minutes, maybe hours, to find a solution) while control operations must respond as quick as possible because the loads' performance could otherwise be compromised (and consequently, the flight mission). In other words, the control's response must be quick, so it requires fast execution of algorithms and optimizations (probably in the order of milliseconds). Automated design could take from a few hours even to a few days, and there could be several designs for the same aircraft application in case of late adjustments in design specifications during early stage. Nevertheless, one EPS architecture must be chosen after the design process. How to perform EPS architecture design is the focus of this chapter.

3.3. Design Framework proposal

Main idea. The original design problem is divided into several subproblems. A series of abstractions of the problem are used to formulate these subproblems. It is ensured that the abstractions and other assumptions are valid to be able to formulate the subproblems, e.g., it is assumed that power conversion's weight and power are related by a constant power density. These abstractions and assumptions can be considered as proxies or surrogate functions (representing something, models) which will approximate what happens when the details are included, e.g., it is assumed that a constant power density can be used as a surrogate for actual component selection. Determining such abstractions and assumptions enables problem's decomposition into a series of problems of decreasing abstractions, and the validity of the decomposition can be shown by the assumptions. The rest of the chapter goes into deep details on what abstractions and assumptions are valid for the EPS design and how to formulate it as an optimization problem.

3.3.1. Preliminaries

The proposed design framework follows a Platform Based Design (PBD) approach that systematically divides the design problem into sub-problems that are not necessarily revisited (solved again) if the problems' abstractions have been appropriately defined [85]. The lack of iterations within the design steps is the main difference with respect to the traditionally followed Conventional Design [23]. In the context of PBD, abstraction (abstract representation or abstract model) means capturing a quality or characteristic that embeds other characteristics of higher detail. For example, abstraction of a generator corresponds to a device that provides power up to a maximum value (highest abstraction). Then, the next abstraction could consider the (static) relationship between voltage and current that produces that power. Later, other characteristics are included, e.g., magnetic saturation, short-circuit response, etc.

PBD requires a certain level of abstraction in the representation of devices (generators, converters, batteries, etc.) and in the functionalities the system is expected to comply with (e.g., critical sources are always supplied). Therefore, the design problem could be split into subproblems that are solved hierarchically from the most- to the less- abstract. For instance, in a MEA EPS the highest abstraction is based on providing power to the loads, then the first problem could be deciding on the power sources. Then, the connectivity between power sources and loads are determined in a lower abstraction and a second problem decides for the power distribution topology. In contrast, if solving the same design problem with Conventional Design (see **Figure *2.1***), the outcome could take longer to converge given the design loop. Conventional Design might simultaneously consider all the levels of detail in the EPS so that generators could not be selected unless there is an actual distribution grid to supply to. Power distribution cannot be synthesized unless there is a generation system from which power is delivered, so the design inherently circles over a loop until convergence. Whenever the specifications are not met in Conventional Design, the design comes back to iterate (possibly long convergence).

Levels of abstraction

In principle, PBD utilizes an abstraction of the components and sub-systems of the system to be designed, as if those components were known. The process of obtaining an abstract representation of a component or sub-system is closely linked to the multilevel modeling paradigm [8] used for determining a mathematical model. The abstraction's aim is to capture and represent information on a physical, behavioral, functional, and architectural level, where the level of complexity and detail is maximum at the physical level. In brief these levels are:

- Architectural level: focuses on the logical and requirements features. It usually performs studies assuming the nominal or steady state condition and power flow, which is advantageous in the sizing of EPS components.
- Functional level: also considers low-frequency transients to perform studies of dynamics, stability, response to load variations (including load shedding) and low-frequency power quality. This level could be extended to consider ripple, harmonics, and coupling with other engineering domains such as thermal, mechanical, hydraulic disciplines, among others.
- Behavioral level: includes high-frequency dynamics, usually in the order of kilohertz, to study the impact of higher harmonics, switching, and electromagnetic compatibility.
- Physical level: extends to all the domains, frequencies, dynamics, and consequently is highly computationally demanding. It is typically used for behavior verification of specific phenomena in single components or devices.

In the construction of an EPS architecture, only architectural modelling is required while a few components' specifications are described in terms of functionality. The term 'functional' as defined above for the functional level (mathematical models of components) has a different meaning from the term 'functionality'. Here (in PBD), functionality (functional specification) does not refer to a mathematical

model, but to what the system, sub-system, or component is supposed to do, i.e., description of the task that the component is supposed to perform. This concept is kept for the rest of the thesis.

Examples of abstractions

Each component or sub-system is described by a set of functional requirements that allows the construction of a system that integrates all the necessary components. There could be requirements at the architectural level to determine certain characteristics of the system (as a whole), and at the functional level for each one of the components. Assuming an example where there are loads that need a DC supply (high, medium, low) and others which need AC (high and low voltages), some requirements could be:

- Architecture
    - The EPS is divided in two identical (mirrored) zones.
    - Each zone has two sections, there is an AC section and a DC section.
    - There are three voltage levels for the DC section (high, medium, low)
    - There are two voltage levels for the AC section (high and low)
    - DC section is supplied from the AC section and not directly from power sources
    - There are power conversion stages between voltages levels in AC and DC.
- Functionality
    - The power conversion between AC and DC sections is performed by a single converter that can be supplied from multiple buses.
    - The outputs of several AC-DC converters can be paralleled to supply a larger load.
    - No electrical energy is permanently stored in the AC-DC converter.
    - DC loads must be supplied by an alternative battery in case main generation fails.

In most cases, these specifications are based on the load requirements and the necessity to comply to aircraft EPS standards and regulations. Given the current transition to a MEA concept in the aerospace

industry, a comprehensive understanding of the power requirements of the load is essential in the development of a load estimation method, that is, the calculation of the amount of electrical power required during a typical flight cycle. The load estimation is an essential input that has a significant impact in determining the total generation power of an EPS architecture. The outcome of a load estimation method is part of the design specifications and requirements, that is, its assessment happens prior to PBD. A few attempts for electrical load-sizing in commercial aircraft have been reported in the literature [126], [127], which also consider projections in case of migration from conventional aircraft to MEA. The development of a load estimation technique is out of the scope of this investigation but the sizing methodology detailed in [127] is recommended to the reader. It presents mathematical techniques and a structured flow to calculate power consumption and it also reports numeric results for MEA.

3.3.2. Platform Based Design

The PBD is a design methodology that divides the problem into several subproblems based on the level of abstraction. This division is possible due to the formalization of a group of abstractions that allows the fragmentation of the original problem into several parts. This problem separation is far from a simple physical detachment, instead, it is intimately linked with the logical features of the architectural level. For instance, the EPS design is not divided into a design of each component, e.g., generator, bus, autotransformer, converter, battery, power controllers etc., and then assembling all of them together. Instead, the design is divided according to the abstractions, from the highest to the lowest. At the highest level, an aircraft EPS generation system is capable of supplying all of the loads at all times. Deciding between many small generators or a few large generators in this case requires knowledge of how weight, reliability, efficiency, and cost influence this selection. This knowledge will be referred to as industry insights because the relationships between weight, reliability, efficiency, and cost are specific to a particular industry.

Each PBD subproblem takes the outcome from the previous one and includes it in its input. The first problem to solve has the highest abstraction. The following problem has a lower abstraction, and the level of detail is increased. Thus, complexity increases for every subproblem solved. At some point, the level of detail becomes very high (when the abstraction is very low), which means that the system is converging to a physical implementation (close to a real system). In other words, the system to be designed starts at the top with the highest abstraction and continues towards a real physical implementation. As an example, the multilevel modelling paradigm (architectural, functional, behavioral, and physical) could be used to sketch the abstractions in the EPS design. However, this does not mean that that there are necessarily four sub-problems - there could be more subproblems in between -.

Key concepts in PBD

The PBD takes its name because of the existence of platforms. A platform is a library of components (building blocks) that can be arranged (assemble by connecting them) into a structure (network) that has a certain abstraction (the platform has captured certain characteristics). The process of arranging the components is outlined by the formulation of a subproblem that needs to be solved usually with optimization formulations or other search-and-select techniques. The component arrangement is known as a *refinement* step because the level of complexity with respect to a previous step is increased, i.e., the features of the step's input have been raised (increased) to form a refined output. The utilization of platforms eliminates loop iterations (such as in Conventional Design) and restricts the design space on each refinement step. However, the number and location of intermediate platforms between architectural and physical levels is a crucial task; it could lead to a sub-optimal architecture if the abstractions were inaccurate. Therefore, sharp, and careful understanding of the system architectural and functional specifications is required, as well as accurate industry insights.

An EPS basically produces electrical energy and distribute this energy to where it is needed, i.e., to the loads. Assuming that all loads are of the same type and size (unrealistic) and could receive power directly from the generators (also unrealistic), the distribution would be simpler (fewer components), and loads could be connected to the same single bus. Then, the distribution system is comprised of a single bus, with power and energy management controlling generation supply (with parallel or non-parallel operation between generators). A more realistic scenario is a distribution system requiring several conversion stages to supply loads at different voltage levels. The distribution and control system are then more complex because there are more components and operation modes. The first case, the system would be lighter and cheaper (fewer components) in comparison to the second case. Reliability in the second case could be higher (if there are alternative paths to account for failures) or lower (fewer components to fail) than in the first case. Therefore, translating the industry insights into clear and accurate relationships between weight, reliability, efficiency, and cost, helps in providing accurate input to the PBD.

Industry's observations for the EPS design

Generally, the best performance from a power source is obtained when it supplies at its rated power because its efficiency is at maximum, since generators are usually designed/built to provide maximum efficiency at rated or nominal power. Unfortunately, a large percentage of loads require variable or pulsating power rather than continuous power, that is, loads' consumption is zero for some periods of time and non-zero for others, and not necessarily at the same value every time. Sizing a power source at rated power to meet the power requirements avoids adding unnecessary weight to the EPS as well as ensuring a good efficiency and low wasted power generation. Because the power sources are not connected directly and simultaneously to the loads, a distribution system is used for transmission and distribution tasks between power sources and loads.

In any phase of a flight mission, some power sources are connected to specific loads, while other sources supply the rest. Hence, in addition to the selection and sizing of power sources in the design process, an arrangement describing which power sources must be connected to which loads must be obtained as well in the design. This arrangement directly influences the size and cost of the distribution system, i.e., an EPS that switches a load between a few power sources to operate at high efficiency would require a more complex distribution system and consequently potentially a costlier one. In fact, transmission and distribution of power must be as reliable as possible to ensure that power available at any power source's terminals is correctly directed to the appropriate loads' terminals. Therefore, the size and cost of the distribution system depends on the power source-load arrangement. The abovementioned perceptions can be extended to the following observations [16]:

- The number of power sources and their power ratings (size) drives the trade-off between cost and efficiency. Maximum efficiency is achieved when rated powers match the load requirements. Also, more power sources are required to maintain the system's reliability above a certain value (in case of failures), so the cost (and possibly the weight) of the system is increased. If weight is favored over efficiency, a larger generator matching peak load would be selected. However, this generator would be inefficient the rest of the time.
- The reliability performance of the EPS is assessed as the availability of power at the loads' terminals.
- The cost of power distribution is driven by the power source-load connection arrangement (or combination) and the topology of the EPS. The power source-load arrangement is the assignment of generator(s) to specific load(s) during a specific time. If the load demand does not vary, there could be only one assignment. Power distribution must be able to reconfigure and form alternative paths in case of failures.

- The weight of the power conversion is driven by the power density (kW/kg) and the amount of power to convert [16], [128]; thus, it is independent from the power source-load combination.

The observations listed above represent the relationship between weight, reliability, efficiency, and cost, in other words, the main industry drivers (industry insights). Where needed, power conversion stages in the distribution system are dominated by the power density of the power electronics components and devices. A simple EPS with one power source and load could have a single power conversion device sized to convert power equal to the maximum load's demand. However, it is also possible to have two or three power conversion devices in parallel for the same system, either for backup purposes, reliability enhancement, or the implementation of a modular conversion topology [17]. Hence, the power conversion is not necessarily influenced by the power source-load arrangement. Nevertheless, the efficiency and cost of the EPS is mainly driven by the efficient utilization of the power sources and much less by the power distribution arrangement (performing mainly power transmission) [129], [130] .

Abstractions in the EPS design

Having reflected on the industry insights, it is possible to determine the first abstraction in the EPS design:

- The EPS produces (generates) electrical power from power sources and this power is delivered to the loads. Therefore, the EPS consists of a group of power sources supplying the loads. There is an assignment on which power source supplies each load and this assignment represents the 'work' or task that the power distribution performs.

This is the highest level of abstraction. Efficiency and cost of the EPS are mainly driven by the EPS generation system. The second abstraction in the EPS design is:

- A pre-defined power source-load assignment can be used to define a power distribution system (connections and components) that distributes (transmits) electrical power.

In this abstraction, the power source-load assignment is assumed to be available, then, this must be provided after processing the first abstraction in the PBD. If the assignment is simple, power distribution is simpler, but the complexity at this stage is higher because of the reliability requirements. In the next section we explain how these abstractions are translated into an EPS design using a PBD based design.

3.3.3. A Framework for designing the EPS

Based on the outlined relations between weight, reliability, efficiency, and cost (industry insights), which helped to determine the necessary abstractions for the proposed PBD-inspired design framework, it is possible to divide the EPS architecture design problem into two subproblems:

- power source selection and power source-load arrangement (GS&GLP), and
- power distribution design (PDD)

Subproblems for the EPS design

The former subproblem (GS&GLP) constructs the generation system that supplies the loads, so there is a library of power sources (the first platform), and the latter subproblem (PDD) constructs a topology for the distribution system by selecting distribution components from another library (second platform). Both subproblems represent refinement steps towards obtaining a physical EPS (real system). The synthesized EPS architecture resultant from the sequential solution of both subproblems could be further refined by solving for the power management control, in which case a third platform would be considered. For this platform, time is a compulsory variable because the system's behavior (response) at any time depends on the system's conditions, then, a library of operational states (specific arrangement of the system) could exist and the third subproblem would construct a control system that decides upon the operational state based on the actual conditions (occurrence of unexpected failures, load variations, etc.). Recall from Chapter 2 that computer science tools have already been used to synthesize such controllers with specialized computer languages. As an alternative, the author has proposed a less complex control

scheme for a system's reconfiguration upon the occurrence of unexpected failures for a testbed in Chapter 7. Nevertheless, successive refinements and abstractions are allowed until convergence to a physical solution (real system).

On each platform, components are defined in terms of their functionality and logic performance. However, in occasional cases, a component whose functionalities are required in a previous platform, may not yet have been defined. These are considered to be virtual, referring to the fact that only the highest abstraction has been captured, with the need to anticipate its definition in a previous platform. This is the case for power distribution. In the platform for the power source selection and source-load arrangement subproblem, the distribution components are not yet defined but the functionality allowing connection (power transmission) between a power source and a load is expected. Then, a virtual distribution component (representing all of the distribution system) is considered such that it has as many input and output terminals as required. Hence, it contains any number of connections (between power sources and loads) as required, and these connections have their own reliability and efficiency. In the next subproblem, each of these connections will be synthesized, i.e., distribution components will be assigned to these connections. The weight, reliability, efficiency, and cost of these distribution components will be determined in the power distribution design step.

Original EPS design problem

At this point, the design problem must be revisited to understand the potential of design frameworks from the point of view of the design exercise. Thus, before continuing with the development of the proposed PBD-inspired EPS design framework, it is necessary to analyze the design problem to determine the advantages and disadvantages of the proposed framework. Let the main industry drivers, i.e., weight, reliability, efficiency, and cost, be represented as $\boldsymbol{w}$, $\boldsymbol{r}$, $\boldsymbol{\eta}$, $\boldsymbol{c}$ respectively. The purpose of the EPS design problem is to produce an electrical system (real system) that can be installed and operated inside an

aircraft vehicle. This problem is referred to as the original EPS design problem, and it is assumed that the design problem starts from scratch (no upgrades or iterations from known aircraft vehicles). In this design problem, the designer must select and size every single component and integrate them into an EPS that has a certain $\boldsymbol{w}, \boldsymbol{r}, \boldsymbol{\eta}, \boldsymbol{c}$. A control system manages all the operational functions in the EPS, e.g., power and energy management, fault recovery, communications, etc., and the designer must also account for its implementation. Currently, there are hundreds of aerospace companies with large portfolios of thousands of components (products) to choose from. Having all these devices available in a pool of components to choose from, corresponds to a large **implementation space**. Solving the original problem requires handling a large number of design variables, even assuming that such a design could be formulated (including selection, sizing, location, connection, etc.); this is the **application space,** i.e., perform a search to achieve a specific $\boldsymbol{w}, \boldsymbol{r}, \boldsymbol{\eta}, \boldsymbol{c}$. Considering selection only, there is a huge design space that could lead to an intractable problem, i.e., a problem that is difficult to formulate, hard to find a solution to in an acceptable time, and for which available algorithms are not efficient. This original EPS design problem can be depicted in **Figure 3.2**.

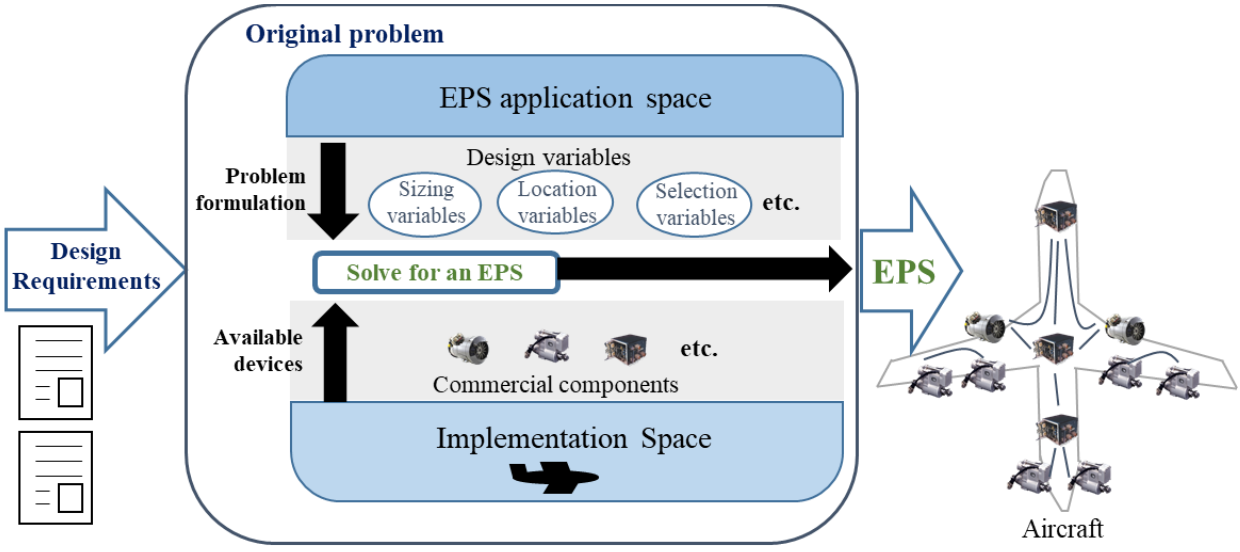

Figure 3.2 Original problem for the design of an EPS

Not only is there a huge implementation space in **Figure 3.2**, but there is also a large application space because there are several ways a design problem could be formulated. Such formulation is complex because there are real variables (powers flows, currents), integer variables (number of converters, generators), binary variables (components are active or inactive), etc.

EPS design and the proposed design framework

On the other side, the proposed PBD-inspired EPS design framework aims to reduce the problem complexity shown in **Figure 3.2** by limiting the design space exploration through the definition of platforms and abstractions that allow a formulation of subproblems. These subproblems are solved in a hierarchical manner, from the subproblem with the highest abstraction, to the subproblem with the lowest abstraction. For this reason, industry insights (observations and relationships between $\boldsymbol{w}$, $\boldsymbol{r}$, $\boldsymbol{\eta}$, $\boldsymbol{c}$) and abstractions must be as accurate as possible to avoid invalidation of results in intermediate refinement steps or incomplete platforms that could lead to suboptimal architectures. The proposed design framework is depicted in **Figure *3.3***.

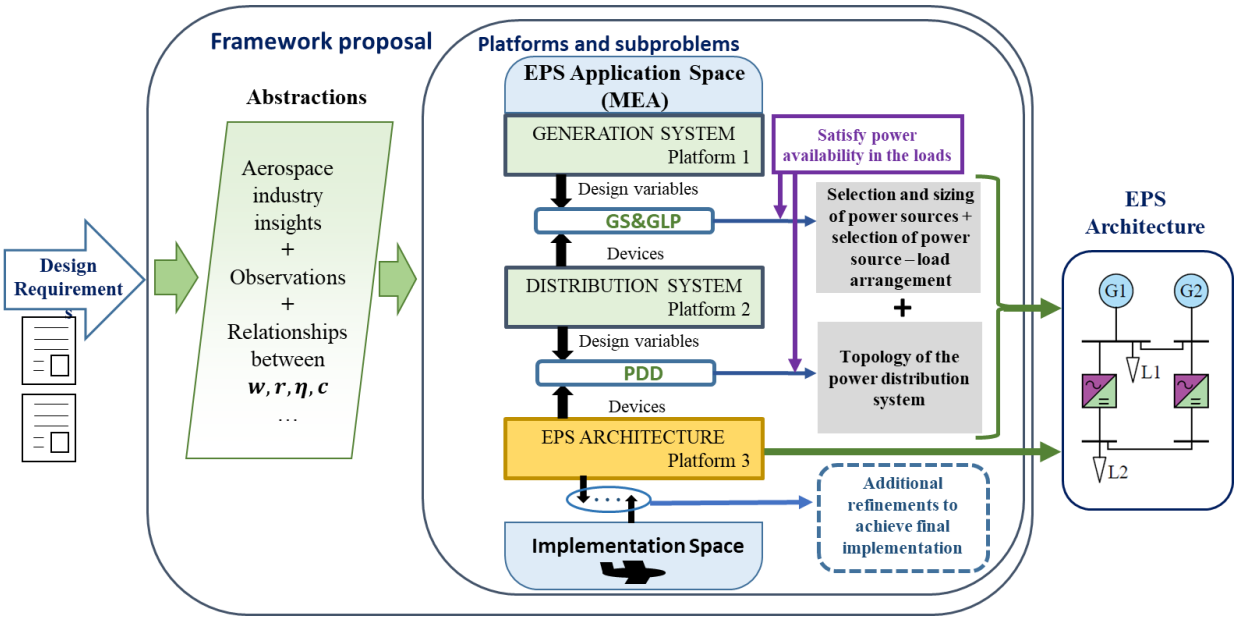

Figure 3.3 Design Framework Proposal (conceptual)

There is a subproblem between any two platforms, i.e., the GS&GLP is a subproblem between the generation system (platform 1) and the distribution system (platform 2), and the PDD is a subproblem between the distribution system (platform 2) and the EPS architecture (platform 3). This structure (subproblem between two platforms) is known as meet-in-the-middle, i.e., synthesis of a solution between two levels of different abstraction (the platforms converge to a solution). Notice that in **Figure *3.3***, the outcome at the right of the figure is called an EPS architecture, which is not the same as the real system shown in **Figure *3.2*** at the same location. Comparing **Figure *3.3*** and **Figure *3.2***, it can be seen that the design framework could reduce the design effort because instead of searching through all possible combinations in the original design problem, the abstractions help in delimiting the design space according to the corresponding platform. This does not mean that the design space is arbitrarily cut and reduced, on the contrary, it is narrowed based on the current abstraction.

By using the design framework in **Figure *3.3***, it is possible to obtain optimal results in limited time. However, the abstractions could fail to accurately represent the functional requirements and there could be some unexplored design space that would lead to a suboptimal solution. Accurate abstraction and design requirements are compulsory if this methodology is used. Generation and verification of accurate abstractions and requirements are out of the scope of this work. From now on, it is assumed that the design requirements are correct (not contradictory), and the abstractions proposed are sufficiently accurate to synthesize an EPS architecture. Similarly, the power source selection and source-load arrangement, and the power distribution design subproblems are going to be referred as GS&GLP and PDD, which stand for Generator Selection and Generator-Load Pairing and Power Distribution Design, respectively. The main type of power source in an aircraft is an electrical generator, for which reason the name GS&GLP more accurately describes the generation system design subproblem.

The GS&GLP platform contains a library of power sources that are considered potential candidates for comprising the generation system. In addition, the distribution system is represented by a virtual

component with many inputs and outputs terminals that connects generators and loads. The number and direction of such connections is determined in the GS&GLP as well. On the other hand, the PDD platform contains a library of power distribution components that are candidates for constructing the generator-load connections previously obtained. Among these components there are buses, switches, contactors, interruptors, breakers, distribution boxes, autotransformers, power converters, energy storage devices, etc. At the architectural level, these components are described in terms of functionality and logic integration with the rest of the system.

The mathematical description of the GS&GLP and PDD subproblems is going to consider reliability at the center of the design within an optimization formulation.

3.3.4. Optimization and Reliability in the Design Framework

In the MEA context, reliability can be defined as the ability of the aircraft to perform a complete flight mission. This ability is quantified by a measurable performance index (a reliability index), usually the probability of not failing to complete the mission. Similarly, the reliability of the EPS is the ability to deliver electrical power to the loads so that no unexpected events could compromise safety. Assuming that flight controls are electrically driven, failure in providing electrical power could lead to disaster. The reliability in EPS is quantified as the availability of power at the load's terminals. With availability being a value between 0 and 1 (0: never available, 1: always available), it can be used to drive the search through the design space using a formal mathematical method. Because the industry drivers are conflicting, it is necessary to obtain the best possible compromise between them, the reason for which optimization is imperative.

General optimization formulation

An optimization problem consists of the maximization or minimization of a real function by selecting the best available value (maximum or minimum) within an allowed set of available alternatives (the design

space). The function that drives the search is a mathematical expression in terms of the design and the system's variables (problem's variables) and the design space could either be constrained or not. This function is known as the objective, and the outcome of the optimization is the set of variables' values (solution) that achieved this value of the objective – i.e., that evaluate to the maximum or minimum in the objective's function. A constrained optimization includes other mathematical expressions that the solution must satisfy, i.e., the conditions in terms of the problem's variables that limit infeasible portions of the design space, whereas unconstrained optimization lacks these conditions. There are several constraints in the EPS design either because resources are limited, or a certain level of performance is expected as a minimum. Generally, an optimization problem (**O. P.** for the rest of the Thesis) is written as follows.

O.P. 1 $\min f(\mathbf{x})$ or $\max f(\mathbf{x})$ (1)

subject to $g_i(\mathbf{x}) = a_i \quad \forall\, i = 1, 2, \dots, n$ (2)

$h_j(\mathbf{x}) \leq b_j \quad \forall\, j = 1, 2, \dots, m$ (3)

Where (2) is the set of equality constraints, (3) is the set of inequality constraints, $f(\cdot)$ in (*1*) is the objective function, $g_i(\cdot)$ and $h_j(\cdot)$ are equality and inequality functions respectively, representing the technical and economical constraints the system must satisfy. The decision variables are represented by the vector $\mathbf{x}$; a_i and b_j are resources or performance limits (fixed upper or lower boundaries).

Types of optimization problems

Considering reliability as the fundamental performance characteristic in the EPS design, optimization can be formulated in several manners. The reliability-based optimization problems can be broadly classified into four main formulation types, as shown in **Table 3.1**.

Table 3.1 Types of Reliability-based formulations.

Type	Reliability-based formulations		
I	$\mathbf{max}\, r_S(\mathbf{x})$		
	subject to	$g_i(\mathbf{x}) = a_i$	$\forall\, i = 1, 2, \dots, n$
		$h_j(\mathbf{x}) \leq b_j$	$\forall\, j = 1, 2, \dots, m$
		$r_S(\mathbf{x}) \geq r_0$	
II	$\mathbf{min}\, c_S\,(\mathbf{x})$		
	subject to	$g_i(\mathbf{x}) = a_i$	$\forall\, i = 1, 2, \dots, n$
		$h_j(\mathbf{x}) \leq b_j$	$\forall\, j = 1, 2, \dots, m$
		$r_S(\mathbf{x}) \geq r_0$	
III	$\mathbf{max}\big(\alpha \cdot r_S(\mathbf{x}) + \beta \cdot c_S(\mathbf{x})\big)$		
	subject to	$g_i(\mathbf{x}) = a_i$	$\forall\, i = 1, 2, \dots, n$
		$h_j(\mathbf{x}) \leq b_j$	$\forall\, j = 1, 2, \dots, m$
		$r_S(\mathbf{x}) \geq r_0$	
IV	$[\mathbf{max}\, r_S(\mathbf{x}), \mathbf{min}\, c_S(\mathbf{x})]$		
	subject to	$g_i(\mathbf{x}) = a_i$	$\forall\, i = 1, 2, \dots, n$
		$h_j(\mathbf{x}) \leq b_j$	$\forall\, j = 1, 2, \dots, m$
		$r_S(\mathbf{x}) \geq r_0$	

r_S : system S reliability
r_0 : a minimum target (reliability performance) for R_S
c_S : resource or performance (weight, cost, efficiency)
α, β *:* equation's weighting coefficients

In all types, there is a minimum reliability constraint enforcing the system to achieve a minimum reliability target r_0. Type 1 formulates a single-objective reliability optimization problem where $r_S(\mathbf{x})$ represents the function that evaluates the system's reliability. Reliability is the only performance metric that drives the design, while other technical and economic resources (weight, cost, efficiency) are constrained. In Type 2, any resource or performance metric different from reliability is selected to drive the design, e.g., to minimize cost or maximize efficiency. A minimum reliability constraint allows a certain reliability level to be achieved, at least. Type 3 formulation is a linear combination of two or more performance indexes

where reliability is always included (linear refers only to the summation of functions). The weighting coefficients represent the order of magnitude of the different performance indexes so that a scale of importance between them is established. For instance, a reliability value in the range [0, 1] must be properly scaled in order to be compared to cost which is in the range of thousands or even hundreds of thousands. Finally, type 4 corresponds to a multi-objective optimization problem where two or more objectives are simultaneously optimized. One way to tackle multi-objective optimization is to formulate the problem as in type 3 where the objectives are combined linearly; the solutions may vary significantly depending on the selected values for the weighting coefficients. In general, the existence of more than one objective deserves a selection of the best compromise, i.e., a tradeoff among objectives, because these often conflict (e.g., an inversely proportional relationship). For example, high reliability could demand duplicated components in case of component failures, at the cost of increasing the economic cost and the system's weight, which are supposed to be minimized. If objectives are not weighted in advance, then there may be several sets of solutions for the multi-objective optimization in type 4, known as the Pareto-front sets [32], representing different trade-offs between objectives, and further analytical decisions must be conducted to select the best trade-off.

3.4. General Mathematical Formulations

The design of an EPS architecture has been divided in two subproblems, generator selection and generator-load pairing (GS&GLP) and power distribution design (PDD), as mentioned before. These subproblems are formulated as optimization problems where reliability can drive the design space search as it is one of the main industry drivers (along weight, efficiency, and cost). The formulation of a reliability-based optimization problem can be expressed in four main types of problems, from which the remaining industry drivers (weight, reliability, efficiency, and cost) can be used as objectives or as limiting conditions (constraints or scarce resources).

The EPS architecture consists of a group of interconnected power sources (generators) and distribution components that supply power to the loads through several paths to provide high reliability, where path is defined as a route that electrical power traverses from generator to load terminals through a series of buses, switches, contactors, transmission and distribution devices, and power converters. In fact, a resilient power distribution network should provide as many alternative paths as required to keep critical loads supplied. When the system is resistant to failure and catastrophic event, is it said that the system is resilient, so that resiliency is a desirable feature in the EPS. Synthesizing a resilient EPS from scratch requires defining a set of continuous (e.g., power flows, currents, etc.) and discrete decision variables (e.g., selection of components, connections, etc.).

Concerning the selection process, a Boolean decision variable for each component aims to reserve that component for the synthesized architecture. If 0, the component in the platform is excluded, while if it is 1, the component is included in the architecture. On the other hand, continuous decision variables are used in assigning a real value to a system's performance index, power rating, size, location, power flow, voltage, etc. In some cases, these parameters and states are functions of other decision variables. In its simplest form, the general formulation that achieves the architecture synthesis goal includes,

1. Optimization of design drivers: weight w, reliability r, efficiency η, and cost c. These drivers are included in the optimization's objective as minimization of cost and weight, and maximization of efficiency and reliability.
2. Static power balance (power flow equations). There is a condition of power balance in every component of the electrical network. The power balance includes connectivity constraints that allow the formation of paths from generators to loads. The power balance is a set of equations expressing the relationship between input and output power flows and could be extended to express relationships between voltages and currents. In its simplest form, assuming specific conditions in the network (e.g., voltage magnitudes are close to their rated values), the power

balance in the EPS equates the delivered generation power (from all power sources) to the load power (consumption) plus system losses.

3. Condition for a minimum system reliability (lower boundary). Similarly to the reliability constraint, which is included in the reliability-based optimizations of **Table *3.1***, EPS's reliability r must achieve at least a reliability target r_{TARGET}. It could be higher but must be at least r_{TARGET}.

This optimization formulation can be compactly written as,

O.P. 2 $\min c, w \ \& \ \max \eta, r$ (4)

subject to $P_{GENERATORS} = P_{LOADS} + P_{LOSSES}$ (5)

$r \geq r_{TARGET}$ (6)

The optimization goals in **O.P. 2** (4) are conflicting, and the system's reliability evaluation in **O.P. 2** (6) depends on the arrangement of components (series, parallel, combination of series and parallel, or more complex). When the system's reliability is too complex to be evaluated, (6) can also be replaced by resilience and survivability constraints. The problem in **O.P. 2** can be directly proposed to solve the original problem in **Figure 3.2**, however, it is advantageous to adopt the proposed framework and divide the problem into two subproblems. For each subproblem, the formulation in **O.P. 2** still applies, but it needs specific adaptations to build the GS&GLP and PDD subproblems.

3.4.1. Generator Selection and Generator-Load Pairing

The GS&GLP attempts to select a number of power sources, determine their ratings (size), and allocate a group of loads to each one, i.e., to produce a set of generator-load connections (as part of the virtual distribution system) such that the loads' demands are matched with generator power, and reliability constraints are satisfied. Recall that the design specifications include all of the load requirements, i.e., a preliminary load sizing assessment has been performed. The GS&GLP platform includes all sorts of candidates for power sources, mainly engine-driven electrical generators, but could also include energy

storage sources. The group of power source candidates (pool of components) and the set of feasible connections between power sources and loads is known as the GS&GLP template, i.e., the template includes all of the legal connections in the GS&GLP (some of them are kept, the rest are discarded according to the outcome of the GS&GLP problem). In the GS&GLP template, generators are not connected between themselves, but only to loads. An example of a GS&GLP template is depicted in **Figure *3.4***.

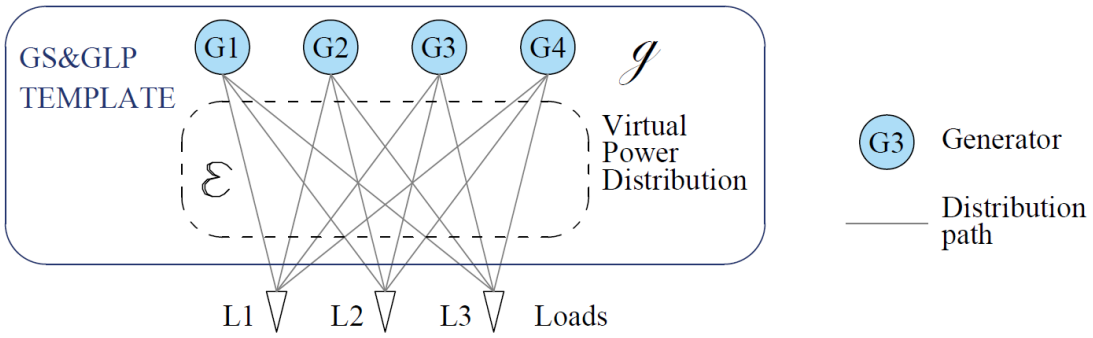

Figure 3.4 An example of a GS&GLP template for the design of a generation system for a 3-load EPS

It is assumed that three loads are to be supplied, thus, a set of loads $\mathcal{L}$ such that $\mathcal{L} = \{L_1, L_2, L_3\}$ is included in the design requirements. The GS&GLP template can be represented as a graph $\mathcal{G} = \{\mathcal{g}, \mathcal{E}\}$ where $\mathcal{g}$ is the set of generators (there are 4 generators available-for-choice here) while $\mathcal{E}$ is the set of generator-load connections (there are 12 connections available-for-choice between generators and loads here),

$$\mathcal{g} = \{G_1, G_2, G_3, G_4\}$$

$$\mathcal{E} = \{G_1 \text{ to } \{L_1, L_2, L_3\}, G_2 \text{ to } \{L_1, L_2, L_3\}, G_3 \text{ to } \{L_1, L_2, L_3\}, G_4 \text{ to } \{L_1, L_2, L_3\}\}$$

The generator-load connections in set $\mathcal{E}$ are the generator *assignments* to the loads of the generator-load pairing, that is, the determination of what loads are supplied from what generators. The connections in $\mathcal{E}$ are referred formally as *assigned pairs* for the rest of the document. All the assigned pairs are part of a virtual power distribution component representing the power distribution to be designed in the next refinement step (PDD subproblem). In the GS&GLP, the highest abstraction of the power distribution

network corresponds to a single virtual component that allows assignment between generators and loads, such that the assigned pairs represent a route of power (or energy) flow (not an actual cable or other device).

The connection of the same load with several generators here (through several assigned pairs) must not be confused with generator paralleling or other operation modes. The template example in **Figure *3.4*** is not a real generation system ready to be implemented in real aircraft, but a highest abstraction that allows the design of an EPS architecture. This proposition is also valid for the outcome of the GS&GLP.

Functional specifications for power sources (generators)

At the functional level, power sources are defined as electrical power generation devices with the following characteristics:

1. Power sources are rotating electrical machines (generators) driven by an engine.
2. For a specific speed design, the weight of a generator is roughly proportional to its power rating [16], [131].
3. The efficiency of a generator is a non-linear function in terms of its loading.
4. The generator's reliability is the probability that it does not fail to deliver power.
5. Generation is only defined by the amount of power supplied from the device's terminals.

Recall that dynamics, thermal issues, and other electromagnetic/mechanical phenomena is not considered at this level, i.e., not considered in this abstraction for the GS&GLP. The functional characteristics listed above can be depicted in **Figure 3.5** for a generator candidate in GS&GLP**.** There are two curves, one representing the linear relationship between power and weight (for a specific speed), and the other representing a quadratic (non-linear) relation between efficiency and loading. The generator's reliability can be represented by the probability of success in producing electrical power, i.e., a (numerical)

bounded magnitude between 0 and 1, where 0 is a completely unreliable device (no power can be drawn) and 1 is a non-fallible device (ideal case generator is perfect, ever fails).

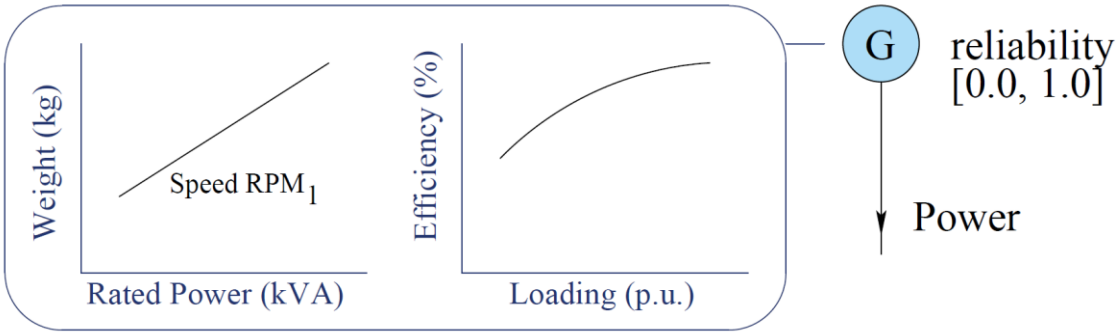

Figure 3.5 Functional abstraction for a generator candidate in the GS&GLP platform

Example of synthesis of a generation system

Assuming the following design specifications for the designed EPS,

- There is a set of loads $\mathcal{L} = \{L_1, L_2, L_3\}$
- L_1 to L_3 demands the same amount of power each one, i.e., they are identical.
- L_1 and L_3 must be supplied from two separate power sources in case of failure in one of them.
- L_2 is supplied by one power source only.
- A power source can only be sized to supply up to two loads simultaneously.
- One of the power sources supplying L_3 must be dedicated to it, i.e., only supply L_3.

By considering the above design specifications, the generators' functional abstraction (depicted in **Figure *3.5***), and the pre-defined template's example of **Figure *3.4***, the synthesis of a generation system in the GS&GLP provides an outcome determining which generators are selected from the ones available for choice (e.g., G1 and G2, or G2, G3, and G4, etc.), their power ratings, and the (virtual) connection arrangement between power sources and loads. An example of such outcome has the following format,

a. G_1, G_2, G_4 are selected with P_1, P_2, P_4 as their power ratings, respectively.

b. The ratings are $P_1 = P_2 = L_1 + L_2, P_4 = L_3$

c. The generator-load arrangement is G_1 to $\{L_1, L_2\}, G_2$ to $\{L_1, L_3\}, G_4$ to $\{L_3\}$

Having presented a feasible outcome example for the GS&GLP, the process of designing a generation system with the GS&GLP subproblem can be fully depicted in **Figure *3.6***.

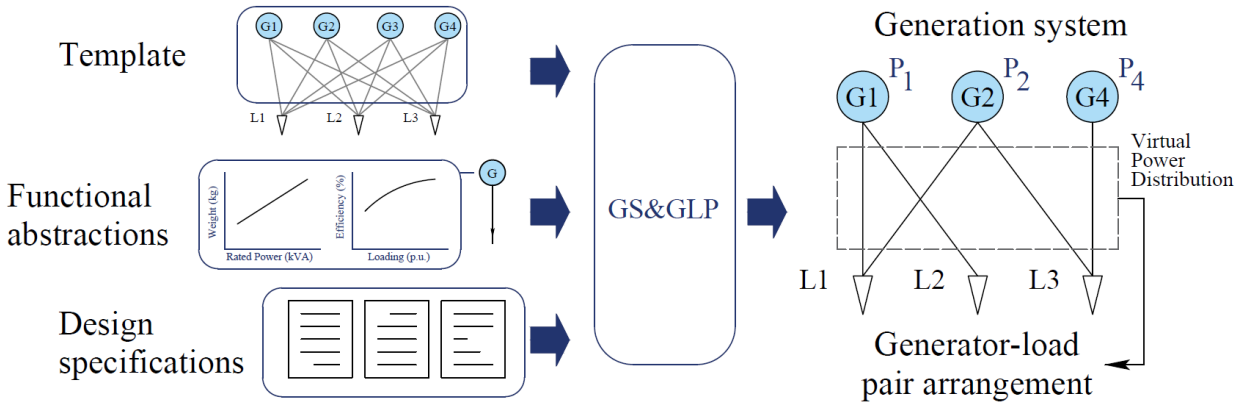

Figure 3.6 GS&GLP process; inputs at the left, optimization-based formulation in the middle, and outcome at the right

The GS&GLP inputs are shown at the left; there is a group of design specifications, a set of functional abstractions (of candidate generators and virtual power distribution), and a template determining all the legal (virtual) connections between generators and loads. These inputs are used to formulate an optimization-based problem (detailed in the next section) shown as a box in the middle of **Figure *3.6*,** whose outcome is shown at the right**.** This outcome includes the generation system and the generator-load pair arrangement. Recall that this arrangement represents routes of energy (power) from generator to loads, and not real electrical connections.

Any change in the template, functional abstractions (power sources, virtual distribution system), or design specifications, can lead to a different generation system. For instance, the functional abstraction for the generator can use relationships (between $\boldsymbol{w}$, $\boldsymbol{r}$, $\boldsymbol{\eta}$, $\boldsymbol{c}$) determined by performing a fitting exercise using characteristics from several commercial electrical machines such as permanent magnet synchronous machine, salient-pole synchronous generator, etc. If a different set of commercial machines are used, the

fitting exercise produces different relationships between $\boldsymbol{w}$, $\boldsymbol{r}$, $\boldsymbol{\eta}$, $\boldsymbol{c}$, then, the input of the GS&GLP changes and the GS&GLP outcome could consequently change. Besides, design specifications can be changed accordingly in order to match the functional characteristics. For example, by considering three-phase alternating AC generators, paralleling could or could not be allowed (functional abstraction), then, design specifications must require that, if a load is connected to more than two generators, only one assigned pair is active to avoid paralleling (if paralleling is not permitted); on the other hand, paralleling could be permitted, and AC synchronization must be used. This condition must be transferred to the power distribution design (PDD) so that the distribution topology prevents parallel operation of generators (or allow parallel operation) by a dedicated switching configuration scheme. There could be other conditions that are transferred to the PDD as well.

General formulation of GS&GLP subproblem

In general, the GS&GLP subproblem can be formulated as in **O.P. 2**, that is, the GS&GLP can be written as a multi-objective optimization problem. In multi-objective problems, there could be a set of optimal solutions (there are multiple objectives to optimize) from which a tradeoff allows to obtain the most convenient compromise for the specific design application.

Optimization objective of GS&GLP

Assuming that the cost of a generator (permanent magnet machine) is directly proportional to its weight [131], then, cost minimization is equivalent to weight minimization. Let the following variables apply to a generator s,

- w_s and η_s as the weight (kg) and efficiency, respectively
- g_s as the Boolean selection variable ($g_s = 1$ if s is selected, $g_s = 0$ if not)
- P_s^G is the continuous variable for sizing power rating (in kW).
- β_s is the loading factor, i.e., ratio between power supplied by generator and its rated power.

A load l has a demand L_l (kW) and the connection between generator s and load l is represented by a Boolean y_{sl}; y_{sl} is an assigned pair in the PDD subproblem. The total power supplied by generator s is,

$$\sum_{l \in \mathcal{L}} L_l y_{sl} \qquad \forall s \in \mathcal{g} \tag{7}$$

The loading factor β_s is,

$$\beta_s = \frac{\sum_{l \in \mathcal{L}} L_l y_{sl}}{P_s^G} \qquad \forall s \in \mathcal{g} \tag{8}$$

Recalling that w_s is approximately proportional to rating P_s^G for a given speed (RPM) [131], i.e., w_s is approximated to a linear function in terms of P_s^G, and that efficiency η_s can be expressed as a function of the machine's loading β_s, i.e., η_s is a function in terms of P_s^G and total supplied power (see **Figure 3.5**), then, the GS&GLP problem's (multi) objective can be written as

$$\min_{w,\eta,g,y} \left(\sum_s w_s g_s \right), \max_{w,\eta,g,y} (\eta_1 g_1), \max_{w,\eta,g,y} (\eta_2 g_2), \ldots \max_{w,\eta,g,y} (\eta_s g_s) \tag{9}$$

There is minimization of generation weight in the first term, i.e., minimize the summation of all generators' weights; the rest of the terms maximize efficiency on each generator. The product of w_s and η_s by g_s in (9) allows to set weight and efficiency of generator s to 0 when it is not selected, so that there is no contribution of an unselected generator to the generation system's weight or efficiency. The conditions or constraints of (9) are directly linked to the design specifications and functional abstractions. The design specifications and abstractions comprise a definition of architectural and functional characteristics of the EPS and the corresponding platform's components that are particular to the application. For instance, the design of an EPS for a 130-passenger narrow body twinjet more-electric-aircraft requires different specifications than the design for a 12-passenger business jet. Some requirements and definitions can be stated as below:

- Operating speed of electrical generator, i.e., the nominal RPM

- Type of electrical machine for generator, e.g., permanent magnet synchronous machine
- Conversion of generator output, e.g., for every generator there is an ATRU unit.
- Mechanical integration to the engine, e.g., CSD-generator into a IDG (constant speed)
- The allowable number of generators is 2 per engine (jet engine).

Having discussed and defined all the requirements, these can be translated into mathematical constraints. Therefore, a set of functional, connectivity, and reliability constraints would then be attached to (9). The reliability constraints ensure power availability at load terminals, while the functional and connectivity requirements allow power balance and other network constraints, e.g., load allocation to generators.

Reliability constraint

The generation system's reliability depends on the reliabilities of generators r_s, and the reliability of the (virtual) distribution (network) component r_{PD}. The former could be available from manufacturer's reports or datasheets, while the latter is unknown at this stage because it is a virtual power distribution. To overcome this uncertainty, the following options apply:

1. Use a new value, $\underline{r_{PD}}$ as a lower boundary for r_{PD} and include this in the formulation, i.e., a minimum reliability is assumed to be achievable in PDD
2. Consider r_{PD} as a continuous variable to solve for, i.e., the GS&GLP also finds r_{PD}
3. Include a set of continuous variables r_{sl} (one per y_{sl} assigned pair), which are included in the model. The set r_{sl} is part of the decision variables of the problem.

First option is a predefined minimum reliability value, while the other two options search for the assigned pairs' reliabilities that satisfies a reliability constraint. Let the load's reliability target be $r_{\text{TARGET},\, l}$ (for any load l), then, the reliability constraint that ensures that the combined reliability of the virtual power distribution and the generator can achieve the target is,

$$r_{PD} r_s \geq r_{\text{TARGET},\, l} \tag{10}$$

Where r_s is the generator's reliability. The reliability constraint in (10) expression is valid for all three options detailed above. $r_{\text{TARGET},\, l}$ is part of the design specifications.

The focus of the EPS design is to increase the power availability at the loads' terminals, reason for which the reliability of the load itself is not included in the left-hand side of (10). The product $r_{PD} r_s$ is the reliability of a series-system (reliability engineering term) assuming independent components' reliabilities, i.e., the probabilities of success or failure of a generator or virtual distribution component are unaffected by the failure of other components. When a load is connected to multiple generators through several assigned pairs, the constraint in (10) changes to,

$$1 - \prod_{s} (1 - r_{PD} r_s) \geq r_{\text{TARGET},\, l} \tag{11}$$

Which is the reliability of a parallel system, that is, the load is assigned to multiple generators. The figure below depicts the series-system and parallel-system in the context of GS&GLP.

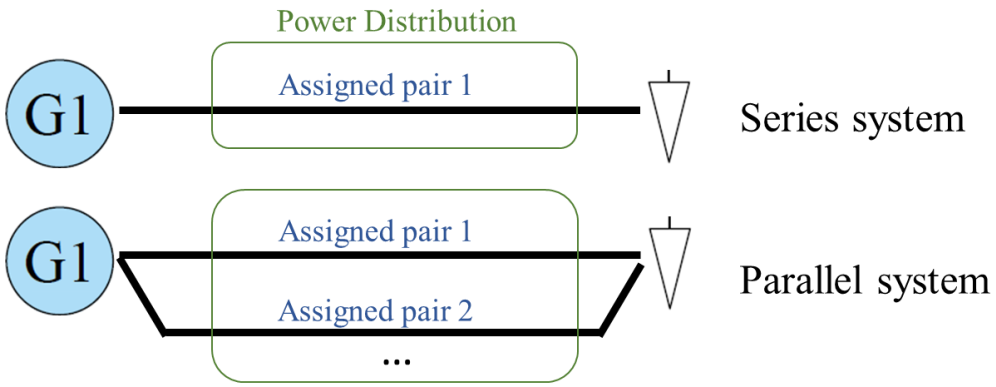

Figure 3.7 Series- and parallel-system in the context of GS&GLP

In a parallel-system, load l is supplied unless all generators (or their associated assigned pairs from the virtual power distribution) fail, in other words, there exists at least one generator that supply power through at least one assigned pair. A healthy distribution pair with no generator available provokes a

failure in the system (and vice versa). It can be inferred from (11) that the lower the generators' reliabilities are, the higher number of generators are required to satisfy any specific $r_{\text{TARGET},\,l}$, to ensure that power availability is still high even when the system has many poor-reliability components (a bulky system). Of course, one of the aims of an EPS design is to reduce weight and cost, and a bulky design is not an option.

GS&GLP general optimization

In summary, the GS&GLP subproblem can be stated as,

O.P. 3 Objective (9)

subject to Connectivity and power balance constraints

Reliability constraints (10), (11)

The optimal solution of **O.P. 3** comprises:

1. A group of selected generators $\mathcal{g}_s \subseteq \mathcal{g}$ with their corresponding ratings P_s^G
2. A group of y_{sl} assigned pairs (generator-load connections) forming a set $K = \{k_1, k_2, \dots\}$. Each pair k from the set K corresponds to a y_{sl} connection (for future notation clarity); $K \subseteq \mathcal{E}$
3. The reliability of the distribution system, either as $\underline{r_{PD}}$, r_{PD}, of a set of r_{sl} (one per y_{sl}).

This solution is then transferred, in addition to other architectural, functional requirements, and abstractions, to the power distribution design (PDD) subproblem for further refinement.

3.4.2. Power Distribution Design

Considering the synthesized optimal power generation system from the GS&GLP, the PDD attempts to find a topology for the distribution system. In PDD, the virtual power distribution of GS&GLP (with the generator-load pairs arrangement) is synthesized with power distribution components. The outcome of

the PDD (i.e., a group of power distribution components and a power distribution topology, combined with the generation system obtained in the GS&GLP) constitute the EPS architecture required.

Similar to GS&GLP, the PDD selects and sizes a group of distribution components from a pool of available components, i.e., the power distribution platform, in order to construct (refine) the assigned pairs determined in the GS&GLP. There is a PDD template (one of the inputs to the PDD subproblem) consisting of the pool of distribution components and all the legal connections permitted between them. These connections allow a route of energy (or power) between components and can be thought of as cabling devices although these connections are not real cables or conductors at this stage yet. In the case study of Chapter 6, abstractions for these connections are used to determine weight, reliability, efficiency, and cost characteristics, but the design of a cabling system as such is out of the scope of the EPS architecture design. Among examples of distribution components there are: distribution box (box or matrix of contactors internally connecting input and output terminals in a specific arrangement or configuration); power converters (X); buses (e.g., LV buses (D)); contactors; switches; interruptors; batteries (voltage stabilization); etc. An example of a template for PDD is shown in **Figure 3.8**.

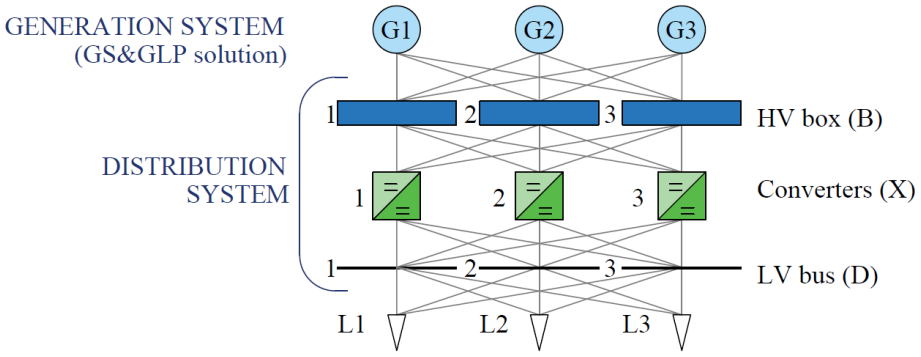

Figure 3.8 An example of a PDD template for the design of a distribution system for a 3-load EPS

In **Figure 3.8**, the generation system is shown but the generator-load pairs arrangement is not shown. The PDD template's example above can be represented by a graph $\mathcal{G} = \{\mathcal{N}, \mathcal{A}\}$ where $\mathcal{N}$ is the set of power distribution devices and $\mathcal{A}$ is the set of connections between them, so that,

$$\mathcal{N} = \{B_1, B_2, B_3, X_1, X_2, X_3, D_1, D_2, D_3\}$$

$$\mathcal{A} = \{B_1 \text{ to } \{G_1, G_2, G_3\}, B_1 \text{ to } \{X_1, X_2, X_3\}, X_1 \text{ to } \{B_1, B_2, B_3\}, X_1 \text{ to } \{D_1, D_2, D_3\}, \dots\}$$

An assigned pair from the generator-load pairs arrangement (obtained in the GS&GLP) is synthesized with a certain number of components from $\mathcal{N}$ and a certain number of connections from $\mathcal{A}$. Then, the power distribution topology is a subset of connected components (and connections) from the template in **Figure 3.8** (example) that enforces all the assigned pairs obtained in GS&GLP.

Functional specifications for distribution components

At the functional level, some distribution components can be defined with the following characteristics:

- Distribution boxes (HV box in **Figure 3.8)**
    - There are multiple input and output terminals to allow several incoming powers from generators and several outputs for power transmission to other boxes, buses, or converters.
    - The weight is directly proportional to the number of input and output terminals.
    - The reliability is the probability that it does not fail to route power between terminals.
    - An arrangement of switches (contactors) inside the box allows implementation of several circuit configurations to route power from specific input to a specific output.
- Power converters
    - The weight is directly proportional to the power transferred.
    - The efficiency is a non-linear function in terms of power transferred.
    - The converter's reliability is the probability that it does not fail to transfer power.
    - Conversion is only defined by the amount of power transferred.

- It contains an arrangement of power electronic switches to transform power from one voltage level to another. In a DC distribution system, one level is assumed to be high voltage, and the second is assumed to be low voltage.
- There is no permanent energy storage inside the power converter electronics.
- Converter should provide galvanic isolation.
- There are several input terminals that allow the converter to be supplied from more than one HV box. The converter can switch between any input.
- The outputs of multiple converters can be paralleled to supply a larger load if required.

- Buses
  - A bus is a single node that allow connections from multiple components.
  - The weight is directly proportional to the number of incoming/outgoing connections.
  - The reliability is the probability that it does not fail to serve as a node.
  - Only one voltage level is allowed at a bus.

Recall that dynamics, thermal issues, and other electromagnetic/mechanical phenomena are not considered at this level.

Example of synthesis of a power distribution system

Assuming the following design specifications (some of them have been transferred from the GS&GLP subproblem (*), and others are linked to the outcome of the GS&GLP optimal solution (**)):

- (*) There is a set of loads $\mathcal{L} = \{L_1, L_2, L_3\}$.
- (*) L_1 to L_3 are identical (i.e., consume the same amount of power).
- (**) There are 3 generators that supply EPS power (previous GS&GLP solution).
- (**) The generator-load arrangement is G_1 to $\{L_1, L_2\}$, G_2 to $\{L_1, L_3\}$, G_4 to $\{L_3\}$
- The distribution has two voltage levels: high voltage (HV), and low voltage (LV).

- There is a power conversion stage between high- and low-voltage.
- Loads are directly connected to LV buses. LV buses can supply more than one load.
- HV distribution boxes distribute generation power to converters or directly to HV loads.
- Loads $\mathcal{L} = \{L_1, L_2, L_3\}$ are LV loads.

By considering the above design specifications, the distribution components' functional requirements, and the template's example of **Figure 3.8**, the synthesis of a distribution system in PDD provides an outcome determining which distribution components are selected and how these components are to be connected (components and connections forming a topology). An example of such an outcome has the following format,

a. B_1, X_1, D_1 are selected. P_1^X as the power rating of converter X_1.
b. The rating X_1 is $P_1^X = L_1 + L_2 + L_3$
c. The components' arrangement is $\{G_1, G_2, G_3\}$ to B_1, B_1 to X_1, X_1 to D_1, D_1 to $\{L_1, L_2, L_3\}$

The intention of this example is just to illustrate the PDD problem in the simplest possible manner. Such power distribution topology is not meant to represent a real MEA EPS power distribution. Having presented a naïve example of a PDD outcome, the process of designing a power distribution with the PDD subproblem can be fully depicted in **Figure *3.9***. The PDD inputs are shown at the left and top; there is a group of design specifications, a set of functional abstractions (on power distribution components), a template determining all the legal (virtual) connections between distribution components, and the outcome of the GS&GLP. The inputs are used to formulate an optimization-based problem (detailed in the next section) shown as a box in the middle of **Figure *3.9***, whose outcome is shown at the right (very illustrative example). This outcome includes the power distribution components and the power distribution topology.

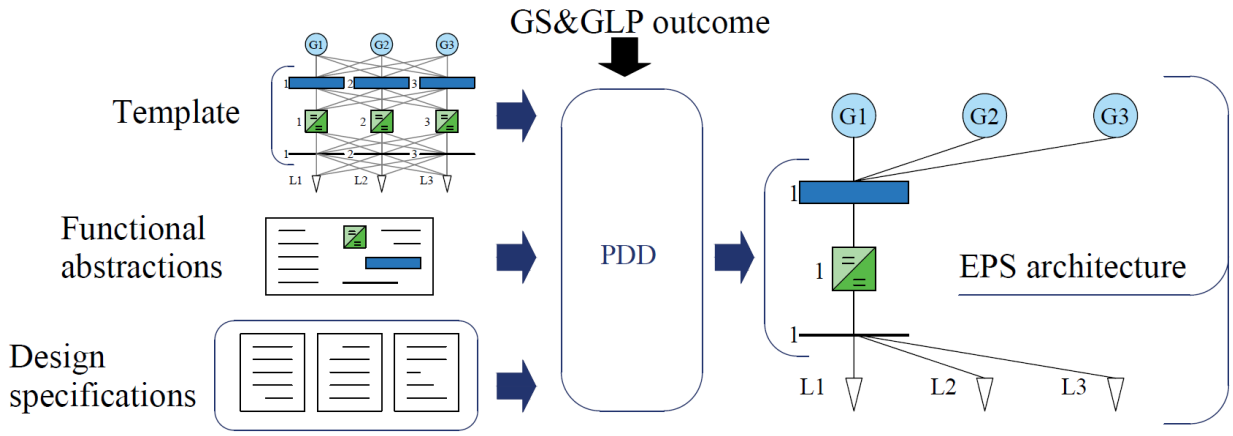

Figure 3.9 PDD process; inputs at the left, optimization-based formulation in the middle, and outcome at the right

It is important to consider how the assigned pairs (from the GS&GLP solution) are enforced in the example of **Figure *3.9*.** Let the **Figure *3.9*** help in identifying each one of the assigned pairs required from the GS&GLP outcome example of **Figure *3.6*.** There are 5 assigned pairs, G_1 to $\{L_1, L_2\}$ (2 pairs), G_2 to $\{L_1, L_3\}$ (2 pairs), and G_3 to $\{L_3\}$ (1 pair). These assigned pairs are highlighted in **Figure *3.10*.** There are 3 generators, G_1, G_2, G_4, that have been renamed to G_1, G_2, G_3 here to ease explanation. In the left, G_1 is connected to L_1 through B_1, X_1, D_1, so the assigned pair is synthesised with components B_1, X_1, D_1 and the corresponding (highlighted) connections.

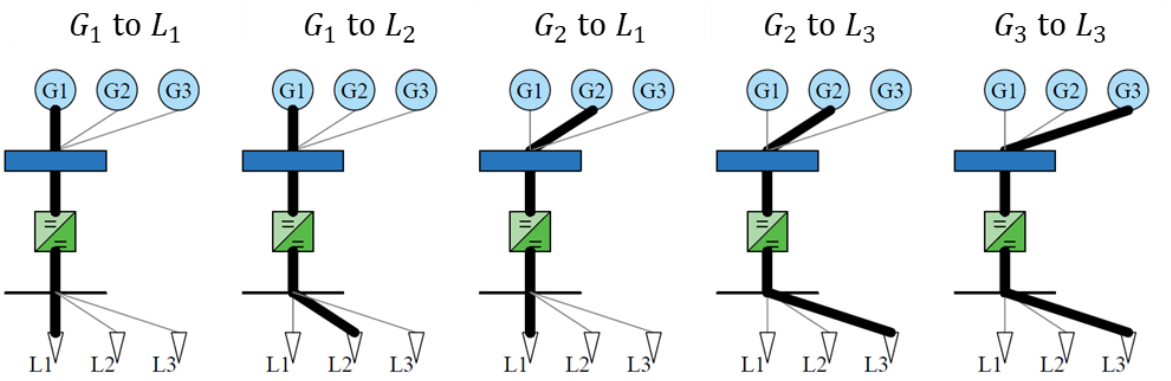

Figure 3.10 Assigned pairs corresponding to the PDD example

Similarly, the other 4 assigned pairs are highlighted in **Figure *3.10***, i.e., in this EPS one can find all the assigned pairs specified in the generator-load arrangement of the GS&GLP. The synthesis of each assigned pair with distribution components produces a *distribution path* or *distribution paths*.

Similar to the GS&GLP case, changes in the template, components' functional abstractions, or design specifications, can lead to a different distribution system. For instance, in the power distribution example above there could be an additional converter in case X1 fails to avoid disconnecting the loads, but there is no specification of what to do in case of failures. Of course, these specifications are a naïve example to illustrate PDD, but in real designs there are usually resilience requirements and more complex reliability specifications that can be included in the PDD design specifications.

Design specifications and requirements must be very specific in providing all functional requirements. If required, backup components would be available to avoid power interruptions in critical (or essential) loads. These conditions are common in network design and comprises a problem generally known as *resilient* design. For instance, conditions for resiliency could include a system's adequacy in case of failure of certain components, that is, there is enough additional components that replace the failed ones in case of contingencies. Besides, there could also be sufficient components and connections to form distributions paths in several ways (for the same generator-load pair). This is usually known as a *reconfigurable* system because different distribution paths can be established by interconnecting components in more than one arrangement (many possibilities). Hence, the EPS architecture must have generation/component adequacy, i.e., sufficient generation units and distribution devices to avoid prologued power interruptions. The system's power management, i.e., the establishment of a specific reconfiguration (interconnection arrangement), is part of the following refinement step or subproblem. This subproblem leads to performance optimization within the controller synthesis task.

General formulation of the PDD subproblem

In general, the PDD subproblem can be written as in **O.P. 2** (general optimization formulation). The balance condition in (5) must be applied to all components, i.e., incoming is equal to outgoing power. PDD is also a multi-objective optimization with multiple sets of solutions from which a tradeoff must be applied. Assuming that the cost of distribution components is directly proportional to their weight, then, cost minimization is equivalent to weight minimization as well. Cost is assumed to have two factors: a fixed cost, and a variable cost, e.g., installation is a fixed cost, while variable cost depends on the amount of power transferred. Also, it is possible that a component or connection serves more than one assigned pair, in other words, several assigned pairs utilize the same component or connection, so that the total power through it must account for the summation of powers from all assigned pairs it belongs to.

Optimization objective of PDD

Recall that assigned pairs are grouped in the set $K = \{k_1, k_2, \dots\}$, where $k \in K$. Let the following variables apply to components and connections between them,

- For a connection $i, j \in \mathcal{A}$
    - $x_{i,j}$ is the Boolean selection variable for connection i, j
    - Fixed cost is $c_{i,j}$ and c_{ij}^{kW} is the variable cost (real value). The *kW* super-index stands for the assumption that variable cost is proportional to the power flow (in *kW)* flowing through this connection.
    - The power flow through connection i, j is $P_{ij} = \sum_{k \in K} P_{ij,k}$, where $P_{ij,k}$ is the existing power from i to j for assigned pair *k*. In other words, many assigned pairs can exist between connection i, j (connection i, j can be part of many assigned pairs).
    - $r_{i,j}$ is the reliability, i.e., the probability that connection i, j connects i and j
    - $\eta_{i,j}$ is the efficiency, which is directly related to the losses

- For a distribution component $i \in \mathcal{N}$
    - v_i is the selection variable (Boolean) for i; $v_i = 1$ if component i is selected
    - m_i is the fixed cost and m_i^{kW} is the variable cost (continuous)
    - Power flow through i is $P_i = \sum_{k \in K} P_{i,k}$, where $P_{i,k}$ is the existing power through i for assigned pair k.
    - r_i is the reliability, i.e., the probability that component i works as expected.
    - $\eta_{i,}$ is the efficiency of component i.

The distribution system's fixed cost is the sum of all the connections and components' fixed costs, i.e.,

$$\sum_{(i,j) \in \mathcal{A}} \left(c_{ij} x_{ij}\right) + \sum_{i \in \mathcal{N}} (m_i v_i)$$

The variable cost is proportional to the amount of power transferred. For each connection and component, the variable cost is $c_{ij}^{\text{kW}}\left(\sum_{k \in K} P_{ij,k}\right)$ and $m_i^{\text{kW}}\left(\sum_{k \in K} P_{i,k}\right)$, respectively. Then, the total variable cost is,

$$\sum_{(i,j) \in \mathcal{A}} \left(c_{ij}^{\text{kW}} \left(\sum_{k \in K} P_{ij,k} \right) \right) + \sum_{i \in \mathcal{N}} \left(m_i^{\text{kW}} \left(\sum_{k \in K} P_{i,k} \right) \right)$$

Now, the objective of the PDD optimization subproblem can be written as,

$$\min_{P,x,v} \sum_{(i,j) \in \mathcal{A}} \left(c_{ij} x_{ij} + c_{ij}^{\text{kW}} \left(\sum_{k \in K} P_{ij,k} \right) \right) + \sum_{i \in \mathcal{N}} \left(m_i v_i + m_i^{\text{kW}} \left(\sum_{k \in K} P_{i,k} \right) \right), \quad (12)$$

$$\max_{P,x,v}(\eta_1 v_1) \, , \ldots \max_{P,x,v}(\eta_i v_i) \, , \ldots \max_{P,x,v}\left(\eta_{1,2} x_{1,2}\right) , \ldots \max_{P,x,v}\left(\eta_{i,j} x_{i,j}\right)$$

PDD's objective in (12) includes efficiency maximization as in (9), e.g., converters' efficiency can be expressed as a function of the converter's type, loading, switching technique, etc. Also, the efficiency of

the distribution system is related to the power losses in connections and buses. These power losses are proportional to the square of the current flowing through them (copper losses).

The costs in (12) have been divided into two main summation terms, i.e., connections' and components' total costs (including fixed and variable costs). $P_{i,k}$ is the summation of all power from incoming (or outgoing) connections related to pair k, i.e., $P_{i,k} = \sum_j P_{ji,k}$. Thus, all components' power flows can be expressed in terms of connection flows, i.e., $P_{ij,k}$.

Power flow relations in PDD components

To help in visualizing the relationships between $P_{i,k}$, P_i, $P_{ij,k}$, P_{ij}, **Figure *3.11*** illustrates power flows applied to a component i (converter).

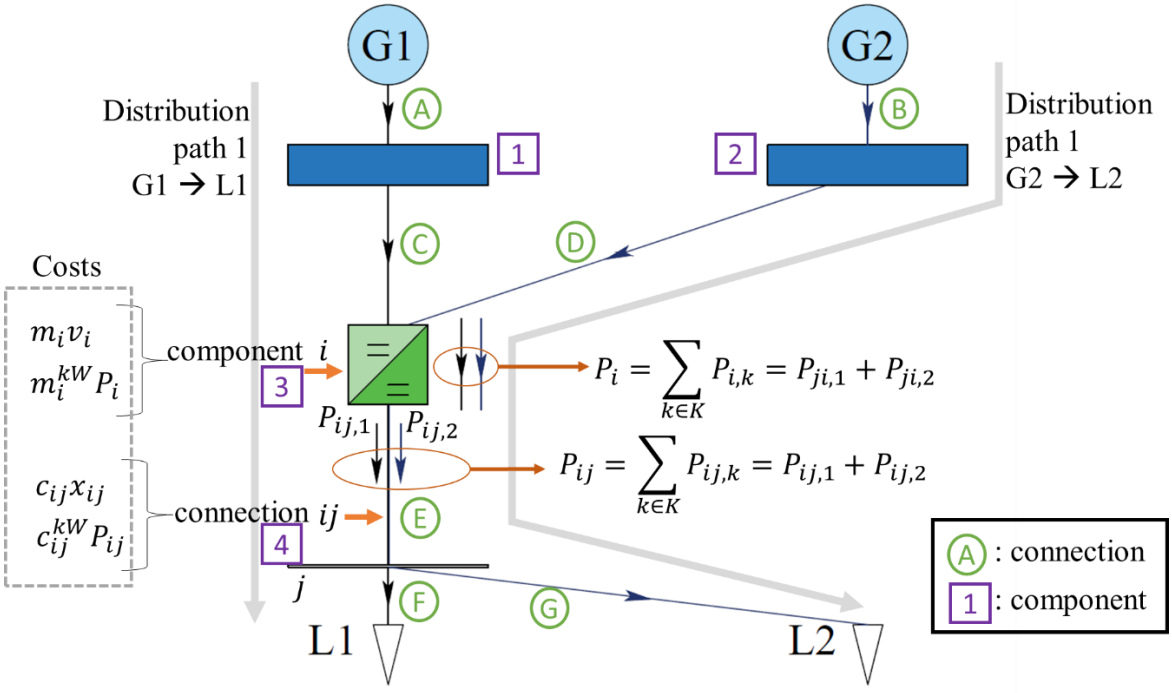

Figure 3.11 Example of EPS detailing power flow relationship for component i in PDD.

In the example of **Figure *3.11***, there are two assigned pairs, $k = 1$ that connects G1 to L1, and $k = 2$ that connects G2 and L2. Components 1, 3, and 4 and connections A, C, E, and F form the assigned pair 1, while components 2, 3, and 4 and connections B, D, E, and G form the assigned pair 2. For component 3

(converter), total power flow P_i ($i = 3$) is equal to the summation of all incoming flows from pairs 1 and 2 (coming from connections C and D). The total power flow P_{ij} for connection E ($i = 3, j = 4$) is equal to the power flow coming from the converter 3, i.e., the flows from C and D. Because component 3 and connection E have been selected, $v_3 = 1$ and $x_{3,4} = 1$. Then, costs are easily calculated using the cost coefficients c_{ij}, c_{ij}^{kW}, m_i, and m_i^{kW}. This analysis is repeated for the rest of components (1, 2, 4) and connections (A, B, C, D, F, G) to find the total system's cost.

In some cases, the connection's fixed cost c_{ij} could include the component's fixed cost $m_i v_i$, for instance in applications where components are modular. Then, the component's fixed cost $m_i v_i$ can be dropped from (12). Some examples of EPS modular components could be modular converters, bus-bar systems that are sized depending on the number of input terminals (each output is matched to its corresponding input), etc.

In the variable cost terms, c_{ij}^{kW} and m_i^{kW} represent a cost/power ratio. Also, it was assumed that cost is roughly proportional to weight, so that a numerical value for a cost/weight ratio can be defined. Hence, both ratios have the following relationship:

$$\frac{\text{cost}}{\text{power}} = \frac{\text{weight}}{\text{power}} \times \frac{\text{cost}}{\text{weight}}$$

It is observed that if a weight/power ratio is multiplied by the cost/weight ratio, we can obtain c_{ij}^{kW} and m_i^{kW}. The weight/power ratio is the inverse of the power density. In general, any component's weight is proportional to the power carried by this component. For example, a converter's power density is the relation between the amount of power that can be converted vs the power electronics' weight to achieve such conversion, then, m_i^{kW} for this converter is the product between the converter's power density and the cost/weight ratio. If cost is in dollars ($), power in kW, and weight in kg,

$$m_i^{\text{kW}}\left[\frac{\$}{\text{kW}}\right] = \frac{1}{\text{power density}\left[\frac{\text{kW}}{\text{kg}}\right]} \times \frac{\text{cost}}{\text{weight}}\left[\frac{\$}{\text{kg}}\right]$$

Similar relation can be established for c_{ij}^{kW} in the case of connections. Note that power density and cost/weight ratio can be determined by analysing data from manufacturers or published data from researchers in the case of new constructions and designs.

Reliability constraint

A group of constraints on connectivity, flow balance, and reliability can be added to (12). Assuming independent failure events, the k-th assigned pair's reliability is the reliability of a series system, and it must be at least equal to a target value (lower boundary). Recall that this value is considered in the GS&GLP (Section 3.4.1) as either $\underline{r_{PD}}$, r_{PD}, of a set of r_{sl} (one per y_{sl} or k). If $\underline{r_{PD}}$ is chosen, the target is a fixed lower boundary, otherwise, the reliability is an outcome of the GS&GLP, either as a system's reliability r_{PD} or a set of pair reliabilities r_{sl} (one per assigned pair). The former requires the evaluation of the network's reliability which can be a hard problem to solve, while the latter relaxes this condition and establishes a reliability target for each assigned pair separately. Assuming that there is a reliability target for each assigned pair, i.e., $r_{\text{TARGET},\,k}$, then, the reliability of each assigned pair can be expressed as the reliability of a series system. A series system is a formation where components are attached one after the other. The reliability of an assigned pair k synthesized as a series system is,

$$\left(\prod_{(i,j)\in k} r_{ij}\right)\left(\prod_{i\in k} r_i\right) \geq r_{\text{TARGET}}$$

Where r_{ij} and r_i stands for reliabilities of connections and components, respectively. In the PDD, components and connections are to be selected, then the reliability constraint of an assigned pair in a series system arrangement (single distribution path) must include selection variables, thus,

$$\left(\prod_{(i,j)\in k} x_{ij} r_{ij}\right)\left(\prod_{i\in k} v_i r_i\right) \geq r_{\text{TARGET},\, k} \tag{13}$$

Whenever a component or connection is not selected, $v_i = 0$ or $x_{ij} = 0$, and the left-hand side is 0 and the pair k can't be formed with that component or connection. Otherwise, $v_i = 1$ or $x_{ij} = 1$ and that component or connection is part of the assigned pair k.

Given a certain reliability target, it is possible that (13) cannot be satisfied, i.e., a series system has a lower reliability than the target. An example to illustrate this comes as follows. Consider that $r_{\text{TARGET},\, k} = 0.999$ for a pair k. Now, if the left hand side of (13) evaluates to 0.98 at most for any possible combination in the selection of components and connections, $0.98 \not> 0.999$ and the target can never be achieved. In this case, either the reliability of components and connections must be increased (maybe it is feasible to build such a component or connection), or there must be alternative paths to increase the reliability of the assigned pair. In other words, pair k (connection between a generator and a load) can be formed by several series systems connected in parallel; one series system is the main series system, and the others are the alternative series systems (multiple distribution systems). A series system and parallel-series system in the context of PDD is depicted in **Figure *3.12***.

In the series system of **Figure *3.12***, the distribution path is simply the system formed by components 1, 2, 3, …, and i. On the contrary, the distribution path in the series-parallel system can be formed in several ways, i.e., either 1, 2, 3, …, i or 4, 5, 6, …, j or both. For the series-parallel case, all the components shown in **Figure *3.12*** are part of the same assigned pair, but the series-parallel system allows alternative routes in case the initial path is interrupted due to failures.

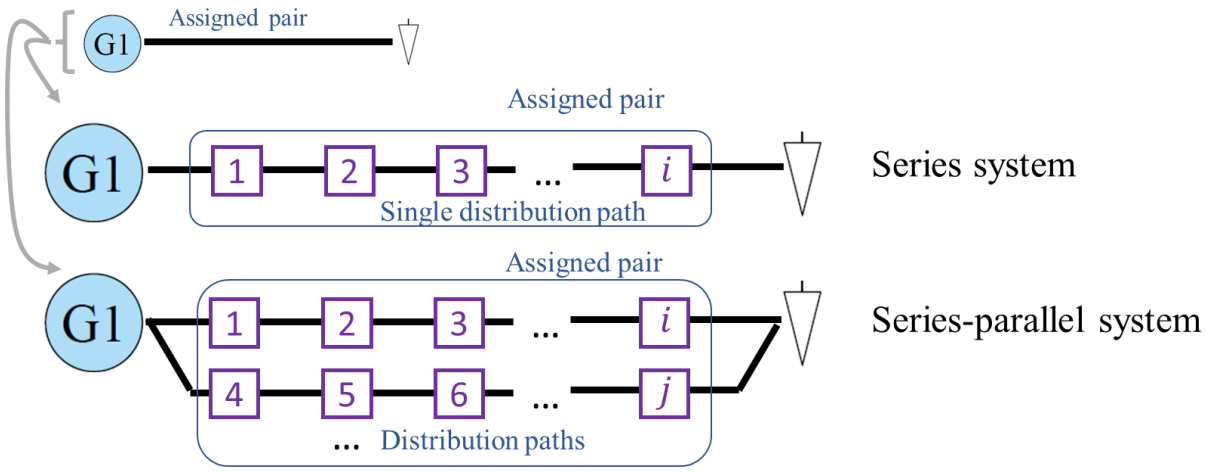

Figure 3.12 Series system and series-parallel system in the context of PDD.

The addition of alternative series-systems increases the system's reliability and incorporates resiliency into the EPS. Consider a number w of alternative and additional independent series systems that are arranged in a parallel-series arrangement (several series systems connected in parallel). The components and connections in this arrangement are part of the pair k (this pair represents an assignment of one generator to a specific load), then the reliability can be written as,

$$1-\prod_{w}\left(1-\left(\prod_{(i,j)\in k} r_{ij}\right)\left(\prod_{i\in k} r_i\right)\right)\geq r_{\text{TARGET}}$$

Similar to the series system case, components and connections are to be selected, so the reliability expression above must include selection variables:

$$1-\prod_{w}\left(1-\left(\prod_{j|(i,j)\in k} x_{ij}r_{ij}\right)\left(\prod_{i\in k} v_i r_i\right)\right)\geq r_{\text{TARGET},\,k} \qquad (14)$$

Whenever a component or connection is not selected, $v_i = 0$ or $x_{ij} = 0$, and the reliability of the corresponding alternative series-system is 0. Otherwise $v_i = 1$ or $x_{ij} = 1$ and those components and connections are part of the alternative series-system. In the GS&GLP, the pair k represents an assignment

of a generator to a load. In PDD, this pair can be implemented as a series-parallel arrangement of series-systems. In PDD, these series-systems are referred as distribution paths; the meaning of a path in PDD is the (series) connection of (some) selected components and connections that allow a power flow between a generator and load. There could be more components and connections that allow this flow, and these components and connections can be also part of the generator-load assignment of pair k (in the GS&GLP sense). Then, alternative paths for the pair k means a series-parallel arrangement.

If an assigned pair k is built as a series system, satisfaction of (13) could be achieved. If not, alternative paths could be required. If the system must be prepared in case of failures, alternative paths are required as well to overcome failure in the main path. Reliability constraint (14) forces the optimization to achieve a certain reliability in the assigned pair by increasing the number of components into a series-parallel system, i.e., build alternative paths. The higher the number of alternative paths, the higher reliability is obtained, at the cost of increasing the size and cost of the system. Once again, there is a compromise between reliability, cost, and weight in the PDD, which leads to a trade-off. The number of alternative paths can be determined by defining a set of failure scenarios or building disjoint paths (paths do not share any component). The intention of the latter is to increase the probability that at least one path delivers power if the other is interrupted due to a component's failure.

PDD general optimization

In summary, the PDD subproblem can be stated as,

O.P. 4 Objective (12)

subject to Connectivity and balance constraints

Reliability constraints (13), (14)

The optimal solution of **O.P. 4** comprises,

1. A group of selected connections $i, j \subseteq \mathcal{A}$ with their corresponding ratings P_{ij}

2. A group of selected components $i \subseteq \mathcal{N}$ with their corresponding ratings P_i
3. Fixed costs and variable costs for selected connections i, j and components i

After explaining in detail, the general mathematical formulation for GS&GLP and PDD, a summary collects the main ideas in this chapter.

3.5. Recap

In summary, this chapter dealt with the design framework proposal for the synthesis of an EPS architecture from scratch. The EPS architecture is not a real aircraft EPS, but a system representation at a functional and architectural level. The PBD principles have been explained and a design framework based on PBD has been proposed. This framework divides the original design problem, which has a huge design space, into several subproblems (GS&GLP and PDD) depending on functional abstractions, industry observations, and relationships between weight, reliability, efficiency, and cost (industry drivers). Accurate observations and relationships allow synthesis of meaningful EPS architectures. Some examples of abstractions and observations were provided for illustrative purposes only; Chapter 6 presents a case study in the design of EPS architecture for MEA. Mathematical formulations for each of the GS&GLP and PDD problems were also provided. These formulations are detailed in Chapter 4 along with linearization methods to solve optimization with MILP commercial solvers and approximate as much as possible to a global solution.

3.6. Conclusion

A Platform Based Design inspired framework is used to solve an EPS design problem in two steps or subproblems: GS&GLP and PDD. Both problems are established based on abstractions of the original design problem. The design of an EPS architecture involves determination of minimal weight and cost, and maximum efficiency and reliability, and these objectives are maintained in both subproblems.

Because there are multiple objectives, a tradeoff is required to select the best compromise between industry drivers. The process of designing an EPS architecture with GS&GLP and PDD problems is depicted in **Figure *3.13***. In this figure, all the inputs are shown at the left, while the optimization-based formulations are shown as boxes labelled GS&GLP and PDD. In the case of PDD, an additional input is the GS&GLP outcome, that is, the generation system and the generation-load pair arrangement.

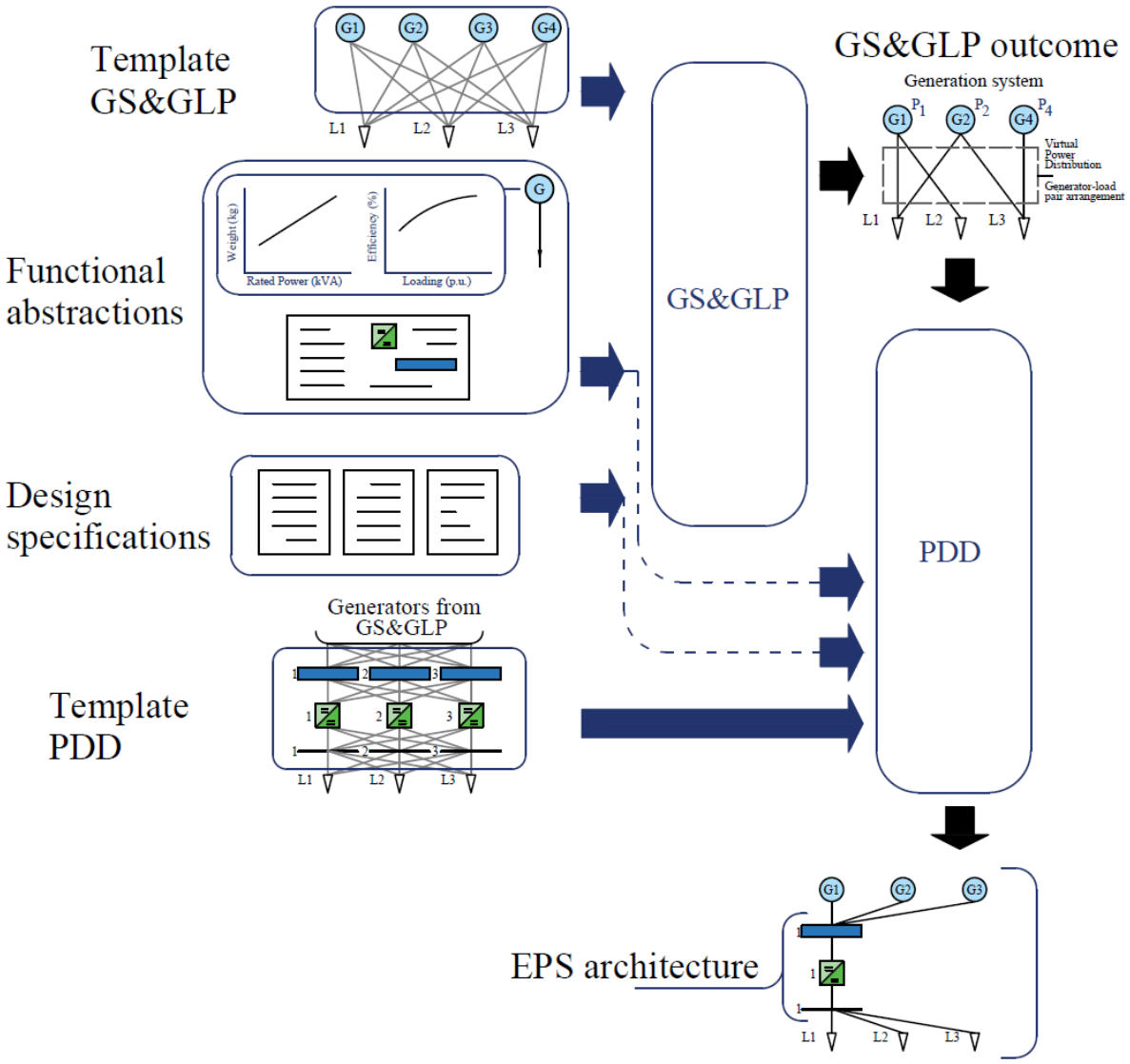

Figure 3.13 Generator Selection and Generator-Load Pairing and Power Distribution Design summary.

In GS&GLP, a group of power sources or generators are selected, sized, and assigned to the loads, that is, the generation system and how they are connected to the loads is synthesized. Then, this optimum solution is used to synthesize a distribution system's topology for the EPS in the PDD step. The power distribution is a group of connected power distribution components and implements the assigned pairs obtained in the GS&GLP.

4. A reliability-based optimization design

4.1. Introduction

The design of an EPS architecture follows the proposed PBD inspired methodology (Chapter 3) where the original design problem is divided into two sequential subproblems: generator selection and generator-load pairing (GS&GLP), and power distribution design (PDD). These subproblems are defined by optimization formulations that aim to find a trade-off between the main industry drivers, i.e., weight, reliability, efficiency, and cost. In principle, these formulations are complex and hard to solve due to the non-linearities intrinsic to the reliability constraints and the mathematical descriptions of functional requirements and specifications. Besides the utilization of heuristics and approximation algorithms to solve such kind of optimization problems, the aim is to find a global optimum and avoid promoting sub-optimal solutions that could compromise the accuracy of each subproblem's outcome. By transforming the optimization subproblems into mixed integer linear equivalents, Mixed Integer Linear Programming (MILP) techniques [120], [132] can be used to decrease the gap between the obtained optimum and the global optimum solution as much as possible. Therefore, linearization methods are applied in the GS&GLP and PDD design problems.

The linearization techniques detailed in Section 2.5 (Chapter 2) are used to transform the non-linear formulations of the GS&GLP and PDD subproblems into MILP formulations that can be solved efficiently with MILP solvers.

4.2. Linear transformations in the EPS design

4.2.1. Generator selection and generator-load pairing

Recall that the GS&GLP subproblem can be defined as in **O.P. 3**. (Section 3.4.1) Total generation weight is minimized while each generator's efficiency is maximized (multi-objective problem). There are power balance constraints to match generation power and load demand, and reliability constraints to ensure the system can achieve a certain level of reliability. The aim of the GS&GLP is to select and size the generation system, i.e., find the number of generators and their ratings, and determine the generator-load pairs (assigned pairs), i.e., which selected generators supply each load.

The GS&GLP optimization is non-linear because the generators' efficiencies are non-linear functions in terms of load supplied and power rating (design variable). Also, the reliability constraints are non-linear because the system's reliability evaluation includes mathematical expressions involving products between variables. The linearization techniques detailed in Section 2.5 are used to convert the GS&GLP into a MILP formulation.

Design variables

Let the design variables (decision variables) of the GS&GLP problem be:

- Boolean g_s: selects generator s. g_s is 1 if generator s is included in model, and 0 otherwise.
- Boolean y_{sl}: assigns generator s to load l (in the assigned pair k). $y_{sl} = 1$ if an assignment between s and l is included, i.e., load l is supplied by generator s.
- Real-valued variable P_s^G: nominal power (rated power) of generator s.

The weight and efficiency of the generators are characteristics that can be expressed in terms of the variables defined above. It has been previously assumed that weight has a roughly proportional relationship with power rating P_s^G, hence, weight can be expressed as a function of power rating P_s^G.

Efficiency of a generator can be written as a function of a generator's loading. Loading is a ratio between the total load connected (to that generator) and the power rating P_s^G. Load connected to a generator includes the variables y_{sl} (assignment of generator s to load l, or assigned pair k) and their corresponding load values L_l, so the loading can be expressed as a function of the variables y_{sl} and power rating P_s^G. Recalling the expressions for total load connected to a generator (7) and generator's loading (8) from Section 3.4.1, the following definitions apply:

- w_s (generator's weight) is a function in terms of P_s^G (rated power, nominal power).
- β_s (generator's loading) is in terms of the number of assigned pairs y_{sl} and rated power. A load l that is supplied (or not) by generator and s can be written as $L_l y_{sl}$. Then, the total load supplied by generator s is $\sum_{l\in\mathcal{L}} L_l y_{sl}$ (see (7)). The generator's loading (ratio between total load and power rating) is then $(\sum_{l\in\mathcal{L}} L_l y_{sl})/P_s^G$ (see (8)), where $\mathcal{L}$ is the set of loads, and L_l is the load demand (kW) of load l.
- η_s (generator's efficiency) is a function in terms of loading β_s. Because β_s is in terms of y_{sl} and P_s^G, efficiency can be consequently expressed in terms of y_{sl} and P_s^G.

The optimization objective of GS&GLP is the minimization of total weight and maximization of each generator's efficiency, see (9) in Section 3.4.1. One alternative in linearizing the objective in (9) consists of reformulating it as a linear combination of objectives (see type 3 formulation in **Table 3.1,** Section 3.3.4). In this case, each objective can have an importance determined by the coefficients a_1, a_2,…, a_n; these coefficients can be normalized, e.g., $\sum_i a_i = 1$. Weight minimization is equivalent to cost minimization because of the assumption that cost is directly proportional to weight (having decided on the generation system's nominal speed). On the other hand, efficiency maximization can become minimization by multiplying efficiency terms by -1. However, it is more convenient to express efficiency in terms of losses, i.e., a loss function in terms of the least number of decision variables, so that total

generation loss can be minimized. Then, both total generation system weight and total generation loss can be minimized.

Efficiency of generator

Recall that efficiency η_s can be expressed as a function of the machine's loading β_s, in other words, η_s can be a function in terms of rating P_s^G and total supplied power ($\sum_{l\in\mathcal{L}} L_l y_{sl}$). A formal expression for generator's efficiency needs to be developed. For an electrical generator, the efficiency is the ratio between electrical output and mechanical input,

$$\eta_s = \frac{\text{output}}{\text{input}} = \frac{\text{output}}{\text{output} + \text{losses}} \tag{15}$$

Where the mechanical input accounts for the generator's losses and the electrical output. The output is the total supplied power, or $\sum_{l\in\mathcal{L}} L_l y_{sl}$ (see (7)). Replacing it in (15):

$$\eta_s = \frac{\sum_{l\in\mathcal{L}} L_l y_{sl}}{\sum_{l\in\mathcal{L}} L_l y_{sl} + \text{losses}}$$

To solve for the efficiency, losses must be known according to the expression above. Losses could be also expressed in terms of the loading, but it also depends on other parameters. It is a common practice to obtain efficiency/losses data during manufacturing tests and use this data to build an approximate function for efficiency/loss [133]. In this occasion, it is considered that data have been used to obtain an approximate efficiency function η_s. An example of such an approximation can be the following quadratic polynomial (see the illustration example in **Figure 3.5** on Section 3.4.1 for GS&GLP),

$$\eta_s(\beta_s) = a_0 + a_1\beta_s + a_2{\beta_s}^2$$

β_s can be expressed in percentage (0-100%) or in normalized value (0-1). The approximation for efficiency can be introduced in the expression (15), and one can clear the variable 'losses'. Then, efficiency maximization in the GS&GLP can be converted to loss minimization. Rearranging (15),

$$\text{losses} = \text{output}\left(\frac{1-\eta_s(\beta_s)}{\eta_s(\beta_s)}\right) \tag{16}$$

The value for 'output' in (16) is again $\sum_{l\in\mathcal{L}} L_l y_{sl}$ and η_s is an approximation function $f(\cdot)$ in terms of loading (as in the quadratic polynomial above), or $\eta_s(\beta_s)$. Let the 'losses' in (16) have the formal notation η_s^{LOSS} (keeping letter η to associate this loss to the efficiency of the machine). Then the power loss in (16) can be written as,

$$\eta_s^{\text{LOSS}} = \left(\sum_{l\in\mathcal{L}} L_l y_{sl}\right)\left(\frac{1-\eta_s(\beta_s)}{\eta_s(\beta_s)}\right) \tag{17}$$

By multiplying and dividing (17) by P_s^G,

$$\eta_s^{\text{LOSS}} = P_s^G\left(\frac{\sum_{l\in\mathcal{L}} L_l y_{sl}}{P_s^G}\right)\left(\frac{1-\eta_s(\beta_s)}{\eta_s(\beta_s)}\right) = P_s^G\beta_s\left(\frac{1-\eta_s(\beta_s)}{\eta_s(\beta_s)}\right) \tag{18}$$

Finally, dividing (18) again by P_s^G, the power loss of a generator can be expressed as a percentage ratio with respect to its nominal power P_s^G (normalized value), then,

$$\eta_s^{\text{LOSS}}[\%] = 100\frac{1}{P_s^G}P_s^G\beta_s\left(\frac{1-\eta_s(\beta_s)}{\eta_s(\beta_s)}\right) = 100\beta_s\left(\frac{1-\eta_s(\beta_s)}{\eta_s(\beta_s)}\right) \tag{19}$$

Now, the power loss of a generator s can be uniquely expressed as a function of its loading β_s, having obtained an approximation function for efficiency $\eta_s(\beta_s)$.

Summing up the power loss of all generators allows for the minimization of total losses. Then, the GS&GLP optimization objective (9) can be written as the minimization of total generation's weight and power loss,

$$\min_{P,g,y}\sum_s \left(a_1(w_s g_s) + a_2\left(\eta_s^{\text{LOSS}} g_s\right)\right) \tag{20}$$

Where a_1 and a_2 are the importance coefficients for generation weight and generation losses, respectively; w_s and η_s^{LOSS} are multiplied by Boolean g_s to exclude unselected generators. Although (20)

is now a summation of weight and losses terms (linear objective), w_s and η_s^{LOSS} need to be linearized. Special ordered sets (SOS), PWL, and/or discretization can help in linearizing w_s and η_s^{LOSS}.

Linearized objective for GS&GLP

Having a finite group (set) of commercial generators available, w_s can be linearized using discretization. The advantage in this option is that there is a finite set of options to choose from. Consider a finite set of $\mathcal{H}$ commercial generators such that a generator selected for the EPS generation system can only take a nominal rating from the set $P_{\mathcal{H}}^G = \{P_1^G, P_2^G, \dots, P_h^G, \dots\}$; P_h^G is the power rating for generator h, e.g., 15kW. Any value of P_h^G has an associated weight value, w_h (also known from commercial datasheets). Then, g_s in the first term in (20) can be replaced with a Boolean $u_{s,h}$, and w_s can be replaced with the coefficient w_h, which is the weight corresponding to a rating P_h^G (from set $P_{\mathcal{H}}^G$). Hence, for each generator candidate (from the set $\mathcal{g}$), $w_h\, u_{s,h}$ selects a rating from $P_{\mathcal{H}}^G$ by setting $u_{s,h} = 1$ for an element h of the set $\mathcal{H}$; for the rest of elements, $u_{s,h} = 0$. This can be written as the following summation:

$$\sum_h w_h u_{s,h}$$

Only one term of the summation above is set to w_h given that $u_{s,h} = 1$ only once for a rating h, and consequently the corresponding value for P_h^G is selected. The set $\mathcal{H}$ can be an ordered set (SOS), by ordering the rating values from low to high, and it can be enforced that only one value can be selected.

Another alternative to discretization is PWL. In this case, w_s can be expressed as a linear function of P_s^G using a slope coefficient and an offset parameter (similar to the equation of a straight line), e.g., $w_h = d_1 P_s^G + w_0$, where d_1 (slope coefficient) is a weight-to-power ratio (inverse of power density), and w_0 is the offset parameter (weight).

Now, power losses η_s^{LOSS} for each generator $P_{\mathcal{H}}^G$ can also be linearized by discretization or PWL. η_s^{LOSS} is a non-linear function in terms of β_s, which is also a function of y_{sl} and P_s^G. Discretization can be used

when load demand is discretized into steps (load steps) and load is not able to take any value between steps, for example, a load bus that has a set of loads working at maximum power or zero power in an on/off operation.

The total load on a bus can take values equal to the summation of the maximum power of the loads connected to the bus. This summation for the total load can also be expressed as $\sum_{l\in\mathcal{L}} L_l y_{sl}$ in this case. Consider then a set of total load values $z_{\mathcal{B}}^{G} = \{z_1^G, z_2^G, \dots, z_b^G, \dots\}$ and an associated set of values $\eta_{h,b}^{\text{LOSS}}$ to represent the losses for a generator with rating P_h^G for a loading condition z_b^G. The values of $\eta_{h,b}^{\text{LOSS}}$ can be pre-calculated using (18) for the set of loading values $z_{\mathcal{B}}^{G}$ corresponding to a generator with rating P_h^G (of the set $P_{\mathcal{H}}^{G}$). Of course, the values $\eta_{h,b}^{\text{LOSS}}$ also then form a related set $\eta_{h,\mathcal{B}}^{\text{LOSS}} = \{\eta_{h,1}^{\text{LOSS}}, \eta_{h,2}^{\text{LOSS}}, \dots, \eta_{h,b}^{\text{LOSS}}, \dots\}$. Similarly, the sets of $\eta_{h,\mathcal{B}}^{\text{LOSS}}$ for the rest of the ratings P_h^G must be calculated. In this case, g_s in the second term in (20) can be replaced with a Boolean $z_{s,h,b}$. Variable $z_{s,h,b}$ is set to 1 ($z_{s,h,b} = 1$) only once, that is, when the generation candidate has a rating P_h^G (from the set $P_{\mathcal{H}}^{G}$) with a loading z_b^G (from the set $z_{\mathcal{B}}^{G}$) corresponding to a power loss of $\eta_{h,b}^{\text{LOSS}}$ (from the set $\eta_{h,\mathcal{B}}^{\text{LOSS}}$). For the rest of options $z_{s,h,b} = 0$. This can be written as the following summation:

$$\sum_{h}\sum_{b} \eta_{h,b}^{\text{LOSS}} z_{s,h,b}$$

Only one term of the summation above is set to $\eta_{h,b}^{\text{LOSS}}$ given that $z_{s,h,b} = 1$ only once for a rating h and loading b; also, the corresponding value for total load z_b^G is selected. There must be a relationship between $z_{s,h,b}$ and $u_{s,h}$ such that both variables point to the same rating P_h^G (from the set $P_{\mathcal{H}}^{G}$) for a generator s.

If discretization is not an option (e.g., power demand can take real values), PWL can be implemented by dividing the non-linear curve of η_s^{LOSS} in (18) or (19) (if efficiency is worked in %) into linear segments (as shown in **Figure *2.7***).

If discretization is used for both a generator's weight and the power losses (there is a set of commercial generators and load demand which can be discretized in load steps), the objective in (20) (weight minimization and power loss minimization) can be now rewritten to,

$$\min_{u,z,y} \sum_{s} \left(a_1 \left(\sum_{h} w_h u_{s,h} \right) + a_2 \left(\sum_{h} \sum_{b} \eta_{h,b}^{\text{LOSS}} z_{s,h,b} \right) \right) \tag{21}$$

The objective in (21) is now a MILP function where generation weight and power losses have been written as MILP functions (discretized in this case). This objective can be considered as the linearized version of the multi-objective non-linear minimization of generation weight and maximization of efficiency in (9).

General constraints for GS&GLP

Now the constraints for the optimization problem for the GS&GLP with objective (21) can be determined. In the constraint (22), each generator must have a unique rating (or power rating = 0 if generator is not chosen), then,

$$\sum_{h} u_{s,h} \leq 1 \qquad \forall s \tag{22}$$

Within a selected rating, a unique generation loss value must be assigned if a generator rating was selected, or none apply if there is no generator rating:

$$\sum_{h} \sum_{b} z_{s,h,b} \leq u_{s,h} \qquad \forall s, \forall h \tag{23}$$

This is the relationship between $z_{s,h,b}$ and $u_{s,h}$ required to select a generator with only one power rating and associate that power rating to a weight value and a power loss value.

Continuing, a load l can be assigned to generator s only if that generator is selected,

$$y_{sl} \leq \sum_{h} u_{s,h} \qquad \forall l, \forall s \tag{24}$$

Each load is assigned at least to one generator,

$$\sum_{s} y_{sl} \geq 1 \qquad \forall l \qquad (25)$$

The total load power cannot exceed the selected generator rating P_h^G for any generator,

$$\sum_{l} L_l y_{sl} \leq \sum_{h} P_h^G u_{s,h} \qquad \forall s \qquad (26)$$

Similarly, the total load power cannot exceed the generator's supply power $\hat{P}_{h,b}^G$,

$$\sum_{l} L_l y_{sl} \leq \sum_{h} \sum_{b} \hat{P}_{hb}^G z_{shb} \qquad \forall s \qquad (27)$$

Where $\hat{P}_{h,b}^G$ depends on the value of β_s, i.e., these values are the load steps that the generator can supply (a discretization of the generator's load). The conditions (22) to (25) are known as the connectivity constraints, while (26) and (27) represent the power balance constraints. Power balance has the form in (5) (**O.P. 2** in Section 3.4) (total generation power equals total load demand plus total losses), however it is an inequality since the generation system is being selected and sized (operation is out of the scope at this stage), and the load for unselected generators must be forced to 0. Now, the reliability constraints can be added.

Reliability constraints for GS&GLP

Reliability constraint in the GS&GLP can be written as the reliability of a series system (load assigned to a single generator in (10)) or the reliability of a parallel system (load assigned to various generators in (11)) as detailed in Section 3.4.1 and included in the general GS&GLP problem in **O.P. 3**. These reliability constraints can be linearized by using logarithms on the product terms. The logarithm of a product of terms results in a summation of the logarithms of each term, i.e.,

$$\log(x_1 x_2 x_3 \dots) = \log x_1 + \log x_2 + \log x_3 + \cdots$$

The case where a load can be assigned to more than one generator (11) (reliability of several generators connected to a load) is more realistic than (10) which is the reliability of a single load assigned to a single generator. Besides, (11) is the generalized case of (10). Hence, it is sufficient to linearize (11). Recall that the distribution paths' reliabilities can be determined either by $\underline{r_{PD}}$, r_{PD}, of a set of r_{sl} (one per assigned pair y_{sl}), then, applying logarithms on both sides of (11),

$$\sum_{s} y_{sl} \ln\left(1 - \underline{r_{PD}} r_s\right) \leq \ln\left(1 - r_{\text{TARGET},\, l}\right) \qquad \forall l \qquad (28)$$

Where $r_{\text{TARGET},\, l}$ is the reliability target for load l and $\underline{r_{PD}}$ is a lower boundary for the distribution system reliability. In the left-hand side, $\ln\left(1 - \underline{r_{PD}} r_s\right)$ is a constant coefficient because both $\underline{r_{PD}}$ and r_s are known coefficients. Therefore, (28) can be directly introduced as a reliability constraint in GS&GLP.

On the other hand, if r_{PD} is considered, a new variable r_{PD} falls inside the logarithmic term in (28). Similarly, when a set of r_{sl} values are included, the logarithms have variables inside. Similar to what has been done with w_s and η_s^{LOSS}, it is possible to linearize the left-hand side of (28) with discretization or PWL. If discretization were chosen, the left-hand side of (28) would be expressed as a summation of elements from a finite set of possible reliability values $r_{s,o}^E$, i.e., $r_{s,O}^E = \left\{r_{s,1}^E, r_{s,2}^E, \dots, r_{s,o}^E, \dots\right\}$ and this set O contains all the values (elements o from the set O) that the term $\ln\left(1 - \underline{r_{PD}} r_s\right)$ can take. Because r_s (a generator's reliability) is known, the subscript o accounts for the discretized values of r_{PD} (or r_{sl}), which at the same time allows the existence of the set $r_{s,O}^E$. A Boolean variable $r_{s,l,o}^S$ can replace y_{sl} and the reliability expression $\ln\left(1 - \underline{r_{PD}} r_s\right)$ can be replaced with a reliability value $r_{s,o}^E$. Of course, $r_{s,l,o}^S = 1$ only for one reliability value, while for the rest of reliability values of the set $r_{s,O}^E$, $r_{s,l,o}^S = 0$. Then, the reliability constraint in (28) can be linearized as,

$$\sum_{s} \sum_{o} r_{s,o}^E r_{s,l,o}^S \leq \ln\left(1 - r_{\text{TARGET},\, l}\right) \qquad \forall l \qquad (29)$$

The Boolean variable $r_{s,l,o}^{S}$ picks only one reliability value $r_{s,o}^{E}$ from the set $r_{s,O}^{E}$ for a selected assigned pair that assigns generator s to load l. This condition can be written as,

$$\sum_{o} r_{s,l,o}^{S} \leq y_{sl} \qquad \forall s, \forall l \qquad (30)$$

A PWL method can also be used for linearizing (28). In this case, the (non-linear) curve contained in the left-hand side of (28) is approximated with piecewise linear segments as in **Figure *2.7***.

GS&GLP Linear Formulation

In summary, the linear formulation for GS&GLP can be written as:

O.P. 5 Objective (21) (minimization of generation weight and losses)

Connectivity constraints (22) to (25)

subject to Power balance constraints (26) and (27)

Reliability constraints, (28) or (29) to (30)

The reliability constraints (29)-(30) provide resiliency in case the main generator supplying the load fails. However, the outcome of GS&GLP depends on the load needs as there can be both non-critical (sheddable) and critical (non-sheddable) loads.

The optimization problem in **O.P. 5** can now be used to synthesize a generation system and obtain a generator-load pair arrangement. Constraints (22)-(30) can be considered as a *basic* set of constraints. Naturally, there could be other design requirements that can be translated to mathematical constraints, and these could be added accordingly to **O.P. 5**.

Clearly, the optimization problem **O.P. 5** works for a set of commercial generators, load steps, and maximum power ratings for both generators and loads. More than one generator can be assigned to the same load, as expressed by (25), and the reliability constraint has been discretized. However, there is no information on *how* the power from generation system is going to be assigned to the loads (power

allocation) for a given load demand profile. Moreover, there is no explicit power balance for a given loading condition (for a certain period or time instant). The only condition is that the total available power rating matches total (maximum) load power; total rating is high enough to supply maximum load although generators will not always supply that much. This (maximum) condition is sufficient for design purposes. The GS&GLP can also be solved for a specific load assignment (power allocation), considering many factors such as that generators can be temporarily overloaded, some loads are pulsating, etc. In fact, a real EPS does not always work at maximum load. This could require the introduction of time as an independent variable in the GS&GLP. Depending on the design specifications, the GS&GLP can provide a power allocation scheme on top of the generation system selection; the generator-load pair arrangement is then a profile that provides information on the activation and deactivation of assigned pairs.

To finalize this discussion, linearization methods with PWL could be used if commercial sets of generators to choose from are not available, or if the designer has the capacity to build a generator tailored for a specific application.

After expanding on the linearization of the GS&GLP subproblem, the PDD is treated.

4.2.2. Power Distribution Design

Recall that the PDD subproblem can be defined as in **O.P. 4** in Section 3.4.2. The aim of the PDD is to synthesize a power distribution system; this system was represented as a virtual power distribution component in the previous step of GS&GLP. This power distribution system is formed by selecting and sizing a group of distribution components that connects generators and loads in the arrangement set by the generator-load pairs (assigned pairs) from the GS&GLP, i.e., the assigned pairs of the GS&GLP are synthesized into distribution paths in the PDD.

The objective of the PDD is the minimization of total fixed and variable costs and the maximization of efficiency on every power distribution component (multi-objective optimization). Also, there are power

balance constraints and the power distribution's reliability is maintained at least above a certain reliability target. The power distribution reliability constraint is expressed as a system's reliability or as the reliability of each distribution path. In the latter case, the distribution path is a series-parallel system, i.e., there could be alternative (parallel) paths in case the main path fails as detailed in Section 3.4.2 and **Figure *3.12***.

The total cost (fixed and variable) minimization objective in (12) is already linear, assuming again that the costs of components and connections are roughly proportional to their weights. However, the maximization of efficiency of every component makes the objective still non-linear. Efficiency and losses are multi-parameter non-linear functions (as observed in the GS&GLP case), and in PDD there are several types of distribution components for which efficiency depends on the voltages and currents held at their terminals (loading condition for electrical generators in GS&GLP does not require knowledge of voltage and current). One way to handle such complexity in the design of PDD is to assume a lossless system, that is, losses can be assumed negligible. Given current advances in power conversion [134], it can be said that distribution components have very high efficiencies and losses are almost negligible. Then, total cost minimization objective in (12) can be considered as the optimization objective of PDD.

Design variables

Recall the variables for selection and sizing of PDD components (HV box, buses, converters, etc.) and connections defined in Chapter 3, then,

- Boolean x_{ij}: selects connection between components i and j. It takes a value of 1 when connection from i to j is selected, and 0 otherwise.
- Boolean v_i: selects component i. It takes a value of 1 when component i is selected, 0 otherwise.
- Real variable $P_{ij,k}$: power flow through connection i, j for assigned pair k.
- Real variable $P_{i,k}$: power flow through component i for assigned pair k.

The total power (for all assigned pairs) flowing through component, i.e., P_i, and connection, i.e., $P_{ij,}$ can be expressed in terms of power variables $P_{ij,k}$ and $P_{i,k}$. Considering the previous variables, the fixed and variable cost of component and connection were expressed in Chapter 3 as follows,

- $c_{ij}x_{ij}$ is the fixed cost for connection ij.
- $m_i v_i$ is the fixed cost for component i.
- $c_{ij}^{\text{kW}}\left(\sum_{k\in K} P_{ij,k}\right)$ is the variable cost for connection ij
- $m_i^{\text{kW}}\left(\sum_{k\in K} P_{i,k}\right)$ is the variables cost for component i, where $P_{i,k} = \sum_{\not{j}} P_{\not{j}i,k}$.

c_{ij}, m_i, c_{ij}^{kW}, m_i^{kW} are cost coefficients included in the design specifications.

Linearized objective for PDD

The optimization objective of PDD, i.e., minimization of total fixed cost and total variable cost, is repeated here for the sake of clarity (see Section 3.4.2),

$$\min_{P,x,v} \sum_{(i,j)\in\mathcal{A}} \left(c_{ij}x_{ij} + c_{ij}^{\text{kW}}\left(\sum_{k\in K} P_{ij,k}\right)\right) + \sum_{i\in\mathcal{N}} \left(m_i v_i + m_i^{\text{kW}}\left(\sum_{k\in K} P_{i,k}\right)\right)$$

Now, the design variables (decision variables) recalled above can be used to define the PDD constraints. There are connectivity and power balance constraints, and reliability constraints.

General constraints for PDD

The power balance is enforced on every component $i \in \mathcal{N}$ by summing all incoming and outgoing power flows, components' losses, generation power, and load demand. Incoming flows (entering the component) and generation power (for generator components) are considered positive $(+)$, while outgoing flows (leaving the component) and power consumption (for loads) are considered negative $(-)$. In other words,

- Total incoming flow is $\sum_{i|(j,i)\in\mathcal{A}} P_{ji,k}$, that is, summation of flows from all components j to i
- Total outgoing flow is $\sum_{i|(i,j)\in\mathcal{A}} P_{ij,k}$, that is, summation of flows from i to all components j.

Note that the components j from which power flows into each component i in the incoming flow are not the same as the components j to which power flows from each component i in the outgoing flows; j is just an index to represent every other component (that i is connected to) in the system. Given the solution of the GS&GLP, each assigned pair k must satisfy a load demand d_k^{LOAD} by supplying a generation power d_k^{GEN}. In other words, each assigned pair k delivers d_k^{GEN} from a power source (generator), this power flows through distribution components (to be synthesized in the PDD), and this power is withdrawn by a load demanding a power d_k^{LOAD}. For the generator-load pair k, it is assumed that,

- $d_k^{LOAD} = 0$ at the generator, i.e., there is no load directly connected to generator.
- $d_k^{GEN} = 0$ at the load, i.e., no generator is directly connected to a load.
- Both $d_k^{LOAD} = 0,\ d_k^{GEN} = 0$ for the rest of the components forming the path, e.g., buses, HV box, converters, etc.

Some observations to the previous assumptions:

- It is assumed that a load is connected to a generator through, at least, one distribution component, but not directly, e.g., a bus or any other distribution component.
- Some buses, that are not necessarily load (or generation) buses, can have loads (or power sources, e.g., batteries) connected to them, i.e., they are also connected to other components such as converters, HV box, other buses, etc. For these buses, $d_k^{LOAD} \neq 0$ and/or $d_k^{GEN} \neq 0$.

Since $P_{ji,k}$ represents an incoming power from component j to i, and $P_{ij,k}$ is an outgoing power from i to other j, the power balance constraint for any component i in the power distribution is then,

$$\sum_{i|(j,i)\in\mathcal{A}} P_{ji,k} - \sum_{i|(i,j)\in\mathcal{A}} P_{ij,k} + d_k^{LOAD} - d_k^{GEN} = 0 \qquad \forall i \in \mathcal{N}, \forall k \in K \qquad (31)$$

Rearranging terms, the power balance in (31) can also be written as,

$$\sum_{i|(j,i)\in\mathcal{A}} P_{ji,k} - \sum_{i|(i,j)\in\mathcal{A}} P_{ij,k} = d_k^{GEN} - d_k^{LOAD}$$

To illustrate the power balance in (31), **Figure *4.1*** shows the power balance for component i (a bus). Power on distribution path 1 flows through components 1, i, 3, and 4 and connections A, C, and D, while power on distribution path 2 flows through components 2, i, 3, and 5 and connections B, C, and E. Component i is a bus connected to the rest of the system through connections A, B, and C. Assuming the power flow directions as shown in **Figure *4.1***, there are two incoming power flows from connections A and B. The single outgoing connection C holds the outgoing flows from both distribution paths.

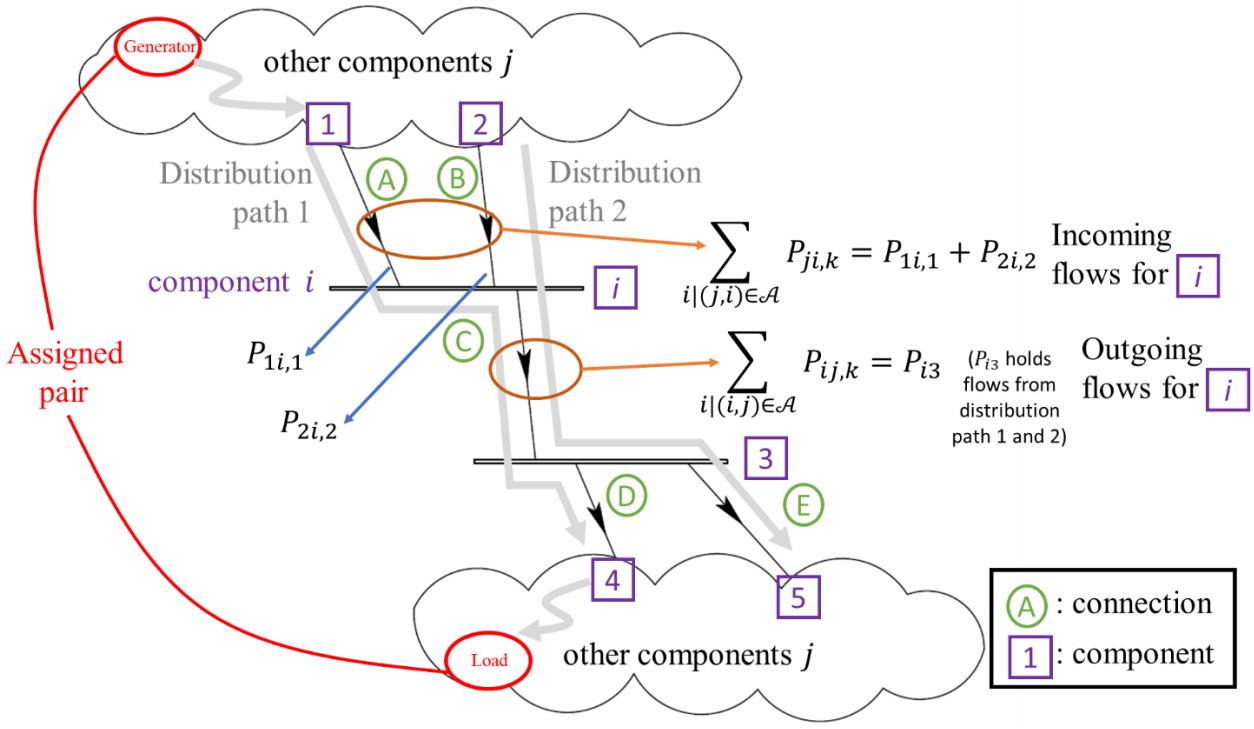

Figure 4.1 Example of power flow balance for a component i.

There are no loads or generators attached to component i, therefore, the power balance for bus i is:

$$\sum_{i|(j,i)\in\mathcal{A}} P_{ji,k} - \sum_{i|(i,j)\in\mathcal{A}} P_{ij,k} = \left(P_{1i,1} + P_{2i,2}\right) + P_{i3} = \left(P_{1i,1} + P_{2i,2}\right) + \left(P_{i3,1} + P_{i3,2}\right) = 0$$

For any components i, j the power flow $P_{ij,k}$ flows in the $i \to j$ direction. However, it is possible to have flow in opposite direction by defining two variables for the same connection between i, j (such that only one can be positive at once) allowing power flow to be reversed, e.g., recovering energy in regeneration modes. The connection from i to j can only be selected (x_{ij} is 1) if components i and j have both been selected (i.e., v_i is 1 and v_j is 1), so,

$$\begin{aligned} x_{ij} &\leq v_i && \forall (i,j) \in \mathcal{A}\ , \forall i \in \mathcal{N} \\ x_{ij} &\leq v_j && \forall (i,j) \in \mathcal{A}\ , \forall j \in \mathcal{N} \end{aligned} \tag{32}$$

Constraint (33) ensures that power $P_{ij,k}$ through any connection i, j and power through any component i can only flow if connection x_{ij} and component v_i have been selected. For the rest of the document, the required flow along the distribution path(s) of the assigned pair k is d_k such that $d_k = \left|d_k^{LOAD}\right|$, for notation simplicity.

$$\begin{aligned} P_{ij,k} &\leq d_k x_{ij} && \forall (i,j) \in \mathcal{A}\ , \forall k \in K \\ \sum_{j\in\mathcal{N}} P_{ji,k} &\leq d_k v_i && \forall i \in \mathcal{N}\ , \forall k \in K \end{aligned} \tag{33}$$

In summary, the conditions (32) and (33) are the connectivity constraints, while (31) is the power balance constraint for any component. Having determined the power balance equation for every component i of the distribution system and the connectivity constrains, the reliability constraints can be introduced.

Reliability constraints for PDD

In Section 3.4.2, it was introduced that an assigned pair k can be synthesized into a series system (single distribution path) or a series-parallel system (multiple distribution paths, see **Figure *3.12***). The reliability

constraints (13) and (14) in **O.P. 4** apply to a series system and a series-parallel system, respectively. The series-parallel system allows alternative routes in case the main path is interrupted due to failures. These alternate routes can be synthesized with resilient design formulation for a failure set or resilient design formulation as two-disjoint path.

Series system or single distribution path

Linearization of the reliability constraint for a series-system in (13) can be done by applying the logarithm function. Thus, the logarithm of the product of the terms is converted into a summation of each term's logarithm (similar to the GS&GLP case) which is a linear constraint for MILP, hence,

$$\log\left(\left(\prod_{j|(i,j)\in k} x_{ij}r_{ij}\right)\left(\prod_{i\in k} v_i r_i\right)\right) \geq \log r_{\text{TARGET},\,k}$$

$$\sum_{j|(i,j)\in k} x_{ij}\log r_{ij} + \sum_{i\in k} v_i \log r_i \geq \log r_{\text{TARGET},\,k} \qquad \forall k \in K \qquad (34)$$

Note that instead of writing $\log x_{ij}r_{ij}$, the term is arbitrarily changed to $x_{ij}\log r_{ij}$ (similar with $v_i \log r_i$). The reason is that the logarithm of 0 (if connection/component is not selected, e.g., $x_{ij} = 0$) is undetermined, and the expression cannot be solved. On the contrary, $x_{ij}\log r_{ij}$ drops the contribution of the term from the overall reliability if connection ij is not selected.

Series-parallel system or multiple distribution paths

On the other side, linearization of the reliability constraint for a series-parallel system in (14) is much more complex due to the nested multiplication terms inside logarithm terms. Rearranging (14) and applying logarithm function,

$$\log\left(\prod_{w}\left(1-\left(\prod_{j|(i,j)\in k} x_{ij}r_{ij}\right)\left(\prod_{i\in k} v_i r_i\right)\right)\right) \leq \log\left(1 - r_{\text{TARGET},\,k}\right)$$

$$\sum_{w} \log\left(1 - \left(\prod_{j|(i,j)\in k} x_{ij} r_{ij}\right)\left(\prod_{i\in k} v_i r_i\right)\right) \leq \log\left(1 - r_{\text{TARGET},\,k}\right) \qquad \forall k \in K \qquad (35)$$

Although there is a summation of logarithmic terms (from the outer multiplication), the expression inside these logarithmic terms contains other products. In this case, there is no straight linearization that could produce a linear constraint amenable for MILP. Discretization and PWL are difficult to apply because there are not only two-variable terms, but *n*-variable terms due to cross multiplication. Instead, network methods are effective in achieving the same goal (produce alternative paths) without the need to evaluate the reliability of a series-parallel system. These network methods are based on the resilient network design, i.e., resilient design for a set of failure scenarios, and resilient design with two-disjoint paths.

In resilient design for failure scenarios, the definition of a failure set is required beforehand. In this case, distribution paths are enforced by selecting sufficient component and connections such that any failure in the distribution path is recovered by forming other path with the remaining components and connections. No reliability for distribution paths is evaluated; instead, there are constraints regarding all the possible failure scenarios assumed to happen in the system. On the other hand, in the resilient two-disjoint path, a distribution path is implemented with two series systems connected in parallel, and these series systems do not share any component or connection (this condition is called *disjointness*). Then, there is a main path and an alternative path in case the former fails. Now, what happens if the reliability target could not be satisfied with two-disjoint paths? It is possible that reliability target must be satisfied with two or three alternative paths depending on the case. Then, reliability in (14) (many paths as required) must be approximated and replaced with other algebraic expressions [30].

PDD with single distribution paths (series-system)

Consider that each assigned pair k of the EPS is implemented as a series-system (single distribution path) and assume that the reliability target for each path can be achieved. The reliability constraint (36)

(linearization of the reliability for a series-system) can be applied on each distribution path. A subset of connections and components connected in series (see **Figure *3.12***) belongs to an assigned pair k. Since connection x_{ij} and component v_i can be used for more than one assigned pair k (as shown in **Figure *4.1***), additional Boolean variables $z_{ij,k}$ and $z_{i,k}$ are used to determine if x_{ij} and v_i are being used for pair k once i, j and i have been selected. In other words, $z_{i,k}$ is a variable that indicates if selected component i has been reserved to the assigned pair k; the same component i can be reserved for another path k (and so on). Then,

$$\begin{aligned} z_{i,k} &\leq v_i && \forall i \in \mathcal{N}\,, \forall k \in K \\ z_{ij,k} &\leq x_{ij} && \forall (i,j) \in \mathcal{A}\,, \forall k \in K \end{aligned} \tag{36}$$

Similar to (33), constraint (37) enforce no power flow (associated with pair k only) in component i or connection i, j if i and i, j have not been reserved for path k, hence,

$$\begin{aligned} P_{ij,k} &\leq d_k z_{ij,k} && \forall (i,j) \in \mathcal{A}\,, \forall k \in K \\ \sum_{j \in \mathcal{N}} P_{ji,k} &\leq d_k z_{i,k} && \forall i \in \mathcal{N}\,, \forall k \in K \end{aligned} \tag{37}$$

Considering $z_{i,k}$ and $z_{ij,k}$, the reliability constraint (series-system) in (36) is written as (38),

$$\sum_{j|(i,j)\in\mathcal{A}} z_{ij,k} \ln(r_{ij}) + \sum_{i \in \mathcal{N}} z_{i,k} \ln(r_i) \geq \ln(r_{\text{TARGET},\,k}) \qquad \forall k \in K \tag{38}$$

Lastly, (39) limits the power flow through i and i, j to their maximum values, i.e., P_i^{MAX} and P_{ij}^{MAX},

$$\begin{aligned} 0 \leq \sum_{k \in K} P_{ij,k} &\leq P_{ij}^{\text{MAX}} && \forall (i,j) \in \mathcal{A}\,, \forall k \in K \\ 0 \leq \sum_{k \in K} P_{i,k} &\leq P_i^{\text{MAX}} && \forall i \in \mathcal{N}\,, \forall k \in K \end{aligned} \tag{39}$$

Constraints in (36) to (39) correspond to the linearized version of reliability constraint (13) introduced in Section 3.4.2 for the reliability of a series-system.

In summary, a MILP formulation (linear objective and linear constraints) for the PDD problem considering that all distribution paths can be implemented as series systems, and assuming that the reliability target for each distribution path can be achieved, can be written as in **O.P. 6**.

O.P. 6 Objective (12)

subject to Connectivity constraints (32) and (33)

Power balance constraints (31)

Reliability constraints, (38) with (36), (37), and (39)

In addition to the design specifications and requirements for the PDD, the generator-load pair arrangement from the GS&GLP (within the virtual distribution system) is also used in the PDD to synthesize a power distribution topology with distribution components and connections. The **O.P. 6** is a standard formulation to synthesize a power distribution in PDD (assigned pairs as single distribution paths or series systems). Logically, there could be other requirements that could be translated into additional constraints or algebraic expressions. In case a series-system is unable to achieve the reliability target, resiliency formulations are introduced.

PDD as a Resilient Design for a set of Failure Scenarios

If a failure event occurs in any component i of the series-system (see **Figure *3.12***), power flow is interrupted, and the load supply is unexpectedly cut. In this case, the single distribution path of the assigned pair k fails to provide an alternative path in case of failures. Failure events can happen even when the reliability target of the series-system in (38) has been achieved. On the other hand, one can argue that (38) might have been unable to achieve the reliability target, and a series-parallel system is required to implement a distribution path. Nevertheless, it has been observed that the reliability of a series-parallel system in (35) cannot be directly transformed into a linear constraint using linearization techniques; it could be possible that other algebraic approximations are necessary. However, the resilient network design methods provide an effective alternative when alternative paths are required in the

power distribution design. A resilient design for a set of failures can be adapted to the PDD such that a failure resistant system is obtained.

Let F be the set of failure scenarios comprising connection failures and/or component failures that the system is expected to survive, i.e., $F = \{\not{f}_1, \not{f}_2, \dots, \not{f}, \dots\}$. This set is defined prior to solving the optimization problem. The failure events in F are assumed to be independent, i.e., failure cases are not related, so that one failure has no effect on the probability of other failures. A failure scenario in F is defined as a list that contains the components and connections that are assumed to fail. However, this list is not related to the set of assigned pairs K, that is, the failure scenarios are not necessarily described per assigned pair and distribution path because, prior to the PDD, which components and connections will be selected is unknown. Besides, there is no reliability assessment on distribution paths or in the power distribution network. The reliability targets are achieved by synthesizing a system that is resilient to failures, although direct reliability assessment is not part of the constraints in this approach.

The advantage of resilient design in the EPS comes when the loads are divided into critical (essential) and non-critical (non-essential) loads. The EPS must continue supplying critical loads even when any of the failure scenarios of the set F occurs, although non-critical loads can be shed. A critical load would require that the EPS still delivers power supply under any failure event occurring in the components and connections between generator's terminals and the load's terminals. Then the failure set F contains failure scenarios for all the components in each level of the PDD template.

For each failure $\not{f}$ of the set F, the power balance constraint (31) for any component i of the power distribution system still applies, i.e., power balance is maintained in any failure condition. The connection's power flow $P_{ij,k}$ corresponds now to the maximum value from all the power flows existing for every failure $\not{f}$, that is,

$$P_{ij,k} = \max_{\not f} P_{ij,k}^{\not f} \tag{40}$$

Where $P_{ij,k}^{\not f}$ is the power flow on connection i,j for assigned pair k during failure scenario $\not f$. Thus, power balance in (31) is,

$$\sum_{j|(i,j)\in\mathcal{A}} P_{ji,k}^{\not f} - \sum_{j|(j,i)\in\mathcal{A}} P_{ij,k}^{\not f} + d_k^{LOAD} - d_k^{GEN} = 0 \qquad \forall i \in \mathcal{N}, \forall k \in K, \forall \not f \in F \tag{41}$$

Let $\not f_{ij}$ represent the existence of a failure in connection x_{ij}, then $\not f_{ij} = 0$ if there is no failure, and $\not f_{ij} = 1$ when failure occurs. Power flow in connection i,j is guaranteed if, for the failure scenario $\not f$, this connection has not failed, otherwise, power flow is 0, then,

$$P_{ij,k}^{\not f} \leq d_k x_{ij}\left(1 - \not f_{ij}\right) \qquad \forall (i,j) \in \mathcal{A}, \forall k \in K, \forall \not f \in F \tag{42}$$

Finally, the condition that Boolean x_{ij} (selection of connection i,j) can only take two values, i.e., 0 or 1, is called the *integrality* constraint for x_{ij}, hence,

$$x_{ij} \in \{0,1\} \qquad \forall (i,j) \in \mathcal{A} \tag{43}$$

The PDD as a resilient network design for a set of failure scenarios can then be formulated as follows:

O.P. 7 Objective (12)

subject to Connectivity constraints (40)

Power balance constraints (41)

Resiliency constraints (42), and (43)

Note that the optimization in **O.P. 7** has been built with selection variable x_{ij} only, and v_i for the selection of component i has been dropped from the formulation. This is not an issue since the failure in a component can be modelled as a failure in all its incoming and outgoing connections. However, variations of **O.P. 7** can be created to explicitly declare failures in components and include v_i.

Although the determination of an exhaustive failure set (all possible failures) could be cumbersome because of the large number of components/connections and simultaneous failure combinations, it is possible to determine a partial failure set, e.g., limited number of hazardous events that could compromise critical functions. At this point, it might be desirable to have an alternative if the set F could not be determined. This situation might appear when considering disruptive designs based on experimental technologies. In these cases, there is limited information on the failure modes of the system because technology can be at the prototype level, which is likely to happen in MEA designs. Hence, in addition to the resilient design for failure scenarios, a two-disjoint path formulation is introduced.

PDD as a Resilient Design with two-disjoint paths

In the resilient design with two-disjoint paths, each distribution path of the assigned pair k must have an alternative, completely separate (disjoint, having no component in common), path to transfer power in case a failure of any component/connection from the 'main' path interrupts power supply. In this case, both paths must be disjoint because the failure of any component on one of them must not limit the distribution capacity of the other, i.e., they must not share any component which could fail.

In practice, it is possible that the alternative path supplies power from a different generator or power source, however, a two-disjoint path arrangement uses the corresponding generator-load pair k obtained in GS&GLP (one generator assigned to one load). Assignment from the same load to other generators have already obtained in GS&GLP given that a load's reliability target must have been satisfied.

In a two-disjoint path arrangement, only one of both paths are active at any time, i.e., either disjoint path 1 or 2 serves for the assigned pair k. This approach is known as the *two-disjoint* path problem [135]. Disjointness increases the probability that at least one path survives. Considering a set of critical and non-critical loads, two-disjoint paths can be built for the assigned pairs whose loads are critical (non-critical loads can be shed, e.g., when supplied from a series-system).

Let q be the disjoint-path index, i.e., $q \in \{1,2\}$. When connection i,j is selected, it can either allow power distribution for the first or the second disjoint-path, thus $P_{ij,k}^{q=1} = 0$ or $P_{ij,k}^{q=2} = 0$. Similarly, when component i is selected, it can either transfer power for the first or second disjoint-path, that is, $\sum_{j \in N} P_{ji,k}^{q=1} = 0$ or $\sum_{j \in N} P_{ji,k}^{q=2} = 0$. Let the Boolean $u_{ij,k}$ and $u_{i,k}$ select which disjoint-path the connection i,j and component i is reserved for. The connection disjointness can be established as follows,

$$\begin{aligned} P_{ij,k}^{q=1} &\leq d_k u_{ij,k} && \forall (i,j) \in \mathcal{A}, \forall k \in K \\ P_{ij,k}^{q=2} &\leq d_k (1 - u_{ij,k}) && \forall (i,j) \in \mathcal{A}, \forall k \in K \end{aligned} \tag{44}$$

Boolean $u_{i,k}$ reserves component's power flow $P_{ij,k}^{q}$ for disjoint-path 1 or 2 only (not both) because either $u_{i,k} = 0$ or $1 - u_{i,k} = 0$. Similarly, the component disjointness can be established as,

$$\begin{aligned} \sum_{j \in \mathcal{N}} P_{ji,k}^{q=1} &\leq d_k u_{i,k} && \forall i \in \mathcal{N}, \forall k \in K \\ \sum_{j \in \mathcal{N}} P_{ji,k}^{q=2} &\leq d_k (1 - u_{i,k}) && \forall i \in \mathcal{N}, \forall k \in K \end{aligned} \tag{45}$$

Now, the power balance must be established for every disjoint-path q, thus, it can be written as,

$$\sum_{j|(i,j) \in \mathcal{A}} P_{ji,k}^{q} - \sum_{j|(j,i) \in \mathcal{A}} P_{ij,k}^{q} + d_k^{LOAD} - d_k^{GEN} = 0 \qquad \forall i \in \mathcal{N}, \forall k \in K, q \in \{1,2\} \tag{46}$$

If x_{ij} is set, $P_{ij,k}^{q}$is allowed to flow on either disjoint-path, so,

$$P_{ij,k}^{q} \leq d_k x_{ij} \qquad \forall (i,j) \in \mathcal{A}, \forall k \in K, q \in \{1,2\} \tag{47}$$

The integrality constraint for the additional Booleans $u_{ij,k}, u_{i,k}$ is,

$$u_{ij,k}, u_{i,k} \in \{0,1\} \qquad \forall (i,j) \in \mathcal{A}, \forall k \in K, \forall i \in \mathcal{N} \tag{48}$$

Up to now, the disjointness constraints are (44) and (45), the power balance is (46), and connectivity constraints are (47) and (48). What follows is the reliability calculation of a two-disjoint path arrangement,

such that the reliability target can be achieved. The reliability of two-disjoint paths is comparable to calculating the probability (of occurrence) of two events, say a and b (any of the two paths is successful in supplying a load). Let $\mathrm{P}(\cdot)$ be the probability of occurrence of any event. Then, the probability of occurrence of any two events a and b is equal to the summation of probability of a and b minus probability of both events happening simultaneously, then,

$$\mathrm{P}(a \cup b) = \mathrm{P}(a) + \mathrm{P}(b) - \mathrm{P}(a \cap b) \tag{49}$$

As long as events a and b are independent, the last term of the right-hand side of (49) is $\mathrm{P}(a \cap b) = \mathrm{P}(a)\mathrm{P}(b)$, i.e., the product between the probabilities of occurrence of a and b. The probability of occurrence in (49) can be used to determine the probability of successfully supplying a load from two-disjoint paths. Let r_k^q be the reliability of the disjoint-path q, then, based on (49), the probability that at least one path survives (successfully supply power to the load) must at least reach target $r_{\mathrm{TARGET},\,k}$,

$$r_k^{q=1} + r_k^{q=2} - r_k^{q=1} r_k^{q=2} \geq r_{\mathrm{TARGET},\,k} \qquad \forall k \in K \tag{50}$$

For the calculation of each disjoint-path's reliability r_k^q, reliability constraint in (38) suffices (reliability of a series-system or single path). Considering (38), the product $r_k^{q=1} r_k^{q=2}$ in (52), that is, multiplication of the disjoint-paths' reliabilities, produces an extensive number of products terms between variables. For instance, the term $r_k^{q=1} r_k^{q=2}$ has the following form,

$$r_k^{q=1} r_k^{q=2} = \left(\sum_{j|(i,j)\in\mathcal{A}} z_{ij,k} \ln(r_{ij}) + \sum_{i\in N} z_{i,k} \ln(r_i) \right) \left(\sum_{j|(i,j)\in\mathcal{A}} z_{ij,k} \ln(r_{ij}) + \sum_{i\in N} z_{i,k} \ln(r_i) \right)$$

Which produces many product terms. To avoid performing linearization on each of these products, a simpler approach to represent the disjoint-path's reliability is introduced.

Simpler calculation for the reliability of two-disjoint path

The main idea of a simpler calculation for the reliability of two-disjoint path is to avoid linearization of an extensive number of product terms. Instead of using an expression that calculates reliability over two paths (considering series-parallel system), an expression for the reliability of reaching a component i after arriving from component j through connection i, j can be used. Starting from a generator, this reliability is calculated for every component i (on both paths of the two-disjoint path arrangement) until it reaches the load. It can be said that, along the trail of components, the reliability of reaching the next component is updated with the reliabilities of all the previous components. At the load, constraint (50) can be calculated using the current reliabilities at the load. There is still a product term to solve for, but only one per assigned pair (if synthesized as a two-disjoint path). Whenever the current paths configurations do not meet the reliability target, the reliability constraints are forced through other sets of components and connections.

Let a set of variables $\mathcal{s}_{i,k}^{q}$ be defined as the probability of power successfully reaching component i (the starting position is the generator or power source) when component i is reserved for disjoint-path q (recall that assigned pair k consists of two disjoint-paths). Then, the reliability $\mathcal{s}_{i,k}^{q}$ of succesfully reaching a component can be written as,

$$\mathcal{s}_{j,k}^{q} \leq r_{ij} r_i \mathcal{s}_{i,k}^{q} + \left(1 - \mathcal{u}_{ij,k}\right) \qquad \forall k \in K, q \in \{1,2\}, \forall (i,j) \in \mathcal{A} \qquad (51)$$

Of course, there is no reliability target in (51) except when it reaches the load. If component i is selected, $\mathcal{u}_{ij,k} = 1$, and (51) becomes $\mathcal{s}_{j,k}^{q} \leq r_{ij} r_i \mathcal{s}_{i,k}^{q}$; otherwise (51) relaxes $\mathcal{s}_{j,k}^{q}$ to an arbitrary value (0 or 1) if component i is not selected, i.e., $\mathcal{u}_{ij,k} = 0$. In the power sources,

$$\mathcal{s}_{GEN,k}^{q} = 1 \qquad \forall k \in K, q \in \{1,2\} \qquad (52)$$

When (51) is applied to the load corresponding to the assigned pair k, $s_{j,k}^{q}$ is the probability of successfully reaching the load and $s_{j,k}^{q}$ can be replaced with $s_{LOAD,k}^{q}$. Then, $s_{LOAD,k}^{q}$ is the reliability of the disjoint-path q, so that $s_{LOAD,k}^{q} = r_k^q$ (r_k^q in constraint (50)). Now, considering the variables $s_{LOAD,k}^{q}$, the reliability constraint at the load can be written as,

$$s_{LOAD,k}^{q=1} + s_{LOAD,k}^{q=2} - s_{LOAD,k}^{q=1} s_{LOAD,k}^{q=2} \geq r_{\text{TARGET},\, k} \qquad \forall k \in K \qquad (53)$$

Which finally includes the reliability target that needs to be satisfied. Both values in (53) has to be set ($s_{LOAD,k}^{q=1}$ and $s_{LOAD,k}^{q=2}$), so the optimization search has to investigate both, in other words, $s_{LOAD,k}^{q=1}$ is set and then $s_{LOAD,k}^{q=2}$ can be determined, and vice versa. In fact, the values of $s_{LOAD,k}^{q=1}$ and $s_{LOAD,k}^{q=2}$ in (53) could be interchangeable. This could originate from an algorithmic issue in MILP known as *symmetry*, which can produce high computational effort during MILP optimization. Symmetry exists when the order of variables can be interchanged without producing a different outcome (the optimal solution is the same). Then, there are portions of the design space that are unnecessarily searched, and this situation consumes computational effort (optimization can take unnecessarily longer). To break the potential symmetry (and avoid searching equivalent portions of the design space), an additional constraint is introduced to speed up MILP optimization,

$$s_{LOAD,k}^{q=1} \geq s_{LOAD,k}^{q=2} \qquad \forall k \in K \qquad (54)$$

In (54), it is ensured that $s_{LOAD,k}^{q=1}$ is set in advance with respect to $s_{LOAD,k}^{q=2}$. Before introducing constraints (51)-(54) in the MILP formulation of PDD, constraint (53) have to be linearized. The linear constraints (51), (52), and (54) are already amenable for MILP.

Linearization of two-disjoint path reliability constraint

In (53), the product $s_{LOAD,k}^{q=1} s_{LOAD,k}^{q=2}$ is a bilinear term, i.e., multiplication of two real variables. An alternative to the linearization of bilinear terms is to implement McCormick envelopes as explained in

Section 4.2 in the case of two-variable functions. These envelopes try to enclose the two-variable function (bilinear term) inside a parallelogram limited by linear functions. Other alternative is discretization by replacing the left-hand side of (53) with a set of Boolean variables multiplied by fixed coefficients. Let the discretization approach linearize (53) in this occasion.

Allow each $\mathcal{s}_{LOAD,k}^{q}$ to be discretized into a vector containing disjoint-path' reliability values, i.e., $\boldsymbol{\alpha} = [\alpha_1 \dots \alpha_a]$ and $\boldsymbol{\beta} = [\beta_1 \dots \beta_b]$ for $q = 1$ and $q = 2$ paths, respectively. Also, allow a matrix $\boldsymbol{\Gamma}$ of dimension $[a \times b]$ have elements $\gamma_{a,b}$ such that $\gamma_{a,b} = \alpha_a + \beta_b - \alpha_a\beta_b$, i.e., each row corresponds to a vector $\boldsymbol{\gamma}_a = \alpha_a + \boldsymbol{\beta} - \alpha_a \cdot \boldsymbol{\beta}$. Let a Boolean variable $\sigma_{ab,k}$ select a unique value from $\boldsymbol{\Gamma}$, then, (55) ensures that only one element $\gamma_{a,b}$ is selected,

$$\sum_a \sum_b \sigma_{ab,k} = 1 \qquad \forall k \in K \qquad (55)$$

The two-path reliability constraint in (53) can be written as,

$$\sum_a \sum_b \gamma_{a,b}\sigma_{ab,k} \geq r_{\text{TARGET},\,k} \qquad \forall k \in K \qquad (56)$$

A condition for (55) and (56) is that a unique value for each disjoint path's reliability (α_a and β_b) must be selected. For the disjoint path $q = 1$, such a condition can be written as,

$$\sum_a \sum_b \alpha_{a-1}\sigma_{ab,k} \leq \mathcal{s}_{LOAD,k}^{q=1} \leq \sum_a \sum_b \alpha_{a+1}\sigma_{ab,k} \qquad \forall k \in K \qquad (57)$$

α_{a-1} and α_{a+1} act as an upper and lower bound (window) for α_a. Similarly, for $q = 2$,

$$\sum_a \sum_b \beta_{b-1}\sigma_{ab,k} \leq \mathcal{s}_{LOAD,k}^{q=2} \leq \sum_a \sum_b \beta_{b+1}\sigma_{ab,k} \qquad \forall k \in K \qquad (58)$$

In (56), $\gamma_{a,b}$ could be stuck around $r_{\text{TARGET},\,k}$ even when the disjoint paths' reliabilities are higher. To prevent this, an additional term in the optimization objective is needed to push $\mathcal{s}_{LOAD,k}^{q}$ to its actual value

(i.e., to adopt the highest value within the constrained range by preference). This term should be comparatively small with respect to the total cost to avoid biasing the cost optimization. Then, the objective for the MILP optimization formulation of the PDD is,

$$\min_{P,x,s,u} \sum_{(i,j)\in\mathcal{A}} \left(c_{ij}x_{ij} + c_{\mathrm{kW}}^{ij}\left(\sum_{k\in K} P_{ij,k}\right)\right) + \sum_{i\in\mathcal{N}} \left(m_i v_i + m_{\mathrm{kW}}^{i}\left(\sum_{k\in K} P_{i,k}\right)\right) - \sum_{k\in K}\sum_{q} s_{LOAD,k}^{q} \tag{59}$$

In summary, the optimization formulation for the PDD considering a resilient design with two-disjoint path approach (assigned pair k is implemented as a two-disjoint path system) and linearization of reliability constraints with discretization, is formulated as follows:

O.P. 8 Objective (59)

subject to
- Connectivity constraints (44), (45) (disjointness), (47), (48)
- Power balance constraints (46)
- Disjointness constraints, (51), (52), (53)*, (54)
- *Constraint (53) is replaced by (55) - (58)

A drawback of the discretization approach is that a large number of variables $\sigma_{ab,k}$ are needed if higher accuracy is required. Alternatively, if McCormick envelopes or 2-PWL approximations were used (see Section 2.5) , careful analysis is required to test the effectiveness of the approximation, that is, that the segments (pieces of surfaces) resemble as much as possible the non-linearities of the two-variable function (it is a tight approximation).

4.3. Recap

Up to this point, the PDD problem for the synthesis of a power distribution system has been linearized to produce a MILP formulation that can produce a global optimum that is very close to the global optimum of the original EPS design. The assigned pairs (from the generator-load pair arrangement) of the GS&GLP have been synthesized in three forms: as a series-system (single distribution path), as a resilient system

for a failure set, and as a resilient system with two-disjoint paths (multiple distribution paths). In the first case, reliability target on each load is achieved by a series system. Whenever it is not possible to achieve the reliability target, alternative paths are required. If the loads could be separated into critical and non-critical loads, the resilient design for a failure set offers an alternative to produce a power distribution that always supply critical loads, even under the occurrence of a pre-defined set of failure scenarios. The synthesis of an alternative path in case the main path fails can be done with a two-disjoint path formulation. In this approach, no component or connection is shared between both paths, and it is assumed that two-disjoint paths that satisfies the reliability target of the load can be synthesized. Whenever the reliability target of the load is not satisfied by any of these methods, the designer must provide other algebraic approximations for the calculation of reliability of series-parallel system where three or more paralleled paths are required to satisfy the reliability target of the load. The latter is not part of the scope of this work.

4.3.1. PDD Linear Formulations

In summary, three linear formulations for PDD have been presented,

1. **O.P. 6**: assigned pair k built as a series-system (single distribution path); reliability constraint is satisfied with one path.
2. **O.P. 7**: Resilient design for a set of failure scenarios; the system accommodates sufficient components and interconnections (system's adequacy) to continuously supply power to critical loads. Loads are separated into critical and non-critical loads. Critical loads must be always supplied, while non-critical loads can be shed. Several distribution paths can be formed between the same generator-load pair, but the reliabilities of these paths are not evaluated in the optimization formulation.

3. **O.P. 8**: Resilient design with two-disjoint paths (two disjoint paths per assigned pair k); the main distribution path has an alternative path to route power to critical loads. Both paths do not share any connection and component. It is assumed that the load's reliability target can be achieved by a two-disjoint path.

In this chapter, linearization of the objectives and constraints of the GS&GLP and PDD subproblems (**O.P. 3** and **O.P. 4** respectively) for the design of an EPS architecture has been applied. The goal is to convert the non-linear optimization formulations into MILP optimization problems. The optimal solution of a MILP problem is a global optimum solution. If the linear approximations of objectives and constraints are tight and represent very closely the non-linear functions, the optimal solution is also very close to the optimal of the original non-linear problem. Besides, MILP problems can be solved with powerful and efficient commercial solvers, then, the designer focuses on the design framework (problem modelling) rather than how the mathematical optimization is going to be solved. The accuracy of the linear approximations comes with the sacrifice of increasing the number of variables and constraints, however, this can be effectively managed by current commercial solvers. A case study explaining the use of GS&GLP and PDD in the design of an EPS architecture (from scratch) is presented in Chapter 6.

4.4. Conclusion

This chapter presented the MILP reliability-based optimization formulations for the GS&GLP and PDD subproblems. By solving GS&GLP and PDD sequentially, a new EPS architecture is synthesized. A graphical summary of the MILP formulations within the EPS architecture design framework is shown below.

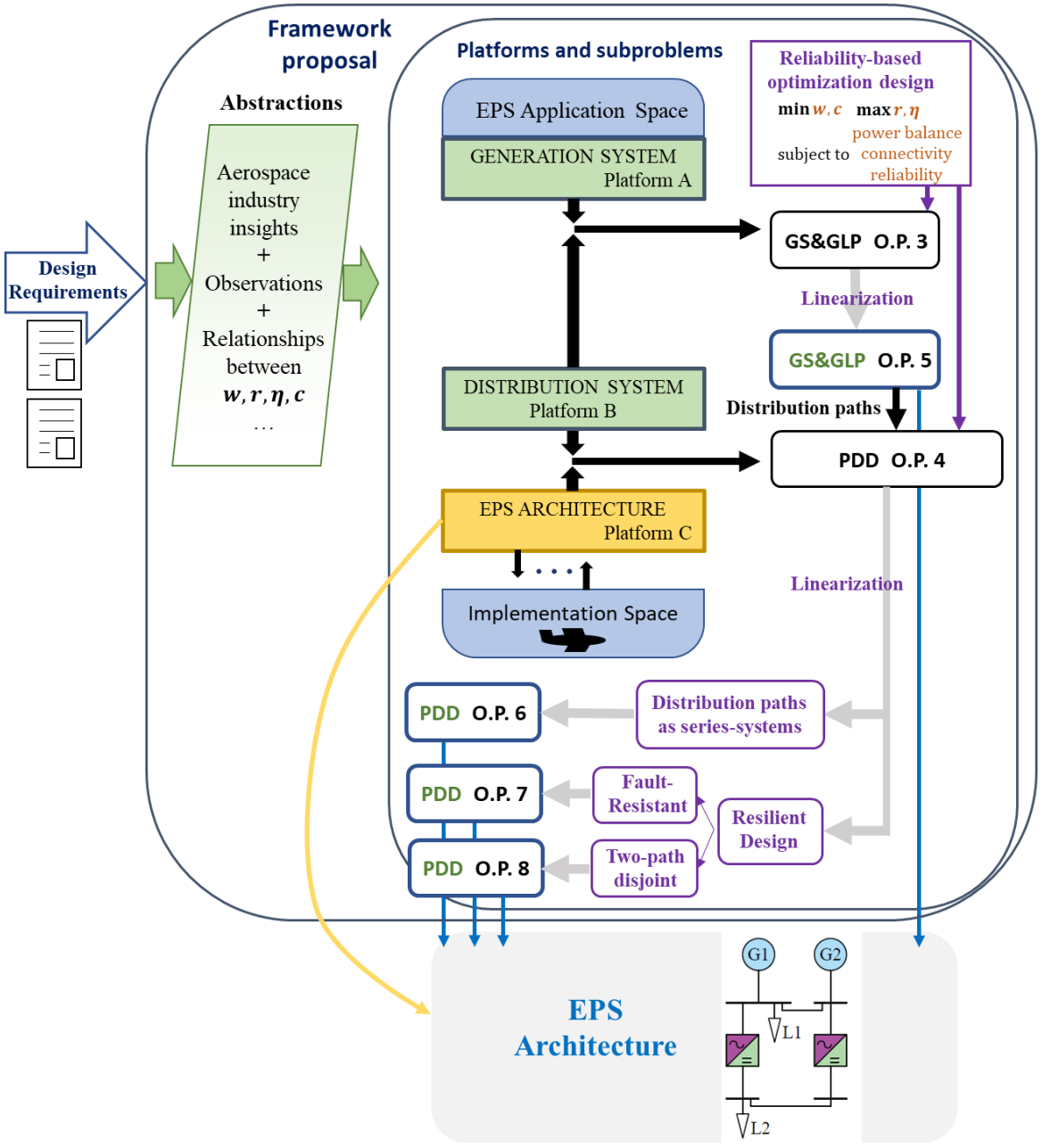

Figure 4.2 Graphical summary of the MILP reliability-based formulations for the EPS design framework proposal.

The design framework follows a Platform Based Design methodology, but it has been adapted to the design needs of the EPS architecture design. Resilient network techniques are adopted for designing an EPS architecture that satisfied the reliability targets. The original EPS design problem is divided into two subproblems, i.e., GS&GLP and PDD. The design outcome is not a real system ready to be installed in

aircraft because its abstraction is still at the architectural and functional level. However, at this stage it complies to the design requirements through minimization of cost and weight, and maximization of efficiency and reliability. In order to increase power availability in the loads, GS&GLP let the loads be supplied from multiple generators, while resilient design in the PDD introduced network methods to generate alternative paths that ensure that critical loads are always supplied. Resiliency was achieved by designing an EPS that tolerates the occurrence of failures either by preparing the system for a set of pre-defined failure scenarios or by providing two-disjoint paths for every assigned pair. The design framework depicted in **Figure *3.3*** is expanded in **Figure *4.2*** to show the MILP formulations studied in this chapter.

An EPS architecture synthesized with the MILP formulations for the GS&GLP and PDD problems is still not ready for deployment in real aircraft. There is a gap between the architecture abstraction and the physical implementation (real system) that needs to be addressed. Although the number of components, the size of components, and the EPS topology are known at this stage, electrical performance of the system is not possible to assess because the system's voltage has not been decided yet. In fact, the system's voltage allows obtention of voltages and currents essential to evaluate the performance of any power and energy management system, i.e., control system during EPS operation. To shorten the gap between the EPS architecture and a real system implementation, performance optimization of an EPS architecture is studied in the next chapter.

5. Performance Optimization in EPS Designs

5.1. Introduction

Having obtained an optimal EPS architecture by following the PBD inspired framework (Chapter 3) and solving the reliability-based optimization formulations for the GS&GLP and PDD subproblems (Chapter 4), performance evaluation is mandatory to ensure the system works according to the architectural requirements and functional specifications. The evaluation tests if the system were responding appropriately for a given condition. Further to responding in an appropriate manner, the system can optimize its response as well, so that there could be an optimal response for that condition as well. This is referred as performance optimization in this work.

A vital task in performance optimization is the obtainment of the corresponding operating parameters under each condition. This is achieved by solving a *load flow* problem. The load flow is the steady state analysis of the EPS that determines the operating state, i.e., it solves each optimisation problem to determine the unknown variables at each bus, such as voltages, currents, and powers. For this purpose, the system's voltage and the components' electrical characteristics must have been predefined so that *power flow* equations can be established. Therefore, a way to select an optimal operation voltage and the steady state (electrical) models of connections and components are required, to establish a load flow for performance optimization afterwards.

Electrical models of components and connections are not necessary during architecture synthesis. However, once the architecture has been synthesized, some aspects of physical implementation can be decided upon, to be able to bring the system to an optimized performance during operation. In the case of each of the connections, the electrical model is not only driven by the cable's type, but also by the length and the power transferred. The length directly depends on the location of components, while the

power transferred depends on the current it carries and the voltage at which it distributes power. Similarly, electrical characteristics for components must be decided upon, to establish power flow equations. With a complete electrical representation of the system, the load flow can be introduced into optimization formulations for optimal performance. During operation, optimal performance is required to optimize use of the available resources (e.g., energy consumption, efficiency, etc.). Optimization during operation is implemented in the power and energy management system whose main tasks are topology reconfiguration and performance optimization, e.g., efficiency maximization through loss minimization. These problems are an extension of the load flow problem and thus are presented in this chapter as a tool that can be used to evaluate synthesized EPS architectures. Thus, this chapter follows the flow diagram depicted in **Figure *5.1***.

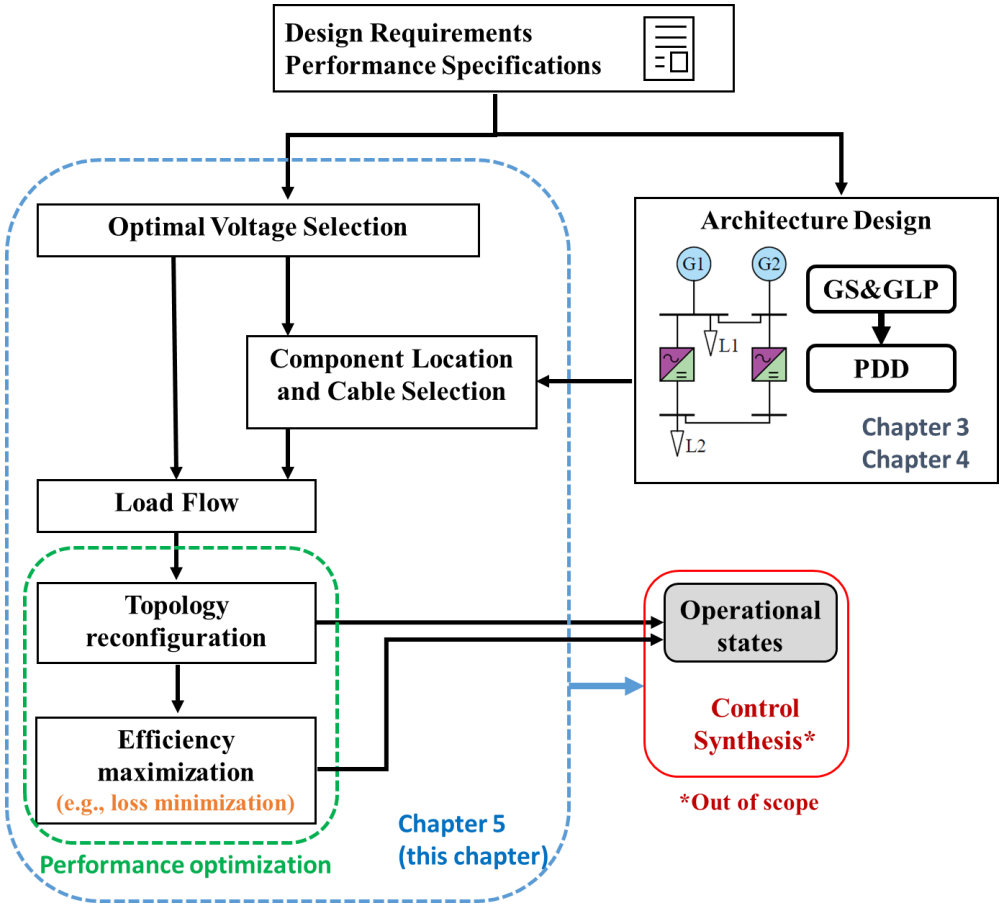

Figure 5.1 Flow diagram for performance optimization of EPS architecture.

First, optimal voltage selection is introduced. Once the system's voltage can be determined, component location and cable selection can be performed. Having determined the electrical models of connections and components, a load flow problem can be established. Then, the load flow problem can be introduced in performance optimization problems for topology reconfiguration and efficiency maximization. Both lead to the definition of operational states that are part of the controller synthesis task which is outside of the scope of this work.

5.2. Optimal Voltage Selection

Before any power flow equation can be established, the system's voltage must be determined [136]. The selection of the EPS' voltage is a compromise between weight and power transfer capability, constrained by partial discharge phenomena at high altitudes and the available space (volume) inside the aircraft. In general, voltage selection in any electrical system depends mainly on the following factors,

1. Type and size of the loads to be supplied.
2. Transmission and distribution distances from power sources to loads.
3. Load growth, e.g., additions of new loads throughout system's lifetime.
4. Electrical installation standards
5. Life cycle costs: initial cost, maintenance cost, and end of lifetime

The second and third factors are much less decisive in selecting the EPS voltage because the aircraft's EPS is an autonomous grid that, contrary to what happens in ground power systems, does not experience significant overall load increases over time (e.g., from the addition of new energy users, new devices, etc.), and its loads are not geographically dispersed over a large territory. Instead, the aircraft EPS is confined to a limited space and the electrical network is not expanded with large additions (new devices or subsystems). Besides, the aircraft EPS always serves for roughly the same maximum power on each flight phase; there are variations due to number of passengers and flight distance. Some spare capacity to

incorporate new subsystems could be expected, but continuous long-term significant increments are not expected – an aircraft redesign or replacement would be more common if this was necessary. The fourth factor is much more decisive because aerospace and aircraft regulations drive the design towards certification and aircraft permission to fly. In the MEA context, current aerospace and aircraft regulations are expected to experience profound transformations to include new technologies, disruptive topologies, and innovative ways of distributing power and energy onboard. However, current standards are still being observed, with most requirements and specifications being exceeded to provide enhanced safety and reliability.

In completely new installations, the choice of the system's voltage should also consider achieving the most efficient power conversion at the lowest cost [137], while carefully observing safety and reliability. In electrical propulsion cases, the load's performance (the performance of the electrical motors driving the propulsors/fans) has the highest impact on the system's reliability, and the operating voltage is one of the main decision variables in the overall propulsion system optimization [138]. On the other hand, for the non-electrical propulsion case, the operating voltage mainly depends on the system's weight and the distribution power transfer capability.

It has been previously observed that the EPS's weight depends on several factors (see Chapter 3) determined by the observations and industry insights,

- The system's weight and efficiency are mainly influenced by the number of power sources and their ratings. These power sources match load demand at all flight stages and there is generation adequacy in case of loss of generation.
- The total power distribution weight is roughly proportional to the amount of power to convert.
- Power conversion's weight is driven by a power density (kW/kg) figure that depends on the power converter topology and semiconductor selection.

- The EPS reliability performance is assessed as the availability of power at load's terminals, so that higher availability demands more distribution capacity to cope with contingencies.

The factors above were considered in the formulation of the GS&GLP and PDD subproblems to obtain an optimal EPS architecture. At the function model level, connections between components are represented by lossless transmission lines with unlimited capacity. However, all connections constitute a cabling system that has inherent physical limitations, and their performance depends directly on the voltage level at which power is transmitted. Therefore, voltage selection must be included in the EPS architecture design. The MEA will also experience a substantial increase in electrical energy consumption with respect to current aircraft [139], so that the generation system and power distribution will be larger and power demand will definitely be higher. Given that current state-of-the-art commercial systems operate at 230/400 VAC and ±270VDC, increased demands would require thicker conductors for the same voltage levels, which would consequently increase the weight payload. In contrast, increasing the voltage levels could increase the insulation weight (increase in the insulation vs. conductor ratio) to avoid the risk or partial discharge (PD), and beyond a certain value, increased voltage is not a reasonable option. The aim is to find a voltage value that optimizes insulation and conductor weight such that there is no risk of partial discharge (PD). Partial discharge is considered as the presence of a physical electromagnetic phenomena at high altitude that could result in the EPS malfunction, failures, and potential risk of fatalities.

5.2.1. Physics of Power System Voltage

Consider a connection between components i, j implemented as a cable segment of finite length (line). This cable is built with an electrically conductive solid material known as *conductor* covered by a jacket of *insulation* of certain thickness. Ideally, insulation has no imperfections during manufacturing processes and the cable has experienced no degradation during its lifetime. On the contrary however, cables contain microscopic deficiencies, and also develop some form of degradation due to exposure to harsh

environments. In this case, a physical phenomenon known as *dielectric breakdown* could occur. When a breakdown happens, the risk of PD is high.

PD is the dielectric breakdown of the conductor's insulation or airgap between cables at a specific location along the line in the presence of a certain electric potential of voltage level. The insulation aims to decrease as much as possible, or even eliminate, the presence of electric potential on the cable's surroundings. The thicker the insulation, the better is the voltage attenuation outside the cable at the expense of increasing the weight payload. The insulation's efficiency deteriorates with material degradation due to water presence, defects in joints and terminations, ionic contamination, electrical treeing, and other mechanical damages that could result in high stress on microscopic voids. During a cable's operation these voids can get filled with extraneous solid and liquid materials [140]–[142]. On the other hand, the risk of PD between cable and other conducting elements such as other cables, ground surfaces, metallic plates, busbars, metallic ducts, etc., is reduced by increasing the insulation level between them, so that the electric potential is heavily attenuated. Unless electrical conductors were installed in pressurized chambers (see [143] for futuristic cryogenic cabling proposals), the surrounding environment of cabling systems is air, which acts as a natural insulation element. If PD occurs in a cabling system, dielectric breakdown of air is present, which is the reason for which the definition of an appropriate airgap is required.

The scientific study of PD has traditionally been conducted by testing two electrodes (conductors with a special shape) immersed in a pressurized chamber filled with a gas or liquid material, so that dielectric breakdown figures for such gases or liquids are obtained. The electrodes are separated by an adjustable distance (gap) and a variable voltage difference between them is applied. The PD inception voltage (PDIV) is defined as the voltage at which at least one single PD occurs, i.e., an apparent charge equal to or greater than 100 pC (pico-Coulomb) [144] (see IEC TR 61294 Determination of the Partial Discharge Inception Voltage) is present. The PDIV that produces a dielectric breakdown depends on pressure, gap length

between conducting elements, and temperature experienced by the conductors (testing conditions). The relationship between these factors is illustrated in the Paschen's curve [145] as shown in **Figure *5.2***. This curve is used to formulate design criteria for insulation systems.

The Paschen's curve usually shows the breakdown voltage as a function of gap length for a fixed pressure and temperature. In an aerospace application in which conductors and cables are surrounded by air, the Paschen's pressure is the atmospheric pressure at which the aircraft is flying, which is associated to the flying altitude, e.g., 10kPa is equivalent to 53 kft (16.1 km) above sea level. In **Figure *5.2***, air breakdown takes place at a voltage of 2kV for a 3.75mm gap. This is a conservative figure because flights operate at lower altitudes, e.g., common cruise altitude in commercial flights is between 33 kft and 36 kft (10 km – 10.97 km).

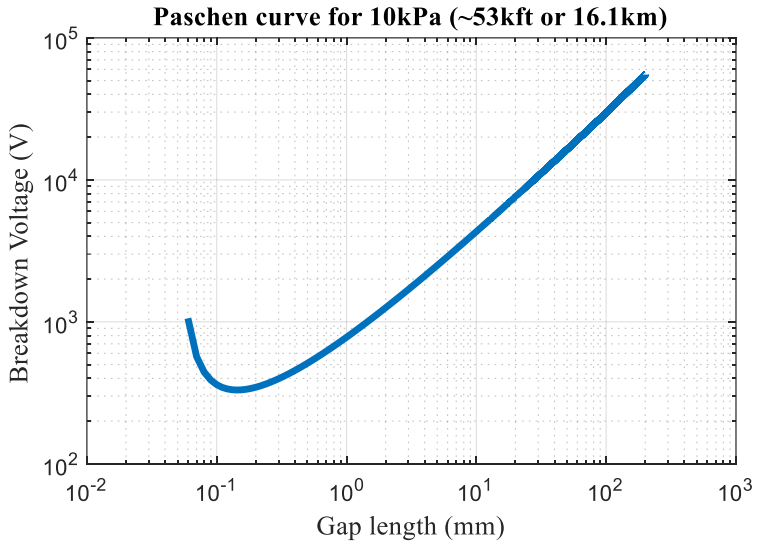

Figure 5.2 Paschen's curve for Air at a pressure of 10kPa, temperature of 15°C.

It can be observed in **Figure *5.2*** that larger gaps require higher voltages to produce air breakdown (at the same pressure). There is a specific gap length for which the breakdown voltage is a minimum; below this value, there are smaller gap lengths that also require higher voltages to produce air breakdown. Once a breakdown is triggered, a variable amount of charge starts to flow (an electrical current) from one

conductor to the other through the air. This condition could result in a potential system's damage and/or risk of fire, i.e., electrical current in certain materials could cause a dangerous temperature rise (thermal losses). Essentially, a safety margin is necessary in cabling system designs to avoid any risk of PD. This margin is obtained by calculating a safe field gap margin considering the minimum breakdown voltage of the Paschen's curve. The main idea is that, if a system is operating below the minimum breakdown voltage, any gap length between cables in its cabling system prevents the risk of breakdown.

5.2.2. Calculation of a Safe Operating Voltage

The field gap is the electric field (in voltage per unit of length, V/m) existing in the gap separating two conductors. In order to obtain the maximum field gap within a complex cabling installation, numerical analysis techniques such as Finite Element Analysis (FEM) [146] are used. Consider a simple power cabling installation consisting of a cable installed at a certain distance *e* from a conductive wall, i.e., ground plane, as shown in **Figure *5.3***. In this arrangement, e is the *clearance* distance (shortest airgap), c is the conductor's diameter, i is the insulation thickness, D is the distance between the conductor's center and the ground, and d is any distance of arbitrary length for which the field gap is calculated. The field gap for this cable-ground arrangement can be obtained by using the uniform field gap method [147],

$$V_d = 100\frac{d}{d + \left(\frac{i}{\varepsilon_r}\right)} \tag{60}$$

Where V_d is the percentage of the voltage across the gap, and ε_r is the relative permittivity of the cable's insulation. If $i = 0$ (naked cable or wire), V_d is 100%, i.e., full voltage is present across the gap; for any $i > 0$ in (60), $V_d < 100\%$ and a partial voltage (with respect to the nominal voltage at which the cable is operating) is present across the gap because the insulation has served as an attenuation material. Smaller ε_r provides better insulation because the field gap decreases.

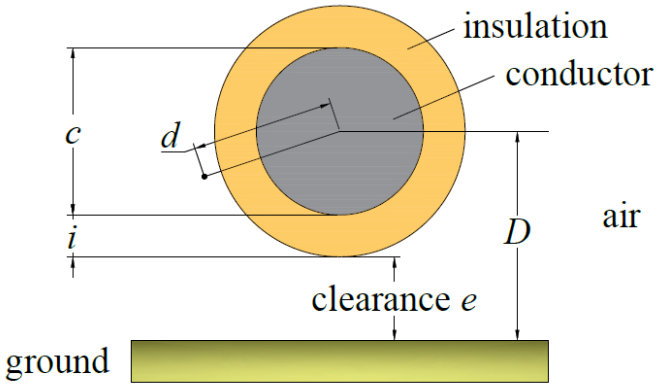

Figure 5.3 Basic cable arrangement for a power conducting cable.

The product of V_d with the system's voltage provides the actual voltage (in V) across the gap. By matching this product to the breakdown voltage from the Paschen's curve, the actual voltage now represents a safe operating voltage (SOV), in other words,

$$(V_d)(SOV) = V_{PASCHEN} \tag{61}$$

Thus, the maximum SOV for any gap d could be considered as the safe operating voltage for a particular set of parameters (altitude, temperature, insulation thickness i and permittivity ε_r). By variating d, (60) and (61) can be used to obtain V_d and SOV curves. To illustrate the variation of V_d and SOV with respect to air gap d, let the insulation thickness i be 0.09mm and the permittivity ε_r be 4.4. V_d and SOV versus variations in air gap length can be shown in **Figure *5.4***. The maximum SOV in this example is approximately 375.5 V for a $d = 0.16mm$. Therefore, the system's voltage in this case must be at most 375.5V. Any voltage above this value could potentially generate a voltage breakdown, a risk of PD, and of unexpected failure events.

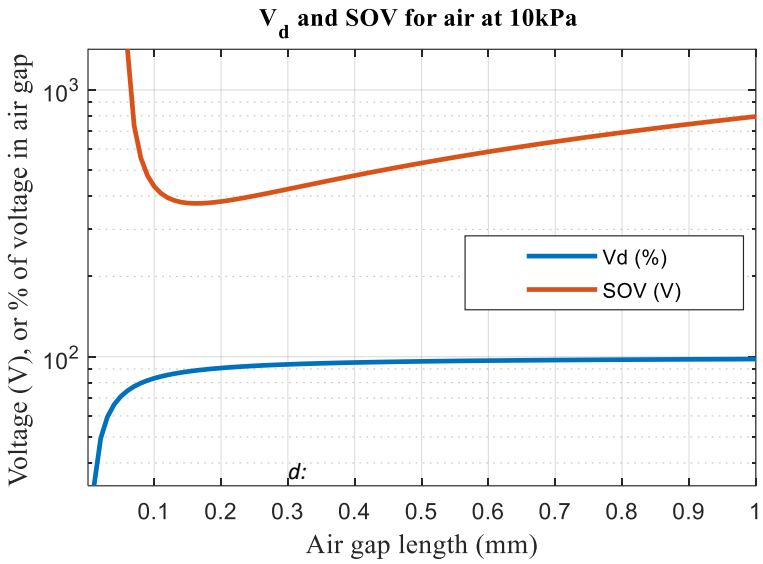

Figure 5.4 V_d and SOV curves for a cable with $i = 0.09mm$, $\varepsilon_r = 4.4$, at an air pressure of 10 kPa and T = 15°C.

Electrical cables and wires in real applications have insulation thicknesses that are greater than 1mm and insulation materials with permittivity ranging between 2.3 (low density polyethylene) and 9.0 (polyvinyl fluoride, chloro-sulfonated polyethylene compounds) [148]. To obtain the optimal system's voltage, appropriate selection of insulation thickness and material must be performed. Moreover, this selection depends on the EPS's power requirements and space limitations.

For the same airgap on an existing installation layout, the risk of PD increases if higher voltages are considered, reason for which upgrading the system's voltage demands a redesign of its cabling. Any voltage desired to be implemented in the EPS must be a SOV to ensure the system's safety. Besides, extending the airgap continuously for every voltage increment is not an option in the aircraft industry due to the strict limitations on space and volume. Given the conflicting outcomes between adopting thicker insulation and increasing cables' separation, an optimization method for selection an appropriate voltage is required.

5.2.3. Safe Operating Voltage Optimization

By selecting the appropriate insulation's parameters (thickness i, and relative permittivity ε_r), constrained by the power requirements and space limitations (installation constraints), the optimal safe operating voltage for an EPS can be found.

Let the cabling system be modelled as in **Figure *5.3***; the clearance distance can be written as,

$$D - \frac{c}{2} - i = e \tag{62}$$

The clearance distance e corresponds to a feasible distance a cable can be installed from ground. There is a minimum distance e_{TARGET} that installation must observe for any cable; shorter distances than e_{TARGET} are unpractical to implement. Maximum distance is determined by space limitations, but cabling systems are always deployed as close as possible to the fuselage or any internal wall. The installation constraint requires that the clearance distance (between cable and ground plane) must be at least equal or greater than the lower boundary e_{TARGET}, then,

$$D - \frac{c}{2} - i \geq e_{TARGET} \tag{63}$$

D is also known beforehand as it is a geometrical requirement. Thus, conductor diameter c and insulation thickness i are the only variable (unknown) parameters. The conductor's diameter depends on the power requirements (ampacity) while the insulation thickness is related to the SOV value. There is an inversely proportional relationship between c and the EPS voltage given a fixed power requirement: a higher voltage results in a smaller c, a higher c allows implementation of lower voltages. Besides, insulation thickness depends on the SOV, that is, safer systems demand thicker insulations. Allow the calculation of SOV be performed with uniform field gap, i.e., using (60) and (61). By combining both equations, i can be calculated as,

$$i = \frac{\left(D - \frac{c}{2}\right)\left(\frac{V_{PASCHEN}}{SOV} - 1\right)}{\frac{V_{PASCHEN}}{SOV}\left(1 - \frac{1}{\varepsilon_r}\right) - 1} \tag{64}$$

$V_{PASCHEN}$ can be obtained by determining the lowest breakdown voltage (from a Paschen's curve similar to **Figure *5.2***) within the entire range of gap length for a specific application, given a flight altitude and expected environmental EPS temperature. The thickness in (64) is modified either by varying c or SOV, and it can be replaced in (63) so that a generalized geometrical constraint can be written.

Given the fact that cable manufacturers use standardized conductor's diameters, e.g., American AWG, British SWG, the diameter c belongs to a set of discrete conductors' values,

$$\mathcal{C} = \{c_1, c_2, \dots, c, \dots\}$$

However, some of the conductors in $\mathcal{C}$ can satisfy (63), while others cannot, for a given value of permittivity and SOV. Therefore, for a specific insulation material (fixed ε_r) and SOV, there is a subset $\mathcal{D} \subseteq \mathcal{C}$ that satisfies the geometrical installation constraint. The cable with the highest ampacity that satisfies this constraint is said to be the cable for which maximum power transfer $\mathcal{P}_{\mathcal{D}}$ capability occurs, therefore, for this SOV there is a maximum $\mathcal{P}_{\mathcal{D}}$ constrained by (63), in other words,

$$\mathcal{P}_{\mathcal{D}}|_{SOV} = \max(\{\mathcal{P}_1, \mathcal{P}_2, \dots\}) : (\mathcal{P}_{\mathcal{D}} \in \mathcal{D}) \wedge (\mathcal{D} \subseteq \mathcal{C}) \tag{65}$$

Consider a set of SOV values,

$$\mathcal{N} = \{n_1, n_2, \dots, n, \dots\}$$

By repeating this calculation for the n SOV values of set $\mathcal{N}$, several maximum power transfers are obtained, so that there are a set of n pairs of values {SOV, $\mathcal{P}_{\mathcal{D}}|_{SOV}$}. Then, the optimal voltage V^* can be determined by selecting the SOV* that provides maximum power transfer among all the n values of $\mathcal{P}_{\mathcal{D}}|_{SOV}$, then,

$$V^* = SOV^* \in \{SOV_1, SOV_2, \dots, SOV_n\} : \mathcal{P}_{\mathcal{D}}|_{SOV^*} = \max_n\left(\left\{\mathcal{P}_{\mathcal{D}}|_{SOV_1}, \mathcal{P}_{\mathcal{D}}|_{SOV_2}, \dots, \mathcal{P}_{\mathcal{D}}|_{SOV_n}\right\}\right) \quad (66)$$

By considering other insulation materials with different ε_r, a different V^* can be obtained.

In addition to maximum power transfer, cable weight can be introduced in the optimal voltage selection by considering the cable's power density, or relationship between power capacity and weight.

Let a cable have linear densities ρ_c and ρ_i for the conductor and insulation materials, respectively. The linear density represents the density per unit of wire length when the conductor's cross-sectional area is known (recall that volume equals the area of the cross-section multiplied by the length). For instance, a 10 mm^2 pure copper conductor (diameter is 3.57 mm) with a density of ~8.96 g/cm^3 results in a linear density of 0.448kg/m. The power to weight ratio ρ of the cable can be defined as,

$$\rho = \frac{\mathcal{P}}{\rho_c + \rho_i} \quad (67)$$

Which represents the amount of power capacity per unit of weight and length, i.e., the power density (in kW/kg/m). Similarly to the selection of optimal voltage based on maximum power transfer, an optimal voltage can be found by selecting the SOV that provides the maximum power density.

$$V^* = SOV^* \in \{SOV_1, SOV_2, \dots, SOV_n\} : \rho_{\mathcal{D}}|_{SOV^*} = \max_n\left(\left\{\rho_{\mathcal{D}}|_{SOV_1}, \rho_{\mathcal{D}}|_{SOV_2}, \dots, \rho_{\mathcal{D}}|_{SOV_n}\right\}\right) \quad (68)$$

$$\text{Where } \rho_{\mathcal{D}}|_{SOV} = \max(\{\rho_1, \rho_2, \dots, \rho_{\mathcal{D}}\})$$

The SOV for maximum power density is not necessarily the same as the one for maximum power transfer. However, it has been observed that both SOV values are close, so that a value in between suffices as the optimal voltage for the EPS.

5.2.4. General formulation for optimal voltage

The optimal voltage can be manually obtained by executing the following steps.

1. Set the aircraft application parameters, i.e., flight altitude and average temperature. These parameters are used to generate the Paschen's curve.
2. Set the requirements for e_{TARGET} and D according to geometrical specifications.
3. Obtain the Paschen's curve and determine $V_{PASCHEN}$ (lowest value for any gap length) [145].
4. Get the set $\mathcal{C}$ of power distribution cables, e.g., 10 AWG (5.26 mm^2) to 4/0 AWG (107 mm^2), with a specific insulation type with permittivity ε_r.
5. Calculate the corrected ampacities and linear densities ρ_c, ρ_i for the set $\mathcal{C}$.
6. Get a range of potential values for SOV, i.e., set $\mathcal{N}$. There can be n discrete SOV candidates.
7. Determine subsets $\mathcal{D}$ that satisfy the geometrical constraint (63) for each SOV.
8. Determine the maximum power transfer capability on sets $\mathcal{C}$ for each SOV, using (66).
9. Determine the maximum power density on sets $\mathcal{C}$ for each SOV, using (68).
10. Locate the maximum value among all the maximum power transfer capabilities and power densities. Identify the SOV voltages at which each maximum happens. The optimal voltage for the EPS is within both voltage values.

Corrected ampacity in step 5 refers to ampacity correction factors due to temperature difference, number of power cables in a bundle, altitude (pressure), alternating or direct current, and conductor type (copper, aluminium). Although the optimal SOV voltage can be manually obtained by following the steps above, an alternative optimization formulation is possible. This formulation can then be included in other design formulations and methodologies; (63) to (68) can be used to formulate the problem as follows,

O.P. 9 Objective: $\max \mathcal{P}$, $\max \rho$

$$D - \frac{c_{n,c}}{2} - \alpha_{n,c} i_{n,c} \geq e_{TARGET} \qquad \forall n \in \mathcal{N}, \forall c \in \mathcal{C}$$

subject to:

$$\mathcal{P} = \alpha_{11}\mathcal{P}_{11} + \alpha_{12}\mathcal{P}_{12} + \cdots \alpha_{21}\mathcal{P}_{21} + \alpha_{22}\mathcal{P}_{22} + \cdots \alpha_{\mathcal{N},\mathcal{C}}\mathcal{P}_{\mathcal{N},\mathcal{C}}$$

$$\rho = \alpha_{11}\rho_{11} + \alpha_{12}\rho_{12} + \cdots \alpha_{21}\rho_{21} + \alpha_{22}\rho_{22} + \cdots \alpha_{\mathcal{N},\mathcal{C}}\rho_{\mathcal{N},\mathcal{C}}$$

$$\sum_{n=1}^{\mathcal{N}}\sum_{c=1}^{\mathcal{C}}\alpha_{n,c}=1$$

$$\alpha_{n,c}\in\{0,1\} \qquad \forall n\in\mathcal{N},\forall c\in\mathcal{C}$$

Insulation $i_{n,c}$ is calculated with (64). **O.P. 9** is an integer programming (IP) problem because the search space is comprised of integer values: the cable set as well as the potential SOV values are finite sets (vectors of values). Still, steps 1 to 6 need to be performed. The coefficients $\mathcal{P}_{n,c}$ (power transfer) are obtained by calculating the power that the cable can transfer, e.g., voltage (SOV candidate) multiplied by current (cable's ampacity) for DC EPS, while $\rho_{n,c}$ (power density) coefficients are obtained with (67). The geometrical constraint in **O.P. 9** includes multiplication by Boolean $\alpha_{n,c}$ to discard the cable-SOV combination pairs that do not satisfy the constraint.

The optimal voltage selection problem in **O.P. 9** has linear constraints. However, it is a multi-objective problem because both power transfer and power density are maximized simultaneously. Following the formulation type 3 from **Table 3.1** where the objectives of a multi-objective problem can be written as a linear combination of objectives,

$$\max(c_1\cdot\mathcal{P}+c_2\cdot\rho)=\max\left(c_1\sum_{n=1}^{\mathcal{N}}\sum_{c=1}^{\mathcal{C}}\alpha_{n,c}\mathcal{P}_{n,c}+c_2\sum_{n=1}^{\mathcal{N}}\sum_{c=1}^{\mathcal{C}}\alpha_{n,c}\rho_{n,c}\right) \tag{69}$$

By replacing (69) in **O.P. 9** as the optimization objective, the optimal voltage selection can be solved as Mixed Integer Linear Programming (MILP) problem.

O.P. 10 Objective (69) (maximize power transfer and power density)

$$D-\frac{c_{n,c}}{2}-\alpha_{n,c}i_{n,c}\geq e_{TARGET} \qquad \forall n\in\mathcal{N},\forall c\in\mathcal{C}$$

subject to

$$\mathcal{P}=\alpha_{11}\mathcal{P}_{11}+\alpha_{12}\mathcal{P}_{12}+\cdots\alpha_{21}\mathcal{P}_{21}+\alpha_{22}\mathcal{P}_{22}+\cdots\alpha_{\mathcal{N},\mathcal{C}}\mathcal{P}_{\mathcal{N},\mathcal{C}}$$

$$\rho=\alpha_{11}\rho_{11}+\alpha_{12}\rho_{12}+\cdots\alpha_{21}\rho_{21}+\alpha_{22}\rho_{22}+\cdots\alpha_{\mathcal{N},\mathcal{C}}\rho_{\mathcal{N},\mathcal{C}}$$

$$\sum_{n=1}^{\mathcal{N}} \sum_{c=1}^{\mathcal{C}} \alpha_{n,c} = 1$$

$$\alpha_{n,c} \in \{0,1\} \qquad \forall n \in \mathcal{N}, \forall c \in \mathcal{C}$$

The formulation for finding an EPS optimal voltage in **O.P. 10** can be used to determine the system's voltage. Given that the optimal voltage selection is not influenced by the EPS architecture but only driven by maximum power transfer and power density (included in the performance specifications), it can be separately solved and adjoined to the architecture for evaluation and testing.

Now, having defined a voltage level, and prior to establishing a load flow problem, electrical characteristics for components and connections must be determined. First, the component location and cable selection problem can determine the length and type of cables, so that their electrical characteristic (i.e., admittance or impedance) can be calculated and then included in the admittance matrix of the load flow problem.

5.3. Component location and cable selection

Component location and cable selection are problems that are tied together because the cable selection mainly depends on the power transferred and the length between the components being connected (always observing standard and codes for aircraft installations). The distance between components directly depends on where they are located. In aircraft, component location is a 3D problem that is complex and difficult to solve. Consider the plane and side views of the aircraft shown in **Figure *5.5***.

The B373-400 aircraft shown in **Figure *5.5*** has an approximate total width of 28.7m, while the fuselage's width is approximately 3.7m. Components can be located along the fuselage and wings (plan view), and also along the fuselage's cross section (side view). Two components, A and B, are shown, connected by a blue line. In 3D, there are three variables (x, y, z) for the location of each component, and three variables for each turn, elbow, and harness for the connection between A and B. During preliminary design, such a

level of detail can be very time- and resource-consuming. Hence, approximations can be affordable at the cost of having a certain error.

If the 3D location problem for components A and B were approximated to a 2D location problem, two variables (x, y) for the location of each component and two variables per turn, elbow, and harness for connections are required. In this case, height is ignored, and the maximum error is around $\frac{3.7}{28.7}100 = 12.8\%$ assuming the fuselage is circular. If the approximation limits the location along the fuselage and wing lines of **Figure *5.5*** only, the error could reach up to $\frac{3.7\times2}{28.7}100 = 25.7\%$ during the preliminary design. This coud be acceptable in some cases, while for others the only option is designing in 3D.

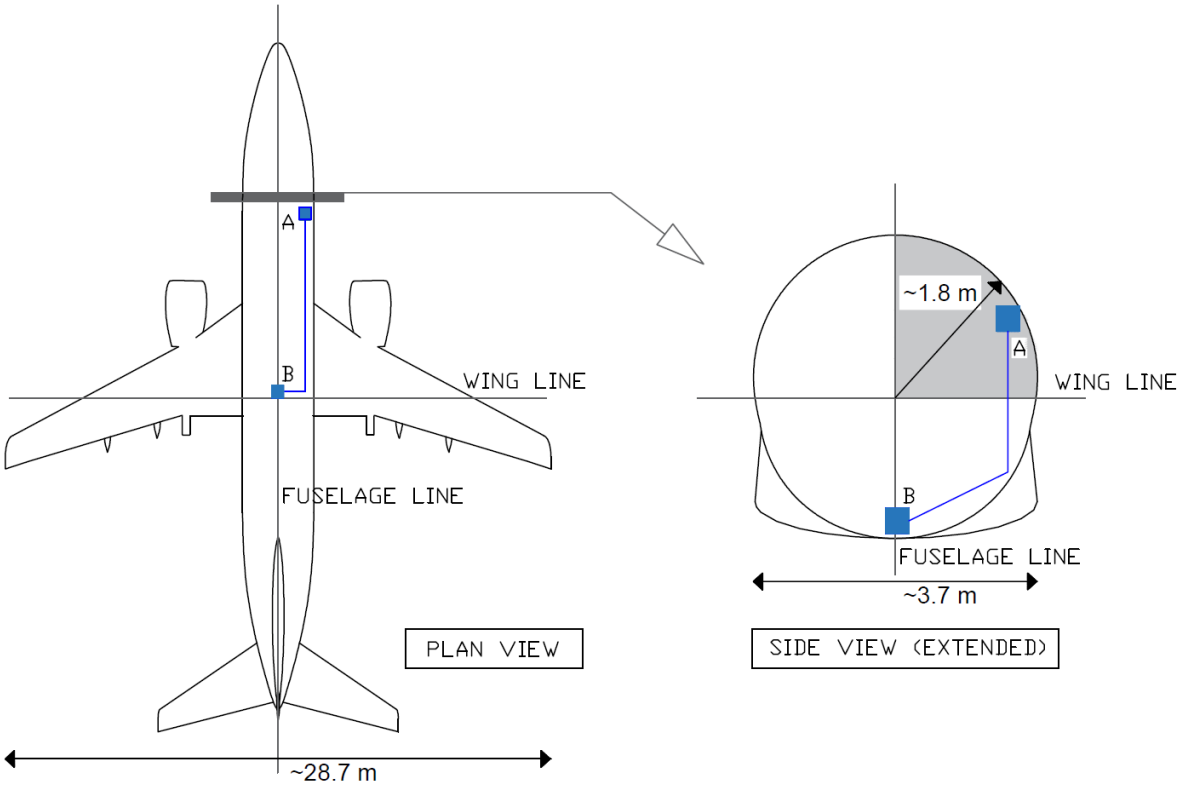

Figure 5.5 Plan and side view of a B737-400 aircraft.

Assume that the 3D location problem can be approximated to a 2D problem. Let the 2-dimensional space availability be represented with two straight lines, one horizontal line spanning from the tip of the left

wing to the tip of the right wing (wing line), and the other, vertical, line crossing from the cockpit to the aircraft's tail (fuselage line), as shown in **Figure *5.5***. The components can be in any position along each one of these two lines. If selected, a component i is in a unique position (m, n), then,

$$\begin{aligned} m_i^{\text{MIN}} x_i \leq m_i \leq m_i^{\text{MAX}} x_i \\ n_i^{\text{MIN}} x_i \leq n_i \leq n_i^{\text{MAX}} x_i \end{aligned} \qquad \forall i \in \mathcal{N} \qquad (70)$$

Where m_i, n_i are the abscissa and ordinate location variables for component i; $m_i^{\text{MIN}}, m_i^{\text{MAX}}$ are the permissible minimum and maximum abscissa location, and $n_i^{\text{MIN}}, n_i^{\text{MAX}}$ are the minimum and maximum ordinate location. If $x_i = 0$ in (70) (component i not selected), the location variables m_i, n_i are automatically set to 0. The connection's length l_{ij} connecting components i and j can be determined by,

$$l_{ij} = |m_i - m_j| + |n_i - n_j| \qquad \forall (i,j) \in \mathcal{A} \qquad (71)$$

In (71), the length is measured as the sum of the absolute difference of the components' locations (1-Norm). Euclidean distance (2-Norm) is not necessary as components are located along 2 axes only. To ensure that each component has a unique location, i.e., any component cannot be placed on an occupied position, the constraint for unique location is,

$$l_{ij} \geq \epsilon x_{ij} \qquad \forall (i,j) \in \mathcal{A} \qquad (72)$$

Where ϵ is a tolerance gap (distance gap) to force either $|m_i - m_j| \geq \epsilon$ or $|n_i - n_j| \geq \epsilon$ when connection x_{ij} is selected, hence $m_i \neq m_j$ or $n_i \neq n_j$. In addition to the location constraints (70) -(72), cable selection according to distribution line's length, voltage drop, and ampacity can be performed.

Once an optimal safe operating voltage (SOV) has been determined with **O.P. 10** considering maximum power transfer and power density for the specific aircraft application, the cable selection is a task that optimizes the cabling weight. Although the optimal SOV occurs at a specific wire gauge, it does not necessarily mean that all transmission and distribution lines are implemented with the same wire gauge. What this means is that there is a power transfer that is maximum at a voltage that is safe and such

transfer is achieved with a certain wire gauge. In fact, the system would be wasting energy carrying a payload that is not efficiently used. Then, the cable for each connection is selected based on the power requirements, length, and voltage drop.

For example, let a connection i, j require transporting 5 kW at 540 V in a DC system. The current in this circuit is 9.26 A and a 12 AWG cable (copper, 3.31 mm^2, 5.208 Ω/km) suffices to transport such current. Considering that a 1.5 % allowable voltage drop in a 540 V system is 8.1 V, the 12 AWG cable's length cannot go beyond 1560 m (this length is not the length within the aircraft, it is just an upper bound), otherwise, the voltage drop is higher than 8.1 V. If a larger distance were required in that installation, e.g., 1800 m, the cable must be changed to the next gauge (bigger cross-sectional area) to reduce the resistance and consequently reduce the voltage drop. Then, the connection's power requirement and length influence the gauge type or ampacity while observing the permissible voltage drop. Ampacity is determined by the power requirement, i.e., power flow transferred from i to j, while the voltage drop depends on the current established to achieve the power required.

Consider a set $\mathcal{O}$ of standard wire gauges that are commercially available (as in the optimal voltage selection problem of Section 5.2). Let a Boolean $c_{ij,o}^{\mathrm{AWG}}$ select a wire gauge o ($o \in \mathcal{O}$) such that $c_{ij,o}^{\mathrm{AWG}} = 1$ if selected (0 otherwise). Then, each connection x_{ij} that has been selected must have a unique wire gauge,

$$\sum_{o \in \mathcal{O}} c_{ij,o}^{\mathrm{AWG}} \leq x_{ij} \qquad \forall (i,j) \in \mathcal{A} \qquad (73)$$

Each wire gauge o has an ampacity coefficient I_o^{AWG}, and a resistance and weight per unit of length coefficients (linear resistance and linear weight) r_o^{AWG} and w_o^{AWG} respectively. Note that w_o^{AWG} is different from w_{ij}^{kW}, which is the inverse of the power density or power-to-weight ratio. Let the connection's voltage be V_{ij}^{SOV} (consider that there is a system's pre-defined SOV determined by the optimal voltage

selection in **O.P. 10**). The ampacity constraint ensures that the connection's i,j current is less than or equal to the ampacity I_o^{AWG} from the wire gauge o, then,

$$\frac{P_{ij}}{V_{ij}^{\mathrm{SOV}}} \leq \sum_{o \in \mathcal{O}} I_o^{\mathrm{AWG}} c_{ij,o}^{\mathrm{AWG}} \qquad \forall (i,j) \in \mathcal{A} \qquad (74)$$

Where the left-hand term represents the current flowing through connection i,j. Now, let the maximum permissible voltage drop be V_{MAX}^{DROP} in p.u. (per unit). The drop constraint ensures that the voltage drop across the connection is less than or equal to the maximum permissible voltage drop, then,

$$\frac{P_{ij}}{V_{ij}^{\mathrm{SOV}}} r_o^{\mathrm{AWG}} l_{ij} \leq V_{MAX}^{\mathrm{DROP}} V_{ij}^{\mathrm{SOV}} + V_{ij}^{\mathrm{OP}} \left(1 - c_{ij,o}^{\mathrm{AWG}}\right) \qquad \forall (i,j) \in \mathcal{A}, \forall o \in \mathcal{O} \qquad (75)$$

Where (75) has been written in Big-M notation [32]. V_{ij}^{SOV} is the value of the optimal voltage (SOV) calculated with **O.P. 9**. When $c_{ij,o}^{\mathrm{AWG}} = 1$, (75) enforces the voltage drop to be less than or equal to $V_{MAX}^{\mathrm{DROP}} V_{ij}^{\mathrm{SOV}}$, otherwise the voltage drop is arbitrarily set. Finally, the cable selection constraints (73) -(75) allow cabling weight minimization.

In summary, constraints (70)-(75) are introduced as component location and cabling selection constraints to optimize system weight and achieve higher performance. To complete the component location and cable selection problem, the objective of the optimization problem can be written as the minimization of total cabling weight, in other words,

$$\min\left(\sum_{(i,j) \in \mathcal{A}} \sum_{o \in \mathcal{O}} c_{ij,o}^{\mathrm{AWG}} w_o^{\mathrm{AWG}} l_{ij}\right) = \min\left(\sum_{(i,j) \in \mathcal{A}} w_{ij}\right) \qquad \forall (i,j) \in \mathcal{A} \qquad (76)$$

Where w_o^{AWG} is the linear density of the cable type o (as defined previously), $c_{ij,o}^{\mathrm{AWG}}$ is the wire gauge selection Boolean, and l_{ij} is the cable's length given by (71). In the weight minimization of (76), the cable weight w_{ij} is equal to the product of linear density (in units of weight per unit of length) and length. In

summary, the optimization formulation for the component location and cable selection problem can be written as follows.

O.P. 11 Objective: (76) (minimization of cabling weight)

subject to: Location constraints (70)-(72)

Cable selection constraints (73)-(75)

A simple inspection of the objective and constraints in **O.P. 11** indicates that the component location and cable selection is a non-linear problem. The linearization techniques detailed in Section 4.2 are valid for linearizing the non-linearities in constraints and the weight minimization objective. Linearization of absolute values in (71) (calculation of the connection's length) can be performed according to techniques in [149]. Besides, there is a bilinear term in the left-hand side of (75) (voltage drop constraint), i.e., $P_{ij}l_{ij}$, that can be replaced by a variable δ_{ij} and a set of linear constraints in the form of a two-dimensional piecewise linear function (PWL), or a McCormick envelope. Finally, the bilinear term in the weight minimization objective in (76) can be straightforwardly replaced by a set of inequality constraints as in [150]. Unlike previous bilinear terms that are products between two real variables, the bilinear term in (76) is the product between a real variable and a Boolean (expressed as 0 or 1). The main idea behind linearization is to produce tight constraints to achieve good accuracy because any linearization is in fact an approximation of the original problem.

After determining the component location and cable selection, the admittance (electrical characteristic) of each connection ij can be calculated as the inverse of the product between the r_o^{AWG} (resistance per unit of length corresponding to the wire gauge o selected for connection ij) and the length of connection ij, thus,

$$\mathrm{admittance}_{ij} = \frac{1}{r_o^{\mathrm{AWG}} l_{ij}} \qquad \forall (i,j) \in \mathcal{A} \qquad (77)$$

This admittance is calculated for all the connections ij. Then these values are used in the construction of the admittance matrix of the load flow problem. Finally, the electrical characteristics of the distribution components (components' models) must be determined before attempting a load flow formulation. In MEA EPS, the majority of distribution components are based on power electronic converters. Such modelling for power converters and other distribution components is comprehensively detailed in references [8], [136], [151], [152].

5.4. Load Flow in EPS architecture

Load flow is a vital task for evaluating the performance of an EPS. It is the steady state analysis of a power system network where the operating state of the system for a given loading is determined. However, load flow of electrical networks can be complex to solve and require iterative methods to obtain a solution due to the non-linear relationship between voltages and currents [136], [152]. An efficient approximation of a load flow problem aims to include performance evaluation in the general design task. First, the load problem demands a representation (model) of the EPS that captures the components' steady state behavior. Then, a set of electrical equations relating voltages, currents, and power magnitudes are solved to obtain the system's state. The load flow uses the system's power balance for solving unknown currents and voltages. Power balance constraints have been already introduced in the EPS architecture design,

- In the original EPS design problem, (5), formulation **O.P. 2**, in Chapter 3
- In the GS&GLP subproblem, (26)-(27), formulation **O.P. 5**, in Chapter 4
- In the PDD subproblem, (31) in formulation **O.P. 6** (distribution path as a series-system), (41) in formulation **O.P. 7** (resilient design for a failure set), (46) in formulation **O.P. 8** (resilient design with two-disjoint paths), in Chapter 4

These power balance constraints considered electrical power as a flow that must be balanced on every component of the system, such that the source (outgoing) flow can reach the load, that is, the system is

lossless. This is because the EPS architecture is an outcome that is topological, i.e., it contains a network structure that allows electrical flow to be transported between sources and loads. The synthesized EPS provides sufficient generation and distribution to achieve the reliability targets (overcome unexpected failures and always supply critical loads).

With the obtention of an optimal EPS voltage (safe operating voltage), the power balance equations are extended to include calculation of voltages and currents to obtain the steady state of the EPS, that is, the power balance equations are extended to become the load flow constraints.

5.4.1. The EPS load flow problem

There is a large variety of components in a power system. Each component has a group of physical characteristics expressing how electricity is transferred from its input to the output. The load flow uses the representation of steady state electrical characteristics of components as a matrix of interconnected components, i.e., network of components, that allows the definition of nodal equations. The interconnection of components is based on the transmission of power through the distribution system, beginning at the power sources' terminals and ending at the loads. In the analysis of systems with two or more components, the network model takes the form of a *network matrix* whose elements are determined by the interconnection characteristics.

The interconnection characteristics basically relate electrical current flow, voltage at the input and output terminals, and power values at steady state, i.e., the behavior is unchanging in time, all dynamics and transients have vanished. In this context, the state of the system is a collection of parameters (state variables) that simply describe the system's behavior at a particular time. In an EPS, the state variables are the currents, voltages, and powers at the different components' terminals or nodes. These terminals are also known as *buses* and are considered as nodes where other components can be connected to. It is between these buses that the network matrix holds the interconnection characteristics. In the load flow

studies, the admittance matrix is the most utilized network matrix because the power flow equations (nodal equations) of the load flow problem are amenable for dropping or adding terms when connections and disconnections occur. This is essential for topology reconfiguration and efficiency maximization.

The mathematics of the load flow problem is covered in detail in textbooks on power system analysis, e.g., [136], [152]. Material on load flow analysis (for the non-electrical background reader) has been condensed and explained in Appendix I to avoid overloading this section with power system analysis details. This appendix is self-contained and has detailed explanation of how to formulate the load flow problem from scratch for an EPS. Load flow problems for DC and AC systems are also determined. Because DC systems are attractive for future MEA, the load flow formulation for a DC EPS is presented here:

$$\begin{gathered}\text{Find unknowns given a set of specified } V \text{ and } P\text{, such that: } \operatorname{diag}(\boldsymbol{V})[\mathbf{G}]\boldsymbol{V} = \boldsymbol{P} \\ [\mathbf{G}]\boldsymbol{V} = \boldsymbol{I}\end{gathered} \tag{78}$$

Where $\boldsymbol{V}$ is the voltage vector (voltages in all buses), $\boldsymbol{I}$ is the current vector (currents in all buses), $\boldsymbol{P}$ is the power vector (powers in all buses), and $\mathbf{G}$ is the admittance matrix that represents the electrical characteristics of the EPS components (load flow in matrix notation). For a DC system, $\mathbf{G}$ is known as the *conductance* matrix. Because there are components that can supply or consume power and current at each bus (no connection to other buses is involved), the current vector $\boldsymbol{I}$ in (78) can also be written as below:

$$[\mathbf{G}]\boldsymbol{V} = \operatorname{diag}(\boldsymbol{G^0})\boldsymbol{V} + (\boldsymbol{P}^0 \oslash \boldsymbol{V}) + \boldsymbol{I}^0 \tag{79}$$

Where $\boldsymbol{P}^0$ is the local (in the bus) power consumption (or supply), $\boldsymbol{I}^0$ is the local (in the bus) current consumption (or supply), and $\boldsymbol{G^0}$ is the conductance of a component that consumes power or current. The $\oslash$ symbol represents the division-wise operation. In any bus i, the current is,

$$\sum_{n=1}^{N} G_{in}V_n = g_i^0 V_i + \frac{p_i^0}{V_i} + i_i^0 \tag{80}$$

Where p_i^0, i_i^0, and g_i^0 are the local bus power, current, and conductance. When both sides of (80) are multiplied by V_i, the following power expression applies,

$$V_i \sum_{n=1}^{N} G_{in} V_n = g_i^0 V_i V_i + p_i^0 + i_i^0 V_i \tag{81}$$

Which is the power flow equation for bus i. Following the power balance notation in (31) (see Section 4.3.2 on power distribution design), (81) can be written as,

$$\sum_{n=1}^{N} P_{in} = \sum_{n=1}^{N} P_{in} - \sum_{n=1}^{N} P_{ni} = P_i \tag{82}$$

Where $P_{in} = G_{in} V_i V_n$ and $P_i = g_i^0 V_i V_i + p_i^0 + i_i^0 V_i$ according to (81). The left-hand side of (82) is divided into incoming ($i \rightarrow$ other buses n) and outgoing (other buses $n \rightarrow i$) power flows in the middle equivalence of (s). Also, P_i is equivalent to $d^{GEN} - d^{LOAD}$ as bus i can be injecting/consuming power via connected devices. Still, power balance is preserved and the expressions (31), (81) and (82) are equivalent.

5.4.2. Linearization of the DC Load Flow

The set of power flow equations for the DC load flow of (78) is quadratic, non-affine [153], and non-convex which can lead to multiple solutions [154]. Solving a DC load flow is not trivial due to the non-convexities of the solution space, hence gradient-based iterative methods are also used. The main drawback of iterative methods is the processing time required. Besides, these methods are not amenable to be introduced directly as constraints into design optimization problems. Some issues are,

- The initial conditions of the load flow problem must remain unchanged until a solution is reached.
- A set of internal auxiliary parameters are continuously updated but are not part of the solution.
- Iterative steps are dependent upon each other, previous results are used to recalculate new ones.

If initial conditions must remain unchanged to solve a load flow (evaluate the EPS's performance), then tasks such as LP-based optimal topology reconfiguration are not possible because during the optimization

search, potential candidates' performance must have been already evaluated to select the optimal among them[2] (or at least the candidates' performance must be a linear function). Besides, it is not possible to solve load flow for all the elements of the search space. On the other hand, if iterative steps are dependent from each other (result from previous step is used in the next), parallel processing is hard to implement. Therefore, an accurate approximation aims to simplify the obtention of a solution very close to the global solution (of the original non-linear problem).

The aim is to convert the load flow problem into a Mixed Integer Linear Programming (MILP) optimization for achieving an optimal performance, e.g., minimum losses. Several techniques have been developed to increase the effectiveness of a MILP such as piecewise linearization, rolling horizon approach (problems with several time-periods), dimensionality reductions, among others [108]. The non-linearity comes from the bilinear terms $V_i V_j$ and V_i^2 in (81). The presence of these quadratic terms means the following:

- V_i^2 can be accurately approximated with a PWL function.
- $V_i V_j$ can be linearized with two-variable piecewise linear functions (2-PWL) or using McCormick envelopes (McCE).

The tightness of these approximations must be ensured so that the solution is accurate at least by a tolerance $\epsilon \leq \epsilon_{TARGET}$. **Figure *5.6*** depicts a voltage bilinear term; in the operational range [0.8, 1.2] p.u. (p.u. is the normalized value), a linear approximation is feasible because the search space resembles a plane, although it is not.

[2] On the other hand, any non-linear load flow solver can be freely used with heuristic algorithms, e.g., Particle Swarm Optimization, because search is then performed by iteratively repeating a set of steps.

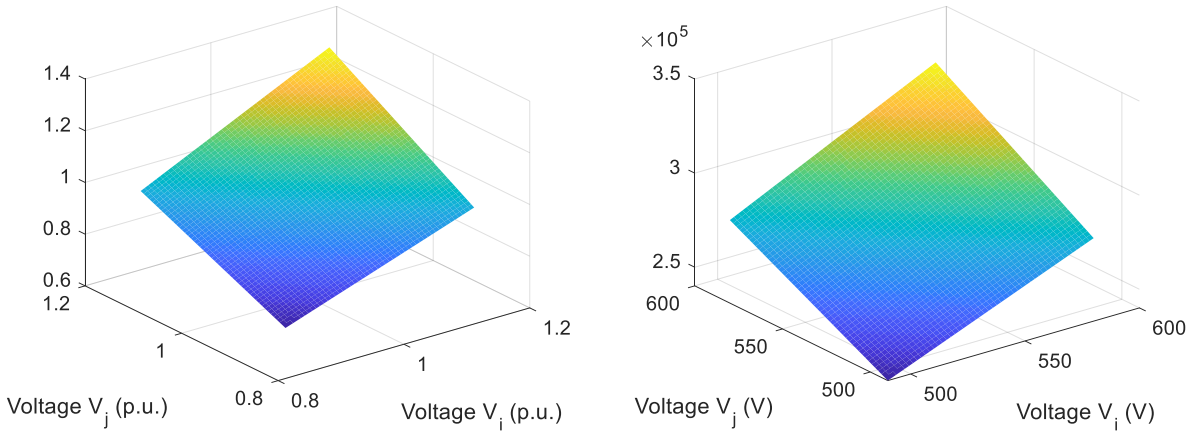

Figure 5.6 Bilinear term $V_i V_j$ in the feasible operating range, in p.u. (left), in real values around 540 VDC (right).

For quadratic terms V_i^2, PWL approximates the square function to linear segments between breakpoints. While a large number of breakpoints provides higher accuracy, the number of variables increases as well. However, there are methods that obtain an optimal number and location of breakpoints along the feasible range of values that the variable can take [155], [156].

Approximations of bilinear terms with 2-PWL generates an explicit function that is not necessarily continuous and differentiable by using Special Ordered Sets of order *k* (SOS*k*) [120] or other techniques based on interpolation [157]. The two-variable function is divided into a grid (surface segments) and a set of Boolean and continuous variables are used to select a value within a single segment only.

The McCE is also based on the piecewise principle, but it generates a surface that is limited by a set of 4 inequalities (upper and lower boundaries), i.e., an envelope that wraps the function between the bilinear feasible range. These boundaries have the following form:

$$\begin{aligned} w_{ij} &\geq V_j V_{MIN} + V_i V_{MIN} - V_{MIN} V_{MIN} \\ w_{ij} &\geq V_j V_{MAX} + V_i V_{MAX} - V_{MAX} V_{MAX} \\ w_{ij} &\leq V_j V_{MAX} + V_i V_{MIN} - V_{MAX} V_{MIN} \\ w_{ij} &\leq V_j V_{MIN} + V_i V_{MAX} - V_{MIN} V_{MAX} \end{aligned} \tag{83}$$

Where the bilinear term $V_i V_j$ has been replaced with a continuous variable w_{ij}, V_{MIN} and V_{MAX} are the minimum and maximum values (within the operating range) that V_i, V_j can take. Then, the power balance for bus i in (81) (DC EPS), can be written as below.

$$\sum_{n=1}^{N} G_{in} w_{in} = g_i^0 V_i^2 + p_i^0 + i_i^0 V_i$$

In addition, the constraints in (83) are included for every bilinear term $V_i V_j$. Now, the linearized version of the DC load flow problem can be compactly written as below:

O.P. 12 Objective: find unknowns given a set of specified V and P

$$\sum_{n=1}^{N} G_{in} w_{in} = g_i^0 V_i^2 + p_i^0 + i_i^0 V_i$$

subject to

Constraint (83) $\forall i \in N$ (all buses)

$$w_{in} = V_i V_n$$

Power flow formulation in **O.P. 12** can be used in any DC system.

Recap (intermediate)

At this point, an optimal voltage selection (based on [158]), a component location and cable selection, and the load flow problems have been presented. Having calculated the optimal voltage (Section 5.2, problem **O.P. 10**), the component location and cable selection can be performed (Section 5.3, problem **O.P. 11**) (admittances of connections can be determined with (77)), then the load flow (Section 5.4, problem **O.P. 12**) can be solved. The load flow determines the system's state in steady state, i.e., no dynamics or transients are considered. The relationship between the proposed design framework and the performance evaluation through optimal voltage selection, component location and cable selection, and load flow is depicted in **Figure *5.7***.

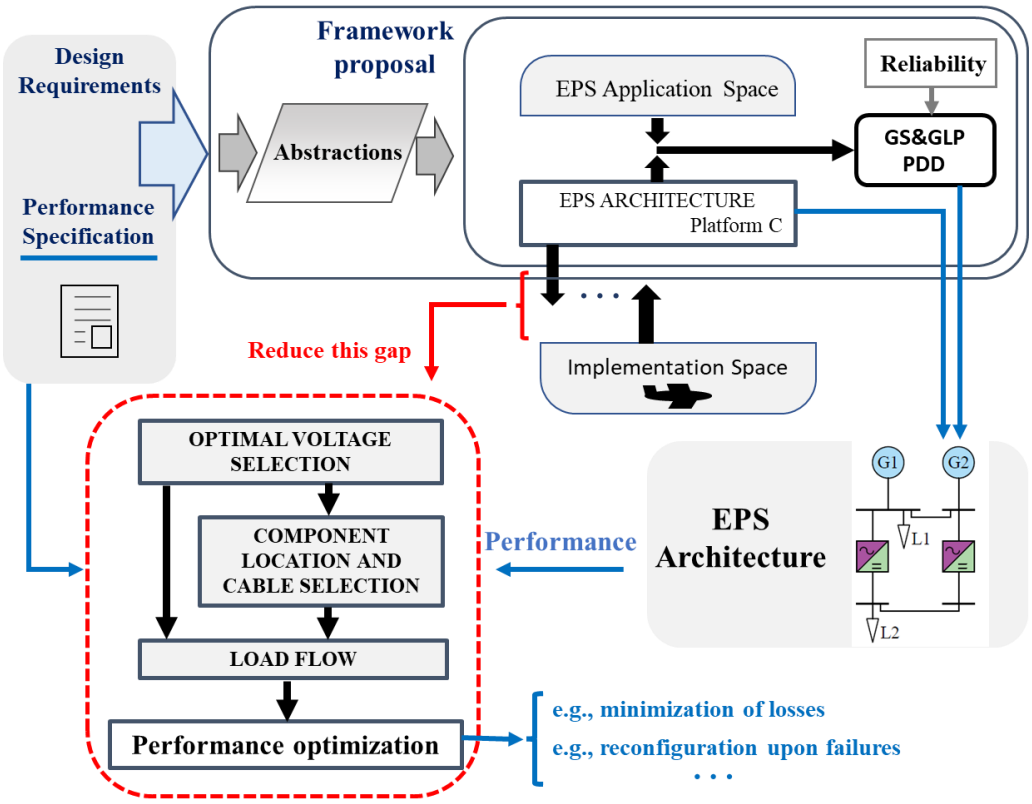

Figure 5.7 Performance evaluation within EPS architecture design.

With the definition of an optimal voltage, a component location and cable selection can be performed. Cable selection provides the admittance of connections via (77), which then can be used to build the admittance matrix for the load flow problem. The rest of the power distribution components can be modelled (for static or steady state analysis) following references [136], [151], [152]; modelling of power distribution components is out of the scope of this work. After component location and cable selection, the load flow problem can be solved, and the steady state can be identified for a given EPS condition. The system's state can then be improved (optimized for the same EPS condition) in order to make the best out of the available resources, i.e., performance optimization, which is considered next.

5.5. Performance Optimization

The evaluation/testing of a power system architecture according to the conventional design flow (CDF) has been depicted in **Figure *2.1***. The main disadvantage of this approach in the design of disruptive architectures is the iterative loop (for performance evaluation and consequent new specifications) that consumes a lot of resources, time, and effort. The design framework proposed in Chapter 3 aims to reduce the design effort by non-iteratively solving two subproblems (GS&GLP and PDD with reliability-based formulations in Chapter 4) having identified the relationship between the industry drivers (observations and insights) and defined a series of abstractions. EPS operation is realized by the control system that achieves the required performance. However, the synthesis of this controller belongs to a new problem following PDD. The controller determines the operational state (for any given condition) and optimization of resources during operation. Within these requirements, there are performance specifications that need to be satisfied during operation of the EPS architecture.

The system's required performance is part of the specifications, and it is also used in the evaluation/testing step. It can be assumed that, because the system was built to satisfy the specifications, it must also successfully comply to the testing assessment. It is possible to formulate architectural design and performance evaluation into one problem that is solved for all the states before operation[3]. However, such a problem can dramatically increase complexity as all the system's states must be solved for, and the design objectives (weight and cost minimization, and efficiency and reliability maximization) will share their importance with the system's performance indexes as well, thus, extending the complexity of the

[3] There is an approach for special systems that experience very-fast changes in the operating conditions for which it is more appropriate to solve for all the future operational states and perform a quick look-up, rather than re-calculate every time there is a change. This is known as *multi-parametric programming* [188] and it helps in dividing the parameters' space into regions. The regions are separated by functions and the parameters fall within a certain region bounded by these functions. Nevertheless, it is not a complete enumeration but a function evaluation.

trade-off in the multi-objective optimization. It is not necessary to follow such an approach as the performance specifications serve both problems (architecture design and evaluation), such that the same specifications, expressed differently, drive architecture design (task one) and putting the system in a certain state (task two), separately.

5.5.1. Operation after EPS design

Consider the following example. Let the construction of an EPS architecture be performed using the GS&GLP and PDD formulations, such that the system is resilient for a set of failures in components. Let this EPS architecture be as shown in **Figure *5.8***. Features of this architecture are,

- It has enough components and connections to re-route power in case of failures in a converter and/or generator
- Its topology allows the formation of alternative distribution paths to route power in case of failures.

Neither are all the components in the architecture energized, nor are all the connections closed during normal operation. In the normal state, G1 is supplying L1 and L2, and no failure has occurred yet.

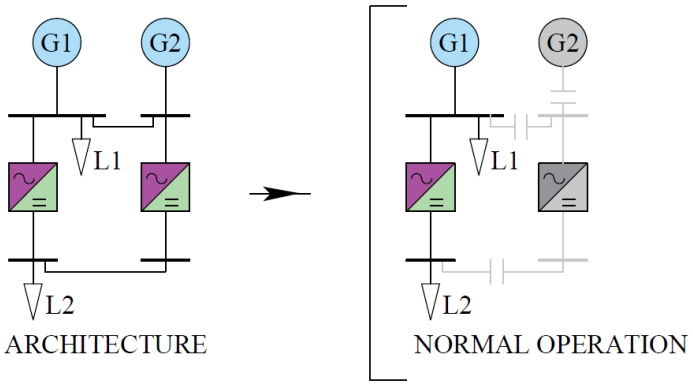

Figure 5.8 Example of EPS architecture in normal operation.

In case unexpected failure happens, the system can no longer remain in the normal state. Assuming that failure events cannot happen simultaneously, a reconfiguration method must be determined. The system is brought to a new operational state by forming alternative distribution paths (different than the normal state); this is known as reconfiguration of the system. In fact, the EPS has been designed to have alternative paths in case of failures, so the system's topology is reconfigurable. This reconfiguration can be the result of performance index optimization, e.g., minimum number of disconnections and re-connections, minimum losses, etc. In order to execute performance optimization, the system state must be known in order to make the transition to a new (reconfigured) state. Then, the load flow can be used to determine the next state as shown in **Figure *5.9***. The optimal voltage (using **O.P. 10**) has been determined to be 1.2 kV (just as an example). Then, component location and cable selection have provided admittances for connections; the rest of component static (steady state) models have also been determined. Under the occurrence of failures, a performance optimization (minimization of losses) is performed to find the new reconfiguration states (at the right of **Figure *5.9***).

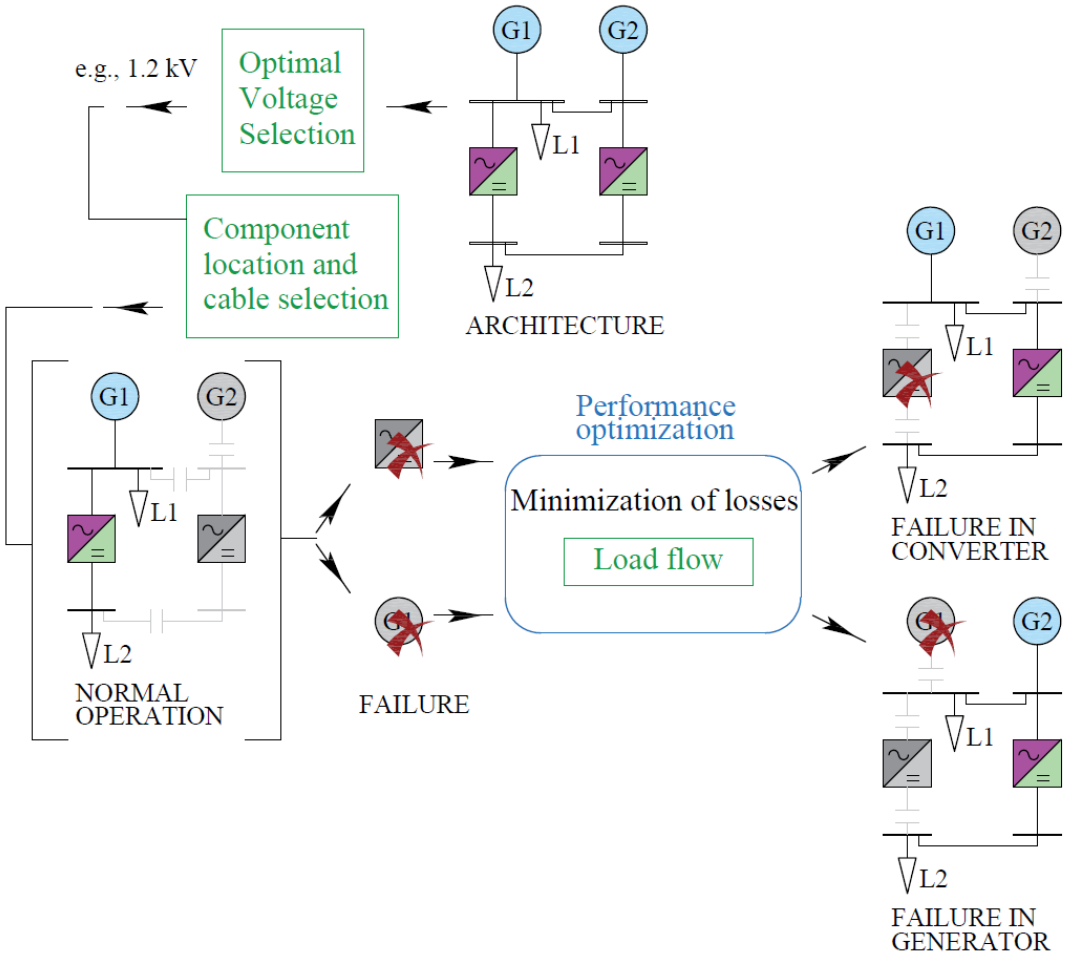

Figure 5.9 Example of EPS reconfiguration after performance optimization with load flow.

In the case that a second failure occurs (after the first one), the performance optimization is triggered and executed again so that a new state (EPS topology) can be obtained. Reconfiguration is possible because there is a sufficient number of alternate distribution paths; the EPS has been designed to allow formation of alternate paths, and the tests verify the response of the EPS during the reconfiguration (as presented in the experimental testbed in Chapter 7).

Performance optimization is not the only method that can be used to find a new state and reconfigure the system. The optimization problems in GS&GLP and PDD can also serve as a base to formulate reconfiguration problems for EPS operation, e.g., to minimize the number of generators used, maximize generators' efficiency under low load conditions, etc. Besides, other algorithms also brought from the

network design field can be used to find a new reconfiguration state. For example, the shortest path algorithm is amenable to finding alternative paths in case the main path breaks. Also, a combinatorial logic can be determined to perform a lookup task, based on the current condition, to pick a new state. In combinatorial logic, there is a state enumeration, i.e., it lists all the possible states the system can support, and each state has an associated list of conditions that are to be met if that state is enforced. The disadvantage of combinatorial logic is that it is not easy to scale-up to large EPS; only small EPS can be supported, e.g., an EPS with fewer than 9 fallible components can generate fewer than a few hundred states. An example of a combinatorial logic implementation for an EPS testbed is presented in Chapter 7. On the other hand, more complex control techniques including performance optimization and reconfiguration can be synthesized (see literature review in Chapter 2) but these approaches demand expertise in computer science languages and tools. In general, the formulation of such control for an EPS architecture corresponds to controller synthesis techniques, which are outside of the scope of this work.

5.5.2. Types of performance optimization problems

There are dozens of problems related to the optimization of the EPS performance, but they can be broadly enclosed in the following types of problems:

- Topology reconfiguration in case of failure in components (or connections)
- Optimization of a performance index to achieve maximum efficiency

The latter type, optimization for maximum efficiency involves the former type, topology reconfiguration and adjustment of power flows of generators and power distribution components (power allocation, distribution of power among generators and converters, etc.). However, the former type, topology reconfiguration, does not necessarily involve the latter type, optimization for maximum efficiency, (see **Figure *5.10***) because reconfiguration can be triggered by a failure event and the system is just brought to a new state to avoid interrupting power supply to critical loads.

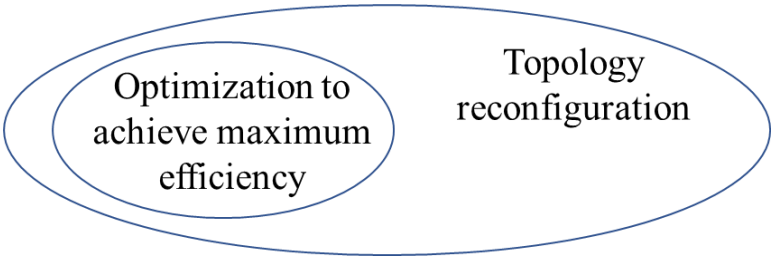

Figure 5.10 Relation between topology reconfiguration and optimization for maximum efficiency.

Both topology reconfiguration and optimization for maximum efficiency can be directly related to efficiency maximization. The system must be efficient enough to meet the aviation sustainability targets (see Chapter 1), that is, to reduce the emissions through an increasing reduction in fossil fuel consumption. If the EPS is not efficient, the generation system will consume more fuel than is required and the distribution system will transfer this energy to the loads at the cost of increasing losses.

Because the EPS architecture is constructed by reliability-based optimization formulations (centered on achieving a certain level of reliability), topology reconfiguration is the first performance optimization problem. In this problem, the system's connections are opened/closed in order to form a group of distribution paths that route power from sources to loads. In the normal state, some connections are normally opened, and others are normally closed. Any unexpected failure event triggers the task of determining a new state, i.e., entering a reconfiguration state (different from the normal state) that delivers power to the loads through alternative distribution paths (some connections are closed, and others are opened to form these alternative paths). This problem has been extensively studied in the power system field as optimal transmission switching [70], however, it has rarely been applied in the aerospace field.

The problem is the optimization of a performance index for achieving maximum efficiency. There could be several indexes to determine the system's performance, e.g., efficiency, reliability, among others. At the same time, efficiency can be measured by the losses the system has, by the consumption of fuel due

to electrical generators, by the amount of emissions that the engine has released to the environment, etc. In the EPS context, the efficiency can be effectively quantified as the losses the system incurs. Then, the optimization of efficiency during operation can be stated as a loss minimization problem.

5.5.3. A performance optimization problem

Having designed the EPS architecture by optimization of weight, reliability, efficiency, and cost in the GS&GLP and PDD problems, the next problem to solve is how to operate the system in an optimal manner. Efficiency becomes the main operational parameter to optimize because:

- After designing the EPS architecture, the system's weight is fixed, i.e., all the components included in the generation and distribution systems are known, and their weight has been established.
- There is enough generation and distribution capacity to consider the system as resilient, hence, it provides high reliability. In normal state, there are distribution paths that deliver power to the loads. Upon unexpected failures, other distribution paths can be formed. Thus, the reliability constraints used for designing the EPS architecture can be dropped during the operation optimization. However, reliability can be included in operational problems whenever safety is critical under exceptional circumstances, for example, a sequence of multiple failures that require reconfiguration for maximum reliability and safety (regardless of efficiency).
- The EPS design costs no longer apply once the system has been synthesized. As in the case of weight, the system's design costs can be dropped from operational optimization. Although there are operational costs, these costs can be directly related to the operational efficiency. In fact, there is a roughly proportional relationship between efficiency and operational cost; an inefficient system wastes more and consequently has higher costs, while an efficient system keeps the operational costs to a minimum.

Therefore, the optimal performance problem is centered around finding an optimal efficiency point of operation for a given condition. The core of the optimal efficiency problem (optimization of performance) is the determination of the state variables such that the efficiency (in terms of the state variables) is maximized. For such determination, the system's model (steady state) must be defined via the obtention of an admittance matrix. However, the EPS architecture designed with the GS&GLP and PDD problems contains components and connections whose characteristics are still declared at the functional level, i.e., components are defined in terms of functionalities to allow synthesis of an architecture. The admittance matrix requires a steady state model of each component, that is, the relationship between voltages and currents at their terminals. This demands an increase in the level of detail (decreasing the level of abstraction), from functionality to establishing steady state electrical behavior. Therefore, the optimal voltage selection and load flow problems were introduced as tools to achieve this transition.

In this work, performance optimization has been focused on the steady state, that is, obtaining a new state (new point of operation) after the system has experienced a change in its conditions. This is common practice in power system engineering [136], [152]. However, there is also optimization *during* the transition between two states, that is, optimization of the dynamic response of the system. This is out of the scope of the present work. The relation between steady state and dynamic performance optimization is shown in **Figure *5.11***. Nevertheless, dynamic performance optimization will be studied in the future as a part of controller synthesis within the power and energy management systems.

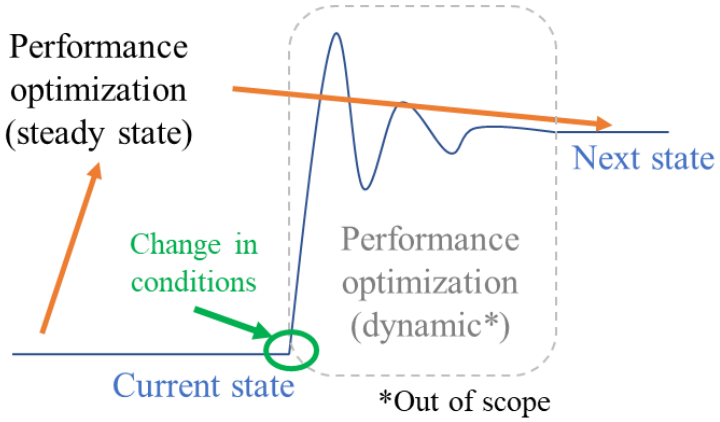

Figure 5.11 Performance optimization including steady-state and dynamic.

The state of the system can be obtained by solving a load flow problem. Given that DC systems are attractive for the implementation of electrical networks for MEA, the rest of the chapter's formulations are focused only on DC systems (see formulation for DC load flow in **O.P. 12**). The power flow equations of the DC load flow can replace (31) (power balance) in the PDD subproblem because,

- The cabling losses are not negligible. This loss depends on the cable's resistance and the square of the current flowing through it. Cable ohmic loss minimization aims to maximize the system's efficiency. In the component location and cable selection of Section 5.3, the positions of components within the aircraft and the cabling length were solved, that is, the optimization solves for the optimal location and the shortest cabling length. Afterwards, during operation, cabling losses depend only on the current.
- The converter's losses depend on the voltage levels at its terminals. Delivering constant power requires continuous adjustment of current values whenever there are changes in voltage values. Ideally, non-variant voltages produce no changes in current, and output power is constant. When output power is modified, current is stepped up or down accordingly. The values of voltages, currents, and power flows can be mapped to generate an efficiency map (efficiency chart) that could be used for the converter's efficiency calculation in the load flow problem.

In general, there are efficiency functions in terms of voltages, currents, temperature, etc., for every component in the EPS. Apart from voltages and currents, the rest of the parameters could be ignored given that their impact is insignificant, or these parameters can be represented as functions of other parameters at a nominal operation point. For instance, a cable that operates normally at a high temperature can be modelled with an ampacity corrected by temperature, that is, instead of including the temperature as a variable in the problem, corrections factors (coefficients) for current capacity can be used.

Topology reconfiguration

A reconfiguration is the arrangement of open/close connections including the activate/disactivate command sent to components (by the controller). The idea is that different distribution paths are formed in the EPS so that power from generators to loads can be re-routed based on a given criterion. Among the criteria, there are,

- Shortest path from generator to loads. This is a classical network problem where each connection and component have a 'weighting factor' which is used as a parameter to drive the total 'weight' value of the path. The path that has the least total weight value is the shortest one.
- Maximum throughput. The aim is to arrange the system such that the maximum amount of flow (power in this case) from sources to loads can occur. The components and connections are mostly working at their maximum possible rating.
- Minimum operational cost. This can be also translated to a maximum efficiency problem, as previously mentioned in Section 5.5.2. Note that the operational cost includes fuel consumption, losses, etc, but excludes design cost.
- Assignment and matchings. The formation of a distribution path follows a pre-specified assignment between source and load, similar to the generator-load pairing arrangement

established in GS&GLP. For any system's state, several assignments could be implemented based on different system's parameters, e.g., the sudden increase of a load could temporarily demand a different generation assignment.

- Failure recovery. Reconfiguration can be driven by load criticality, in other words, the system is reconfigured such that critical loads continue to be supplied. The aim is to overcome the interruption, continue supplying power, and possibly isolating the fault. In this criterion, any of the previous criteria can also be included.

In general, the reconfiguration formulation can be similar for all the criteria above, the difference resides in the reconfiguration's purpose. Hence, each criterion can provide a different outcome. Let y_{ij} be a Boolean that performs the selection of connection i,j ($y_{ij} = 1$ when selected, 0 otherwise) as in Chapter 3 and Chapter 4. The reconfiguration of an architecture's topology is similar to the Optimal Transmission Switching problem proposed in [70], then, for the open/close selection of connection i,j the constraints are,

$$\begin{aligned} P_{ij} &\leq G_{ij}\left(V_i^2 - V_iV_j\right) + M\left(1 - y_{ij}\right) \\ P_{ij} &\geq G_{ij}\left(V_i^2 - V_iV_j\right) - M\left(1 - y_{ij}\right) \end{aligned} \qquad \forall (i,j) \in \mathcal{A} \qquad (84)$$

Where M is a big and positive value to enforce the following when $y_{ij} = 1$, otherwise P_{ij} is unconstrained by this inequality[4] [32]:

$$P_{ij} = G_{ij}\left(V_i^2 - V_iV_j\right)$$

The quadratic term V_i^2 and bilinear term V_iV_j can be linearized (see Chapter 4). The topology reconfiguration based on the switching constraints in (84) has the following formulation:

[4] In Operations Research field, this is known as a *Big-M* constraint. The idea is to transform both inequalities into a single equality when a certain condition is satisfied, otherwise, the variables take an arbitrary value.

Optimization objective

$$\text{subject to: } P_{ij} \le G_{ij}\left(V_i^2 - V_iV_j\right) + M\left(1 - y_{ij}\right) \qquad \forall (i,j) \in \mathcal{A}$$
$$P_{ij} \ge G_{ij}\left(V_i^2 - V_iV_j\right) - M\left(1 - y_{ij}\right)$$

power flow constraints (81)

Topology reconfiguration can be implemented with switching constraints (84) in any optimization problem that optimizes a specific performance index, e.g., a loss minimization problem. In the case that performance requires a minimum number of connections closed, a topology reconfiguration problem can be written as the following optimization problem:

$$\min y_{ij}$$

$$\text{subject to: } P_{ij} \le G_{ij}\left(V_i^2 - V_iV_j\right) + M\left(1 - y_{ij}\right) \qquad \forall (i,j) \in \mathcal{A}$$
$$P_{ij} \ge G_{ij}\left(V_i^2 - V_iV_j\right) - M\left(1 - y_{ij}\right)$$
$$P_i = g_i^0 V_i V_i + p_i^0 + i_i^0 V_i = G_{ii}V_i^2 + \sum_{\substack{j=1 \\ j \ne i}}^{\mathcal{N}} G_{ij}V_iV_j \qquad \forall i \in \mathcal{N}$$
$$y_{ij} \in \{0,1\} \qquad \forall (i,j) \in \mathcal{A}$$

In addition to the switching constraints in the topology reconfiguration problem above, there is also the power flow constraint for every bus in the system.

In addition to the transmission switching constraints (84) in a performance optimization problem, topology reconfiguration can also be based on a pre-defined response scheme in case of failures. Although operation under failure may not be optimal, reconfiguration ensures that the critical systems and loads are supplied to avoid fatalities. There could be a list of all possible failures and the response that the system needs to perform, i.e., state enumeration or combinatorial logic. Then, this information could be used to create a finite state machine (FSM) that decides upon the next state based on the actual conditions. An example of such approach is illustrated in the testbed of Chapter 7 where an FSM is used

to control transitions between normal states and reconfigured states. A simple FSM has the flow depicted in the figure below:

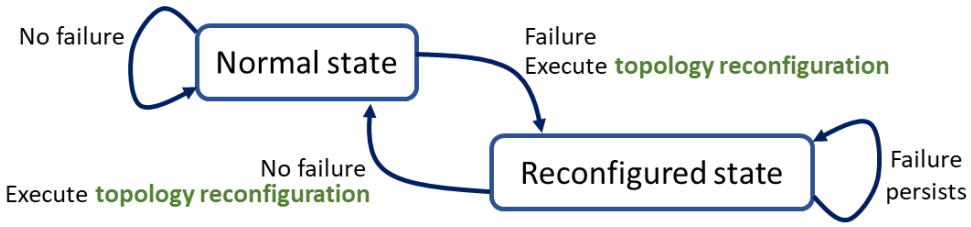

Figure 5.12 Example of simple Finite State Machine.

In some cases, there could be nested optimization formulations (e.g., power allocation) within some states [159], while in other cases no optimization is executed. When the system's size is moderately large, state enumeration could be cumbersome, this being the reason for which approaches based on reactive synthesis have gained attention recently [36], [39], [40]. The goal of reactive synthesis (and similar methods) is to synthesize and verify an FSM-based controller without the need to do state enumeration. In fact, the states of this FSM do not necessarily correspond to all possible states the system could be in. Instead, the states are those which are required to allow safe operation due to synthesis through an advanced decision-making algorithm. However, these approaches are still under research as no conclusive method to synthesize (create) such class of controllers has been found yet.

Loss minimization problem in DC system

Recall that loss minimization is equivalent to efficiency maximization. In a DC EPS, there are ohmic losses due to connections (cabling) and components (power distribution components, generators, etc.). Then, the objective of the loss minimization problem can be written as:

$$\min\left(\sum(\text{cable losses}) + \sum(\text{component losses})\right)$$

Ohmic losses in connection ij (within the cabling system) are calculated as the product between the squared current (I_{ij}^2) (flowing through ij) and the resistance (R_{ij}). Ohmic losses in component i depend

on the voltage and current values at their terminals, i.e., ohmic loss η_i^{LOSS} is a function of V_i and I_i, or $\eta_i^{LOSS} = \mathrm{f}(V_i, I_i)$. Usually, ohmic losses can be calculated from the efficiency maps (charts) as in the case of converters. Now, the objective for the loss minimization problem can be written as,

$$\min_{V,I,\mathcal{Y}} \sum_{(i,j)\in\mathcal{A}} \left(R_{ij} I_{ij}^2\right) + \sum_{i\in\mathcal{N}} \eta_i^{LOSS} \tag{85}$$

In general, the components' ohmic losses depend on a variety of factors, for which reason loss functions η_i^{LOSS} are unique for each type of component. Recent advances in power electronics and topologies for power converters have resulted in very efficient converters, even in the range between 97% and 99% from zero to full load [160]. Thus, in some cases the second term in (85) can be assumed to be negligible. Most of the distribution components, apart from buses, perform a power conversion, so, there is a large number of converters in the EPS, i.e., voltage step-up or -down, or DC-AC / AC-DC converters for AC and DC actuators. Special cases of component types are the source matrix contactor and load matrix contactor, in general any matrix contactor box, where an arrangement of contactors (switches) is configured to interconnect input and output terminals.

The constraints of the loss minimization problem are:

- Power flow equations (81), enforced on every bus of the system.
- Transmission or distribution switching equations that allow reconfiguration of the EPS by opening/closing connections to re-route power through different paths. This can be based on the switching constraint (84). Reconfiguration of the system due to failure in components relies on switching constraints to decide which connections must be opened or closed.
- Limiting constraints for power flow and voltage magnitudes, i.e., values must be maintained within upper and lower permissible boundaries.

- Additional efficiency constraints or any other converter's or component's power equation that sets a specific relation between voltage and current that is not expressed in the power flow equations.

The quadratic term I_{ij}^2 in the loss minimization objective in (85) can be linearized with a piecewise Linear (PWL) function, i.e., I_{ij}^2 can be replaced with a new variable $\mathcal{i}_{ij}$. Similarly, the V_i^2 term in (81) can be linearized with PWL (new variable is $\mathcal{v}_i$), and the bilinear terms $V_i V_j$ can be replaced with a new variable w_{ij} so that McCormick envelopes in (83) can be used in the feasible region depicted in **Figure *5.6***. Thus, the left-hand side of the power balance in (81) can be written as,

$$P_i = g_i^0 V_i V_i + p_i^0 + i_i^0 V_i = G_{ii}\mathcal{v}_i + \sum_{\substack{j=1 \\ j\neq i}}^{\mathcal{N}} G_{ij} w_{ij} \qquad \forall i \in \mathcal{N} \qquad (86)$$

The power balance in (86) is the same power balance constraint as in the DC load flow problem in **O.P. 12**. The rest of the constraints for the loss minimization problem are:

- The switching equations in (84)
- Symmetry for power values (power from i to j is the negative of the power from j to i) (88), commutative property in the voltage product ($V_i V_j$ is the same as $V_j V_i$) (89), and symmetry for current values (current from i to j is the negative of the current from j to i) (90).
- Conditional constraint for current I_{ij} (91) -(92), i.e., if connection ij is selected, current exists.
- Limiting constraints for connections' power (94) and voltage (93), e.g., $P_{ij} \leq P_{MAX} y_{ij}$. P_{ij} is forced to be 0 when connection i, j is not selected.

Now, the loss minimization problem can be stated as,

O.P. 13 Objective (85)

subject to: (86), (84)

$$P_{ij} = P_i - P_j \qquad \forall i, \forall j \in \mathcal{N} \tag{87}$$

$$P_{ij} = -P_{ji} \qquad \forall (i,j) \in \mathcal{A} \tag{88}$$

$$w_{ij} = w_{ji} \qquad \forall (i,j) \in \mathcal{A} \tag{89}$$

$$I_{ij} = -I_{ji} \qquad \forall (i,j) \in \mathcal{A} \tag{90}$$

$$I_{ij} = G_{ij}(V_i - V_j) \qquad \forall (i,j) \in \mathcal{A} \mid y_{ij} = 1 \tag{91}$$

$$I_{ij} = 0 \qquad \forall (i,j) \in \mathcal{A} \mid y_{ij} = 0 \tag{92}$$

$$V_{MIN} \leq V_i \leq V_{MAX} \qquad \forall i \in \mathcal{N} \tag{93}$$

$$P_{MIN} y_{ij} \leq P_{ij} \leq P_{MAX} y_{ij} \qquad \forall i \in \mathcal{N} \tag{94}$$

$$V_{SLACK} = 1.0 \text{ p.u.} \tag{95}$$

$$y_{ij} \in \{0,1\} \qquad \forall (i,j) \in \mathcal{A}$$

Where (91) is the same as Ohm's law. Finally, (95) is the fixed voltage condition for the slack bus (reference bus). In every EPS, there must be a slack (reference) bus, i.e., its voltage is controlled to remain in a specific value, and this bus provides power compensation for any power imbalance in the system. Other buses can have a fixed voltage as well, but they could not provide power compensation.

5.6. Recap

In this chapter, performance optimization has been presented. Performance optimization is an extension of the proposed design framework from Chapter 3. The GS&GLP and PDD problems produce an EPS architecture from scratch, i.e., a generation system and a power distribution topology. The performance evaluation of this architecture requires a controller that can bring the system to a new state depending on the actual system's conditions. Controller synthesis is outside of the scope of this work. However, the tools presented in this chapter aim to shorten the gap between the EPS architecture and a real EPS by

defining formulations that can be used during EPS operation, that is, the main contributions are main methods that allow performance optimization and evaluation.

First, the optimal voltage of the EPS can be calculated (Section 5.2). Once the system's voltage is known, a component location and cable selection problem can be executed (Section 5.3) to determine the admittances of connections (steady state electrical characteristics). Having determined the admittances of the rest of the distribution components, the admittance matrix can be built, and the load flow problem can be formulated (Section 5.4). The load flow problem opens up the possibility to formulate the two main types of performance optimization, both related to efficiency maximization during operation (Section 5.5): topology reconfiguration, and loss minimization. For a performance optimization based on a loss minimization problem, the optimization formulation can be compactly written as:

$$\min_{V,I,y} \sum_{(i,j)\in\mathcal{A}} \left(R_{ij} I_{ij}^2\right) + \sum_{i\in\mathcal{N}} \eta_i^{LOSS}$$

subject to: $P_i = g_i^0 V_i V_i + p_i^0 + i_i^0 V_i = G_{ii} v_i + \sum_{\substack{j=1 \\ j\neq i}}^{\mathcal{N}} G_{ij} w_{ij}$	$\forall i \in \mathcal{N}$
$P_{ij} \leq G_{ij}\left(V_i^2 - V_i V_j\right) + M\left(1 - y_{ij}\right)$	$\forall (i,j) \in \mathcal{A}$
$P_{ij} \geq G_{ij}\left(V_i^2 - V_i V_j\right) - M\left(1 - y_{ij}\right)$	
$P_{ij} = P_i - P_j$	$\forall i, \forall j \in \mathcal{N}$
$P_{ij} = -P_{ji}$	$\forall (i,j) \in \mathcal{A}$
$w_{ij} = w_{ji}$	$\forall (i,j) \in \mathcal{A}$
$I_{ij} = -I_{ji}$	$\forall (i,j) \in \mathcal{A}$
$I_{ij} = G_{ij}\left(V_i - V_j\right)$	$\forall (i,j) \in \mathcal{A} \mid y_{ij} = 1$
$I_{ij} = 0$	$\forall (i,j) \in \mathcal{A} \mid y_{ij} = 0$
$V_{MIN} \leq V_i \leq V_{MAX}$	$\forall i \in \mathcal{N}$
$P_{MIN} y_{ij} \leq P_{ij} \leq P_{MAX} y_{ij}$	$\forall i \in \mathcal{N}$
$V_{SLACK} = 1.0$ p.u.	
Other constraints for η_i^{LOSS} (efficiency maps, charts, etc.)	
$y_{ij} \in \{0,1\}$	$\forall (i,j) \in \mathcal{A}$

The formulation above includes a topology reconfiguration problem, however, there are constraints on the components' efficiencies η_i^{LOSS} that are not shown. These constraints are specific to the problem formulation. For example, generation efficiency can be included in the loss minimization problem by using the generation losses expression obtained in (18)-(19) (see the derivation in Section 4.3.1). Then, load flow and topology reconfiguration can be used to optimize performance. The relationship between the EPS architecture design and the performance optimization methods detailed in this chapter is depicted in **Figure *5.13***.

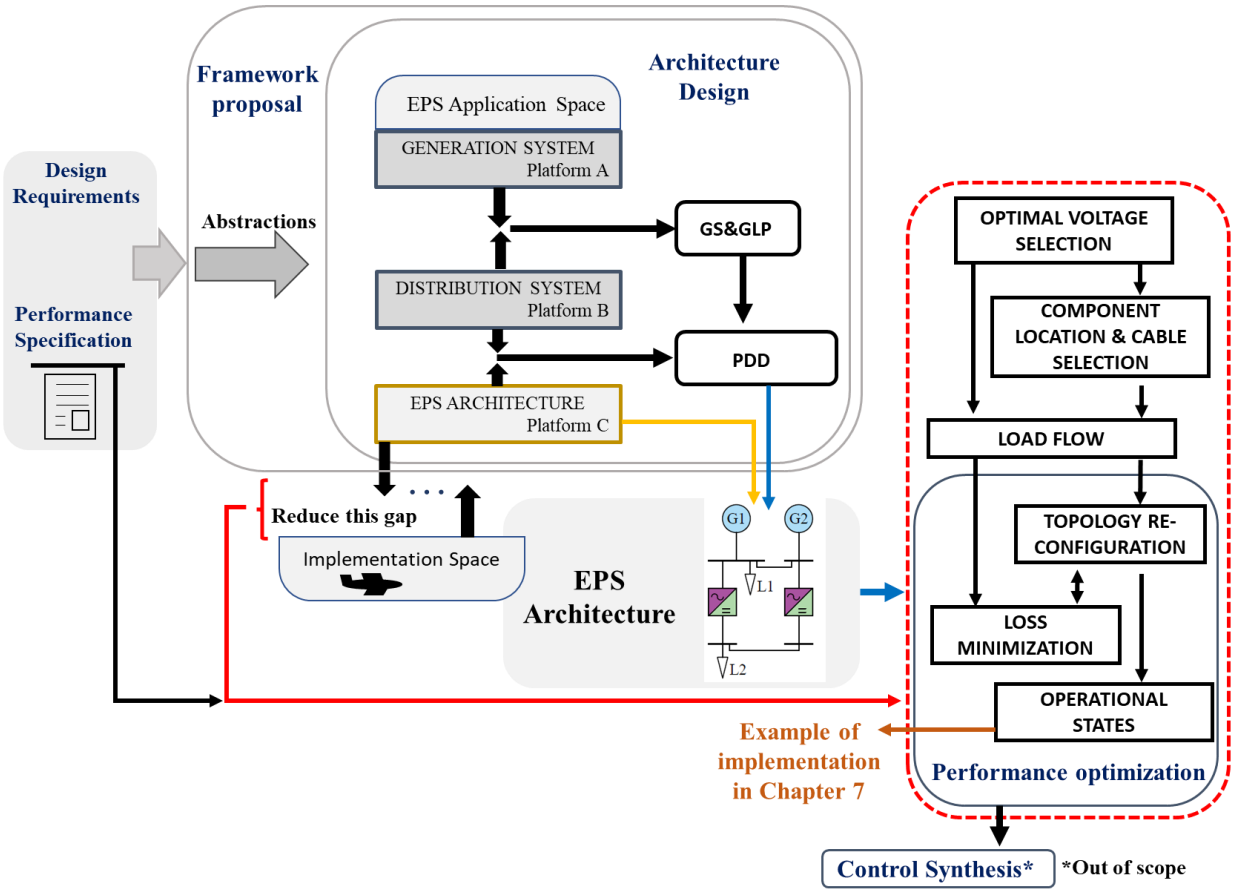

Figure 5.13 Performance optimization in the context of architecture design (all methods).

The performance optimization methods illustrated in **Figure *5.13*** are used in controller synthesis (outside of the scope of this work); this controller is part of the power and energy management system. The optimal voltage selection is an independent step from the architecture design. Then, the architecture and the optimal voltage are used to determine the component location and cable selection. At this stage, the EPS architecture has been brought closer to a real aircraft implementation, but not yet a real aircraft EPS. In order to evaluate and optimize performance during operation, a load flow problem can be formulated. The load flow and topology reconfiguration are tools that are used within efficiency maximization problems. A main loss minimization problem has been proposed as an application of performance optimization. There is a large list of other performance optimization problems in the literature that are outside of the scope of this work. The last two chapters of this thesis present a case study for the design of an EPS architecture (Chapter 6) and an experimental testbed assembled with electronic devices that implements a topology reconfiguration technique based on state enumeration (Chapter 7).

5.7. Conclusion

The EPS architecture has been brought closer to a real EPS implementation by proposing methods for achieving optimal performance during operation. Once the EPS architecture design has been completed, the next step is to optimally operate the EPS architecture under the conditions that the system is supposed to be successful, in other words, to achieve optimal performance by adjusting the system's parameters. Because the system has been designed to comply with a set of functional and safety specifications, the optimal performance problem must hold a close relationship with the design problem. The proposed methods for shortening the gap between architecture and real system are detailed below.

- Optimal voltage selection. This decides on the system's voltage considering maximum power transfer and maximum power density in the distribution system.

- Component location and cable selection. Assuming that the aircraft can be approximated to a 2D layout, components are located such that minimum cabling weight is achieved.
- Approximation of the DC load flow. This problem is the basis for the steady state calculation.
- Topology reconfiguration with switching constraints. The switching devices of the EPS architecture can be arranged in such a way that alternative distribution paths can be formed.
- Loss minimization (efficiency maximization) with load flow and switching constraints.

The conceptual relations between design and performance optimization are depicted in **Figure *5.1***, **Figure *5.7***, and **Figure *5.13***. A Mixed Integer Linear Programming (MILP) structure for both the optimal voltage and load flow problems has been presented so that the performance evaluation can be introduced in the EPS architecture operation (controller) and testing. The advantage of such a formulation is that performance optimization problems that involve topology reconfiguration tasks can be efficiently solved as MILP models. This offers an effective alternative when compared to other controllers that have been synthesised using a large number of languages and tools. The aim of reconfiguration based on performance optimization is to solve an optimization problem to determine the EPS's next state. The change in the EPS topology is triggered by changes in input parameters during operation. These changes could be due to loading variations, failures in components, or generation outages, among others, then, the topology of the distribution system is reconfigured from a normal state to a different state that optimizes a performance index.

6. Case study in the EPS design

6.1. Introduction

This chapter presents a case study of the design framework proposed in Chapter 3 using the MILP formulations for the GS&GLP and PDD detailed in Chapter 4. Some of the performance optimization techniques from Chapter 5 are also used to bring the EPS architecture a step closer to a real EPS implementation. As mentioned in previous chapters, controller synthesis is outside of the scope of this work, but the optimization formulations for performance optimization of Chapter 5 can be used to generate a controller, i.e., a power and energy management system. This case study does not pretend to comprehensively present a recipe to design EPS architectures for all types of aircraft. Even better, this chapter illustrates the numerical application of the optimization formulations studied throughout all this work to synthesize an EPS architecture from scratch. The intention is that the designer can apply the concepts studied in this work in their own numerical applications.

The design of an EPS is intimately linked to the aerodynamic aircraft design because the electrical loads are the implementation of (electrically driven) actuators, propulsion systems, and other mechanical subsystems and devices that provide power and energy to take-off, cruise, and land. Then, the EPS is tailored to comply to the loads' requirements and a set of functional and safety specifications. Optimal performance is required to achieve the best possible operation, e.g., maximum power transference and power density, minimum losses, reconfiguration in case of failures, etc. Therefore, this endeavor demands a multi-disciplinary effort to make sense of the proposed tools and formulations. However, assumptions are taken to simplify the exposition of the design framework proposal. The design framework for the synthesis of an EPS architecture is here applied to the construction of a direct current (DC) EPS for MEA. The proposed framework can be used in an extensive variety of prototype's designs; however, a case

study has been chosen to exemplify its potential. The outcome presented in the case study represents an architectural solution for a particular case that has been built by the author.

6.2. Design of an EPS architecture

The design specifications and requirements (built by the author) are presented first. It is assumed that an aircraft preliminary design (out of the scope of this work) has been assessed and its outcome has been used for a preliminary load sizing exercise (see [126], [127]). Therefore, there are load specifications and requirements that the EPS (to be synthesized) must satisfy.

The design flow of **Figure *5.13*** (architecture design with performance optimization in Chapter 5) is followed, so that the optimal voltage selection can be completed independently from the EPS architecture synthesis. Thus, the optimal voltage selection can be carried out prior to the EPS architecture synthesis or after it. For convenience, optimal voltage selection problem is run before the EPS architecture design. The synthesis of the architecture is based on the reliability-based MILP formulations for GS&GLP and PDD in Chapter 4. GS&GLP and PDD optimization formulations exemplify the design framework presented in Chapter 3. Although there are a number of important MEA applications (electric propulsion, turbo-electric, etc.) and EPS structures (DC, AC, hybrid AC and DC, single bus, ring, etc.), a particular and complete design assessment for a small aircraft DC architecture is provided here, so the designer perceives the potential of the framework proposal for wider applications. The optimization formulations are solved using a Windows High Specification PC Intel Xeon 64-bit 3.60 GHz running CPLEX Studio IDE 12.9.0 [110].

CPLEX Studio IDE 12.9.0 is an integrated development environment based on Eclipse (Java) that allows declaration of optimization problems in OPL (Optimization Programming Language). In OPL of CPLEX Studio 12.9.0, formulations can be written in two separate files, one for data (parameters, numerical values, data arrays, coefficients, etc.), and the other for writing the optimization problem as code. A

standard view of the CPLEX Studio 12.9.0 is shown in **Figure *6.1***. At the left, all the projects containing optimization program code and/or data are shown. In the middle, there is space to view the program and data files. At the bottom, the panes show the optimization results and the variable values for the optimal solution.

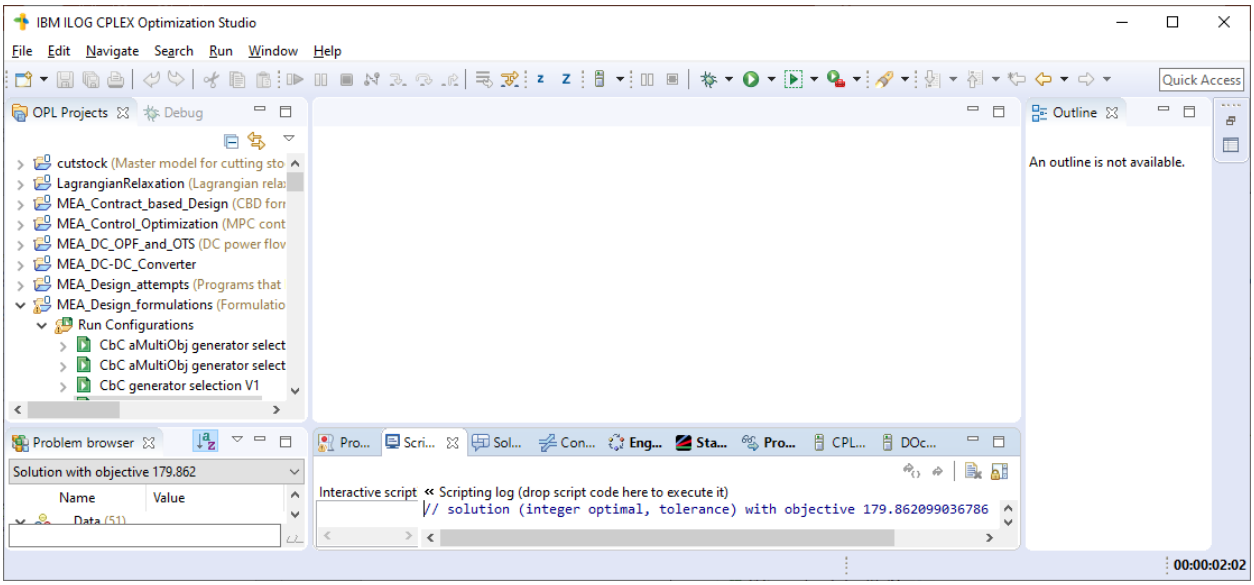

Figure 6.1 Standard view of CPLEX Studio 12.9.0 for programming and solving optimization problems.

The optimization program is written in OPL. An excerpt for GS&GLP is shown below.

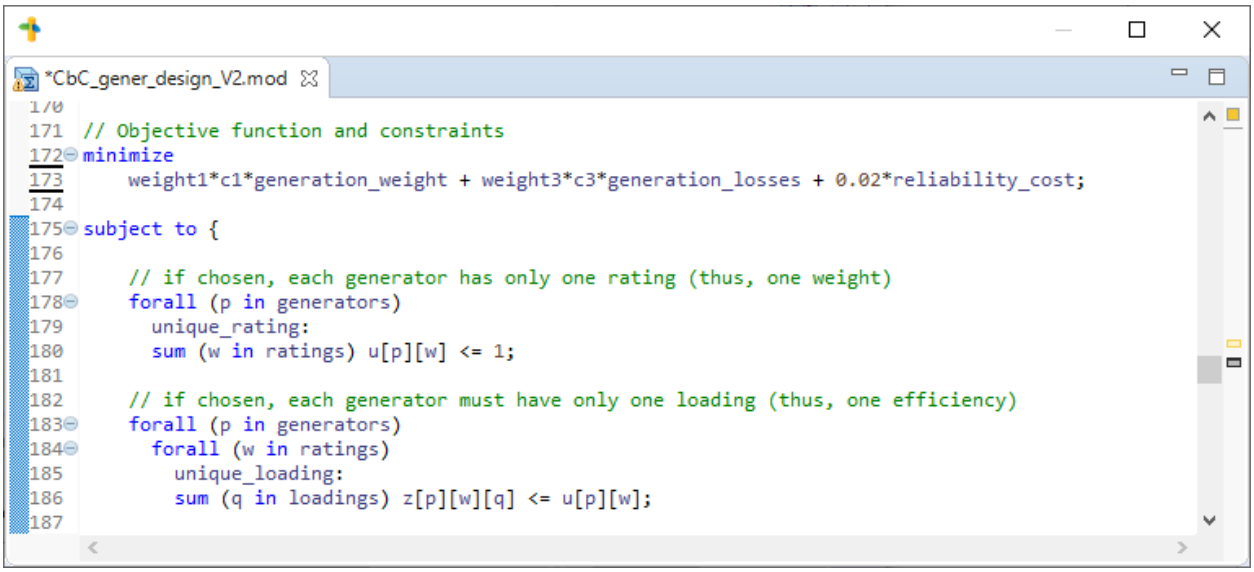

Figure 6.2 Zoomed view of optimization program file in CPLEX Studio 12.9.0.

Finally, a close-up view of a data file (excerpt) is shown below (for the same GS&GLP example above).

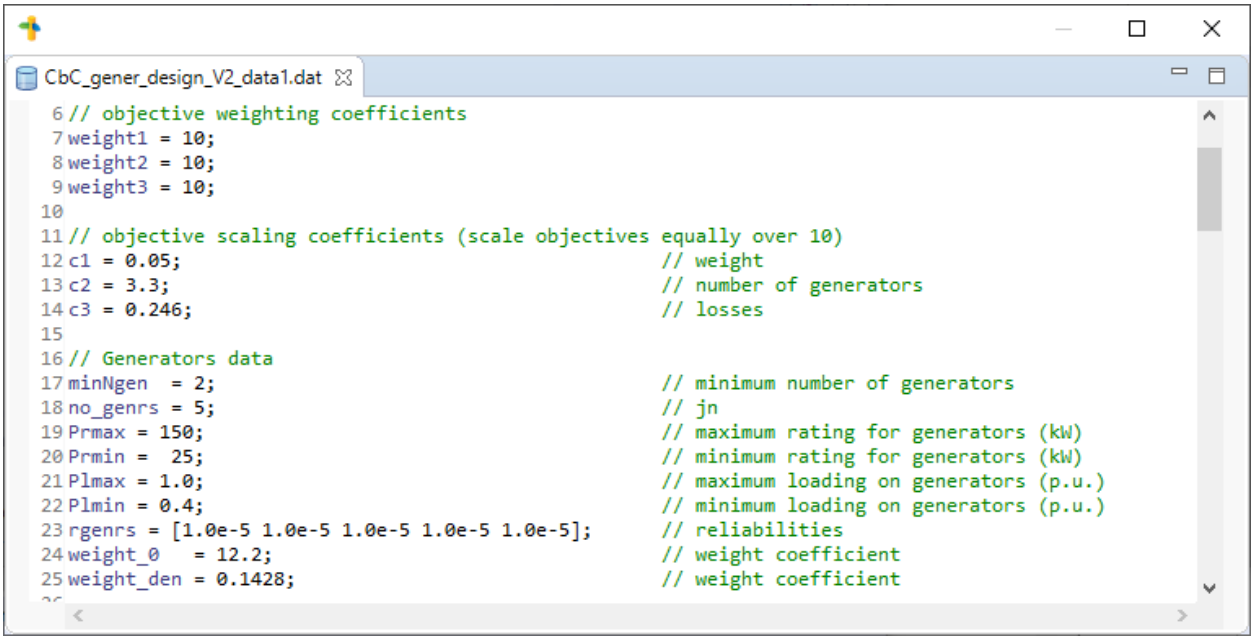

Figure 6.3 Zoomed view of data file in CPLEX Studio 12.9.0.

Now, the design specifications and requirements are detailed.

6.2.1. Design Specifications and Requirements

The initial design assumptions for the MEA EPS design are detailed below:

1. Aircraft conceptual design has been performed to produce a prototype for a small MEA application, i.e., short range flight (up to 1.5 hr.) in a 19-passenger airplane.
2. Loads have been sized to drive main aircraft subsystems, e.g., main actuators (pumps), flight controls, environmental control system (ECS), wing anti-icing, and heating.
3. Loads have been segregated into high- and low-voltage loads.
4. The devices' locations are fixed within the aircraft.

The functional and safety specifications are detailed below. Also, abstractions for power generation and distribution platforms are presented.

1. The MEA EPS is a DC network with two voltage levels, high- and low-voltage (HVDC and LVDC).
2. There are the following types of components:
    a. Source matrix contactor bus (HV bus bar) distributes generation power to converters, i.e., the bus bar is a power distribution box that routes power from inputs to outputs. It has several inputs and outputs to connect to more than one generation device and converter. It can be configured to avoid generator paralleling. An example of an HV bus bar with 3 inputs and 3 outputs is depicted in **Figure *6.4***.

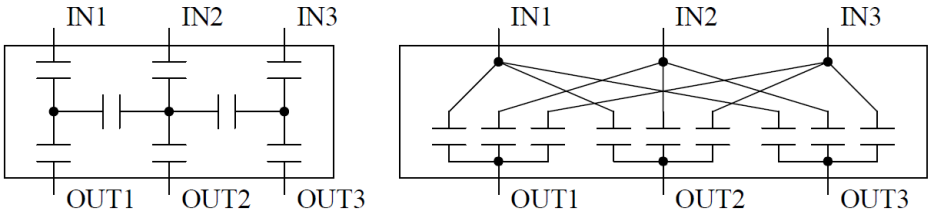

Figure 6.4 Example of source matrix contactor bus (HV bus bar).

    b. DC/DC converter steps down voltage from high- to low-voltage. Each converter can be supplied from several HV bus bars simultaneously, and its output can be paralleled to increase the power capacity to supply larger loads. The converters do not hold any kind of permanent energy storage devices inside. Also, the converters shall provide galvanic isolation.
    c. LV loads are connected to LV buses (LV buses are connected to converters). A LV bus can feed one or more loads and the LV bus can be fed through one or more converters.
3. HVDC loads are connected to a HV source matrix contactor bus (see **Figure *6.4***).
4. PMSM generator with power density of 17.0 kW/kg is assumed to be available [161]. This assumption follows expected technology trends for low carbon MEA propulsion [162].
5. The number of generators is arbitrarily limited to 5, considering the possibility of installing multiple small generators.

6. A power density of 15 kW/kg is assumed for power electronic conversion in DC/DC converters [162], considering high power density SiC-based (Silicon-Carbide) power electronics technology.
7. The weight of power conversion is assumed to be proportional to the maximum power flow transferred, and this maximum flow is assumed to be proportional to the cost.
8. The connections between each pair of components includes a contactor (open/close switch) device that connects or disconnects the components it is connected to.
9. There are 4 loads with the following power and reliability requirements.

Table 6.1 Design requirements for electrical loads.

	L_1	L_2	L_3	L_4
L_l [kW]	50	25	40	10
Type	LVDC	LVDC	LVDC	HVDC
$1 - r_{\mathrm{TARGET},l}$	1.25×10^{-5}	1.25×10^{-5}	1.25×10^{-5}	1.25×10^{-5}

Now, the platform abstractions and templates can be determined.

Platform abstractions and templates

The abstractions are the result of processing the design specifications and requirements, the industry insights (observations), and the relationships between weight, reliability, efficiency, and cost (see Chapter 3). There must be significant input from the aircraft industry in order to estimate the numerical relationships between weight, reliability, efficiency, and cost for generators and power distribution components. Most of this information is not publicly available due to intellectual property and business contracts (sensitive content and reserved as top secret). It is a challenge, for example, to obtain real power generation profiles during flights (assuming there is a data acquisition system installed that could record such data), or efficiency charts from real 90 kVA electrical generators. Few academic references contain information on electrical ratings and number of generators, but further information is locked to manufacturers. To overcome this difficulty, the author has assumed or approximated numerical values to

illustrate the design process. Some values are based on technical projections for MEA, which is the most common practice in this field these days.

The power generation is assumed to have the abstractions and characteristics detailed in **Table *6.2***. These abstractions are part of the GS&GLP step described in Chapter 3. Also, the template for GS&GLP is shown in **Figure *6.5***. The ratings P_s^G of generators are allowed to be in the range from 25kW to 150kW (as a reference, the generator rating for an A380 is 150kVA [163]). Considering a power density of 17.0 kW/kg (from the specifications above, see also [164]), a roughly linear relationship between power and weight can be used to determine a generator's weight w_s (as a function of power P_s^G), as follows:

$$w_s(P_s^G) = \text{weight offset} + \frac{1}{17\frac{kW}{kg}} = 0.5 + 0.058P_s^G$$

Where a weight offset of 0.5 kg has been chosen to account for mounting accessories [164]. Given the scarce information available on operational data of generators, the generator's efficiency has been arbitrarily approximated to a quadratic function in terms of loading β_s and rating P_s^G,

$$\eta_s(\beta_s) = 22.09 + 0.2563P_s^G + 95.23\beta_s - 0.0004374(P_s^G)^2 - 0.1324P_s^G\beta_s - 40.46{\beta_s}^2$$

Where the parameters of η_s above were obtained from interpolating generation efficiency of several electrical generators. This approximation must only be taken for illustrative purposes. The efficiency η_s can be converted to a loss function η_s^{LOSS} following the derivation in Section 4.3. The cost of generators (assumed to be roughly proportional to weight) is arbitrarily set to a ratio of £250 per kilogram considering a higher cost of production than a 90 kW PSMS (64 kg, at a commercial price of $ 6.9k) for an electric vehicle [165]. The generator reliability is assumed to be 0.99999 (unreliability of 1.0×10^{-5}). Finally, the distribution path's reliability targets are in the range shown in **Table *6.2***.

Table 6.2 Power generation platform abstraction.

P_s^G [kW], β_s [p.u.]	$P_s^{MIN} = 25,\ P_s^{MAX} = 150;\quad \beta_s^{MIN} = 0.4,\ \beta_s^{MAX} = 1.0$
$w_s(P_s^G)$ [kg]	$0.5 + 0.058P_s^G$
$\eta_s(P_s^G, \beta_s)$ [%]	$22.09 + 0.2563P_s^G + 95.23\beta_s - 0.0004374(P_s^G)^2 - 0.1324P_s^G\beta_s - 40.46{\beta_s}^2$ Approximated function for values of $P_s^G \in [P_s^{MIN},\ P_s^{MAX}]$
$\eta_s^{\text{LOSS}}(P_s^G, \beta_s)$ [%]	$P_s^G\beta_s(100(\eta_s^{-1}(\beta_s)) - 1)$
Cost ($w \propto c$)	$250\ £/kg$
$1 - r_s$	1.0×10^{-5}
r_{VS}	$[0.999900,\ 0.999988]$ or $1 - r_{VS}$: $[1.0 \times 10^{-4}, 1.2 \times 10^{-5}]$

The GS&GLP template shown in **Figure *6.5*** allows all generator candidates to be connected to all the loads, i.e., it is assumed that there are no restrictions in connecting any load with any generator. The connections between generators and loads correspond to the assigned pairs that are refined (designed) into distribution paths in the power distribution design (PDD) step.

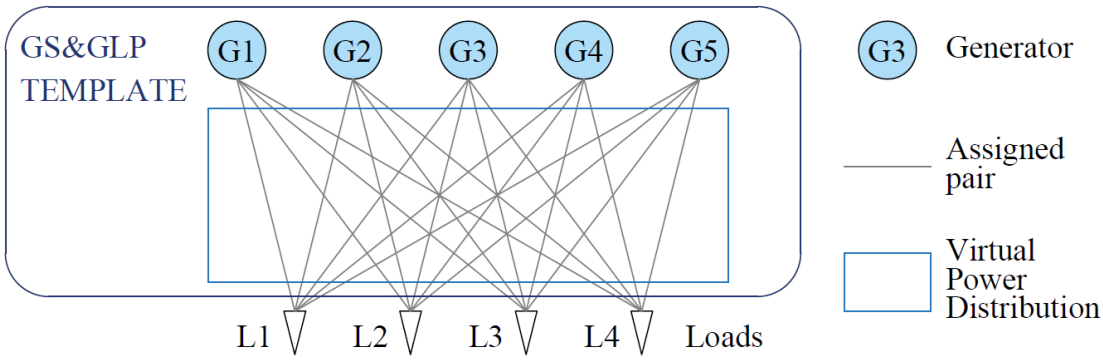

Figure 6.5 GS&GLP template for the EPS design example.

In the template of **Figure *6.5***, it is assumed that the generators' output is in DC, that is, each generator is connected to the EPS through a rectifier unit that supplies power in DC. After determining the GS&GLP abstractions and template, a similar task is done for the PDD. The power distribution components are assumed to have the abstractions and characteristics tabulated in **Table *6.3***. There are three types of components, HVDC bus bar (see **Figure *6.4***), DC/DC converter, and LVDC bus. For each type of component there are six characteristics: power density, weight, variable cost, fixed cost, reliability, and upper

boundary for power flow. These parameters are also defined for connections. Some values for power density shown in **Table *6.3*** come from the report on Commercial Aircraft Propulsion and Energy Systems Research for Reducing Global Carbon Emissions [162]. Other values are based on the EPS design example for MEA reported in [36] and the roadmap toward MEA discussed in [166].

Table 6.3 Power distribution platform abstraction.

	HVDC bus bar	*Converter*	*LVDC bus*	*Connection* (ij)
Power density [kW/kg]	12.0	15.0	25.0	60.0
Cost/weight [k£/kg]	1.4	4.0	2.9	1.2
m_i^{kW}, c_{ij}^{kW} [k£/kW] (var. cost)	0.117	0.267	0.116	0.020
m_i, c_{ij} [k£] (fixed cost)	0.28	0.80	0.29	0.12
r_i, r_{ij} (reliability)	1.0×10^{-6}	1.0×10^{-5}	1.0×10^{-6}	1.0×10^{-8}
P_i^{MAX}, P_{ij}^{MAX} [kW]	800	900	800	1000

The values of $m_i^{\mathrm{kW}}$and c_{ij}^{kW} are equal to the product of the cost/weight ratio to the inverse of the power density. It has been assumed a cost range between 1.2 k£/kg and 4.0 k£/kg for components and connections of the distribution system. The values of m_i and c_{ij} were obtained by multiplying the cost/weight ratio by a fixed weight value representing mounting accessories (small weight value). Some of these weight values were assumed for illustration purposes. Most of this information is publicly unavailable, so some of these estimations are arbitrary. In the PDD solution, any cost can be divided by the cost/weight ratio to obtain the weight value.

The template for the power distribution design (PDD) is shown in **Figure *6.6***. All distribution component candidates in each level are allowed to be connected to their corresponding upper and lower levels indistinctively, in other words,

1. HVDC bus bar(s) connect to generators (upper level) and converters (lower level)

2. Converters connect to HVDC bus bars (upper level) and LVDC buses (lower level)
3. LVDC buses connect to converters (upper level) and LVDC loads (lower level)

HVDC loads are directly connected to HVDC bus bars.

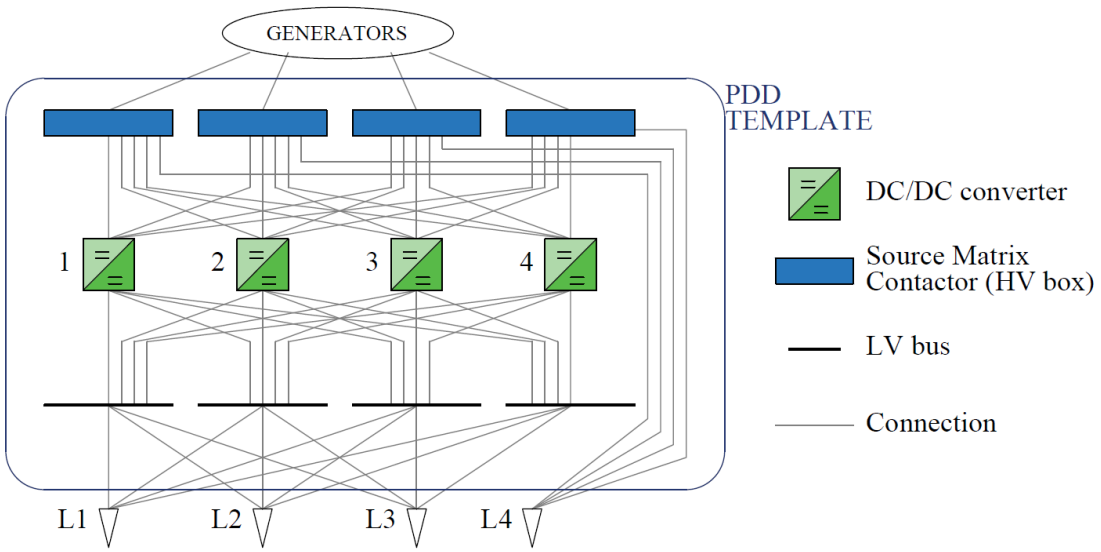

Figure 6.6 PDD template for the EPS design example.

This concludes the platform abstraction and templates for GS&GLP and PDD. These abstractions built by the author are based on estimations and projections for MEA. With an open support and collaboration from industry, these values could be improved (updated) to reflect the reality (manufacturing costs, weights) and increase the accuracy of the results.

The design of the EPS architecture utilizes the abstractions and platforms, the design specifications, and the load requirements (part of the design specifications) detailed in **Table *6.1***. The load's reliability target is expressed as a probability of not being supplied with power, e.g., load L_1 requires to be supplied with generation power with a probability of at least $1 - 1.25 \times 10^{-5}$. In the GS&GLP, such a reliability target may be achieved by assigning more than one generator to a load, so that unexpected events do not interrupt power supply to this load. In the PDD, the assigned pairs of the GS&GLP are synthesized into distribution paths. Using the assigned pairs' reliability targets from the GS&GLP, it is possible to synthesize

the assigned pair as a single distribution path (series system). If the reliability target cannot be satisfied with a series system, an alternative disjoint path can be built by a two-path disjoint formulation. Otherwise, we set the load to be critical or non-critical and design a power distribution system to be resilient for a failure set. In this case study, we run all these PDD options assuming that the reliability target can be satisfied with all of them. The purpose is to illustrate all the MILP formulations in Chapter 4. Then, the reader can compare the different results and perform a trade-off. Therefore, the loads' reliability targets in **Table *6.1*** are satisfied by a group of different PDD resiliency specifications as listed in **Table *6.4***.

Table 6.4 Proposed resilient design scenarios for the same EPS design application.

Scenario	**1**	**2**	**3**	**4**	**5**	**6**	**7**
Formulation	Single path	PDD Design for a Failure Set					
Critical loads	**N/A**	**All**	**1, 3**	**1, 3**	**1, 3**	**4**	**1, 4**
Failure set F	-	Converter & HV box	Converter	Converter & LV bus	N-1	HV box	Converter & HV box
Optimization	**O.P. 6**	**O.P. 7**					

Scenario	**8**	**9**	**10**	**11**	**12**	**13**	**14**
Formulation	PDD with Two Disjoint Path						
Critical loads	**All**	**1, 3**	**1, 4**	**4**	**2, 3**	**2, 4**	**1**
Failure set F	-	-	-	-	-	-	-
Optimization	**O.P. 8**						

In **Table *6.4***, 14 scenarios to synthesize the EPS architecture are presented including synthesis of distribution paths as a series system, as a two-disjoint path, or a resilient design of power distribution for a failure set. In scenario 5, 'N-1' is a criterion that requires supply for critical loads if any single component fails, i.e., all components except one are still available. Several combinations of critical loads are proposed,

just to illustrate all the MILP formulations. The purpose is to demonstrate the flexibility of the design framework in producing several architectures that differ because of the resiliency constraints utilized. In other words, given that there is no one-size-fits-all solution, a palette of optimal architecture solutions is presented. Choosing between any of them is strictly determined by the resiliency requirements selection. For instance, if the required resiliency equals the conditions in scenario 4, then the optimal architecture for that scenario is the final solution. On the other hand, if the only resiliency required is that which is expressed in scenario 9, then the optimal architecture for that scenario is the EPS architecture to be implemented. Note that in real application, only one PDD formulation (e.g., resilient design for a failure set) is used and its optimal is the optimal EPS architecture. Whenever there were multiple resiliency specifications for the same application as in **Table *6.4***, the designer must practice a tradeoff considering the available resources (recall that the drivers of cost, weight, efficiency, and reliability, are conflicting) to select one that fits the budget and resources.

Having described the design specifications, the abstractions, and templates for GS&GLP and PDD and proposed several scenarios to illustrate all the PDD formulations, the design framework and MILP formulations for the EPS architecture design can be formally executed. According to **Figure *5.13***, the optimal voltage selection does not depend on the architecture design, and it can be independently performed. For convenience, the optimal voltage is here calculated prior to GS&GLP and PDD.

6.2.2. Optimal voltage for an EPS

The aim of the optimal voltage selection (Chapter 5) is to determine the voltage rating of the EPS, based on the maximum power transfer and maximum power density of the power cables, i.e., cables distributing power from generators to loads; the other cables for control, avionics, etc., are not part of this selection. The physics of cabling systems and the optimal voltage selection procedure has been explained in detail in Chapter 5 and the general formulation follows the ten steps in Section 5.2.4. The first seven steps are

related to pre-determining flight conditions, setting $V_{PASCHEN}$, setting the cabling arrangement, establishing a set of power distribution wire gauges (set $\mathcal{C}$), applying ampacity correction, and defining a voltage range from which the SOV must be selected (set $\mathcal{N}$). In the last three steps, the optimization formulation in **O.P. 9** and MILP formulation in **O.P. 10** are used to solve for the optimal voltage.

The specifications in **Table *6.5*** are considered as an example of design requirements. Polyvinyl chloride (PVC) insulation and an aluminum conductor were chosen due to their extensive use in the industry [148]. Although other insulation materials are exclusive to newer aircraft designs [167] (Tefzel, PTFE/Polyimide/PTFE, etc.), PVC is selected in this example as it has been used in older aircraft as well. Aluminum is attractive because of its lower density compared to copper, e.g., it could be lighter at the same ampacity, thus reducing the weight payload. A conservative value for $V_{PASCHEN}$ has been selected so that there is a safety margin even though an aircraft typically flies at lower altitudes (see minimum of the Paschen's curve shown in **Figure 5.2)**. The target clearance e_{TARGET} is 0.25 mm, and it represents the minimum distance between the cable and ground that must be observed. The cabling arrangement shown in **Figure 5.3** is used in this case study (conductor at a certain distance from the ground plane).

Table 6.5 Design specification example for optimal voltage selection.

ε_r of PVC insulation	2.1
$V_{PASCHEN}$ at 40kft of altitude, 13.75kPa	331.4 V
D	10 mm
e	0.25 mm
ρ_c for aluminium conductor	2700 kg/m^3/m
ρ_i for PVC insulation	1400 kg/m^3/m

The set $\mathcal{C}$ of pre-established standard wire gauges for power distribution are listed in **Table *6.6***, and the ampacities of these cables have been corrected (derating factors) by pressure (flight altitude), wire bundle, direct current, and conductor type (aluminium in this case). The MIL-W-5088L (military

specification for aerospace vehicle wiring) has been used to obtain the correction factors [168]. The set of wire gauges in **Table *6.6*** ranges from 10 AWG to 4/0 AWG,

$$\mathcal{C} = \{10, 8, 6, 4, 2, 1, 1/0, 2/0, 3/0, 4/0\} \text{ AWG}$$

These are typical values in aircraft installations [148]. Finally, a set of safe operating voltage values (SOV) ranging from 600 V to 5400 V are explored.

$$\mathcal{N} = \{600, 1200, 1800, 2400, 3000, 3600, 4200, 4800, 5400\} \text{ V}$$

There values have been arbitrarily selected. However, similar values have been considered in previous investigations on optimal voltage selection for aircraft EPS [158].

Table 6.6 Standard wire gauge set $\mathcal{C}$ example for optimal voltage selection, ΔT = 70°C, wire in free air, sea level.

	AWG	10	8	6	4	2	1	1/0	2/0	3/0	4/0
Amp. [A]	Standard	60.8	92.7	121.5	163.9	231.9	271.8	311.8	359.8	415.8	495.7
	Corrected	24.5	37.4	49.0	66.1	93.5	109.6	125.8	145.1	167.7	199.9
	Diameter [mm]	2.588	3.264	4.115	5.190	6.544	7.348	8.252	9.266	10.405	11.684

Once the optimal voltage selection parameters (**Table *6.5***) have been obtained, including the standard wire gauges of **Table *6.6***, the optimal voltage selection can be calculated using **O.P. 10**.

The results for insulation thickness, maximum power transfer and maximum power density are shown in **Table *6.7*** and **Figure *6.7***.

Table 6.7 Maximum power transfer and density with corresponding wire gauges for a set $\mathcal{N}$ of SOV values.

SOV	600	1200	1800	2400	3000	3600	4200	4800	5400
AWG	4/0	4/0	4/0	4/0	3/0	1/0	2	4	8
Insulation thickness [mm]	2.62	3.52	3.75	3.86	4.53	5.60	6.46	7.15	8.12
Max. power transfer [kW]	119.9	239.9	359.8	479.8	503.0	452.7	392.7	317.3	201.9
Max. power density [kW/kg/m]	264.1	457.1	660.9	866.6	954.3	931.7	852.5	712.4	471.1

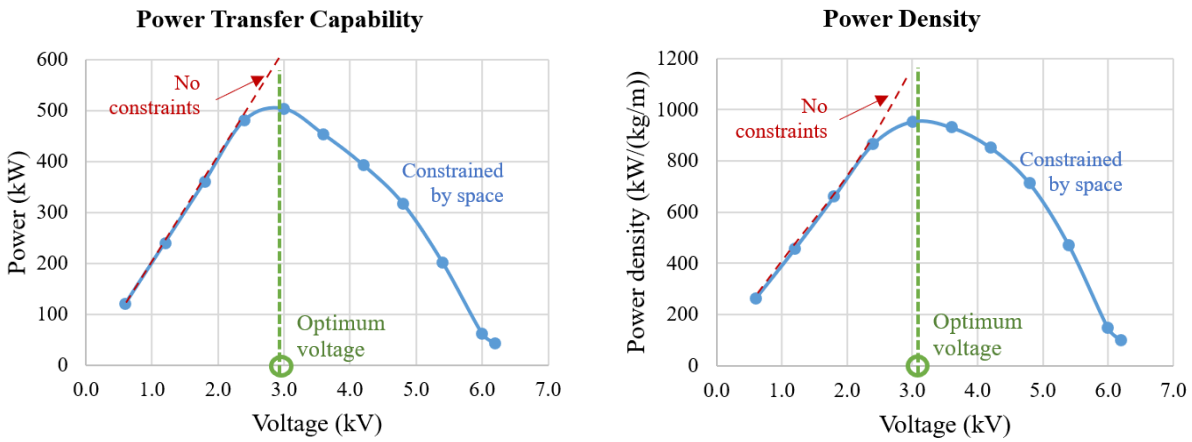

Figure 6.7 Maximum power transfer (left) and power density (right) for optimal voltage selection example.

By visual inspection of **Figure *6.7***, the optimal voltage can be observed to be approximately 3 kV. At this voltage, a maximum power transfer of 503 kW and power density of 954 kW/kg/m is achieved. The cable that allows this maximum is 3/0 with a corrected ampacity of 167.7 A. This result does not mean that all cabling is fixed at 3/0 AWG, it means that the optimal voltage of 3kV allows a maximum power transfer of 503 kW at a power density of 954 kW/kg/m. Could a voltage greater than 3kV improve power transfer? In this case no, because the tradeoff between conductor cross sectional area and the insulation thickness (to prevent risk of PD) is such that a greater voltage reduces the power transfer capacity. If the system has additional cabling levels, the optimal voltage for each level could be obtained by considering different (larger or smaller) sets of standard wire gauges (corresponding to each level) limited by the maximum estimated power (or current) in that level. Also, if there is power conversion between these levels, constraints on the voltage ratio could also be included, so that there are constraints linking the voltage magnitudes between levels.

After determining the optimal voltage for the EPS, the architecture design can be performed. The EPS design starts with the GS&GLP.

6.2.3. Generator Selection and Generator-Load Pairing

The inputs for the GS&GLP consist of: the design specifications and requirements, the platform abstractions, and the GS&GLP template. These inputs have been detailed in Section 6.2.1 including **Table *6.1*** (loads requirements), **Table *6.2*** (GS&GLP abstractions), and **Figure *6.5*** (template).

The generator's rating power is in the range 25 kW – 150 kW and its loading will be restricted to 40% minimum to avoid very low efficiencies; this restriction is enforced by using limiting constraints in loading β_s. The generator's weight is inversely proportional to the power density (17.0 kW/kg), then $w_s \propto \frac{1}{17\ kW/kg}$ or $w_s \propto 0.058 P_s^G$. Efficiency η_s is approximated to a quadratic function in terms of power rating P_s^G and loading β_s to reflect the case that efficiency varies according to different generators' ratings (sizes). This approximation for the efficiency simulates the case where test data has been fitted to a function.

The generator's cost to weight ratio is $£250/kg$ and a reliability of $1 - 1.0 \times 10^{-5}$ is considered in all the generators. The virtual power distribution reliability r_{VS} is in the range $[0.999900, 0.999988]$. All these parameters have been listed in **Table *6.2***. These parameters have been declared as coefficients and constants in CPLEX Studio 12.9.0 as shown in **Figure *6.8***.

The MILP optimization formulation used is **O.P. 5** (Section 4.3.1). The objective's weighting coefficients are here equal, i.e., $a_1 = a_2$. For clarity, the problem is re-written here.

$$\text{Min} \sum_s \left(a_1 \left(\text{generator weight}_s \right) + a_2 \left(\text{generator loss}_s \right) \right)$$

subject to: Connectivity constraints (22) to (25)

Power balance constraints (26) and (27)

Reliability constraints, (28) or (29) to (30)

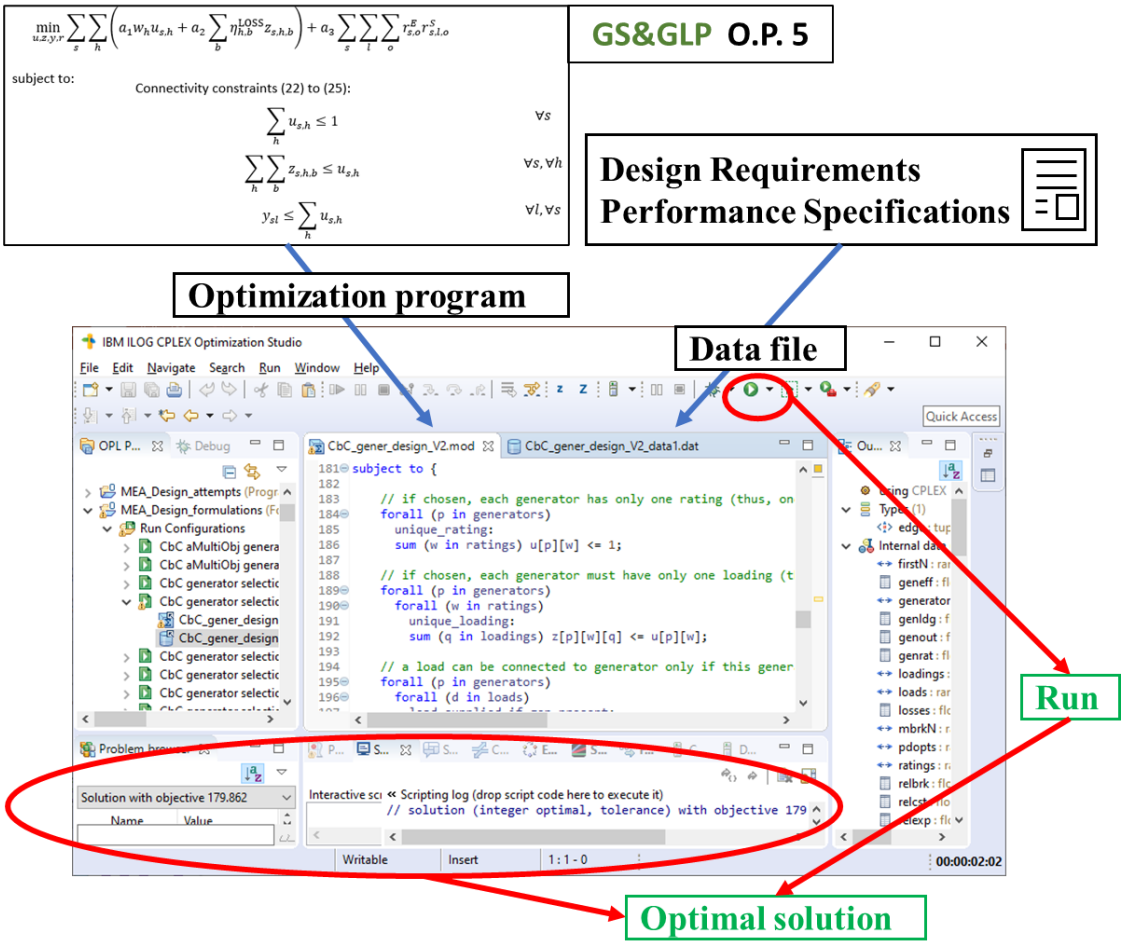

Figure 6.8 GS&GLP programmed in OPL in CPLEX Studio 12.9.0 (excerpt).

The optimization formulation in **O.P. 5** is written in OPL (optimization programming language) and programmed in CPLEX Studio 12.9.0. One feature of OPL is that there can be several data files with different sets of parameters (e.g., different range of generator rating) that can be run with the same optimization program (formulation in **O.P. 5**). The GS&GLP selects and sizes a group of generators (with minimum weight and loss) such that connectivity, power balance and resiliency constraints are satisfied. A generator-load pair arrangement is also obtained as part of the optimization solution. The solution to the GS&GLP in CPLEX Studio 12.9.0 looks like the output shown below in **Figure *6.9***.

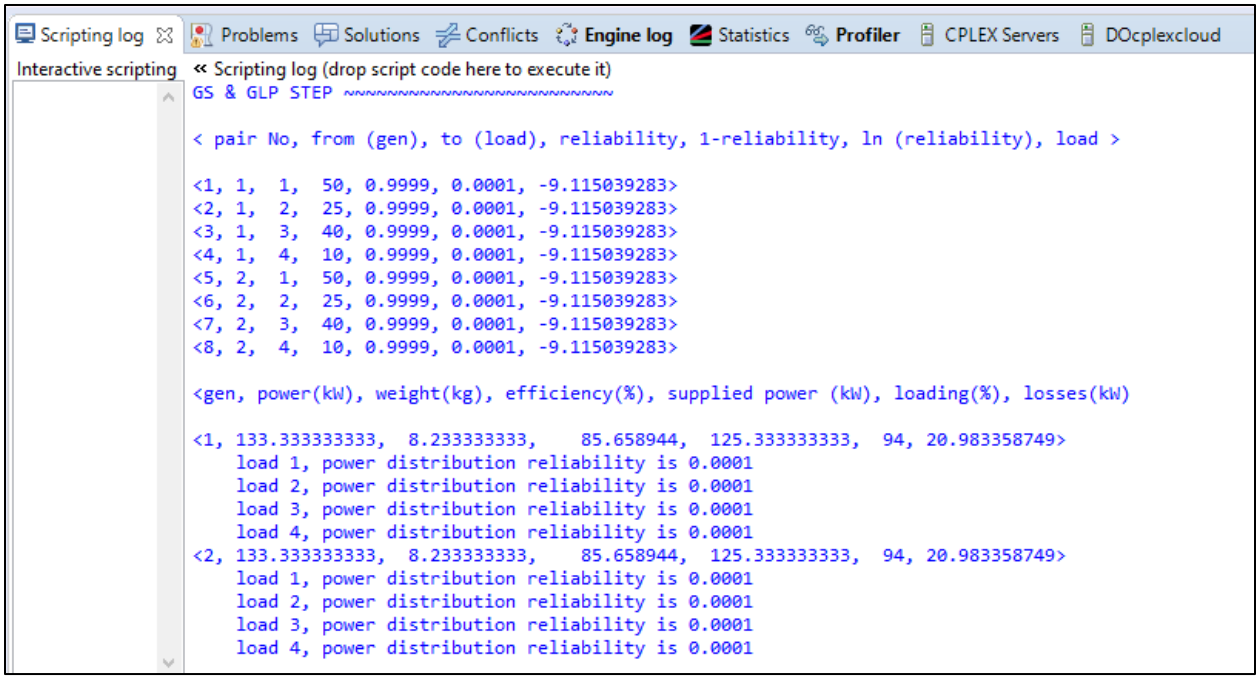

Figure 6.9 GS&GLP outcome in CPLEX Studio 12.9.0 (script excerpt).

The GS&GLP outcome (from CPLEX Studio 12.9.0) depicted in **Figure *6.9*** presents:

- The selected assigned pairs (generator-load pairs, set K), their reliabilities (targets for the following PDD), and the logarithm value of the reliabilities (linearization with logarithms).
- The selected generators, their power ratings (kW), weights (kg), efficiency (%), supplied power (kW), loading (%), and losses (kW). The values for efficiency, supplied power, loading, and losses are for the maximum loading conditions. These values can change during operation.

The GS&GLP solution depicted in **Figure *6.9*** is re-arranged in **Table *6.8*** (generator-load pair arrangement and generator selection) and **Figure *6.10*** (solution overlapped on template of **Figure *6.5***).

The selected generators are shown in a blue colour, while the selected assigned pairs are in bold. Two generators out of five candidates were selected and the total generation capacity is 266 kW. Also, 8 out of 20 distribution paths were selected. Given that the loads' reliability requirements are high, all loads are connected to two generators. Hence, due to the reliability requirements, generation capacity is a little

more than twice the total load demand; total load accounts for 125 kW. Generation capacity could be exactly 125 kW to match total load demand, but any failure event or generation deficiency then would lead to the lack of compliance to the reliability requirements.

Table 6.8 GS&GLP optimal solution for a MEA EPS design example.

	G_1	G_2	G_3, G_5, G_6
P_s^G (kW)	133	133	**Not selected**
Loads served	$\{L_1, L_2, L_3, L_4\}$	$\{L_1, L_2, L_3, L_4\}$	--
Set K	$y_{11}, y_{12}, y_{13}, y_{14}$	$y_{21}, y_{22}, y_{23}, y_{24}$	--
Reliability r_{sl} of the assigned pair k	$1 - r_{11} = 1.0 \times 10^{-4}$ $1 - r_{12} = 1.0 \times 10^{-4}$ $1 - r_{13} = 1.0 \times 10^{-4}$ $1 - r_{14} = 1.0 \times 10^{-4}$	$1 - r_{21} = 1.0 \times 10^{-4}$ $1 - r_{22} = 1.0 \times 10^{-4}$ $1 - r_{23} = 1.0 \times 10^{-4}$ $1 - r_{24} = 1.0 \times 10^{-4}$	--

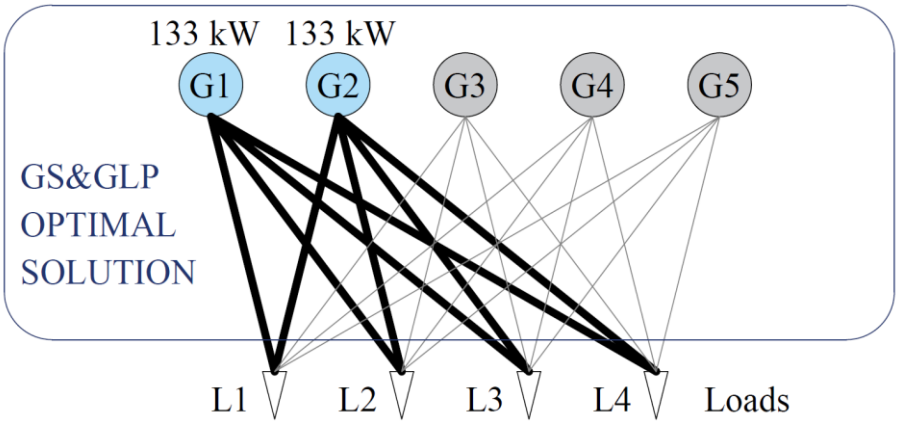

Figure 6.10 GS&GLP optimal solution for the EPS design example (graphical).

In addition, the optimal solution comprises the following:

- The total power generation weight is 16.5 kg.
- The total cost of the power generation is £4.12k.
- The generation loss for each generator is 20.98 kW, i.e., 15.7% with respect to the nominal rating (133 kW) in **Table *6.8***.

The optimal solution of the GS&GLP is used in the PDD step to refine the assigned pairs (of the virtual power distribution) into distribution paths and construct a power distribution system. The reliabilities r_{sl} of each path are used as reliability targets in the PDD step.

6.2.4. Power Distribution Design

The inputs for the PDD consist of: design specifications and requirements, platform abstractions, PDD template, and GS&GLP outcome (generator-load pair arrangement, reliability targets for distribution paths). Recall that the generator-load pair arrangement contains the selected assigned pairs that will be synthesized into distribution paths.

The inputs for the PDD have been detailed in Section 6.2.1 including **Table *6.1*** (load requirements), **Table *6.3*** (PDD abstractions), **Figure *6.6*** (template), and GS&GLP output in **Table *6.8***. The HV bus bar (source matrix contactor in **Figure *6.4***) can allow power generation transference without cross-connecting generators. The power density, weight, fixed costs, variable costs, reliability, and maximum power for all connections and all types of components are the main design coefficients. The power density of the DC/DC converters is 15 kW/kg as previously stated (a conservative value).

In this example, the following assumption applies:

- The cabling distances between components and the components' location are assumed to have negligible impact on the selection of the cabling system, i.e., voltage drop, and power losses are minimal. Then, knowing the required ampacity suffices for the selection of the wire gauge.

The PDD synthesizes distribution paths by considering the optimal solution of the GS&GLP step shown in **Table *6.8*** and **Figure *6.10***, the power distribution platform abstraction in **Table *6.3***, and the MILP optimization formulations presented in Chapter 4. Revisiting the PDD formulations:

- **O.P. 6**: Each assigned pair is built as a series-system (single distribution path).

$$\text{Min} \sum_{(i,j)\in\mathcal{A}} \left(\text{fixed cost}_{ij} + \text{variable cost}_{ij}\right) + \sum_{i\in\mathcal{N}} \left(\text{fixed cost}_i + \text{variable cost}_i\right)$$

subject to: Connectivity constraints (32) and (33)

Power balance constraints (31)

Reliability constraints, (38) with (36), (37), and (39)

- **O.P. 7**: Resilient design for a set of failure scenarios.

$$\text{Min} \sum_{(i,j)\in\mathcal{A}} \left(\text{fixed cost}_{ij} + \text{modules}_i\right) + \sum_{(i,j)\in\mathcal{A}} \left(\text{variable cost}_{ij}\right) + \sum_{i\in\mathcal{N}} \left(\text{variable cost}_i\right)$$

subject to: Connectivity constraints (40)

Power balance constraints (41)

Reliability constraints, (42) and (43)

- **O.P. 8**: Resilient design with two-disjoint paths (per assigned pair).

$$\text{Min} \sum_{(i,j)\in\mathcal{A}} \left(\text{fixed cost}_{ij} + \text{variable cost}_{ij}\right) + \sum_{i\in\mathcal{N}} \left(\text{fixed cost}_i + \text{variable cost}_i\right) - \sum_{k\in K} \sum_{q} \text{path reliability}_k^q$$

subject to: Connectivity constraints (44), (45), (47), (48)

Power balance constraints (46)

Disjointness, (51), (52), (55) – (58), (54)

The PDD formulations above are illustrated through their application in several design scenarios, consisting of different resilient design requirements, as proposed in **Table *6.4***. The idea is to show the potential of all the MILP formulations studied for the design of an EPS architecture for the same application. As previously mentioned, there is no one-size-fits-all solution and the selection between optimal solutions synthesized from several resilient design requirements (whenever the designer has this flexibility) is a trade-off exercise. Hence, there is no 'best' solution among the optimal architectures presented in this section (each satisfying different resilience requirements), e.g., for some applications the resilience requirements in scenario 4 of **Table *6.4*** are sufficient for a specific application, while for

others the optimal architecture from scenario 11 of **Table *6.4*** is adequately, given the available budget and resources for the construction project.

According to the different resilience requirements suggested in the scenarios of **Table *6.4***, loads are divided into critical and non-critical loads, i.e., load criticality is an additional specification for the reliability targets specified in **Table *6.1***. This means that:

- Critical loads are always supplied with power and a certain power availability at loads' terminals is still achieved. Critical loads cannot be shed in case of failures in distribution components.
- Non-critical loads can be shed at some point due to failures in distribution components. However, non-critical loads still comply to a reliability target.

Hence, the set of assigned pairs connecting generators and loads (GS&GLP optimal solution in **Table *6.8***) are divided into two subsets, one that serves non-critical loads K_{NC}, and the other supplying critical loads K_C, i.e., $K = \{K_{NC}, K_C\}$. The power flow P_{ij} in any connection i, j consists of the summation of the power flows from distribution paths supplying critical and non-critical loads. The distribution paths' reliability targets in **Table *6.8*** are tabulated in **Table *6.9***, re-arranged in a per-load format, to ease comparisons for the rest of this section.

Table 6.9 Reliability targets for distribution paths (per load) from optimal GS&GLP solution.

	L_1	L_2	L_3	L_4
Reliability r_{sl} of the assigned pair k	$1 - r_{11} = 1.0 \times 10^{-4}$ $1 - r_{21} = 1.0 \times 10^{-4}$	$1 - r_{12} = 1.0 \times 10^{-4}$ $1 - r_{22} = 1.0 \times 10^{-4}$	$1 - r_{13} = 1.0 \times 10^{-4}$ $1 - r_{23} = 1.0 \times 10^{-4}$	$1 - r_{14} = 1.0 \times 10^{-4}$ $1 - r_{24} = 1.0 \times 10^{-4}$
Minimum reliability required on any path	$1 - 1.0 \times 10^{-4}$	$1 - 1.0 \times 10^{-4}$	$1 - 1.0 \times 10^{-4}$	$1 - 1.0 \times 10^{-4}$

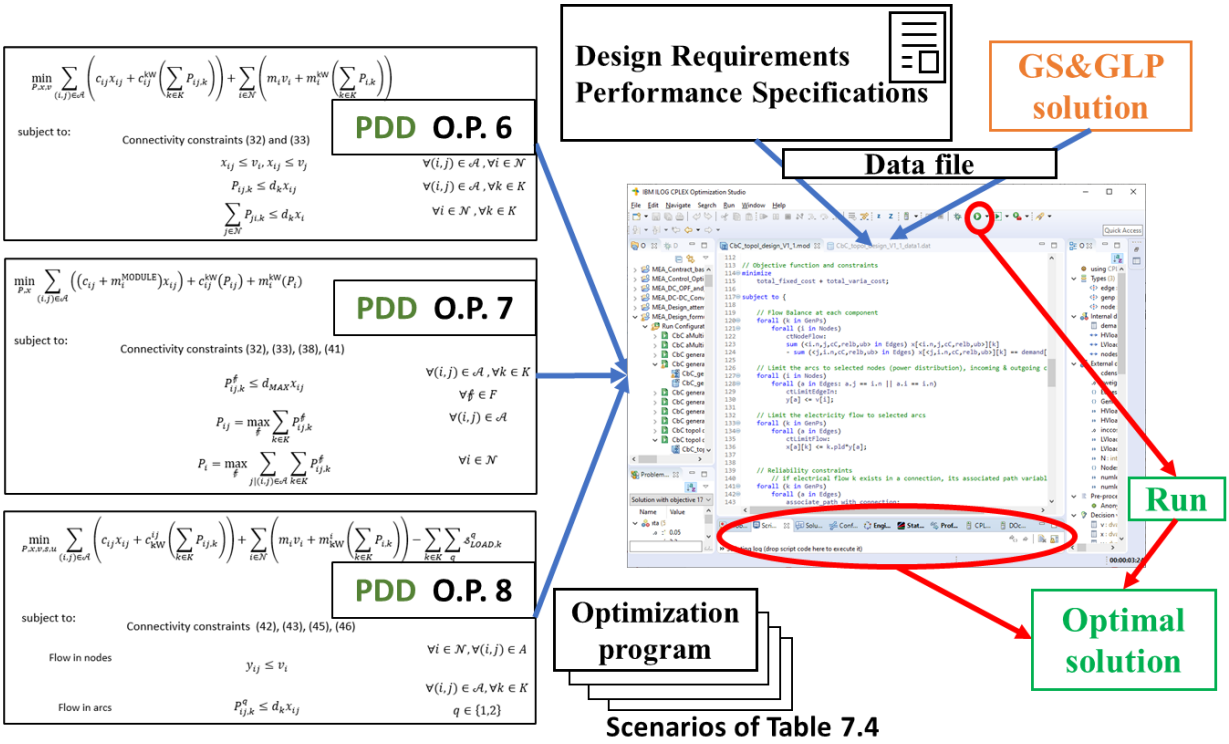

Figure 6.11 PDD programmed in OPL in CPLEX Studio 12.9.0 (excerpt).

The optimization formulations in **O.P. 6**, **O.P. 7**, and **O.P. 8** are written in OPL (optimization programming language) and programmed in CPLEX Studio 12.9.0. Several data files are populated with the parameters of the scenarios proposed in **Table *6.4***. The PDD synthesizes the distribution paths obtained in GS&GLP step, in other words, the PDD selects and sizes a group of distribution components and connections such that connectivity, power balance and resiliency constraints are satisfied. The solution to the PDD in CPLEX Studio 12.9.0 looks like the output shown below in **Figure *6.12*** (formulation **O.P. 6**). In the example of **Figure *6.12***, there are 9 connections selected (out of 48) and 3 components selected (out of 12) according to the template in **Figure *6.6***. The reliabilities of the 9 distribution paths of the GS&GLP solution are also shown and compared to the reliability targets (also determined from the GS&GLP).

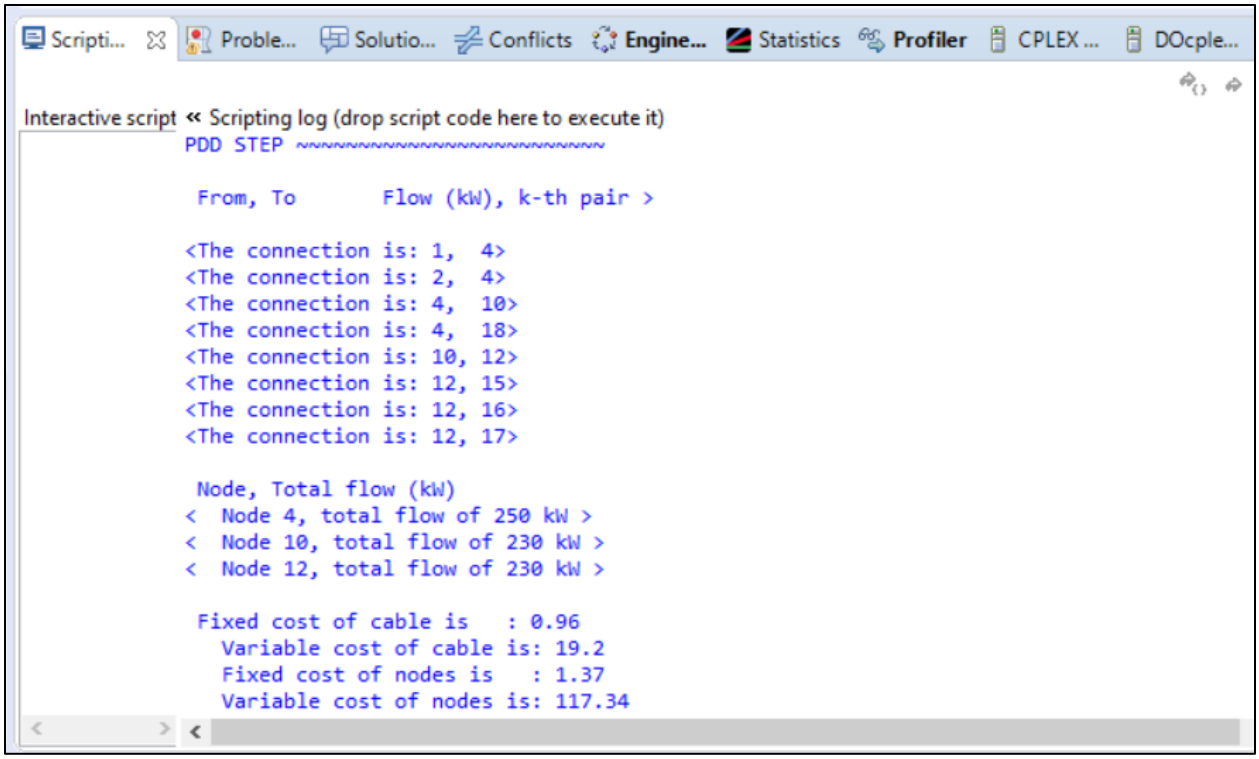

Figure 6.12 PDD outcome in CPLEX Studio 12.9.0 (script excerpt, outcome for formulation O.P. 6).

The scenario 1 (each assigned pair synthesized as a single distribution path) of **Table *6.4*** results in the EPS architecture shown in **Figure *6.13***. The generators supply the LVDC loads through a series system formed by a HV bus bar, DC/DC converter, and LVDC bus (power distribution has 3 components). Each distribution path supplying LVDC loads use the same series-system; L_4 is only supplied through the HV bus bar. The cost, weight, and reliability of this architecture is shown in **Table *6.10***. The reliabilities of the distribution paths are within the targets in **Table *6.9***. Note that if a failure occurred in any component of the EPS in **Figure *6.13***, power supply to LVDC loads is cut. Given the lack of alternative paths to distribute power to the loads in the Scenario 1, resilient designs are used.

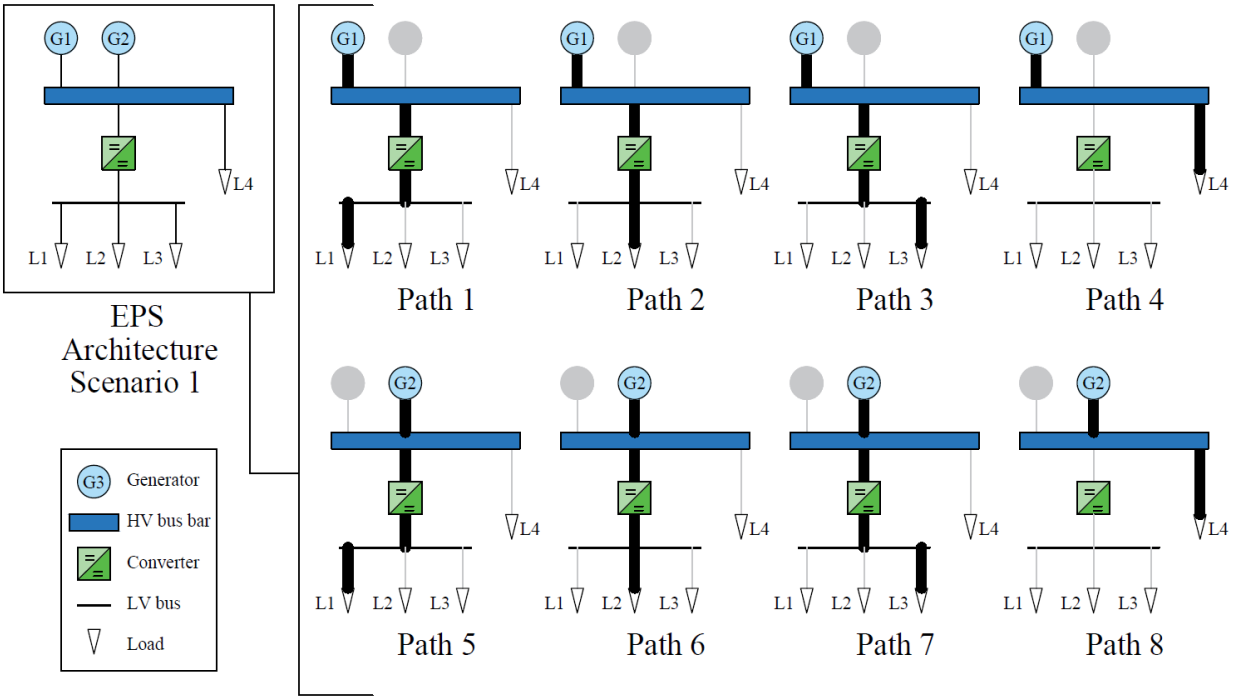

Figure 6.13 MEA EPS for scenario 1 of Table 6.4 (distribution paths of Table 6.8 in bold).

Table 6.10 PDD optimal result for Scenario 1 in Table 6.4.

Cost (k£)*	Weight (kg)*	Reliability at load's terminals			
		L_1	L_2	L_3	L_4
138.0	62.7	1.20×10^{-5}	1.20×10^{-5}	1.20×10^{-5}	1.01×10^{-6}

* only power distribution

The resilient designs for a failure set corresponds to the formulations in Scenarios 2 to 7 of **Table *6.4***, while the resilient designs with two-disjoint paths correspond to the formulations in Scenarios 8 to 14.

The power distribution topologies that result from the synthesis of resilient designs for a failure set (Scenarios 2 to 7 in **Table *6.4***) are shown in **Figure *6.15***. Critical loads are in bold; components that are considered as fallible have an asterisk (*) included. The failures are modelled by determining which connections ij are active and which are not. Each case of the set F has 48 failure elements f_{ij}. Recall that

there are 48 connection candidates as depicted in the PDD template of **Figure *6.6*** ($f_{ij} = 1$ for a failed connection ij). Then, a failure in a component i is determined by setting all incoming and outgoing connections as failed, that is, $f_{ji} = 1$ and $f_{ij} = 1$ for all the components j that are connected to component i. An example is shown in **Figure *6.14*** for the case a failure is declared in converter 1; all the connections ij (in red colour) have $f_{ij} = 1$ (8 in total) for the failure where converter 1 fails. Depending on the set F, the number of selected components varies.

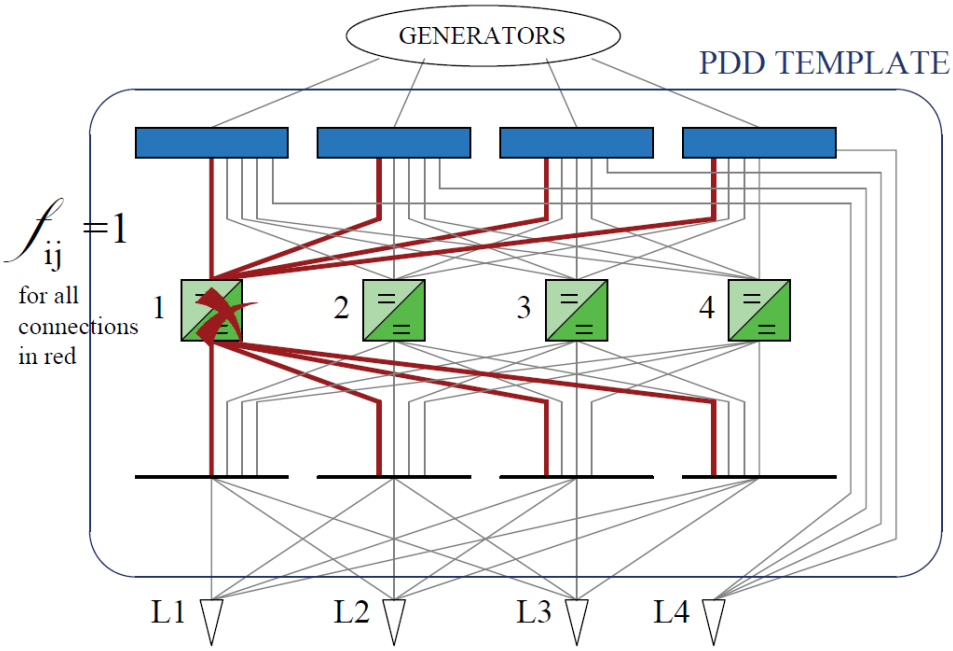

Figure 6.14 Example of failure in converter 1; all connections ij in red are considered as failed.

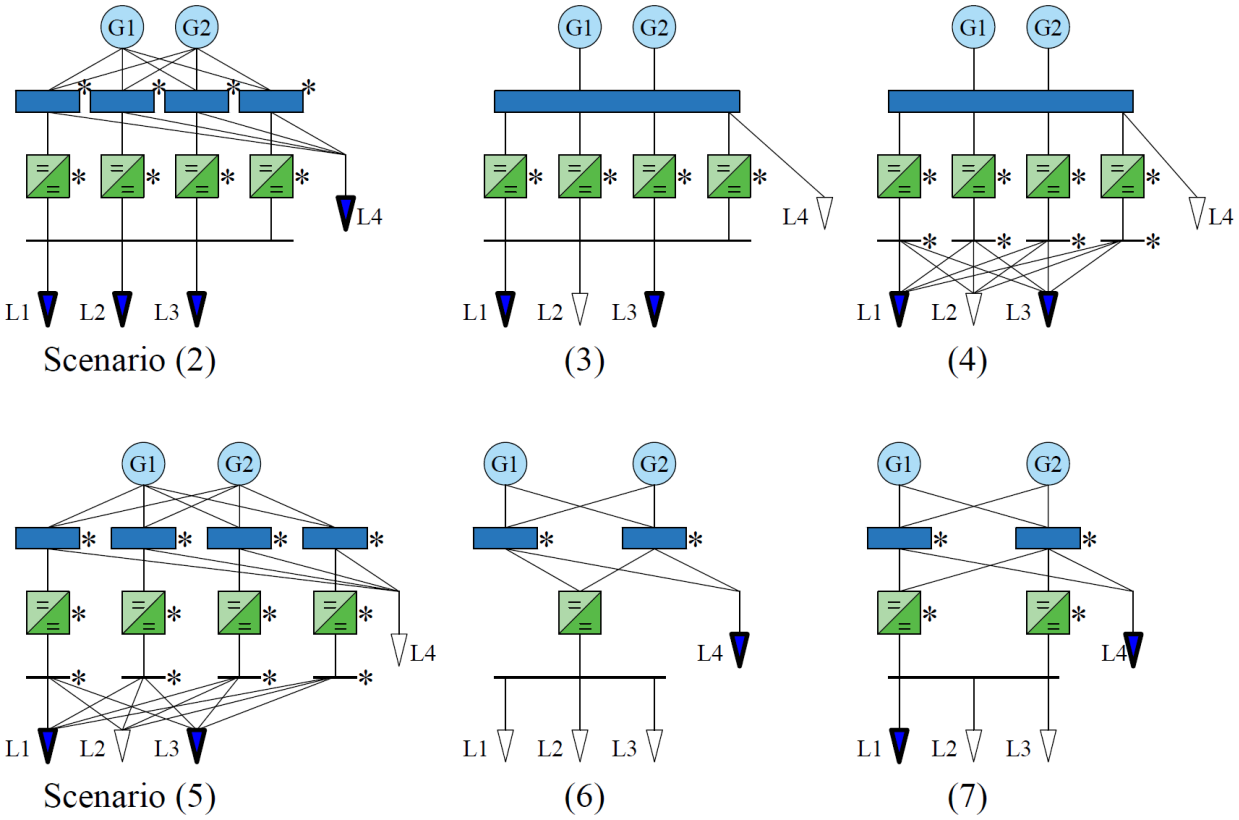

Figure 6.15 MEA EPS optimal architectures for failure-resistant resilient requirements in Table 6.4.

In scenario 2, HV bus bars and converters are fallible; in scenario 3, only converters are fallible, so there is only one HV bus bar and one LVDC bus. In scenario 4, converters and LVDC buses (but not HVDC bus) are fallible, for which reason there is only one HV bus bar. Scenario 5 is the special case where all components can fail, and that is why the number of components is the highest (compared to the rest of cases). Of course, the number of selected components does not only depend on the failure cases included in the corresponding scenario, but also on the combination of critical and non-critical loads. For example, the difference between scenario 6 and 7 is that in scenario 7 there is one additional critical load (L1 in addition to L4) and the converters are fallible, for which reason the number of converters is doubled. The results in terms of total cost, weight, and reliability (at load terminals) are tabulated in **Table *6.11***.

Table 6.11 PDD optimal results for Scenarios 2 to 7 in Table 6.4.

Scenario	Cost (k£)*	Weight (kg)*	Reliability at load's terminals			
			L_1	L_2	L_3	L_4
2	179.0	81.5	1.0×10^{-6}	1.0×10^{-6}	1.0×10^{-6}	1.0×10^{-10}
3	145.0	64.9	2.0×10^{-6}	2.0×10^{-6}	2.0×10^{-6}	1.0×10^{-6}
4	152.3	70.0	1.0×10^{-6}	1.0×10^{-6}	1.0×10^{-6}	1.0×10^{-6}
5	154.8	72.0	1.0×10^{-10}	1.0×10^{-10}	1.0×10^{-10}	1.0×10^{-10}
6	140.4	63.9	1.1×10^{-5}	1.1×10^{-5}	1.1×10^{-5}	1.0×10^{-10}
7	141.4	64.3	1.0×10^{-6}	1.0×10^{-6}	1.0×10^{-6}	1.0×10^{-10}

*only power distribution

Note that the cost and weight values in **Table *6.11*** are only for the power distribution system. In scenario 5, failures are considered in the HVDC bus bars, DC/DC converters, and LV buses. Therefore, it has the highest number of components, 12 in total. Scenario 2 is the heaviest and most expensive option, yet there is only one LVDC bus because failures in LV buses are not considered by this Scenario. In all cases where failure on DC/DC converters are considered (all except 6), the EPS distribution has at least 2 converters, i.e., redundant converters. There is only one HVDC bus bar, but no failures are considered for this component. The lightest and cheapest option is Scenario 6 which considers only HVDC bus bars failures. This EPS is appropriate if critical loads were on the HVDC side. In cases where LVDC loads are critical (L_1 and L_3 in all scenarios except 6), weight and cost can be reduced differently depending on the resiliency requirements. In general, some weight and cost savings are possible depending on the critical load combination and the reliability requirements.

When a failure set cannot be determined, a resilient design with two-disjoint path formulations for critical loads can be used. These options correspond to Scenarios 8 to 14 in **Table *6.4***. The two-disjoint path formulation allow the synthesis of an EPS distribution whose paths are disjoint, hence, there are at least two components of the same type on each level (HVDC bus bar, DC/DC converter, and LVDC bus). Recall

that the disjointness applies on every distribution path for a critical load. In the EPS architecture of scenario 8 shown in **Figure *6.16***, disjoints paths have been highlighted (in bold) to depict disjointness.

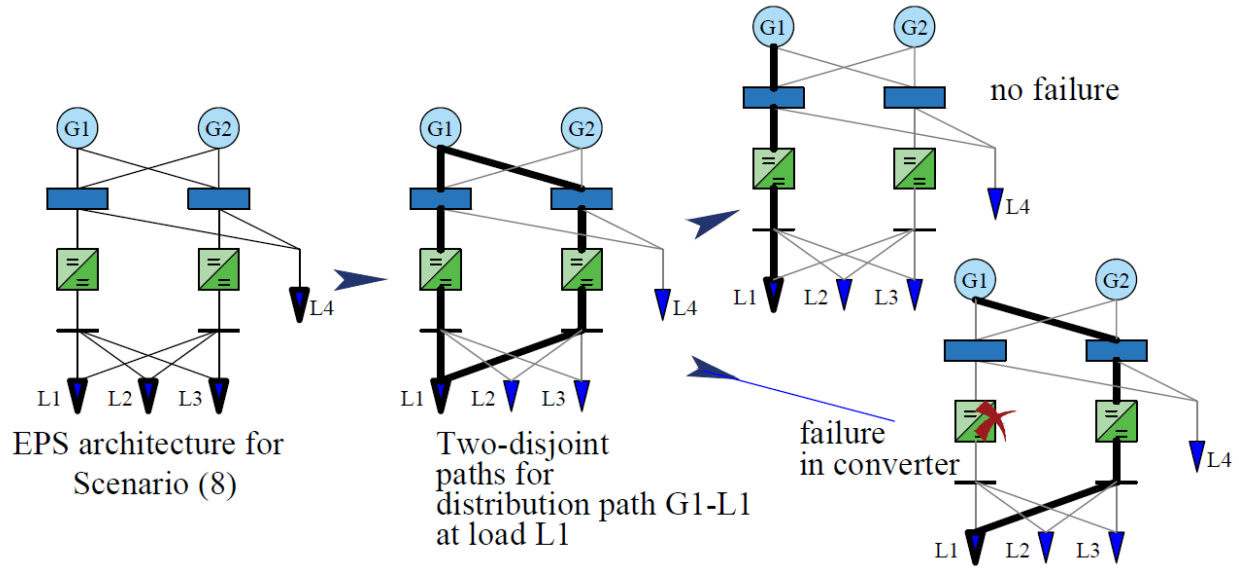

Figure 6.16 EPS architecture for scenario 8 (two-disjoint path); each disjoint path is in bold.

Disjointness is not enforced between distribution paths that supply other critical loads. In other words, one distribution path from a two-disjoint construction can be shared with another path if the connectivity requirements allow. This is precisely what happens in **Figure *6.16***, where disjoint paths for distribution path G1 – L1 (in bold) are shared with distribution path G1 – L2 (components are the same). Enforcing disjointness between all distribution paths serving n critical loads means that there are $2n$ disjoint paths in the distribution system. Almost half of the distribution system could be carried inefficiently during the flight if no failure occurs. Nevertheless, it is not necessary to enforce such disjoint condition, to avoid unnecessary weight; reliability still could be satisfied. The optimal architectures for the two-disjoint paths scenarios 8 to 14 are depicted in **Figure *6.17*** and results are shown in **Table *6.12***.

The disjointness in **O.P. 8** (optimization formulation for the two-disjoint path case) relies on the $u_{ij,k}, u_{i,k}$ variables for the construction of distribution paths that do not share the same components. Similarly to the architectures shown in **Figure *6.15***, it depends on the combination of critical loads and resiliency

requirements to achieve solutions with different costs and weights, thus, obtaining savings in some cases without compromising the system's resiliency.

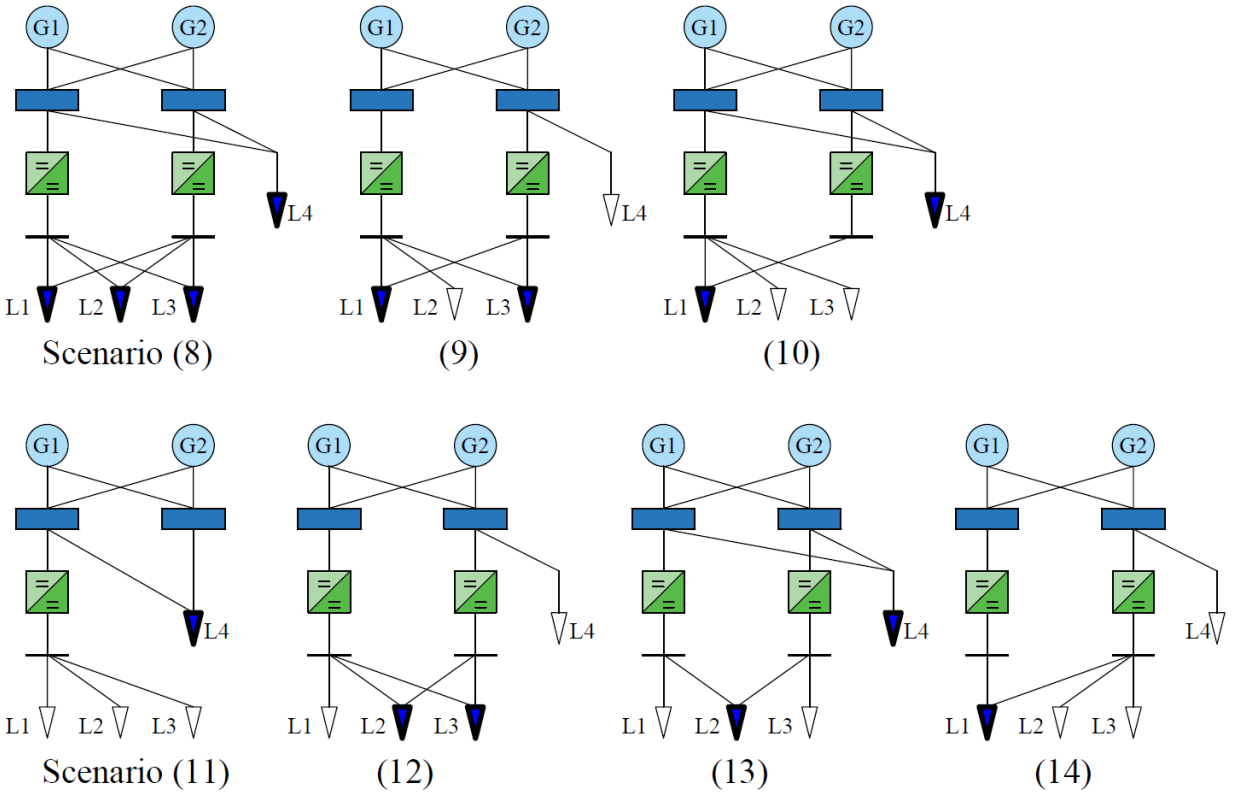

Figure 6.17 MEA EPS optimal architectures for two disjoint path resilient requirements in Table 6.4.

The lightest and cheapest option can be obtained by setting HVDC loads as critical, as in Scenario 11. For the rest of the cases where LVDC loads are critical, the system's cost is increased. The reliability targets of the loads have been satisfied, as well as the reliability targets of the distribution paths (obtained from the GS&GLP).

Table 6.12 PDD optimal results for Scenarios 8 to 14 in Table 6.4.

Scenario	Cost (k£)*	Weight (kg)*	Reliability at load's terminal			
			L_1	L_2	L_3	L_4
8	277.7	125.3	2.4×10^{-10}	2.4×10^{-10}	2.4×10^{-10}	1.0×10^{-10}
9	245.3	110.0	2.4×10^{-10}	1.2×10^{-5}	2.4×10^{-10}	1.0×10^{-6}
10	202.1	91.8	2.4×10^{-10}	1.2×10^{-5}	1.2×10^{-5}	1.0×10^{-10}
11	142.6	65.5	1.2×10^{-5}	1.2×10^{-5}	1.2×10^{-5}	1.0×10^{-10}
12	216.3	97.1	1.2×10^{-5}	2.4×10^{-10}	2.4×10^{-10}	1.0×10^{-6}
13	173.1	78.9	1.2×10^{-5}	2.4×10^{-10}	1.2×10^{-5}	1.0×10^{-10}
14	198.8	89.3	2.4×10^{-10}	1.2×10^{-5}	1.2×10^{-5}	1.0×10^{-6}

*only power distribution

All of the results from the synthesis of EPS architectures for the scenarios 1 to 14 of **Table *6.4*** have been presented in **Table *6.10***, **Table *6.11***, and **Table *6.12*** and **Figure *6.13***, **Figure *6.15***, and **Figure *6.17***. All of these scenarios have been presented to illustrate the potential of the PDD optimization formulations in **O.P. 6**, **O.P. 7**, and **O.P. 8** (distribution path as series system, resilient for a set of failure scenarios, and resilient design with two-disjoint paths, respectively). However, given only one scenario, the optimal is the ESP architecture required. However, it is a common practice in industry to evaluate several scenarios and compare them in terms of weight, reliability, efficiency, and cost, in other words, to perform a tradeoff analysis.

A trade-off example within a single application

A tradeoff is an exercise to compare optimal EPS architectures in terms of weight, reliability, efficiency, and cost. All of the results for the scenarios in **Table *6.4*** and presented in **Table *6.10***, **Table *6.11***, and **Table *6.12*** and **Figure *6.13***, **Figure *6.15***, and **Figure *6.17*** (14 scenarios) are compactly depicted in **Figure *6.18*** in terms of cost, weight, and reliability. In **Figure *6.18***, unreliability is just 1 – reliability (numerical complement). Also, minimum unreliability in **Figure *6.18*** refers to the lowest value among the unreliability of all distribution paths.

It has been already stated that in the case where the designer faces several sets of resiliency requirements for the same application (usually there is only one set), a tradeoff is required. Scenario 1 has been highlighted as the base case (orange circle). The blue dots are the optimal costs, weights, and reliability for the 14 scenarios. These dots have been projected to the cost vs. weight, weigh vs. reliability, and cost vs. reliability planes with light blue-, grey-, and khaki-colored dots respectively.

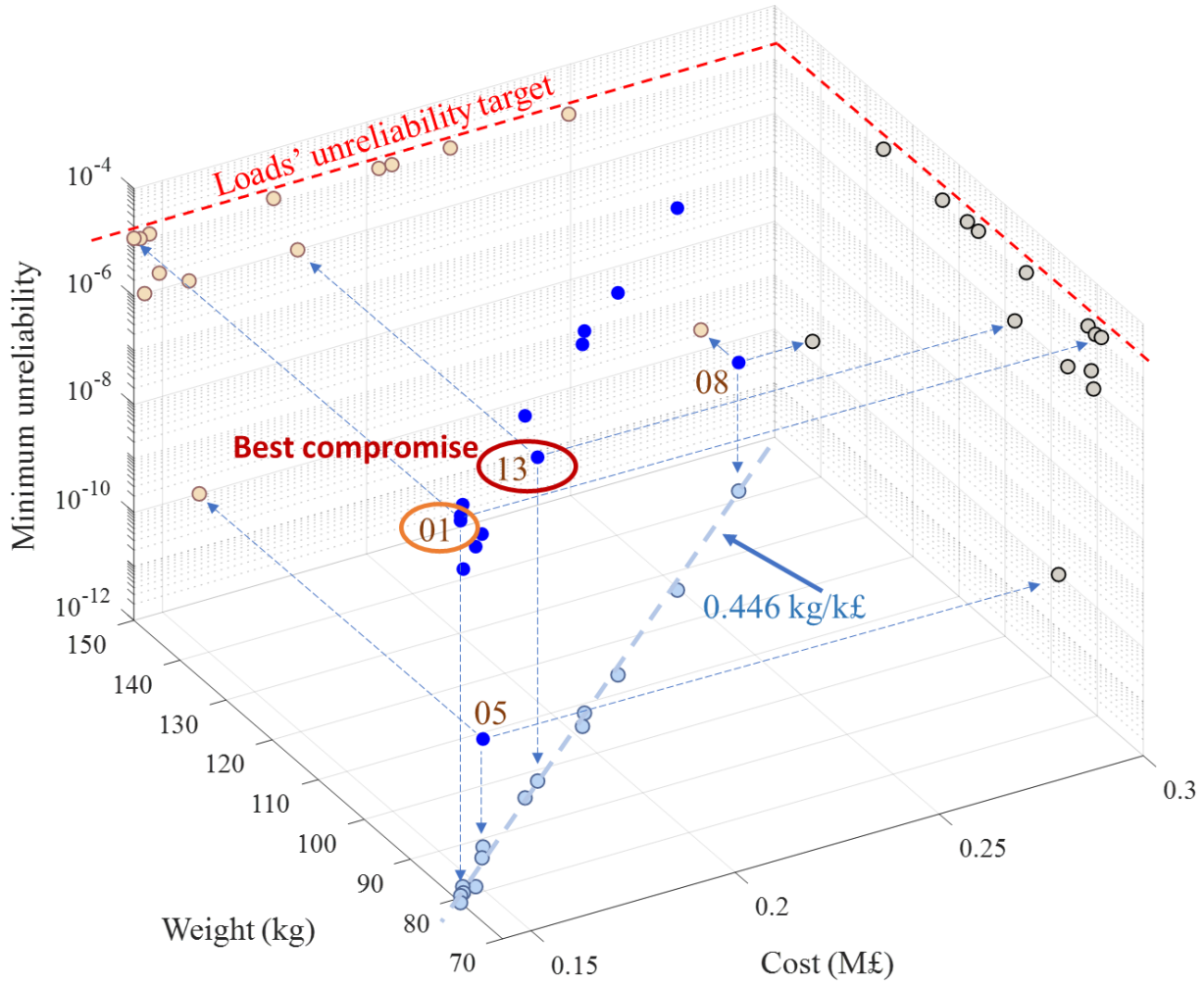

Figure 6.18 Weight, cost, and reliability for the 14 resilient scenarios in Table 6.4.

In the weight vs. cost plane, the projection of the optimal for the 14 scenarios (weight vs. cost relation for all the optimal) does follow a roughly linear relationship with a ratio of ~0.446kg/k£. A mid-cost/mid-weight option that has a reliability around $1 - 1.0 \times 10^{-10}$ is scenario 5 (resilient to a failure set). A

slightly more expensive option is scenario 13 (resilient by being two-path disjoint) reaching a reliability between $1 - 1.0 \times 10^{-5}$ and $1 - 1.0 \times 10^{-10}$.

Having a moderately medium budget (considering a top of 300k£), option 13 is the best weight-cost-reliability compromise according to the results observed (one LVDC and one HVDC load are critical only). Option 13 has been highlighted (red circle) in **Figure *6.18***. A final discussion of the results presented in this study case is detailed below.

6.2.5. Discussion of the design results

An EPS architecture has been synthesized by using optimization formulations for GS&GLP and PDD. The optimal voltage selection has been independently performed. The optimal voltage for a DC EPS in this study has been found to be approximately 3 kV assuming the cabling system specifications is as per **Table *6.5*** and the set of wire gauges available for power distribution is as in **Table *6.6***. A maximum power transfer of 503 kW and a maximum power density of 954 kW/kg/m can be achieved. The wire gauge that allows such a maximum is 3/0 AWG, aluminum conductor, PVC insulation.

After determining the optimal voltage for the system, an EPS architecture has been obtained for all the scenarios of **Table *6.4***. A summary of the results in terms of cost, weight, efficiency, and reliability for each of the optimal EPS synthesized with the proposed framework is presented in **Table *6.13***. This table also tabulates the solution time for comparison purposes. Assuming that the EPS cost is proportional to its weight, the main trade-off analysis can be conducted by looking at the EPS cost and reliability. Most of the optimal solutions provide at least a reliability between $1 - 1.0 \times 10^{-7}$ and $1 - 1.0 \times 10^{-5}$. Based on the results observed, it can be concluded that:

- In all cases, loads' reliability targets were achieved such that $r \geq r_{\text{TARGET},\, l}$
- Although Scenario 1 complies with required reliability at minimum cost, no resiliency is provided.

- In general, failure-resistant optimal architectures have higher reliabilities than two-disjoint path systems.
- The EPS built to comply with two-disjoint paths for critical loads have higher costs compared to failure-resistant EPS.
- Scenarios 6, 7 and 11 are the most economical because the critical load is HVDC which means only one HVDC bus bar is required. On the other hand, LVDC loads require at least one power conversion stage in addition to the HVDC bus bar.
- Scenarios 7, 3, 4, and 5 are the most economical when a set of LVDC loads is critical. The costs increase due to the power conversion stage required.
- Scenario 14 has one LVDC load and its cost is less than having two critical LVDC loads, as in Scenario 9. However, having less stringent requirements for LVDC loads lowers the cost, as seen for Scenario 12.
- The solution times of the failure-resistant designs are higher (on average) than the two-disjoint path resilient designs. This is due to the higher number of constraints per failure case.

Table 6.13 EPS architecture optimal results summary for scenarios in Table 6.4.

	Single Path	Design for a failure set					
Scenario	1	2	3	4	5	6	7
Critical loads	N/A	All	1, 3	1, 3	1, 3	4	1, 4
F	-	Converter & HV box	Converter	Converter & LV bus	N-1 rule	HV box	Converter & HV box
Cost* (k£)	143.0	183.1	149.2	156.5	159.0	144.5	145.6
Weight* (kg)	79.1	97.9	81.3	86.4	88.4	80.4	80.8
***r* L1**	1.2e-05	1.0e-06	2.0e-06	1.0e-06	1.0e-10	1.1e-05	1.0e-06
***r* L2**	1.2e-05	1.0e-06	2.0e-06	1.0e-06	1.0e-10	1.1e-05	1.0e-06
***r* L3**	1.2e-05	1.0e-06	2.0e-06	1.0e-06	1.0e-10	1.1e-05	1.0e-06
***r* L4**	1.0e-06	1.0e-10	1.0e-06	1.0e-06	1.0e-10	1.0e-10	1.0e-10
Solving time (s)	0.796	174.84	11.102	35.42	194.30	7.023	24.652

	Two Disjoint Path						
Scenario	**8**	**9**	**10**	**11**	**12**	**13**	**14**
Critical loads	All	1, 3	1, 4	4	2, 3	2, 4	1
F	-	-	-	-	-	-	-
Cost* (k£)	281.9	249.5	206.2	146.8	220.5	177.2	203.0
Weight* (kg)	141.8	126.4	108.2	82.0	113.6	95.4	105.8
***r* L1**	2.4e-10	2.4e-10	2.4e-10	1.2e-05	1.2e-05	1.2e-05	2.4e-10
***r* L2**	2.4e-10	1.2e-05	1.2e-05	1.2e-05	2.4e-10	2.4e-10	1.2e-05
***r* L3**	2.4e-10	2.4e-10	1.2e-05	1.2e-05	2.4e-10	1.2e-05	1.2e-05
***r* L4**	1.0e-10	1.0e-06	1.0e-10	1.0e-10	1.0e-06	1.0e-10	1.0e-06
Solving time (s)	25.034	3.639	19.722	1.565	16.702	3.582	4.495

* Cost and weight include both generation and power distribution

The optimal EPS architectures synthesized here resemble the results found in [36], [86] and correspond to similar network structures found in [15], [17], [79].

While other design frameworks iterate several times by adding reliability constraints to the EPS architecture candidate until the reliability target is satisfied, our proposed framework has no need for iterations and can synthesize the EPS architecture with one optimization problem. The adoption of network design formulations has helped in providing the tools to formulate reliability-based problems into resilient network design problems. Therefore, the proposed design framework improves the exploration of a vast design space, investigates optimal solutions, and performs a trade-off analysis for several sets of requirements, as evidenced in **Table *6.13***.

6.3. Conclusion

A case study for the design of a direct current (DC) EPS for a small more electric aircraft application has been presented. Several sets of resiliency constraints were proposed to demonstrate the potential of the proposed design framework in producing several architectures depending on the reliability requirements. A trade-off analysis is required if the designer faces several sets of reliability requirements to select according to the available budget and resources. In any other case, a unique set of functional and safety specifications must be determined, such that, having utilized the proposed framework, there is only a single optimal EPS architecture solution.

7. Experimental Testbed

7.1. Introduction

This chapter concludes the work on EPS architecture design by proposing an experimental testbed to evaluate the performance of an optimal architecture synthesized with the proposed design framework (Chapter 3). The MILP optimization formulations for GS&GLP and PDD (Chapter 4) were used to determine an optimal EPS architecture that complies with a new set of functional and safety specifications. Then, a controller which considers topology reconfiguration (Chapter 5) is used to evaluate the system's performance under unexpected failures. In other words, the experimental testbed is built to allow investigation on the performance of a reconfiguration technique and its impact in real time.

An EPS architecture allows flexible routing of power for increased reliability, that is, higher power availability at critical loads. Nevertheless, there is still a gap between having an analytical solution and having a tangible demonstration of the performance of the optimal candidate. In order to close this gap, a scaled testbed representing a DC EPS whose functional and reliability performance can be tested in real time is proposed. The purpose of this prototype is threefold:

- Demonstrate a theoretical EPS architecture with a DC power distribution
- Validate new findings on topology reconfiguration and power management techniques, and
- Provide a platform for testing power transfer and interconnections upon failures in components

In order to validate the theoretical design, a scaled down EPS setup is proposed, built on commercially available electronic components. The development of a physical setup that evaluates the architectural and functional behavior provides valuable performance information to confirm appropriate EPS operation for the range of required conditions. Besides, such a testbed allows the investigation of other control strategies and power management control which is still under early research. The convenience and

limitations of such testbed are explored with the analysis of several failure scenarios and operating conditions.

7.2. The EPS testbed

The intention of a testbed is to provide a means to improve the understanding of the functional requirements and operational behavior of the system [169]. The assembly of an aircraft EPS is a complex and costly task, this being reason for which rapid prototyping and performance analysis is held to be inaccessible in some cases. Research laboratories can be multimillion dollar facilities as in the case of 'The Grid' by Collins Aerospace [170], or fairly limited in other cases. The deployment of a testbed provides a realistic hardware-software environment to test components without having the ultimate system [169]. A limited number of testbeds have been proposed in the literature to validate theoretical advances in control, yet few applications have been dedicated to MEA. The authors in [45] implemented a microscale AC/DC hybrid power system testbed with electronic components resembling a traditional aircraft with left-and right- mirrored zones interconnected by two transfer contactors; the purpose of this testbed is to validate a reactive control. Similar approaches have been reported in [171] and [172] aiming to validate control techniques synthesized with reactive control. Apart from aircraft applications, other efforts have been reported for ground electrical power systems. In [173] an investigation of smart distribution grid scenarios under different load conditions is carried out. Given the unrealistic description of building environments in simulation, the study in [174] introduced a control system paired with a multi-floor scaled building. In [175] a small-scale hardware prototype for a shipboard EPS is developed to allow design and testing of embedded real-time controls including energy management systems. Motorettes (non-rotating machine section of winding and iron) representing complete permanent magnet machines are used in thermal overload and insulation aging studies [176]. In general, testbeds focus on functional verification while other uncertainties are not part of the studies [169].

7.2.1. EPS architecture design

It is assumed that an aircraft conceptual design has been performed and this design has allowed the definition of the electrical loads the EPS will supply. The load sizing for the testbed has followed the recommendations in [126], [127] for electrical loads in typical aircraft and also for MEA. As a reference, the total electrical load in an A320 accounts for approximately 123kW, from which 58% is consumer load, and DC essential load sums up to around 40% (during cruise). By increasing electrification, the electrical load is expected to increase four-fold because the environmental control system, anti-icing, and flight control surfaces are assumed to be supplied completely by electricity. Hence, it is expected that essential loads would account for almost 60%. Therefore, following this projection, the percentage of critical loads in the testbed is 55%, while the rest is non-critical and can be shed if required upon a contingency. **Table *7.1*** tabulates the electrical loads. R1a to R4a are implemented with 50W resistors, while the motor load is implemented with a 5 Vdc electrical motor fed through a driver circuit.

Table 7.1 Load sizing for DC EPS testbed.

Loads per zone	Aircraft system relation (estimation)	Voltage	Power [W]	Critical	% of total load
R1a or R1b	ECS and pressurization, wing anti-icing	HVDC	12.3	Yes	31.9
R2a or R2b	Lighting, entertainment, food heating		12.3	No	31.9
R3a or R3b	Flight and engine control, ECS (shed)	LVDC	5.2	Yes	13.4
R4a or R4b	Cooling, secondary pneumatic and hydraulic		5.2	No	13.4
Motor load a or b	Fuel system, flight & engine control		3.6	Yes	9.3

There are three critical loads and two non-critical loads (per zone) according to **Table *7.1***. There is no reliability target for the loads on this occasion. Instead, critical loads must be supplied at all times regardless of failures in components, while non-critical loads can be shed. Then, resilient design for a set of failure scenarios (PDD in Section 4.3.2) can be used. The design specifications and requirements for the EPS architecture of the testbed are the following (see Section 3.2 and Section 7.2):

- The EPS is divided in two identical (mirrored) zones
- Each zone is supplied with a single power source (main power supply)
- There is a transfer circuit that allows power transfer between zones and power assistance from auxiliary power sources. No loads are connected to the transfer circuit.
- Each zone has two sections, a high voltage (HVDC) and a low voltage (LVDC) section
- Each section has a bus, i.e., there is an HVDC and LVDC bus on each zone
- The power conversion between HVDC and LVDC is performed by a DC/DC converter.
- Two auxiliary power sources are required in case of failure of main power sources.
- Both auxiliary power sources can supply critical loads on the HVDC and LVDC buses
- One auxiliary power source supplies the HVDC loads of either zone in case of generation loss (failure), and the other auxiliary power source supplies the LVDC loads of either zone in case of generation loss or converter loss.
- The auxiliary power sources are part of a transfer circuit with HVDC and LVDC buses, and a DC/DC power conversion between them.
- There are the following types of components: DC/DC converter, HVDC bus, LVDC bus, and power sources.
- The system must be prepared to supply critical loads in case of failure of the main power supply or failure in a power converter (each zone).

Based on the above requirements, the proposed testbed for MEA EPS follows the current aircraft configuration where the electrical system has two mirrored zones (left- and right-) with the same number and size of loads and equal number of buses [177]. Each zone must be capable of supplying its own loads independently from the other, which is the reason for which each zones' power source (engine driving electrical generators in real aircraft) is sized accordingly. In addition, two auxiliary power units provide autonomy on ground and auxiliary power in the event of the loss of a power source. An improvement

with respect to some theoretical proposals based on the patent in [177] is the adoption of DC for the whole system [17] instead of the hybrid AC/DC counterparts. In general, it has been found that the power conversion and transmission could be more efficient in DC than AC [158], [107], and DC could allow maximum generation and battery utilization [178].

Because the EPS is implemented as a micro-scale testbed with commercial electronic devices not necessarily manufactured for aerospace use, the abstractions for MEA detailed in the case study of Chapter 6 (Section 6.2.1) do not apply in this case. Instead, the design space is limited by the local availability of electronic components (see **Figure *7.1*** below).

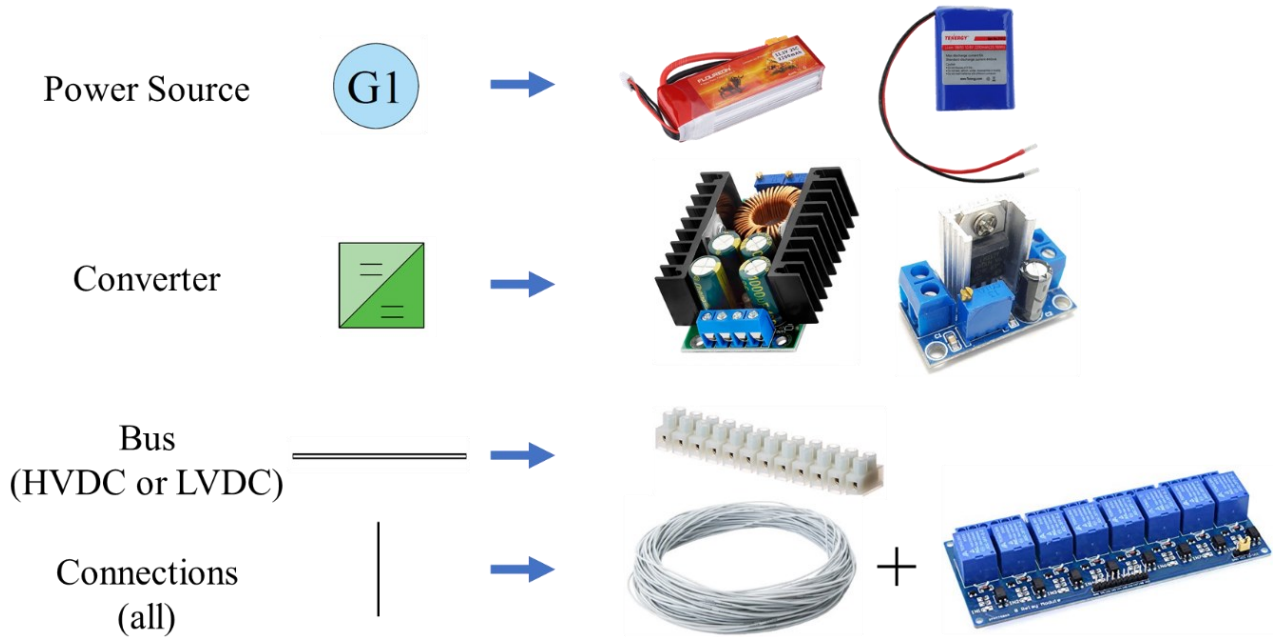

Figure 7.1 Electronic components available for the DC EPS testbed.

The power sources available are Li-Po (Lithium Polymer) and Li-Ion (Lithium Ion) batteries, 2200 mAh, 11.1 VDC; these batteries are used in RC airplanes, drones, and small UAV. The converters can be switched power converters or linear regulators. The buses are H type terminal blocks (screw terminals), and the connections can be PVC insulated cables with relay modules as the switching devices. The availability of 11.1 VDC batteries leads to the arbitrary selection of the EPS voltage as 11.1 VDC. In the case of a real

aircraft, optimal voltage selection can lead to the results as shown in Section 6.2.2. Based on the components of **Figure *7.1***, some abstractions can be performed. However, the design of the EPS architecture for the testbed is atypical. Considering that,

- Although synthesized with abstractions from the aerospace industry, any of the architectures in **Figure *6.15*** and **Figure *6.17*** (case study in Chapter 6) can be implemented as a micro-scale testbed with the available components of **Figure *7.1***. However, performance would not correspond to what has been considered in the abstractions of **Table *6.2*** and **Table *6.3***.
- The design space is significantly limited to the available devices of **Figure *7.1***. In this case, abstractions are substantially reduced. Every component has a matching device only; hence, selection among several options from the same type does not apply.
- Resilient design for a set of failure scenarios (Section 4.3.2 and formulation **O.P. 7**) can be used due to the requirement that the system must supply critical loads even under the occurrence of unexpected failures.

Hence, the abstractions are such that resilient design for a set of failure scenarios (Section 4.3.2 and formulation **O.P. 7**) is used to synthesize the testbed architecture.

In the case of GS&GLP, the 2200 mAh Li-Po can discharge at 25C, which means that up to 610 W can be released if required. The 2200 mAh Li-Ion battery can discharge only at 5 A (54 W). Loading can be between 0 and 100%. The power density is approximately 150 Wh/kg, then battery weight is roughly proportional to the inverse of 150 W/kg, or 6.67 kg/kW. For the Li-Po and Li-Ion batteries, it is assumed that the efficiency in terms of loading is constant, therefore, losses are also constant. The cost of the 2200 mAh Li-Po battery is approximately £20, and the battery weights 130g, so the cost ratio is roughly £153/kg. Reliability of the batteries is assumed to be $1 - (1.0 \times 10^{-5})$.

Table 7.2 Testbed generation platform abstraction (example).

P_s^G[kW], β_s[p.u.]	$P_s^{MIN} = 0.054$, $P_s^{MAX} = 0.610$; $\beta_s^{MIN} = 0.0$, $\beta_s^{MAX} = 1.0$
$w_s(P_s^G)$ [kg]	$6.67P_s^G$
Cost ($w \propto c$)	£$153/kg$
$1 - r_s$	1.0×10^{-5}

The DC/DC switched converters can convert up to 250W and each converter has an approximate weight of 110g. The terminal blocks (for the buses) are 15 A at 450V and each terminal weights around 200g. The fixed costs and variable costs are based on average commercial values found in 2020 on the Internet marketplace (electronic devices retailers) [179], [180]. The connections are implemented with PVC insulated cables and 5VDC relay modules. Finally, the power distribution platform abstractions (for the PDD problem) are listed in **Table 7.3**.

Table 7.3 Testbed power distribution platform abstraction (example).

	Converter	*Bus*	*Connection* (ij)
Power density [kW/kg]	2.27	33.75	3.0
m_i^{kW}, c_{ij}^{kW} [£/kW]	0.1	0.1	0.05
m_i, c_{ij} [£]	5	1.5	1.7
P_i^{MAX}, P_{ij}^{MAX} [W]	250	6750	650

With the abstractions of **Table 7.2** and **Table 7.3** (from the available devices in **Figure *7.1***), the GS&GLP and PDD (resilient design for a set of failure scenarios) can be used to design the architecture. The GS&GLP problem has the condition that a single power source (battery) supplies each zone. Also, there are two auxiliary power sources. Then, the power generation consists of 4 power sources: 2 main batteries, and 2 auxiliary batteries. With this outcome, the PDD synthesizes a power distribution system that is resilient to failures in main power sources and converters (as required by the specification).

The EPS architecture for the testbed is as depicted below in **Figure *7.2***.

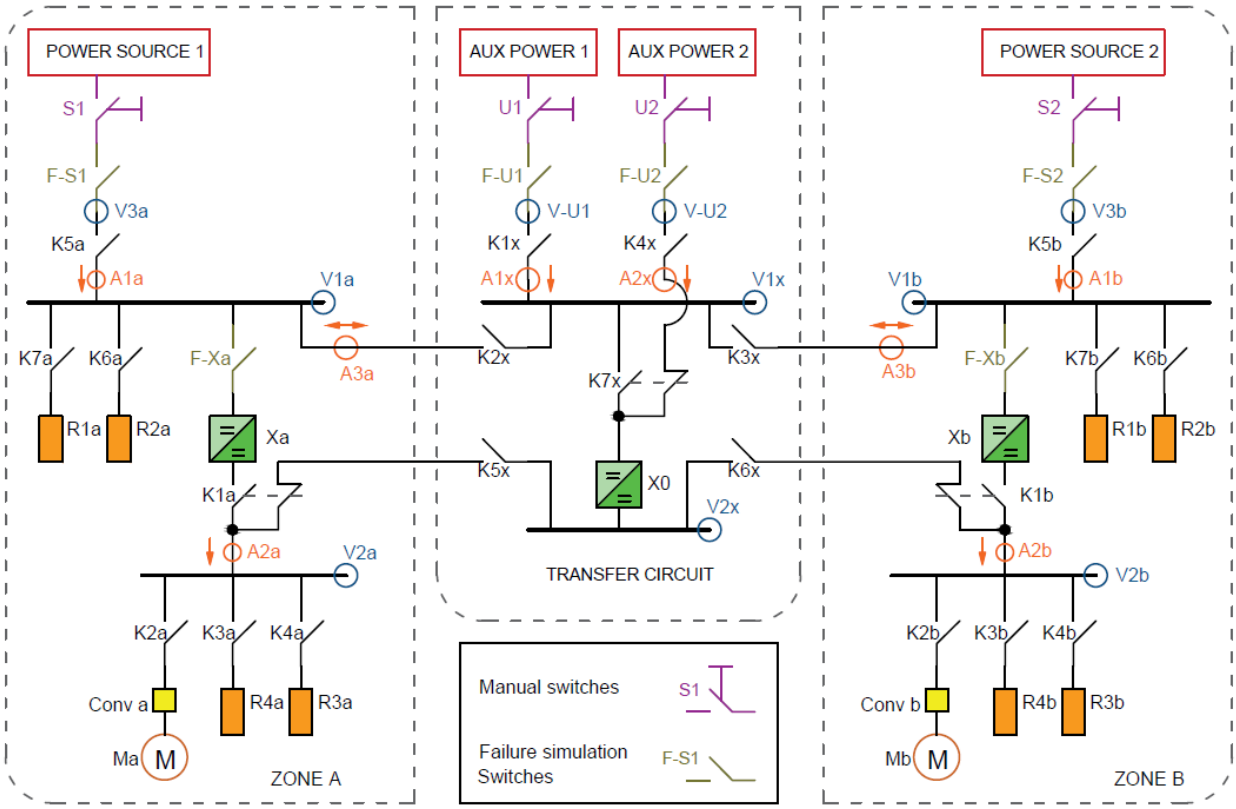

Figure 7.2 Line diagram of the DC EPS testbed.

The converters Xa and Xb are implemented with linear regulators while converter X0 is a switching regulator. Linear regulators can have good ripple rejection with relatively low energy storage, while switching regulators usually store a significant amount of energy in passive elements (inductors and capacitors). These converters are unidirectional, that is, they allow power transfer from HVDC to LVDC only. The transfer circuit in the middle allows power transfer between zones and from auxiliary power sources. Power is distributed at two voltage levels, HVDC (11.1V is the system's voltage) and LVDC (arbitrarily selected as 7.2VDC, to supply motor load). There is a set of manual switches that turns the main (S1, S2) and auxiliary power sources (U1, U2) on. Each side has 5 loads, 2 are HVDC and 3 are LVDC. The assumed essential (critical) loads are R1a, R3a, and Ma in zone A, and R1b, R3b, and Mb in zone B.

The main power sources are implemented with Li-Po batteries, while the auxiliary power sources are Li-Ion batteries. The main power sources can directly supply the HVDC buses, while the LVDC buses are supplied through a power converter. There are several voltage sensors (V1a to V3a, V1b to V3b, V1x, V2x) and current sensors (A1a to A3a, A1b to A3b, A1x, A2x) to provide energization status feedback and analog values for power consumption computation. The set of failure simulation switches (F-S1, F-U1, F-U2, F-S2) allows the disconnection of power sources and converters to simulate failures and evaluate the performance of the EPS reconfiguration method. The highlights of this EPS are,

1. It maintains the mirrored configuration usually found in aircraft industry.
2. It features the proof-of-concept of DC distribution with two voltage levels and a power conversion between them.
3. It incorporates two auxiliary power sources in the transfer circuit, which can supply either a single zone or both if required.
4. Network reconfiguration is possible via control of switches (contactors) which makes this testbed also amenable for testing other control protocols and power management strategies.
5. Compared to the latest micro-scale testbeds available in the literature, this setup allows load shedding in HVDC and LVDC buses under the occurrences of failures in power sources and converters.

As mentioned before, interconnections switches (K1x to K7x) allow several reconfiguration possibilities upon failures in power sources and converters. All switches K1a/b/x to K7a/b/x are implemented with 5VDC relay modules. The transfer circuit can supply both HV- and LVDC loads, and there is an additional DC/DC converter in case of failures in converters Xa or Xb. The transfer circuit could remain inoperative if no contingencies are experienced. Now, performance evaluation is detailed in brief.

7.2.2. EPS controller

Performance evaluation of the testbed in **Figure *7.2*** can be realized through the implementation of a controller that reconfigures the system upon the occurrence of unexpected failures in power sources and converters (as specified in the requirements). In this case, no performance optimization, as described in Chapter 5, is assessed. Given that the controller synthesis is outside of the scope of this work, a simplified implementation in a microcontroller board is proposed to be able to assess the testbed EPS in terms of reconfiguration response. In addition to the microcontroller board, a set of electronic boards are used for data acquisition, measurement, and signal distribution. Each one of the zones and the transfer circuit has their own board with the following capabilities:

- Analog voltage- and current- sensing
- Signal distribution for sending/receiving digital and analog status feedback
- Receive open/close commands to operate controllable switches (K1a/b/x to K7a/b/x).

The zones' and transfer circuit's boards are connected to the main controller board that executes the reconfiguration task, performs power calculations, and registers the system's status. The controller board receives an external interruption signal that triggers the interruption service routine. This signal is generated in an interruption signal generator circuit which is built with logic gates and is triggered by any failure in power sources and converters.

The failure(s) of power sources and converters are triggered by a failure simulation board. This board performs a failure simulation routine, and a reconfiguration time measurement task, i.e., the time the controller takes from the moment the failure happened until the reconfiguration is completed. Hence, it is possible to compare different power transfer techniques and algorithms based on their time response. The digital signal layout of the EPS is shown in **Figure *7.3***. This implementation simulates failures by

disconnecting power sources and converters via open/close commands sent to the failure switches (F-S1, F-S2, F-U1, F-U2, F-Xa, F-Xb).

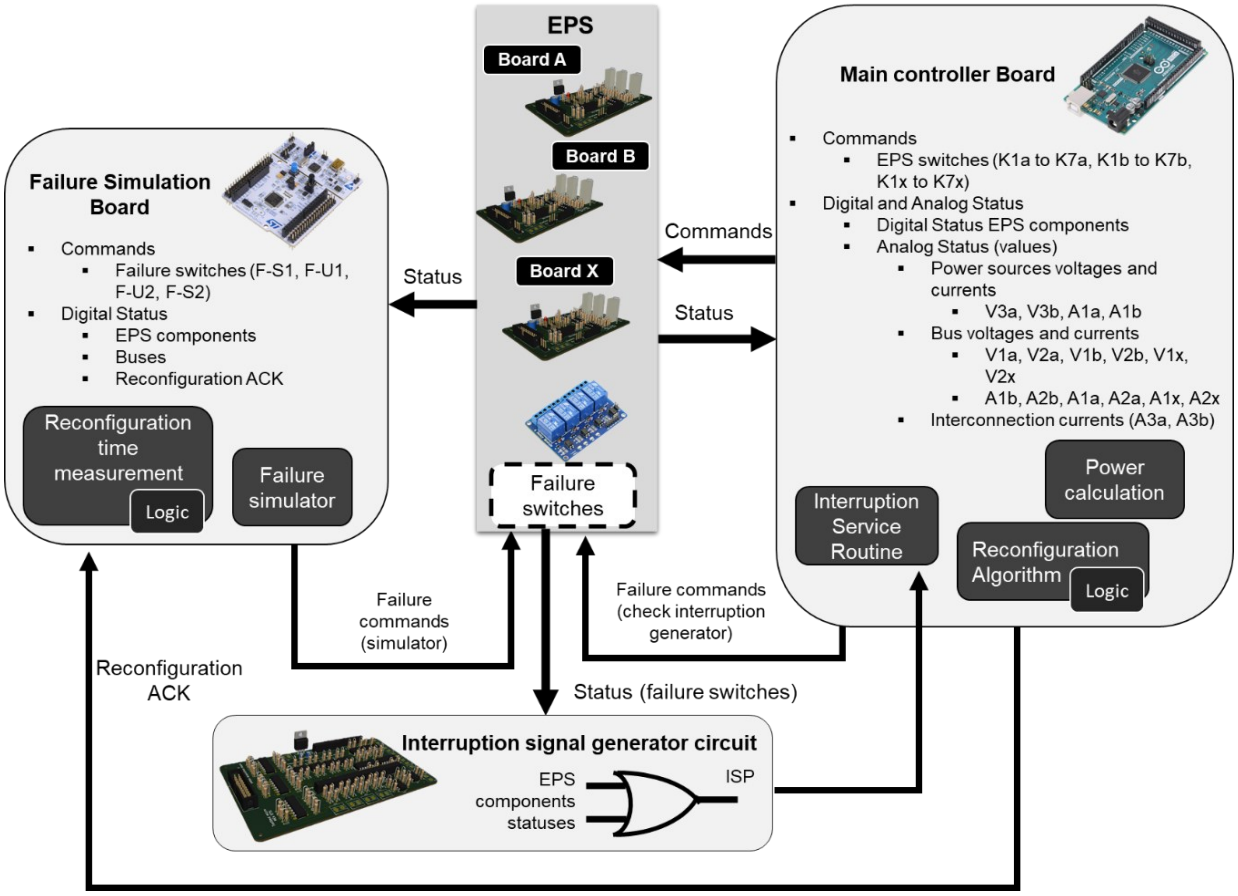

Figure 7.3 Control and data acquisition signal layout for the DC EPS testbed.

In a typical aircraft implementation, the failure switches are removed, and power sources and converters have their own power management electronics that provide status and authentic signals to other external controllers and data acquisition systems. Also, the failure simulation board can be removed, and data acquisition can be included in the main controller. Depending on the reconfiguration logic selected, the interruption signal generator circuit can be maintained as an external circuit or included in the main controller as well.

7.2.2.1. Main controller

The controller is implemented with an Arduino Mega 2560 Rev 3 16 MHz microcontroller that has capacity to handle up to 16 analog inputs, 54 digital input/output pins, and 6 interruption inputs on different pins. One interruption pin has been configured to receive an external interruption signal that triggers the interruption service routine; hence, reconfiguration is the main task of the controller. The controller board must initialize all communication services, input & output ports, and perform calibration routines on the analog data acquisition circuits (voltage and current signals to compute power). Then, it must check the status of components and the interruption signal generator circuit to ensure proper functioning of the interruption signal which is crucial for triggering the reconfiguration algorithm. Following this task, the controller executes and checks the power ON sequence, and the EPS system is up and running normally (state 1, reconfiguration flag (RF) is 0). Afterwards, the controller remains in a loop governed by a two-state FSM, in the first state EPS is normal, and in the second state, EPS is reconfigured. The controller manages an interruption service (IS) triggered by the interruption signal generator circuit, and this service performs (with the highest priority) the reconfiguration task, which leads to the second state once the system is reconfigured. The main controller's procedure is detailed in the pseudocode of **Algorithm *2***.

7.2.2.2. Failure simulation board

The failure of power sources and converters are triggered by a failure simulation board which is implemented on a STM32 Nucleo-64 F446RE microcontroller board. After initializing communications, input and output ports in the failure simulation board, the main loop is governed by a three state FSM. In the first state, there is no request for failure simulation; in the second state, the time the controller board takes to reconfigure (after a failure is provoked in the EPS) is measured. The board remains in the third state (system reconfigured) until it receives an external trigger signal that returns the system to normal. Recall that in practical applications, this board could only measure reconfiguration time, and failure

simulation is no more a practical task. The procedure for the failure simulation board is detailed in the pseudocode of **Algorithm *2***.

Failure Simulation Board	**Main Controller Board**
Initialize serial communication	**Initialize** serial communication
Set input and output configurations	**Set** input and output configurations
Initialize STATE 1, RF = 0	**Calibrate** voltage input signals
While (*true*)	**Calibrate** current input signals
Read SET/RST buttons	**Check** power sources statuses
Switch (STATE)	**Check** interruption signal generator circuit
STATE 1, RF = 0, EPS is normal	**Execute** power ON sequence
If (SET button is *true*)	**Check** power ON sequence
Go to STATE 2	**Enable** Interruption Service (IS)
Else, remain in STATE 1	**While** (*true*)
End if	**Read** EPS component statuses
STATE 2, failure time measurement	**Check** failure status on components
Read manual request input	**Switch** (STATE)
If (manual request is no failure)	STATE 1, RF = 0, EPS is normal
Go to STATE 1	**Read** voltages and currents
Else, **disconnect** failed components	**Compute** power consumption
While (*true*)	**If** (IS or failed components)
Read buses statuses **and** ACK	**Execute Reconfiguration Task**
If (*logic* matched **or** ACK)	**Set** interruption ACK = 1
break	Go to STATE 2
End if	**Else**, remain in STATE 1
End while	**End if**
Measure reconfiguration *time*	STATE 2, RF = 1, system has reconfigured
End if	**Read** voltages and currents
STATE 3, RF = 1, EPS is reconfigured	**Compute** power consumption
If (RST button is *true*)	**If** (no failure in components)
Go to STATE 1	Go to STATE 1
Else, remain in STATE 2	**Else**, remain in STATE 2
End if	**End if**
End switch	**End switch**
End while	**End while**

Algorithm 2 Pseudocode for failure simulation board (left), and main controller board (right).

The pseudocodes of **Algorithm *2*** are programmed in the controller (Arduino Mega 2560) and the failure simulation board (STM32 Nucleo-64 F446RE). Both boards are programmed using the Arduino IDE

(development environment for various types of microcontrollers) with a programming language similar to C/C++. The (physical) experimental testbed is presented in the next section.

7.2.3. Experimental setup

The assembled experimental testbed is shown in **Figure *7.4***. There are four interconnected modules: zone A, zone B, transfer circuit, and control & data acquisition. All modules are built in two levels; the top level holds the electronic boards, 8-channel 5 VDC relay modules, and converters, while the bottom level holds the EPS loads, buses, and power sources.

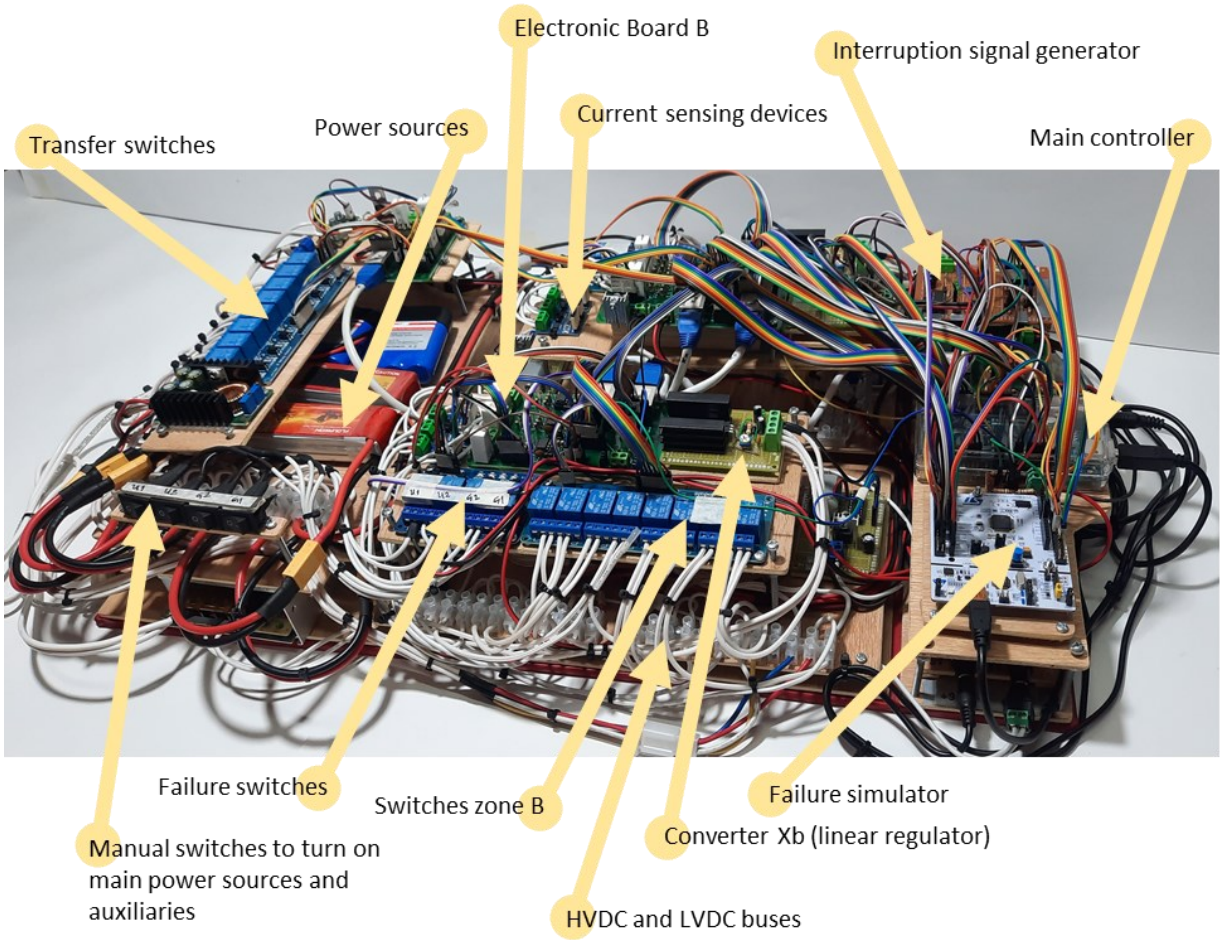

Figure 7.4 Experimental setup of the DC EPS testbed.

In the case of the transfer circuit module, the bottommost level is reserved for the power supplies that energize all of the 5VDC and 9VDC electronics (assumed to be 100% reliable). The control & data acquisition module holds the main controller, failure simulation board, interruption signal generator circuit, and other acquisition boards such as oscilloscopes, and user control panel.

7.2.4. Operation

The system configuration is in the *normal mode* as shown in **Figure *7.5***. Recall that the system has a topology that allows several reconfiguration schemes by switching on/off the controllable switches. All HV and LV loads on each zone are supplied by their corresponding power source. The transfer circuit is not being utilized, so switches K1x to K7x are opened and there are no interconnections between zones.

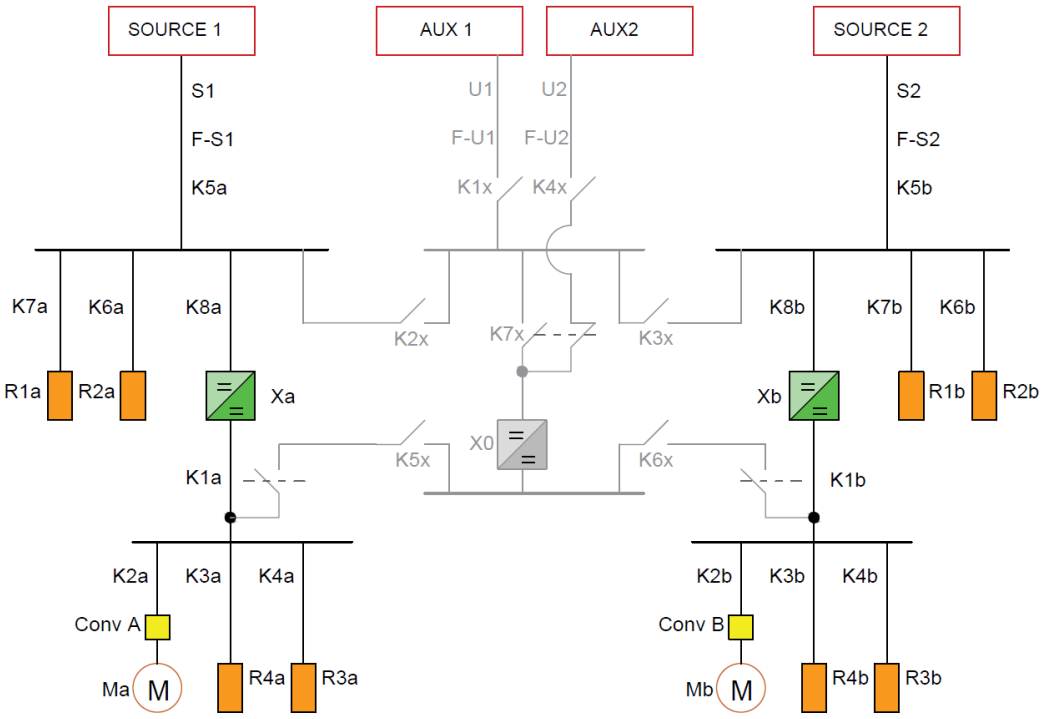

Figure 7.5 Configuration for normal operation (normal mode) in DC EPS testbed.

Whenever a failure occurs in main power sources (Source 1, Source 2), auxiliaries (Aux 1, Aux 2), or converters (Xa, Xb) while in the normal mode, the system requires a new configuration by switching

open/closed the controllable switches so that power is re-routed, and critical loads are continuously supplied with power (non-critical load shedding is also possible). After the new configuration has taken place, it is assumed that the system is in a reconfiguration state (or mode), and it requires returning to a normal mode, so no nested reconfigurations from previous reconfiguration states are allowed. The failure of any source or converter is an independent event, i.e., its failure is not conditioned to any other event. If a failure on any auxiliary source occurs during normal mode, the system remains as it is in **Figure *7.5*** with the difference that the auxiliary is disabled. Failure events where more than one failed component exist are allowed, so there is a combination set between failed components; since there are 6 components that could fail, there are $2^6 = 64$ possible failure combinations. In most cases, the disconnection of two or more components could result in a reconfiguration that only supplies critical loads. For instance, two independent reconfiguration states in case of failure in Source 1 and converter Xa are shown in **Figure *7.6***.

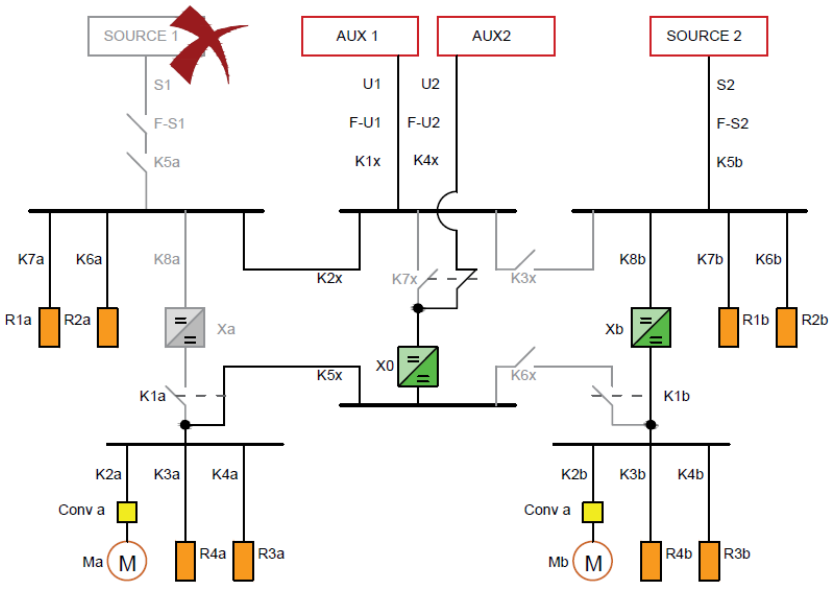

(a)

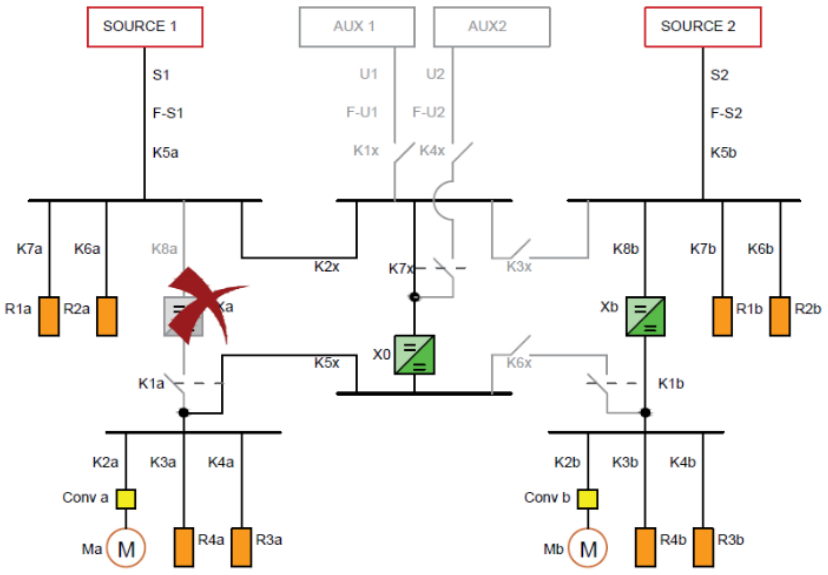

(b)

Figure 7.6 System reconfiguration in case of failures in Source 1 (a), and Xa (b).

In the former case (**Figure *7.6*** a), both auxiliary sources supply HVDC and LVDC buses in zone A because of the disconnection of Source 1 (zone B continues its supply from Source 2), while in the latter case (**Figure *7.6*** b), the load of converter Xa is temporarily supplied through X0. In these cases, load criticality played no significant role because both auxiliary sources could replace Source 1. However, the situation is different if Aux 1 has been disabled (failed) on top of Source 1, so that Aux 2 and Source 2 are the only power sources available, and some load must be shed to avoid prolonged overload. Other reconfiguration options in case of unexpected failures are stated below:

1. On the occurrence of a failure in the main power source of either zone, R2a/b and R4a/b are disconnected, and the system can be temporarily supplied by the live remaining power source only. The HVDC buses could be interconnected through K2x and K3x.
2. On the occurrence of a failure in the power converter of either zone, R1a/b and R2a/b are supplied by the remaining main power source while Aux 2 supplies LVDC loads through X0. The

option of transferring Xa/b load to X0 (activating K2x, K5x, K7x or K3x, K6x, K7x) is also possible as shown in **Figure *7.6***.

3. If both main sources are disconnected, only critical loads are supplied (R1a/b, R3a/b, and motor a/b).
4. Both auxiliary sources could supply critical loads on both zones if requested.
5. Auxiliary power sources should not be overloaded for more than a specific period of time.

The options stated above represent some of the conditions needed to build the control algorithm. These conditions are part of the design specifications, i.e., functional and safety requirements.

7.2.5. Reconfiguration implementation

The reconfiguration task in **Algorithm *2*** can be programmed with the formulations of Chapter 5, i.e., topology reconfiguration and performance optimization. In this case, topology reconfiguration is performed after an unexpected failure occurs (simulated failure in the testbed). Optimization and power management systems are left for future work.

It is possible to build a finite state machine (FSM) that makes transitions between reconfiguration states based on the status feedback of failure signals. In this case, there are 64 failure states and a few hundred transitions between these states which demands a significant amount of diagramming and programming (6 components can fail, that is, 2 main batteries, 2 auxiliary batteries, and 2 converters, then $2^6 = 64$). Another option is to solve successive shortest path problems [67] to match loads with power sources. A shortest path problem can either be formulated using Dijkstra's algorithm [181], or as an optimization problem based on network flow techniques [24]. The former could be programmed in a microcontroller similar to the one used in the testbed, while the latter deserves more powerful computer modules capable of managing extensive optimization libraries and algorithms. An interesting option is SCIP Optimization Suite [182] which is a toolbox for generating and solving Mixed Integer Non-Linear and Linear

Programming problems and has the advantage that is a non-commercial platform that has been implemented in a low-cost Raspberry PI [183] computer [184]. Applications with commercial solvers are restrictive for autonomous implementation in low-cost high-performance computers in terms of licence fees/restrictions, memory space, hardware, and compatibility. In most cases, MATLAB and Simulink [112] is used as the case platform to perform real-time control and call other commercial optimization engines, but such control architectures demand careful configuration as significant processing resources could be diverted to non-control tasks, e.g., other operating system tasks performed required on any desktop computer.

Aside from the above options to implement a reconfiguration algorithm, a combinatorial logic lookup table is also feasible due to the small number of combinations, although, for larger systems it could be cumbersome and inefficient. Once programmed in a microcontroller, such a method is less resource-intensive than an FSM made of 64 states and the hundreds of transitions between them. The combinatorial logic lookup table could take up more or less memory depending on the numerical representation selection. An extract of the combinatorial table used in the reconfiguration task is shown in **Table *7.4***.

The table section at the left lists the failure combinations, that is, more than one component can fail (0 is no failure, 1 is failure); each failure combination represents a state. On the right, the open/close states for the EPS switches are declared (0 for opened, 1 for closed). The reconfiguration task discriminates between failure disconnection and disconnection by de-energization (input supply absence), e.g., state 9 where Source 1 fails provokes de-energization of converter Xa although it hasn't failed. This discrimination is possible when the controller board knows what failure combination has been simulated in the simulation board. However, there is no failure simulation board in practical applications. In real systems, the controller board is directly fed with failure signals from other local electronic controllers for

generation and power conversion systems, so that any failure is truly triggered by a signal generated from the local controller of the corresponding subsystem (generation, conversion, etc.).

Table 7.4 Extract of the combinatorial table for reconfiguration task.

St.	Failure						Description	Shed?	Zone A				Transfer Circuit						Zone B			
	Xb	Xa	S1	Aux 1	S2	Aux 2			K1	K4	K5	K6	K1	K2	K3	K4	K5	K6	K1	K4	K5	K6
1	0	0	0	0	0	0	Normal state	NO	1	1	1	1	0	0	0	0	0	0	1	1	1	1
2	0	0	0	0	0	1	EPS remains operative	NO	1	1	1	1	0	0	0	0	0	0	1	1	1	1
3	0	0	0	0	1	0	Aux 1 and Aux 2 assist zone B	NO	1	1	1	1	1	0	1	1	0	1	0	1	0	1
4	0	0	0	0	1	1	Aux 1 supplies zone B	**YES**	1	0	1	0	1	0	1	0	0	0	1	0	0	0
5	0	0	0	1	0	0	EPS remains operative	NO	1	1	1	1	0	0	0	0	0	0	1	1	1	1
6	0	0	0	1	0	1	Aux 1 and 2 disconnected	NO	1	1	1	1	0	0	0	0	0	0	1	1	1	1
7	0	0	0	1	1	0	Aux 2 supplies LVDC of section B	**YES**	1	0	1	0	0	1	1	1	0	1	0	0	0	0
8	0	0	0	1	1	1	**Only Source 1 is active, alarm**	**YES**	1	0	1	0	0	1	1	0	0	0	1	0	0	0
9	0	0	1	0	0	0	Aux 1 and Aux 2 assist zone A	NO	0	1	0	1	1	1	0	1	1	0	1	1	1	1
10	0	0	1	0	0	1	Aux 1 supplies zone A	**YES**	1	0	0	0	1	1	0	0	0	0	1	0	1	0
11	0	0	1	0	1	0	Only auxiliares are ON	**YES**	0	0	0	0	1	1	1	1	1	1	0	0	0	0
12	0	0	1	0	1	1	**Only Aux 1, overload, high-alarm**	**YES**	1	0	0	0	1	1	1	0	0	0	1	0	0	0
13	0	0	1	1	0	0	Aux 2 supplies LVDC from zone A	**YES**	0	0	0	0	0	1	1	1	1	0	1	0	1	0
14	0	0	1	1	0	1	**Only Source 1 is active, alarm**	**YES**	1	0	0	0	0	1	1	0	0	0	1	0	1	0

ON STATE: K2a, K3a, K7a (zone A), K2b, K3b, K7b (zone B)
OFF STATE: K7x (transfer circuit)

The combinatorial logic in **Table *7.4*** allows a relatively fast lookup once the interruption service sequence is triggered. For each failure combination, there is only one reconfiguration setting that the system executes to get to a new state (regardless of the causes of the corresponding failures). Other sources of failure can be included, e.g., failure in the buses, sudden overloads, etc. These additional sources of failures can be added into the combinatorial table (such as **Table *7.4***) and the number of combinations is increased accordingly. When the number of combinations is very large because there are many sources of failure, it could be difficult to build a combinatorial table. For instance, an EPS with 20 components where any of these components can fail, there are more than a million combinations to determine. In this cases, other control approaches must be used, e.g., shortest path algorithm, minimum cuts, etc.

7.3. Performance evaluation

Reconfiguration time and power consumption have been registered for some states as depicted in **Figure *7.7***. There are two scenarios in the reconfiguration time measurement:

1. Time measurement considers the termination of the interruption service in the controller board; main controller board provides feedback of the interruption service signal, and
2. Time measurement acknowledges the status change in the EPS components to determine if reconfiguration has been done

The reconfiguration does not take more than 4 ms when interruption of service feedback is used, while it takes less than 14 ms when checking EPS components statuses. For the cases where time is 0 ms, there were no status changes with respect to the normal mode, with the exception where all power sources and converters were disconnected, which corresponds to a catastrophic blackout event. A simple inspection of **Figure *7.7*** provides an insight into the performance of the switches, that is, it takes between 7 ms and 9 ms to complete reconfiguration once the interruption service in the controller finishes the lookup routine. If the 50 ms maximum disconnection rule is considered, the performance of the current implementation complies satisfactorily.

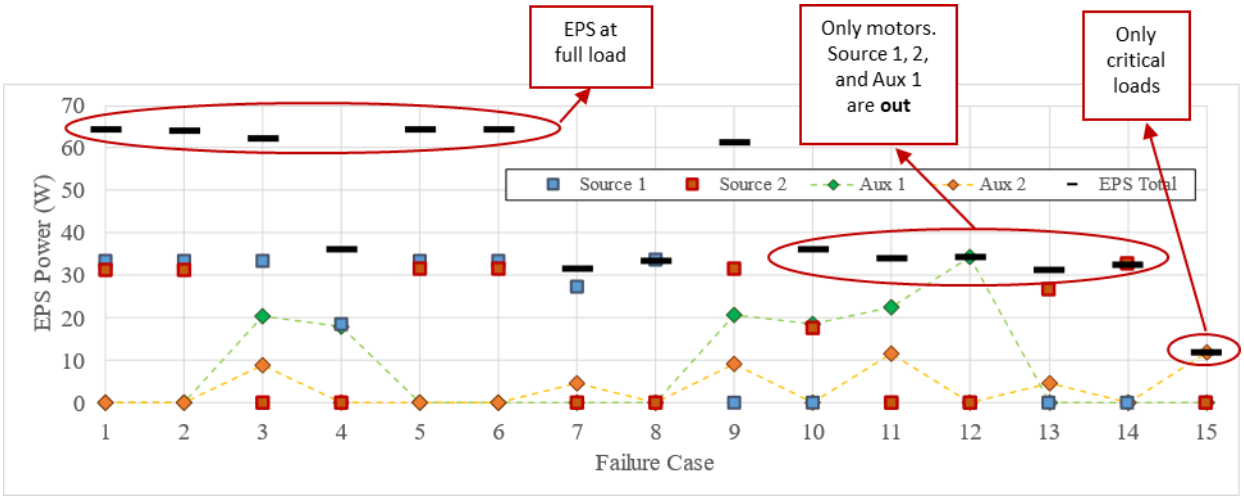

(a)

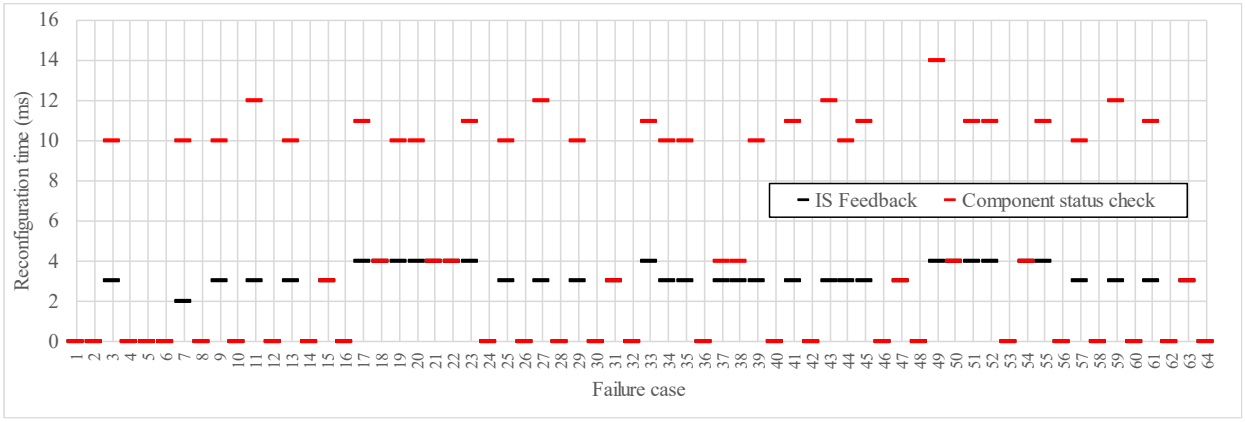

(b)

Figure 7.7 Results from DC EPS testbed, (a) power [W], (b) reconfiguration time [ms].

During normal operation, measured power consumption is around 64.5 W, where each source provides half of this. As expected, the main power sources supply rated load continuously. However, depending on the logic selected for each one of the failure cases, a power source could be temporarily overloaded when failure occurs. Consider a simultaneous failure in auxiliary sources Aux 1 and 2, and converters Xa and Xb, as shown in **Figure *7.8***. The only converter that can supply LVDC buses on both zones is X0, and it could be powered from HVDC bus of zone A or B, given that no parallel operation between power sources is allowed. Then, either Source 1 or 2 is overloaded temporarily (approximately 32% of overload) if no loads were shed, but the power requirements alleviate if non-critical loads were disconnected. An important factor to take into account for such a decision could be the actual condition of the power source, e.g., state of charge of the batteries, so that remaining energy is optimally distributed. Hence, there could be more than one reconfiguration option if other inputs (sources of failure) are included in the logic.

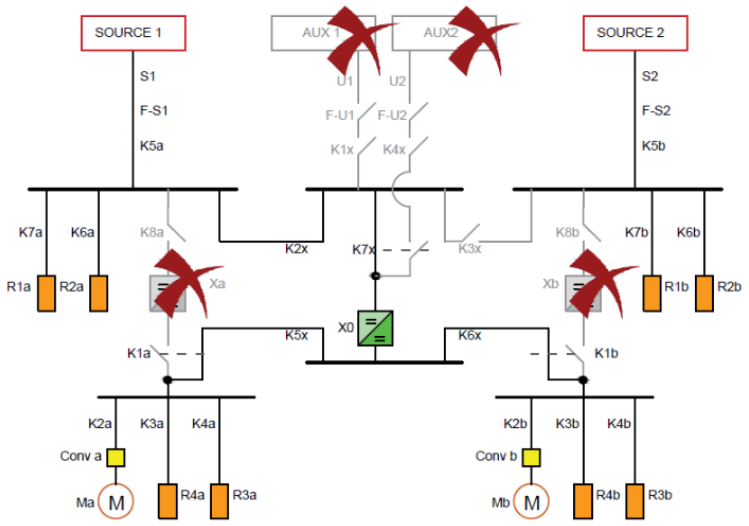

(a)

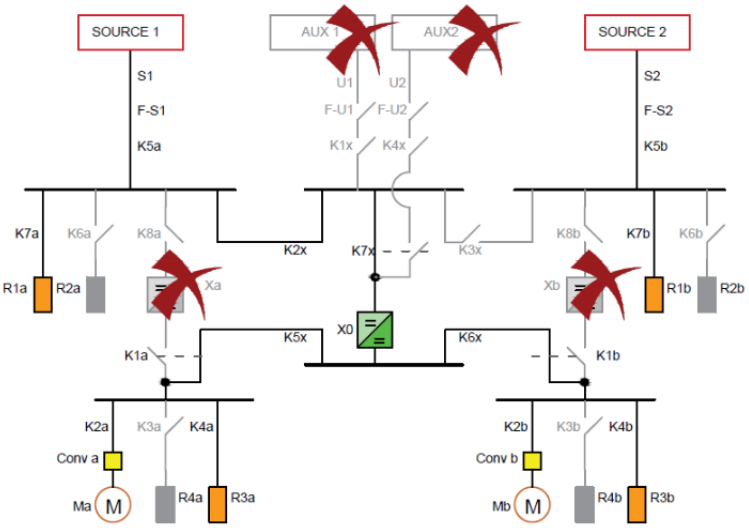

(b)

Figure 7.8 Reconfiguration options in case of simultaneous failure in Aux 1, Aux 2, Xa, and Xb.

Transients during reconfiguration tasks are depicted in **Figure *7.9*** and **Figure *7.10***. Analog data is measured using an OpenScope MZ [185] based on the PIC32MZ2048EFG42 microcontroller (12-bit oscilloscope with a sample rate up to 6.25MS/s). **Figure *7.9*** shows reconfiguration transients after failure in converter Xa.

The LVDC bus is temporarily disconnected (less than 20 ms) in the lapse between the Xa failure and X0 interconnection to this bus (see **Figure *7.9*** around t = 7 s). The slight increment in the HVDC voltage

(around 3.5%) is due to X0 being a switching regulator (step-down buck converter [186]) with less losses than the linear regulator in Xa, hence, switching converters are more energy-efficient [17].

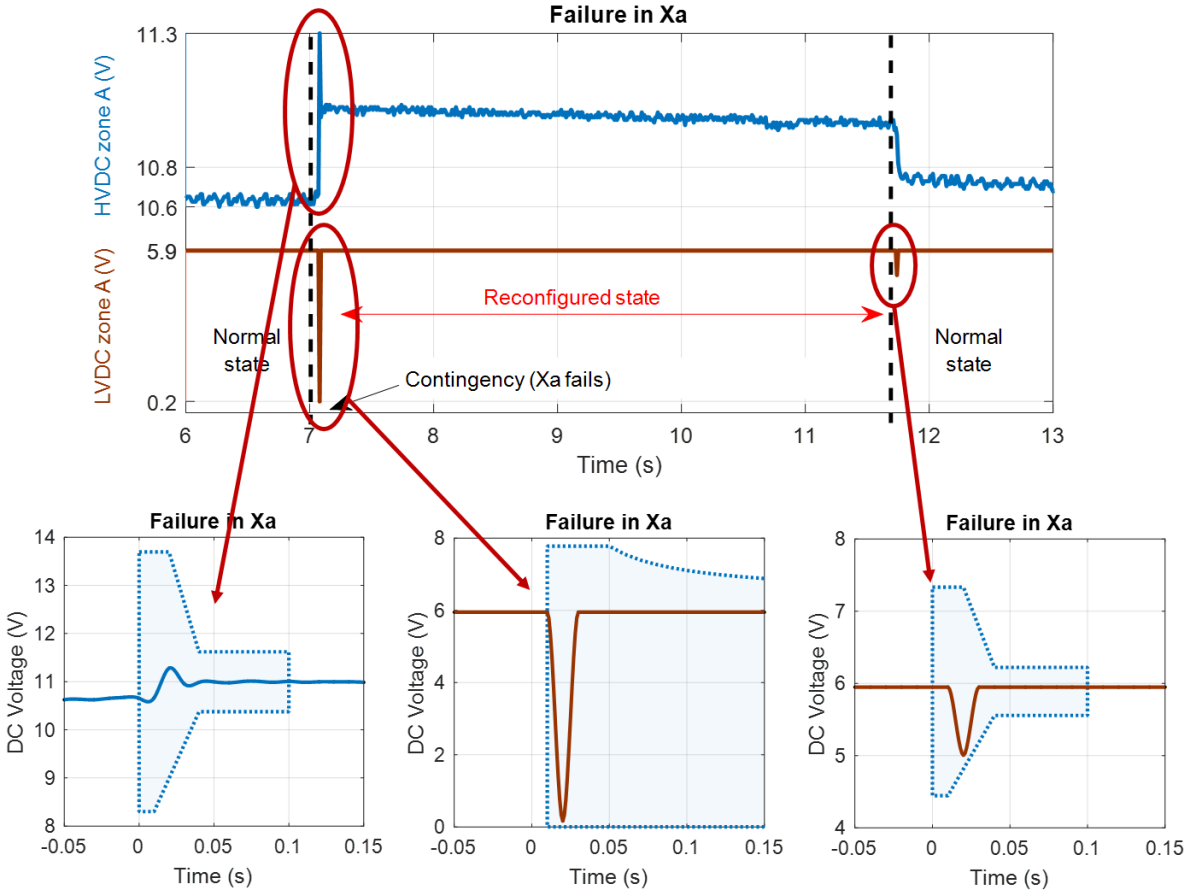

Figure 7.9 Voltage response and transients in HVDC and LVDC buses (zone A) for failure in Xa.

The LVDC voltage is almost constant due to the voltage regulation performed by the converters even though input voltage could vary. At longer simulation times a decreasing slope in power source and HVDC voltages might indicate battery discharging, but the converter output is kept at the LVDC setpoint. The transients observed in **Figure *7.9*** have been enlarged and compared to arbitrary voltage envelopes for comparison. In all cases, the transients are enclosed in these envelopes and limits.

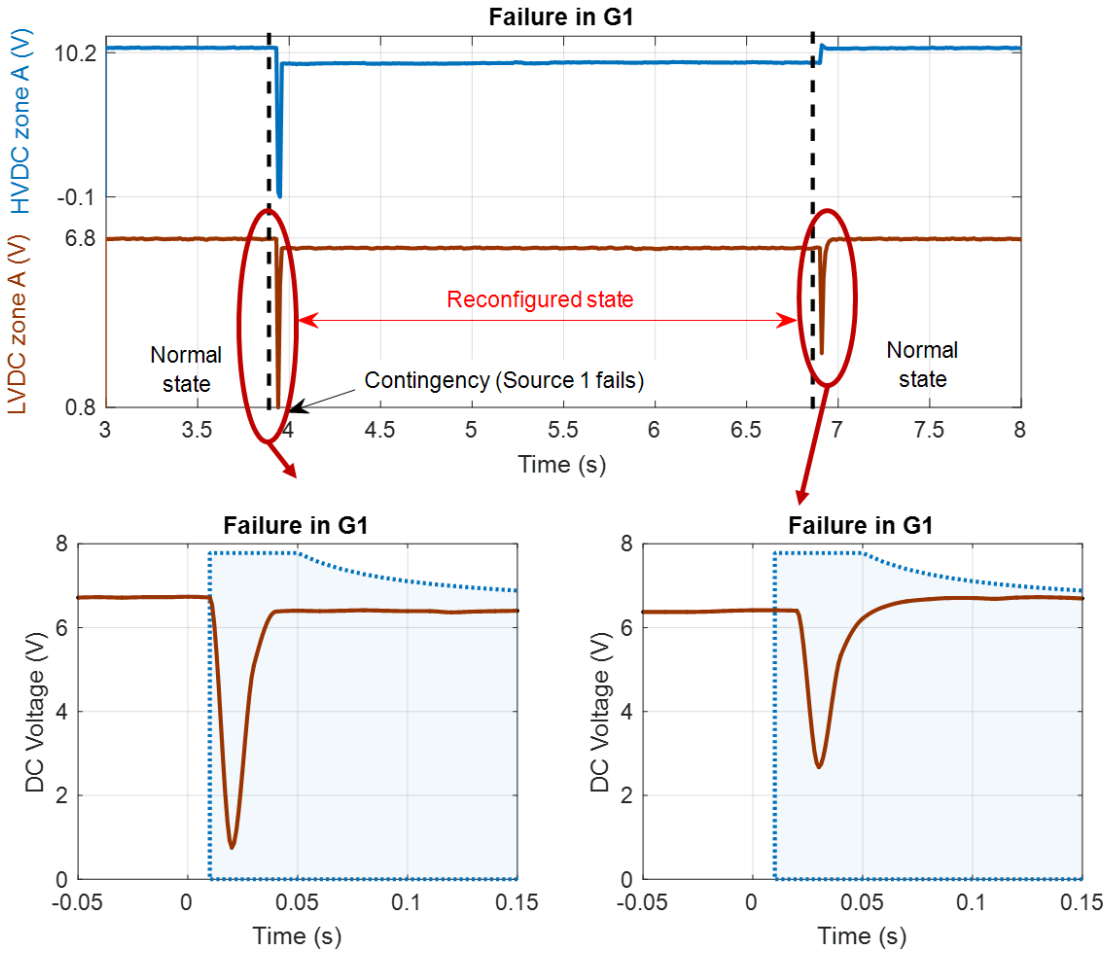

Figure 7.10 Voltage response and transients in HVDC and LVDC buses (zone A) for a failure in Source 1.

Similarly to the results for a failure in Xa, **Figure *7.10*** depicts transients for a failure in power source 1 (Li-Po battery); Aux 1 and Aux 2 assists zone A in this case, Aux 1 supplies HVDC loads and Aux 2 supplies LVDC loads through converter X0. The slight decrement in HVDC voltage is due to the interconnection of Aux 1, which is a Li-ion battery with different electro-chemical characteristics. On the other hand, the minor decrement in LVDC voltage is due to the setpoint in converter X0, which shall be equal to the setpoint in Xa having a more accurate and fine adjustment available. The disconnection in the LVDC bus is less than 20 ms for both reconfiguration transients, that is, power source 1 failure and restoration, and they fall within the assumed limits for over- and under-voltage.

According to **Figure *7.9*** and **Figure *7.10***, the transients' durations of 20 ms are larger than the reported reconfiguration times in **Figure *7.7*** (around 14 ms). This difference can be explained by two factors: the digital reading task (component status check) of the controller, and the sampling time of the oscilloscope. In the former, the electronic interface to produce a signal that the controller could read must accurately translate the bus voltage into a digital signal, while the readings for the latter could be disturbed by cabling factors and energy that can be stored in other components (i.e., some capacitance and inductance effect in cables, tracks, etc.). The transient response is improved when some energy is stored such that HVDC and LVDC buses can use it temporarily during transients. In many applications, LVDC buses are connected to batteries to improve voltage balance and stability, while in others it could be sufficient to provide large energy storage elements in power converters. The transient response of the testbed could also be improved by using faster microcontroller units (these can go up to 200 MHz in some units), switching converters only, and/or batteries attached to buses for power quality enhancement.

7.4. Conclusion

An experimental testbed has been designed and assembled with the purpose of demonstrating the concept of a DC EPS and validating a topology reconfiguration method based on combinatorial logic. This testbed could also serve as a platform for evaluating other reconfiguration methods and control architectures that include optimization-based power management approaches. Physical implementation is based on electronic components and microcontroller boards that are not necessarily designed for aerospace applications; however, the testbed serves as a platform for testing other control systems in the future. The selected reconfiguration technique based on the lookup of a pre-defined combinatorial table is fast enough to rearrange the switches such that critical loads are always supplied with electrical power. Further research could include expansion to accommodate more loads, bidirectional converters, and perform a load allocation and optimal power flow algorithms in the controller.

8. Conclusion

8.1. Summary

The future of aircraft electrification is no longer just a theoretical concept but is now a reality that is becoming tangible with the MEA initiative. Several technological advancements in the design of energy storage and traction systems have enabled the progressive adoption of cutting-edge technology for next-generation aircraft to reduce fuel consumption, improve energy efficiency, and to achieve a more sustainable aerospace industry. Yet, the breakthrough to a new generation of aircraft is still being shaped by advances in several engineering disciplines that seek to optimize the scarce available resources with the objective of being more economical and environmentally responsible. The effort is definitely multidisciplinary, and the complexity demands design strategies that handle the design space appropriately by efficiently exploring the available options. It is in this context that this Thesis proposes a design method for MEA EPS architectures synthesis.

The EPS is a system of systems because it distributes generation power from generation systems and, possibly other energy storage systems, to the rest of the consuming and power conversion sections, which correspond to loads representing traction, actuation, and other electro-mechanical systems, and the associated required power conversion systems. Hence, it is the core of the overall electrical network. By considering the current building blocks of a power system and potential candidate devices and components that are promising, the design space is very large, since multiple potential combinations can be as successful as others, and there could be yet more possibilities that remain unexplored. In order to efficiently explore this design space, a design methodology has been proposed. The aim is to produce an EPS at the architectural level; this architecture complies with the design specifications for a given

application, so that, despite there being no universal solution for MEA, there is a method to generate a system that satisfies a set of requirements.

This thesis presents and explores the architecture design of an aircraft EPS by formulating reliability-based optimization problems whose outcome is a set of selected components and connections between these components that forms a network that distributes generation power to loads. The work presented in this Thesis can be summarized as follows:

- The research on synthesis of EPS architectures from scratch has focused on the development of cyber-physical system design concepts. A few framework proposals have utilized a Platform Based Design (PBD) approach to efficiently explore a vast design space. Other contributions have mostly concentrated on subsystem design, that is, proposals for designing and optimizing specific sections of an aircraft.
- Following a PBD approach, the EPS architecture design is performed in a two-step design framework: generator selection and generator-load pairing (GS&GLP), and then power distribution design (PDD). This partition is enabled by considering the relationship between the main industry drivers, i.e., cost, weight, efficiency, and reliability, and a set of abstractions that allow architectural and functional modelling of power system components.
- Although the idea of designing an EPS by PBD is not new and has been conceptually proposed in the literature before, this work deepens the mathematical formulations and the analysis of actual outcomes that are possible via solving such problems. Hence, in contrast to unreported formulations and solutions, this work attempts to close this gap and completes the design sequence.
- The non-linear original optimization formulations for the design of a power system are linearized into Mixed Integer Linear Programming (MILP) problems to exploit the solution

resources of high-performance commercially available solvers, thus, this work concentrates on the problem formulation rather than on the solution methods. Although MILP has been extensively used in performance optimization problems and other designs in several engineering disciplines, its resources are introduced in the architecture synthesis problem via introduction of network design techniques seldomly utilized in aircraft EPS design.

- Given current advancements in linearization techniques and solution algorithms, the linear approximations of the original design problem can be efficiently formulated such that the approximated optimal solution is close to the global optimum. This characteristic is attractive in MEA where disruptive and innovative designs can be very complex.
- The synthesized architecture is a topology that satisfies a set of functional and safety requirements. Safety requirements are translated into reliability constraints in MILP formulations. Given the burden of calculating a system's reliability where there could be a large number of paths and combinations, reliability in the power system is enforced as a set of resiliency constraints where a reliability target for each load is satisfied. This reliability is defined as the availability of power at load's terminals.
- Further to the topological definition of an architecture, this work attempts to solve for the optimal performance of the synthesized system during operation. Because the system is designed to comply with a set of functional specifications where there are performance targets, there must be a close relationship between the design problem and the operational problem. The architecture design has been complemented with performance optimization methods. An optimal voltage selection, a component location and cable selection, a load flow approximation, and performance optimization via topology reconfiguration and loss minimization problems have been introduced to allow optimization of resources and achievement of an optimal state.

- In order to illustrate the potential of the design framework, a case study was proposed, designing a DC EPS architecture for a small aircraft application. A set of different resiliency requirements are used to demonstrate the difference between architectures provoked by various independent specifications. By proposing such alternatives, within the case study, it is observed that a trade-off assessment between all the optimal solutions is required, but this task is a separate management problem. In principle, there is only one specification containing all the functional and reliability requirements, and one optimal solution is synthesized which is the optimal architecture.
- An experimental testbed has been constructed to demonstrate the concept of a DC distribution system, validate a topology reconfiguration strategy based on combinatorial logic lookup, and provide a platform for testing power transfer interconnections. This testbed is a small-scale two-mirrored zones EPS with a transfer circuit and two auxiliary power sources built with commercially available electronic components. A combinatorial logic lookup table programmed in a low-cost high-performance microcontroller has been the core of the main controller. A separate interruption signal generator and failure simulation board are in charge of artificially triggering a failure. These components can be removed in real aircraft applications.

Proposing a design framework combining a variety of tools has been the main driver of the work done in this thesis. Moreover, the potential of this approach is also applicable to other engineering designs, such as cars, ships, and other aerospace applications. As in any other design problem, the accuracy of the results relies on the careful definition and translation of the specifications and requirements. Also, each application is different to any other, so that each design is tailored to a set of specific needs.

8.2. Future Work

In the MEA context, the existence of the EPS is almost entirely based on the load consumption scheme and profile because the power system is the distributing interface between generation power and the loads. The aircraft loads use power and energy to maintain all vital flight functions, so that loads are intrinsically related to the flight function itself. Hence, the academic visibility (engagement to broader audiences) of the current proposal could be higher if the design started from the aircraft design itself. Of course, the designer can always request the loads' characteristics and commence design from this point. On the other hand, performance evaluation during operation is still an intense area of research, and for more electric aircraft there are still unexplored methods at the experimental stage. Pledging to continue the research presented in this thesis, possible future investigations are listed below:

- Exploration of the generation system design with load profiles. So far, a fixed power demand has been considered in the loads, but no power profile with time-varying and pulsating conditions has been explored. This would aggregate time as a new dimension in the generator selection and generator-load pairing problem, which would have an impact on the sizing of the power sources. Also, an additional set of abstractions and characteristics for power sources would be required.
- Source matrix contactors (bus bar boxes) were assumed to distribute generation power to power converters in the power distribution design problem. These boxes have several inputs and outputs and an internal switch arrangement that matches input with outputs depending on the needs. The synthesis of this device is required to generate a power management strategy that distributes power efficiently.
- It is assumed that power converters' outputs can be paralleled to supply a load bus. The design of such a parallelable converter is the next step in realizing a physical implementation of the architectures proposed in this work.

- Loss minimization has been the main application in optimizing the system's performance. On the other hand, a topology reconfiguration strategy has been implemented in the case of component failures in a DC testbed. Hence, an integrated power management problem can be modelled and investigated considering failures, load varying conditions, power generation shortages, and losses minimization.

With respect to the EPS testbed, there are many investigations that can be performed:

- Converters are unidirectional. However, bidirectional converters are attractive in MEA applications [121], [178] because power from regeneration periods in traction loads could be used to recharge batteries and other electrically rechargeable power sources. Regeneration power could be obtained by including an electro-mechanical drivetrain that simulated the rotational movement of traction wheels or actuators such that at any deceleration (negative speed change), some power could be injected back to the EPS. Nevertheless, this feature requires the usage of controllable converters in the power sources as well, and the implementation of a real-time power and energy management algorithm that optimally distributed supply power and regeneration power when available. The proposed testbed focuses only on the reconfiguration feature of the EPS, but further research could include bidirectional converter additions and replacement, construction of an electro-mechanical drivetrain that simulated regenerative load, and implementation of real-time power management techniques.
- Combinatorial logic and the lookup task have been done for the relatively small EPS testbed. However, larger EPS demand more efficient reconfiguration techniques and power management systems based on performance optimization. Hence, more powerful processing boards are required to handle optimization tasks with digital and analog inputs and outputs. These controllers can replace current controllers in the testbed for real-time performance optimization.

References

[1] T. Balcerzak, “The airline industry in 2050,” *Zesz. Nauk. Uniw. Szczecińskiego Probl. Transp. i Logistyki*, vol. 33, pp. 45–57, 2016, doi: 10.18276/ptl.2016.33-05.

[2] ATAG, “Aviation industry reducing its environmental footprint,” *Aviation Benefits Beyond Borders*, 2021. https://aviationbenefits.org/environmental-efficiency/climate-action/ (accessed Nov. 25, 2021).

[3] Clean Sky, “Clean Sky,” *European Union Funding for Research and Innovation*, 2018. http://www.cleansky.eu (accessed May 10, 2018).

[4] EU, “Clean Aviation Joint Undertaking,” 2022. https://www.clean-aviation.eu/ (accessed Jan. 17, 2022).

[5] B. L. Koff, “Gas Turbine Technology Evolution: A Designers Perspective,” *J. Propuls. Power*, vol. 20, no. 4, pp. 577–595, Jul. 2004, doi: 10.2514/1.4361.

[6] R. Glassock, V. Madonna, P. Giangrande, and M. Galea, “RexMoto-A Range Extender Concept for Light Electric Aircraft,” in *2020 IEEE Transportation Electrification Conference & Expo (ITEC)*, Jun. 2020, pp. 930–935, doi: 10.1109/ITEC48692.2020.9161496.

[7] B. Sarlioglu and C. T. Morris, “More Electric Aircraft: Review, Challenges, and Opportunities for Commercial Transport Aircraft,” *IEEE Trans. Transp. Electrif.*, vol. 1, no. 1, pp. 54–64, 2015, doi: 10.1109/TTE.2015.2426499.

[8] S. Bozhko, C. I. Hill, and T. Yang, “More-Electric Aircraft: Systems and Modeling,” in *Wiley Encyclopedia of Electrical and Electronics Engineering*, Hoboken, NJ, USA: John Wiley & Sons, Inc., 2018, pp. 1–31.

[9] R. I. Jones, “The more electric aircraft—assessing the benefits,” *Proc. Inst. Mech. Eng. Part G J. Aerosp. Eng.*, vol. 216, no. 5, pp. 259–269, May 2002, doi: 10.1243/095441002321028775.

[10] R. H. Jansen, C. L. Bowman, S. Clarke, D. Avanesian, P. J. Dempsey, and R. W. Dyson, “NASA electrified aircraft propulsion efforts,” *Aircr. Eng. Aerosp. Technol.*, vol. 92, no. 5, pp. 667–673,

May 2020, doi: 10.1108/AEAT-05-2019-0098.

[11] K. Sharma and G. Srinivas, “Flying smart: Smart materials used in aviation industry,” *Mater. Today Proc.*, vol. 27, pp. 244–250, 2020, doi: 10.1016/j.matpr.2019.10.115.

[12] E. Baharozu, G. Soykan, and M. B. Ozerdem, “Future aircraft concept in terms of energy efficiency and environmental factors,” *Energy*, vol. 140, pp. 1368–1377, Dec. 2017, doi: 10.1016/j.energy.2017.09.007.

[13] C. A. Luongo *et al.*, “Next Generation More-Electric Aircraft: A Potential Application for HTS Superconductors,” *IEEE Trans. Appl. Supercond.*, vol. 19, no. 3, pp. 1055–1068, Jun. 2009, doi: 10.1109/TASC.2009.2019021.

[14] I. Moir and A. Seabridge, *Aircraft Systems- Mechanical, electrical, and avionics subsystems integration*, 3rd ed. West Sussex, UK: John Wiley & Sons, 2008.

[15] J. Chen, C. Wang, and J. Chen, “Investigation on the selection of electric power system architecture for future more electric aircraft,” *IEEE Trans. Transp. Electrif.*, vol. 4, no. 2, pp. 563–576, 2018, doi: 10.1109/TTE.2018.2792332.

[16] A. Pinto, S. Becz, and H. Reeve, “Correct-by-Construction Design of Aircraft Electric Power Systems,” in *10th AIAA Aviation Technology, Integration, and Operations (ATIO) Conference*, Sep. 2010, pp. 1–11, doi: 10.2514/6.2010-9263.

[17] G. Buticchi, S. Bozhko, M. Liserre, P. Wheeler, and K. Al-Haddad, “On-board microgrids for the more electric aircraft - Technology review,” *IEEE Trans. Ind. Electron.*, vol. 66, no. 7, pp. 5588–5599, 2019, doi: 10.1109/TIE.2018.2881951.

[18] K. Keutzer, A. R. Newton, J. M. Rabaey, and A. Sangiovanni-Vincentelli, “System-level design: orthogonalization of concerns and platform-based design,” *IEEE Trans. Comput. Des. Integr. Circuits Syst.*, vol. 19, no. 12, pp. 1523–1543, 2000, doi: 10.1109/43.898830.

[19] X. Roboam *et al.*, *Integrated Design by Optimization of Electrical Energy Systems*, 1st ed. UK: John Wiley & Sons - ISTE, 2012.

[20] Y. Aoues and A. Chateauneuf, “Benchmark study of numerical methods for reliability-based design optimization,” *Struct. Multidiscip. Optim.*, vol. 41, no. 2, pp. 277–294, Mar. 2010, doi: 10.1007/s00158-009-0412-2.

[21] R. K. Ahuja, T. L. Magnanti, J. B. Orlin, and M. R. Reddy, “Chapter 1 Applications of network optimization,” in *Handbook in Operations Research and Management Science*, M. O. Ball, T. L. . Magnanti, C. L. Monma, and G. L. Nemhauser, Eds. 1995, pp. 1–83.

[22] N. E. Antoine and I. M. Kroo, “Framework for Aircraft Conceptual Design and Environmental Performance Studies,” *AIAA J.*, vol. 43, no. 10, pp. 2100–2109, Oct. 2005, doi: 10.2514/1.13017.

[23] A. Rothwell, “The Conventional Design Process,” in *Optimization Methods in Structural Design. Solid Mechanics and its Applications*, Springer, Cham, 2017, pp. 1–28.

[24] R. K. Ahuja, T. L. Magnanti, and J. B. Orlin, *Network Flows*, United Sta. Pearson, 1993.

[25] J. B. Hu, F. Li, J. Wu, J. H. Wang, and L. P. Zhang, “Research on Aviation Electric Power Cyber Physical Systems,” *Adv. Mater. Res.*, vol. 846–847, pp. 126–133, Nov. 2013, doi: 10.4028/www.scientific.net/AMR.846-847.126.

[26] R. D. Telford, S. J. Galloway, and G. M. Burt, “Evaluating the reliability & availability of more-electric aircraft power systems,” in *Proceedings of the Universities Power Engineering Conference*, 2012, doi: 10.1109/UPEC.2012.6398542.

[27] T. Sgobba, P. D. Wilde, I. Rongier, and F. A. Allahdadi, “Introduction to Space Operations Safety,” in *Safety Design for Space Operations*, Elsevier, 2013, pp. 1–25.

[28] P. Wheeler and S. Bozhko, “The more electric aircraft: Technology and challenges,” *IEEE Electrification Magazine*, vol. 2, no. 4, pp. 6–12, Dec. 2014.

[29] L. S. Brandt, N. Krämer, J. Metzger, and U. Lindemann, “Optimization approach for function-partitioning in an automotive electric electronic system architecture,” in *Proceedings of International Design Conference, DESIGN*, 2012, vol. DS 70, pp. 737–746.

[30] P. Helle, M. Masin, and L. Greenberg, “Approximate Reliability Algebra for Architecture Optimization,” in *In International Conference on Computer Safety, Reliability, and Security*, 2012, vol. 1, no. 1, pp. 279–290, doi: 10.1007/978-3-642-33678-2.

[31] M. Todinov, *Flow Networks*, 1st Ed. London: Elsevier, 2013.

[32] E. Burke *et al.*, *Search Methodologies- Introductory Tutorials in Optimization and Decision Support Techniques*, 1st ed. UK: Springer Science & Bussiness Media, 2005.

[33] a. Sangiovanni-Vincentelli, L. Carloni, F. De Bernardinis, and M. Sgroi, “Benefits and challenges for platform-based design,” in *Proceedings. 41st Design Automation Conference, 2004.*, 2004, pp. 409–414, doi: 10.1109/DAC.2004.240381.

[34] A. Sangiovanni-Vincentelli and G. Martin, “Platform-based design and software design methodology for embedded systems,” *IEEE Des. Test Comput.*, vol. 18, no. 6, pp. 23–33, 2001, doi: 10.1109/54.970421.

[35] P. Nuzzo, J. Finn, M. Mozumdar, and A. Sangiovanni-vincentelli, “Platform-Based Design Methodology and Modeling for Aircraft Electric Power Systems,” in *Proceedings of Green Energy and Systems Conference*, 2013, pp. 1–7.

[36] P. Nuzzo *et al.*, “A contract-based methodology for aircraft electric power system design,” *IEEE Access*, vol. 2, pp. 1–25, 2014, doi: 10.1109/ACCESS.2013.2295764.

[37] J. P. Vielma, “Mixed Integer Linear Programming Formulation Techniques,” *SIAM Rev.*, vol. 57, no. 1, pp. 3–57, Jan. 2015, doi: 10.1137/130915303.

[38] A. Benveniste *et al.*, “Contracts for system design,” HAL archives-ouvertes.fr, 2012.

[39] R. Bloem, B. Jobstmann, N. Piterman, A. Pnueli, and Y. Sa’Ar, “Synthesis of Reactive(1) designs,” *J. Comput. Syst. Sci.*, vol. 78, no. 3, pp. 911–938, 2012, doi: 10.1016/j.jcss.2011.08.007.

[40] H. Xu, U. Topcu, and R. M. Murray, “Specification and synthesis of reactive protocols for aircraft electric power distribution,” *IEEE Trans. Control Netw. Syst.*, vol. 2, no. 2, pp. 193–203, 2015, doi: 10.1109/TCNS.2015.2401174.

[41] N. Bajaj, “Synthesis of Reliable and Cost-Effective Cyber-Physical System Architectures,” University of California at Berkeley, 2015.

[42] H. Xu, “Design, specification, and synthesis of aircraft electric power systems control logic,” California Institute of Technology, 2013.

[43] H. Xu, U. Topcu, and R. M. Murray, “A case study on reactive protocols for aircraft electric power distribution,” *2012 IEEE 51st IEEE Conf. Decis. Control*, pp. 1124–1129, 2012, doi: 10.1109/CDC.2012.6426175.

[44] I. Filippidis and S. C. Livingston, “Temporal Logic Planning (TuLiP) toolbox.” https://github.com/tulip-control.

[45] R. Rogersten, H. Xu, N. Ozay, U. Topcu, and R. M. Murray, “An aircraft electric power testbed for validating automatically synthesized reactive control protocols,” in *Proceedings of the 16th international conference on Hybrid systems: computation and control - HSCC ’13*, 2013, p. 89, doi: 10.1145/2461328.2461344.

[46] T. Wongpiromsarn, U. Topcu, N. Ozay, H. Xu, and R. M. Murray, “TuLiP: A Software Toolbox for Receding Horizon Temporal Logic Planning,” in *Proceedings of the 14th international conference on Hybrid systems: computation and control*, 2011, pp. 313–314, doi: 10.1145/1967701.1967747.

[47] I. Filippidis, S. Dathathri, S. C. Livingston, N. Ozay, and R. M. Murray, “Control design for hybrid systems with TuLiP: The Temporal Logic Planning toolbox,” in *2016 IEEE Conference on Control Applications, CCA 2016*, 2016, pp. 1030–1041, doi: 10.1109/CCA.2016.7587949.

[48] Y. Sa’ar, “JTVL Project Home Site,” 2008. .

[49] A. Pnueli, Y. Sa’ar, and L. D. Zuck, “Jtlv: A framework for developing verification algorithms,” *Lect. Notes Comput. Sci. (including Subser. Lect. Notes Artif. Intell. Lect. Notes Bioinformatics)*, vol. 6174 LNCS, pp. 171–174, 2010, doi: 10.1007/978-3-642-14295-6_18.

[50] A. Pinto and A. L. Sangiovanni Vincentelli, “CSL4P: A Contract Specification Language for Platforms,” *Syst. Eng.*, vol. 20, no. 3, pp. 220–234, May 2017, doi: 10.1002/sys.21386.

[51] J. Finn, P. Nuzzo, and A. Sangiovanni-Vincentelli, “A mixed discrete-continuous optimization scheme for Cyber-Physical System architecture exploration,” in *2015 IEEE/ACM International Conference on Computer-Aided Design (ICCAD)*, Nov. 2015, pp. 216–223, doi: 10.1109/ICCAD.2015.7372573.

[52] P. Nuzzo, “Compositional Design of Cyber-Physical Systems Using Contracts,” University of California, Berkeley, 2015.

[53] C. Hang, P. Manolios, and V. Papavasileiou, “Synthesizing cyber-physical architectural models with real-time constraints,” *Lect. Notes Comput. Sci. (including Subser. Lect. Notes Artif. Intell. Lect. Notes Bioinformatics)*, vol. 6806 LNCS, pp. 441–456, 2011, doi: 10.1007/978-3-642-22110-1_35.

[54] N. Bajaj, P. Nuzzo, M. Masin, and A. Sangiovanni-Vincentelli, “Optimized Selection of Reliable and Cost-Effective Cyber-Physical System Architectures,” in *Design, Automation & Test in Europe*

Conference & Exhibition (DATE), 2015, 2015, pp. 561–566, doi: 10.7873/DATE.2015.0913.

[55] A. Sangiovanni-Vincentelli, W. Damm, and R. Passerone, “Taming Dr. Frankenstein: Contract-Based Design for Cyber-Physical Systems*,” *Eur. J. Control*, vol. 18, no. 3, pp. 217–238, 2012, doi: 10.3166/ejc.18.217-238.

[56] B. Wen *et al.*, “Integrated Design by Optimization of Power Systems for More Electric Aircraft,” in *MEA 2015 – More Electric Aircraft –*, 2015, no. February, [Online]. Available: https://hal.archives-ouvertes.fr/hal-01115434.

[57] A. Tardy *et al.*, “Towards More Optimization for Aircraft Energy Conversion Systems,” in *MEA 2015 – More Electric Aircraft –*, 2015, no. February, p. 16, [Online]. Available: https://hal.archives-ouvertes.fr/hal-01114509/.

[58] X. Roboam, *Systemic Design Methodologies for Electrical Energy Systems: Analysis, Synthesis, and Management*, 1st ed. Hoboken, New Jersey: John Wiley & Sons - ISTE, 2012.

[59] J. R. R. A. Martins and A. B. Lambe, “Multidisciplinary Design Optimization: A Survey of Architectures,” *AIAA J.*, vol. 51, no. 9, pp. 2049–2075, 2013, doi: 10.2514/1.J051895.

[60] G. Ezzati, “A reliability-based design optimization model for electricity power networks,” in *Dynamics of Continuous, Discrete and Impulsive Systems*, 1st ed., no. Series B, Applications and Algorithms 22, Watam Press, 2015, pp. 339–357.

[61] S. Ezzati, “Reliability-based Design Optimisation Methods in Large-scale Systems,” *Bull. Aust. Math. Soc.*, vol. 95, no. 01, pp. 172–173, Feb. 2017, doi: 10.1017/S0004972716000691.

[62] S. Seong, C. Hu, and S. Lee, “Design under uncertainty for reliable power generation of piezoelectric energy harvester,” *J. Intell. Mater. Syst. Struct.*, vol. 28, no. 17, pp. 2437–2449, 2017, doi: 10.1177/1045389X17689945.

[63] M. Minoux, “Networks synthesis and optimum network design problems: Models, solution methods and applications,” *Networks*, vol. 19, no. 3, pp. 313–360, May 1989, doi: 10.1002/net.3230190305.

[64] B. Gendron, T. G. Crainic, and A. Frangioni, “Multicommodity Capacitated Network Design,” in *Telecommunications Network Planning*, B. Sanso and P. Soriano, Eds. Boston, MA: Springer US, 1999, pp. 1–19.

[65] R. L. Y. Chen and C. A. Phillips, “K-Edge failure resilient network design,” *Electron. Notes Discret. Math.*, vol. 41, pp. 375–382, 2013, doi: 10.1016/j.endm.2013.05.115.

[66] M. Garg and J. C. Smith, “Models and algorithms for the design of survivable multicommodity flow networks with general failure scenarios,” *Omega*, vol. 36, no. 6, pp. 1057–1071, 2008, doi: 10.1016/j.omega.2006.05.006.

[67] Yu Liu and D. Tipper, “Successive survivable routing for node failures,” in *GLOBECOM 01 IEEE Global Telecommunications Conference*, 2002, vol. 4, pp. 2093–2097, doi: 10.1109/GLOCOM.2001.966150.

[68] T. L. Magnanti and R. T. Wong, “Network Design and Transportation Planning: Models and Algorithms,” *Transp. Sci.*, vol. 18, no. 1, pp. 1–55, 1984, doi: 10.1287/trsc.18.1.1.

[69] M. Carneiro da Silva, P. Morelato Franca, and P. D. Bishop da Silveira, “Long-range planning of Power Distribution Systems : Secondary Networks,” *Science (80-.).*, vol. 22, no. 3, pp. 179–191, 1996, doi: 10.1016/j.ecolmodel.2007.08.027.

[70] E. B. Fisher, R. P. O’Neill, and M. C. Ferris, “Optimal Transmission Switching,” *IEEE Trans. Power Syst.*, vol. 23, no. 3, pp. 1346–1355, Aug. 2008, doi: 10.1109/TPWRS.2008.922256.

[71] H. Dommel and W. Tinney, “Optimal Power Flow Solutions,” *IEEE Trans. Power Appar. Syst.*, vol. PAS-87, no. 10, pp. 1866–1876, Oct. 1968, doi: 10.1109/TPAS.1968.292150.

[72] A. Monticelli, M. V. F. Pereira, and S. Granville, “Security-Constrained Optimal Power Flow with Post-Contingency Corrective Rescheduling,” *IEEE Trans. Power Syst.*, vol. 2, no. 1, pp. 175–180, 1987, doi: 10.1109/TPWRS.1987.4335095.

[73] Y. Zhang, R. Su, C. Wen, M. Y. Lee, and C. Gajanayake, “Distributed power allocation and scheduling for electrical power system in more electric aircraft,” in *IECON 2016 - 42nd Annual Conference of the IEEE Industrial Electronics Society*, Oct. 2016, pp. 102–107, doi: 10.1109/IECON.2016.7793600.

[74] M. Maasoumy, P. Nuzzo, F. Iandola, M. Kamgarpour, A. Sangiovanni-Vincentelli, and C. J. Tomlin, “Optimal load management system for Aircraft Electric Power distribution,” in *IEEE Conference on Decision and Control*, 2013, pp. 2939–2945, doi: 10.1109/CDC.2013.6760330.

[75] X. Giraud *et al.*, “Load allocation problem for optimal design of aircraft electrical power system,”

Int. J. Appl. Electromagn. Mech., vol. 43, no. 1–2, pp. 37–49, 2013, doi: 10.3233/JAE-131708.

[76] E. Kabalci, "Power System Flexibility and Resiliency," in *Power System Resilience Modeling, Analysis and Practice*, 1st ed., N. M. Tabatabaei, S. N. Ravadanegh, and N. Bizon, Eds. Springer Cham, 2019, pp. 81–100.

[77] M. Terörde and D. Schulz, "New real-time heuristics for electrical load rebalancing in aircraft," *IEEE Trans. Aerosp. Electron. Syst.*, vol. 52, no. 3, pp. 1120–1131, 2016, doi: 10.1109/TAES.2016.150001.

[78] M. Terorde, A. Lucken, and D. Schulz, "Weight saving in the electrical distribution systems of aircraft using innovative concepts," *Int. J. energy Res.*, vol. 31, no. August 2007, pp. 135–147, 2007, doi: 10.1002/er.

[79] J. Brombach, A. Lucken, B. Nya, M. Johannsen, and D. Schulz, "Comparison of Different Electrical HVDC- Architectures for Aircraft Application," in *Electrical Systems for Aircraft, Railway and Ship Propulsion (ESARS), 2012*, 2012, pp. 1–6, doi: 10.1109/ESARS.2012.6387380.

[80] A. Engel, Y. Reich, T. R. Browning, and D. M. Schmidt, "Optimizing system architecture for adaptability," in *Proceedings of International Design Conference, DESIGN*, 2012, vol. DS 70, pp. 1677–1688.

[81] K. N. Areerak, S. V. Bozhko, G. M. Asher, L. De Lillo, and D. W. P. Thomas, "Stability study for a hybrid AC-DC more-electric aircraft power system," *IEEE Trans. Aerosp. Electron. Syst.*, vol. 48, no. 1, pp. 329–347, 2012, doi: 10.1109/TAES.2012.6129639.

[82] D. R. Vieira, M.-L. Rebaiaia, and M. C. Chain, "The Application of Reliability Methods for Aircraft Design Project Management," *Am. J. Ind. Bus. Manag.*, vol. 06, no. 09, pp. 967–992, 2016, doi: 10.4236/ajibm.2016.69094.

[83] V. Crk, "Reliability Engineering Challenges in Aerospace Industry," 2011. [Online]. Available: http://ieee.rackoneup.net/rrvs/11/Reliability Engineering Challenges in Aerospace Industry.pdf.

[84] B. Kaiser, P. Liggesmeyer, and O. Mäckel, "A New Component Concept for Fault Trees," in *Proceedings of the 8th Australian workshop on Safety critical systems and software*, 2003, vol. 33, no. January, pp. 37–46.

[85] A. Sangiovanni-Vincentelli, "Quo vadis, SLD? Reasoning about the trends and challenges of

system level design," *Proc. IEEE*, vol. 95, no. 3, pp. 467–506, 2007, doi: 10.1109/JPROC.2006.890107.

[86] S. Messaoud, "Optimal Architecture Synthesis for Aircraft Electrical Power Systems," Technische Universitat Munchen, 2015.

[87] S. Becz, A. Pinto, L. E. Zeidner, R. Khire, A. Banaszuk, and H. M. Reeve, "Design system for managing complexity in aerospace systems," in *10th AIAA ATIO/ISSMO Conference*, 2010, pp. 1–7, doi: 10.2514/6.2010-9223.

[88] X. Roboam, B. Sareni, and A. De Andrade, "More Electricity in the Air," *Industrial Electronics Magazine, IEEE*, vol. 6, no. 4, pp. 6–17, Dec. 2012.

[89] N. P. Tedford and J. R. R. A. Martins, "Benchmarking multidisciplinary design optimization algorithms," in *Optimization and Engineering*, 2010, vol. 11, no. 1, pp. 159–183, doi: 10.1007/s11081-009-9082-6.

[90] I. Kaymaz and K. Marti, "Reliability-based design optimization for elastoplastic mechanical structures," *Comput. Struct.*, vol. 85, no. 10, pp. 615–625, 2007, doi: 10.1016/j.compstruc.2006.08.076.

[91] H. Agarwal, "Reliability based design optimization: formulations and methodologies," University of Notre Dame, 2004.

[92] Y.-G. Zhao and T. Ono, "A general procedure for first/second-order reliability method (FORM/SORM)," *Struct. Saf.*, vol. 21, no. 2, pp. 95–112, 1999, doi: 10.1016/S0167-4730(99)00008-9.

[93] B. D. Youn and K. K. Choi, "Selecting Probabilistic Approaches for Reliability-Based Design Optimization," *AIAA J.*, vol. 42, no. 1, pp. 124–131, 2004, doi: 10.2514/1.9036.

[94] P. Yi, G. Cheng, and L. Jiang, "A sequential approximate programming strategy for performance-measure-based probabilistic structural design optimization," *Struct. Saf.*, vol. 30, no. 2, pp. 91–109, 2008, doi: 10.1016/j.strusafe.2006.08.003.

[95] G. Kharmanda, N. Olhoff, A. Mohamed, and M. Lemaire, "Reliability-based topology optimization," *Struct. Multidiscip. Optim.*, vol. 26, no. 5, pp. 295–307, 2004, doi: 10.1007/s00158-003-0322-7.

[96] R. J. T. Montgomery and S. Galloway, “An Optimisation Based Design Approach for Aircraft Electrical Power Systems,” *SAE Int. J. Aerosp.*, vol. 7, no. 1, pp. 44–52, 2014, doi: 10.4271/2014-01-2121.

[97] L. Laguna, R. Prieto, J. A. Oliver, J. A. Cobos, H. Visairo, and P. Kumar, “Power Conversion Modeling Methodology Based on Building Block Models,” in *Energy Conversion Congress and Exposition (ECCE), 2009 IEEE*, 2009, pp. 3404–3410.

[98] L. Laguna, R. Prieto, J. A. Oliver, J. A. Cobos, and H. Visairo-Cruz, “Fast architecture generation and evaluation techniques for the design of large power systems,” in *2010 IEEE Energy Conversion Congress and Exposition*, Sep. 2010, pp. 3464–3469, doi: 10.1109/ECCE.2010.5618340.

[99] I. Purellku, A. Lucken, J. Brombach, B. Nya, and D. Schulz, “Optimization of the Energy-Supply-Structure of Modern Aircraft By Using Conventional Power System Technologies,” in *CIRED 21st International Conference on Electricity Distribution*, 2011, no. 0973, pp. 6–9.

[100] H. Kim, L. Guo, E. A. Lee, and A. Sangiovanni-Vincentelli, “A Tool Integration Approach for Architectural Exploration of Aircraft EPS with Ptolemy II / Metro II,” in *IEEE 1st International Conference on Cyber-Physical Systems, Networks, and Applications CPSNA*, 2013, no. 1, pp. 38–43, doi: 10.1109/CPSNA.2013.6614244.

[101] Y. Xu, Z. Zhang, J. Li, and Y. Yan, “Architecture analysis and optimization of high voltage DC parallel electric power system for more electric aircraft,” in *AUS 2016 - 2016 IEEE/CSAA International Conference on Aircraft Utility Systems*, 2016, pp. 244–249, doi: 10.1109/AUS.2016.7748054.

[102] H. A. Taboada, J. F. Espiritu, and D. W. Coit, “MOMS-GA: A multi-objective multi-state genetic algorithm for system reliability optimization design problems,” *IEEE Trans. Reliab.*, vol. 57, no. 1, pp. 182–191, 2008, doi: 10.1109/TR.2008.916874.

[103] H. A. Taboada, F. Baheranwala, D. W. Coit, and N. Wattanapongsakorn, “Practical solutions for multi-objective optimization: An application to system reliability design problems,” *Reliab. Eng. Syst. Saf.*, vol. 92, no. 3, pp. 314–322, 2007, doi: 10.1016/j.ress.2006.04.014.

[104] T. M. Cho and B. C. Lee, “Reliability-based design optimization using convex linearization and sequential optimization and reliability assessment method,” *Struct. Saf.*, vol. 33, no. 1, pp. 42–50,

2011, doi: 10.1016/j.strusafe.2010.05.003.

[105] M. Rashki, M. Miri, and M. A. Moghaddam, “A simulation-based method for reliability based design optimization problems with highly nonlinear constraints,” *Autom. Constr.*, vol. 47, pp. 24–36, 2014, doi: 10.1016/j.autcon.2014.07.004.

[106] M. Lukic *et al.*, “State of the Art of Electric Taxiing Systems,” in *2018 IEEE International Conference on Electrical Systems for Aircraft, Railway, Ship Propulsion and Road Vehicles & International Transportation Electrification Conference (ESARS-ITEC)*, Nov. 2018, pp. 1–6, doi: 10.1109/ESARS-ITEC.2018.8607786.

[107] A. Recalde, S. Bozhko, and J. Atkin, “Linear Power Flow Characterization of DC Power Distribution Systems for MEA Optimization,” in *2020 IEEE Transportation Electrification Conference & Expo (ITEC)*, Jun. 2020, pp. 789–794, doi: 10.1109/ITEC48692.2020.9161584.

[108] L. Urbanucci, “Limits and potentials of Mixed Integer Linear Programming methods for optimization of polygeneration energy systems,” *Energy Procedia*, vol. 148, pp. 1199–1205, Aug. 2018, doi: 10.1016/j.egypro.2018.08.021.

[109] G. Srinivasan, *Operations Research, Principles and Applications*, 3rd Editio. Delhi: PHI Learning Private Limited, 2017.

[110] IBM, “IBM ILOG CPLEX Optimization Studio,” 2021. https://www.ibm.com/products/ilog-cplex-optimization-studio (accessed Jun. 01, 2021).

[111] Gurobi, “Gurobi Optimization,” 2021. https://www.gurobi.com/ (accessed Jun. 01, 2021).

[112] Mathworks, “Matlab,” 2021. https://uk.mathworks.com/products/matlab.html (accessed Jun. 01, 2021).

[113] E. Balas, “Disjunctive Programming,” in *Annals of Discrete Mathematics*, Pittsburgh, USA: North-Holland Publishing Company, 1979, pp. 3–51.

[114] G. B. Dantzig, “Origins of the simplex method,” in *A history of scientific computing*, New York, NY, USA: ACM, 1990, pp. 141–151.

[115] J. C. Nash, “The (Dantzig) simplex method for linear programming,” *Comput. Sci. Eng.*, vol. 2, no. 1, pp. 29–31, 2000, doi: 10.1109/5992.814654.

[116] N. Karmarkar, “A new polynomial-time algorithm for linear programming,” in *Proceedings of the sixteenth annual ACM symposium on Theory of computing - STOC ’84*, 1984, pp. 302–311, doi: 10.1145/800057.808695.

[117] C. H. Papadimitriou, “On the complexity of integer programming,” *J. ACM*, vol. 28, no. 4, pp. 765–768, Oct. 1981, doi: 10.1145/322276.322287.

[118] R. Kannan and C. L. Monma, “On the Computational Complexity of Integer Programming Problems,” *Optim. Oper. Res. Lect. Notes Econ. Math. Syst.*, vol. 157, no. 1, pp. 161–172, 1978, doi: 10.1007/978-3-642-95322-4_17.

[119] A. Letchford, “Combinatorial Optimization, Branch & Cut, Benders Decomposition,” in *NATCOR Combinatorial Optimization Coursepack, University of Southampton*, 2019.

[120] C. D’Ambrosio, A. Lodi, and S. Martello, “Piecewise linear approximation of functions of two variables in MILP models,” *Oper. Res. Lett.*, vol. 38, no. 1, pp. 39–46, Jan. 2010, doi: 10.1016/j.orl.2009.09.005.

[121] L. Tarisciotti, A. Costabeber, C. Linglin, A. Walker, and M. Galea, “Evaluation of isolated DC/DC converter topolog for future HVDC aerospace microgrids,” *2017 IEEE Energy Convers. Congr. Expo. ECCE 2017*, vol. 2017-Janua, pp. 2238–2245, 2017, doi: 10.1109/ECCE.2017.8096437.

[122] L. Gan and S. H. Low, “Optimal Power Flow in Direct Current Networks,” *IEEE Trans. Power Syst.*, vol. 29, no. 6, pp. 2892–2904, Nov. 2014, doi: 10.1109/TPWRS.2014.2313514.

[123] F. Gao, S. Yeoh, S. Bozhko, and G. Asher, “Coordinated Control of a DC Electrical Power System in the More Electric Aircraft Integrated with Energy Storage,” in *Energy Conversion Congress and Exposition (ECCE), 2015 IEEE*, 2015, pp. 5431–5438, doi: 10.1109/ECCE.2015.7310424.

[124] V. G. Gkoutzamanis *et al.*, “Conceptual Design and Energy Storage Positioning Aspects for a Hybrid-Electric Light Aircraft,” in *Volume 5: Controls, Diagnostics, and Instrumentation; Cycle Innovations; Cycle Innovations: Energy Storage*, Sep. 2020, doi: 10.1115/GT2020-15477.

[125] D. Raymer, *Aircraft Design: A Conceptual Approach, Sixth Edition*. Washington, DC: American Institute of Aeronautics and Astronautics, Inc., 2018.

[126] G. F. Esdras and S. Liscouet-Hanke, “An Electrical Load Estimation Tool for Aircraft Conceptual Design,” in *SAE Technical Papers*, Sep. 2013, vol. 7, doi: 10.4271/2013-01-2206.

[127] R. Seresinhe and C. Lawson, “Electrical load-sizing methodology to aid conceptual and preliminary design of large commercial aircraft,” *Proc. Inst. Mech. Eng. Part G J. Aerosp. Eng.*, vol. 229, no. 3, pp. 445–466, Mar. 2015, doi: 10.1177/0954410014534638.

[128] J. Biela, U. Badstuebner, and J. W. Kolar, “Impact of Power Density Maximization on Efficiency of DC–DC Converter Systems,” *IEEE Trans. Power Electron.*, vol. 24, no. 1, pp. 288–300, Jan. 2009, doi: 10.1109/TPEL.2009.2006355.

[129] Y.-K. Son, S.-Y. Lee, S. Ko, Y.-W. Kim, and S.-K. Sul, “Maritime DC Power System With Generation Topology Consisting of Combination of Permanent Magnet Generator and Diode Rectifier,” *IEEE Trans. Transp. Electrif.*, vol. 6, no. 2, pp. 869–880, Jun. 2020, doi: 10.1109/TTE.2020.2992474.

[130] Jie Chang and Anhua Wang, “New VF-power system architecture and evaluation for future aircraft,” *IEEE Trans. Aerosp. Electron. Syst.*, vol. 42, no. 2, pp. 527–539, Apr. 2006, doi: 10.1109/TAES.2006.1642569.

[131] J.-K. Mueller *et al.*, “Design Considerations for the Electrical Power Supply of Future Civil Aircraft with Active High-Lift Systems,” *Energies*, vol. 11, no. 2, p. 179, 2018, doi: 10.3390/en11010179.

[132] M. Nozarian, A. H. Nikoofard, and A. Fereidunian, “Efficient MILP formulations for AC optimal power flow to reduce computational effort,” *Int. Trans. Electr. Energy Syst.*, vol. 30, no. 8, Aug. 2020, doi: 10.1002/2050-7038.12434.

[133] J. Lee, K. Nam, S. Choi, and S. Kwon, “Loss Minimizing Control of PMSM with the Use of Polynomial Approximations,” in *2008 IEEE Industry Applications Society Annual Meeting*, Oct. 2008, pp. 1–9, doi: 10.1109/08IAS.2008.226.

[134] Y. Zhang *et al.*, “An Extremely High Power Density Asymmetrical Back-to-Back Converter for Aerospace Motor Drive Applications,” *Energies*, vol. 13, no. 5, p. 1292, Mar. 2020, doi: 10.3390/en13051292.

[135] A. K. Andreas and J. C. Smith, “Mathematical Programming Algorithms for Two-Path Routing Problems with Reliability Considerations,” *INFORMS J. Comput.*, vol. 20, no. 4, pp. 553–564, Nov. 2008, doi: 10.1287/ijoc.1080.0266.

[136] J. J. Grainger and W. D. Stevenson, *Power System Analysis*. McGraw-Hill Education, 1994.

[137] J. A. Sayago, T. Bruckner, and S. Bernet, “How to Select the System Voltage of MV Drives—A

Comparison of Semiconductor Expenses," *IEEE Trans. Ind. Electron.*, vol. 55, no. 9, pp. 3381–3390, Sep. 2008, doi: 10.1109/TIE.2008.924032.

[138] K. Ibrahim, S. Sampath, and D. Nalianda, "Optimal Voltage and Current Selection for Turboelectric Aircraft Propulsion Networks," *IEEE Trans. Transp. Electrif.*, vol. 6, no. 4, pp. 1625–1637, Dec. 2020, doi: 10.1109/TTE.2020.3004308.

[139] P. Kshirsagar, S. Dwari, J. M. Rheaume, R. Taylor, C. E. Lents, and P. Walsh, "Anatomy of a 20 MW Electrified Aircraft: Metrics and Technology Drivers," in *AIAA Propulsion and Energy 2020 Forum*, Aug. 2020, doi: 10.2514/6.2020-3581.

[140] M. Abou-Dakka, A. Bulinski, and S. S. Bamji, "On-site diagnostic technique for smart maintenance of power cables," in *2011 IEEE Power and Energy Society General Meeting*, Jul. 2011, pp. 1–5, doi: 10.1109/PES.2011.6039394.

[141] Omicron, "Partial Discharge Analysis on Power Cables," *Cable Test Monitoring*, 2021. https://www.omicronenergy.com/en/applications/cable-testing-monitoring/commissioning-diagnosis-partial-discharge-analysis-on-power-cables/ (accessed Apr. 27, 2021).

[142] R. Bartnikas, "Partial discharges. Their mechanism, detection and measurement," *IEEE Trans. Dielectr. Electr. Insul.*, vol. 9, no. 5, pp. 763–808, Oct. 2002, doi: 10.1109/TDEI.2002.1038663.

[143] M. J. Armstrong, C. A. H. Ross, M. J. Blackwelder, and K. Rajashekara, "Trade Studies for NASA N3-X Turboelectric Distributed Propulsion System Electrical Power System Architecture," *SAE Int. J. Aerosp.*, vol. 5, no. 2, pp. 2012-01–2163, Oct. 2012, doi: 10.4271/2012-01-2163.

[144] L. Calcara, S. Sangiovanni, and M. Pompili, "Partial Discharge Inception Voltage in Insulating Liquids Dependence from the Definition Used," in *2020 IEEE 3rd International Conference on Dielectrics (ICD)*, Jul. 2020, pp. 736–739, doi: 10.1109/ICD46958.2020.9341822.

[145] E. Husain and R. S. Nema, "Analysis of Paschen Curves for air, N2 and SF6 Using the Townsend Breakdown Equation," *IEEE Trans. Electr. Insul.*, vol. EI-17, no. 4, pp. 350–353, Aug. 1982, doi: 10.1109/TEI.1982.298506.

[146] J. P. Webb, "Application of the finite-element method to electromagnetic and electrical topics," *Reports Prog. Phys.*, vol. 58, no. 12, pp. 1673–1712, Dec. 1995, doi: 10.1088/0034-4885/58/12/002.

[147] N. Trinh, “Electrode Design for Testing in Uniform Field Gaps,” *IEEE Trans. Power Appar. Syst.*, vol. PAS-99, no. 3, pp. 1235–1242, May 1980, doi: 10.1109/TPAS.1980.319754.

[148] “Aerospace and Defense,” *Nexans*, 2018. https://www.nexans.com/business/Industry---Solutions/Aerospace---Defense.html (accessed Dec. 14, 2020).

[149] S. Boyd, B. S. P., and L. Vandenberghe, *Convex Optimization*, 1st ed. Cambridge University Press, 2004.

[150] FICO, “MIP formulations and linearization,” 2009.

[151] R. W. Erickson and D. Maksimovic, *Fundamentals of Power Electronics*, 3rd Ed. Springer, 2020.

[152] A. Wood, B. F. Wollenberg, and G. B. Sheble, *Power Generation, Operation and Control*, 3rd Ed. John Wiley & Sons, 2013.

[153] A. Garces, “Uniqueness of the power flow solutions in low voltage direct current grids,” *Electr. Power Syst. Res.*, vol. 151, pp. 149–153, Oct. 2017, doi: 10.1016/j.epsr.2017.05.031.

[154] O. D. Montoya, L. F. Grisales-Noreña, D. González-Montoya, C. A. Ramos-Paja, and A. Garces, “Linear power flow formulation for low-voltage DC power grids,” *Electr. Power Syst. Res.*, vol. 163, no. March, pp. 375–381, Oct. 2018, doi: 10.1016/j.epsr.2018.07.003.

[155] E. Camponogara and L. F. Nazari, “Models and Algorithms for Optimal Piecewise-Linear Function Approximation,” *Math. Probl. Eng.*, vol. 2015, pp. 1–9, 2015, doi: 10.1155/2015/876862.

[156] A. Imamoto and B. Tang, “Optimal Piecewise Linear Approximation of Convex Functions,” *Lect. Notes Eng. Comput. Sci.*, vol. 2173, no. 1, pp. 1191–1194, 2008.

[157] R. Misener and C. A. Floudas, “Piecewise-Linear Approximations of Multidimensional Functions,” *J. Optim. Theory Appl.*, vol. 145, no. 1, pp. 120–147, Apr. 2010, doi: 10.1007/s10957-009-9626-0.

[158] I. Christou, A. Nelms, I. Cotton, and M. Husband, “Choice of optimal voltage for more electric aircraft wiring systems,” *IET Electr. Syst. Transp.*, vol. 1, no. 1, pp. 24–30, 2011, doi: 10.1049/iet-est.2010.0021.

[159] C. Spagnolo, S. Sumsurooah, C. I. Hill, and S. Bozhko, “Finite state machine control for aircraft electrical distribution system,” *J. Eng.*, vol. 2018, no. 13, pp. 506–511, Jan. 2018, doi: 10.1049/joe.2018.0039.

[160] M. Guacci, D. Bortis, and J. W. Kolar, “High-Efficiency Weight-Optimized Fault-Tolerant Modular Multi-Cell Three-Phase GaN Inverter for Next Generation Aerospace Applications,” in *2018 IEEE Energy Conversion Congress and Exposition (ECCE)*, Sep. 2018, pp. 1334–1341, doi: 10.1109/ECCE.2018.8557754.

[161] D. Golovanov *et al.*, “4-MW Class High-Power-Density Generator for Future Hybrid-Electric Aircraft,” *IEEE Trans. Transp. Electrif.*, vol. 7, no. 4, pp. 2952–2964, Dec. 2021, doi: 10.1109/TTE.2021.3068928.

[162] N. A. of Sciences Engineering and Medicine and C. on Propulsion, *Commercial Aircraft Propulsion and Energy Systems Research*. Washington, D.C.: National Academies Press, 2016.

[163] V. Madonna, P. Giangrande, and M. Galea, “Electrical Power Generation in Aircraft: review, challenges and opportunities,” *IEEE Trans. Transp. Electrif.*, vol. 1, no. 1, pp. 1–14, 2018, doi: 10.1109/TTE.2018.2834142.

[164] R. Sasaki, M. Wada, and O. Sakamoto, “Weight and Characteristics of Aircraft AC Generators Abstract,” *J. Japan Soc. Aeronaut. Sp. Sci.*, vol. 27, no. 305, pp. 296–300, 1979, doi: 10.2322/jjsass1969.27.296.

[165] Alibaba.com, “90KW 90000 watt PMSM ac EV car electrical motor and inverter motors controls,” 2022. https://www.alibaba.com/product-detail/90KW-90000-watt-PMSM-ac-EV_1600055465948.html (accessed Feb. 11, 2022).

[166] J. Benzaquen, J. He, and B. Mirafzal, “Toward more electric powertrains in aircraft: Technical challenges and advancements,” *CES Trans. Electr. Mach. Syst.*, vol. 5, no. 3, pp. 177–193, Sep. 2021, doi: 10.30941/CESTEMS.2021.00022.

[167] Flight-Mechanic, “Wiring Installation - Wire Types,” *Flight-Mechanic*, 2020. https://www.flight-mechanic.com/wiring-installation-wire-types/ (accessed Apr. 28, 2021).

[168] DoD, “MIL-W-5088 Wiring, Aerospace Vehicle,” 1991.

[169] P. J. Fortier and H. E. Michel, “Testbeds as modelling tools,” in *Computer Systems Performance Evaluation and Prediction*, Elsevier, 2003, pp. 1–38.

[170] W. I. Bellamy, “New Collins Electric Aircraft Lab Has High Voltage Goals,” *Aviation Today*, 2019. https://www.aviationtoday.com/2019/04/05/new-collins-electric-aircraft-lab-high-voltage-goals/

(accessed Jan. 14, 2021).

[171] R. Rogersten, H. Xu, N. Ozay, U. Topcu, and R. M. Murray, “Control Software Synthesis and Validation For A Vehicular Electric Power Distribution Testbed,” *AIAA J. Aerosp. Inf. Syst.*, vol. 11, no. 10, pp. 1–14, 2013, doi: 10.2514/1.I010167.

[172] L. Persson, S. C. Livingston, and R. M. Murray, “An improved aircraft electric power testbed for validating synthesis methods,” 2015.

[173] N. S. Tunaboylu, G. Shehu, M. Argin, and T. Yalcinoz, “Development of smart grid test-bed for electric power distribution system,” in *2016 IEEE Conference on Technologies for Sustainability (SusTech)*, 2016, pp. 184–187, doi: 10.1109/SusTech.2016.7897164.

[174] R. Eini, L. Linkous, N. Zohrabi, and S. Abdelwahed, “A testbed for a smart building,” in *Proceedings of the Fourth Workshop on International Science of Smart City Operations and Platforms Engineering - SCOPE ’19*, 2019, pp. 1–6, doi: 10.1145/3313237.3313296.

[175] P. Pant, K. Schoder, and A. Feliachi, “An Integrated Electric Shipboard Power System Testbed,” in *2007 IEEE Electric Ship Technologies Symposium*, May 2007, pp. 438–442, doi: 10.1109/ESTS.2007.372123.

[176] V. Madonna, P. Giangrande, L. Lusuardi, A. Cavallini, C. Gerada, and M. Galea, “Thermal Overload and Insulation Aging of Short Duty Cycle, Aerospace Motors,” *IEEE Trans. Ind. Electron.*, vol. 67, no. 4, pp. 2618–2629, Apr. 2020, doi: 10.1109/TIE.2019.2914630.

[177] R. Michalko, “Electrical starting, generation, conversion and distribution system architecture for a more electric vehicle,” 7439634, 2008.

[178] R. T. Naayagi, A. J. Forsyth, and R. Shuttleworth, “High-Power Bidirectional DC–DC Converter for Aerospace Applications,” *IEEE Trans. Power Electron.*, vol. 27, no. 11, pp. 4366–4379, Nov. 2012, doi: 10.1109/TPEL.2012.2184771.

[179] HobbyKing.com, “Turnigy 2200mAh 3S 25C LiPo Pack,” 2022. https://hobbyking.com/en_us/turnigy-2200mah-3s-25c-lipo-pack.html?___store=en_us (accessed Feb. 08, 2022).

[180] AZ_Delivery, “XL4016 Step-Down Buck Converter,” 2022. https://www.az-delivery.de/en/products/xl4016-step-down-buck-converter-dc-dc (accessed Feb. 08, 2022).

[181] E. W. Dijkstra, “A note on two problems in connexion with graphs,” *Numer. Math.*, vol. 1, no. 1, pp. 269–271, 1959, doi: 10.1007/BF01386390.

[182] T. Achterberg, “SCIP: solving constraint integer programs,” *Math. Program. Comput.*, vol. 1, no. 1, pp. 1–41, Jul. 2009, doi: 10.1007/s12532-008-0001-1.

[183] Raspberry Pi Foundation, “Raspberry Pi,” 2021. https://www.raspberrypi.org/ (accessed Jun. 01, 2021).

[184] S. Pokutta, “SCIP x Raspberry Pi: SCIP on Edge,” 2019. http://www.pokutta.com/blog/random/2019/09/29/scipberry.html (accessed Jun. 01, 2021).

[185] DIGILENT, “OpenScope MZ,” *Digilent Reference*, 2021. https://reference.digilentinc.com/test-and-measurement/openscope-mz/start (accessed Jun. 08, 2021).

[186] M. Rashid, *Power Electronics Handbook*, 4th Ed. Butterworth-Heinemann, 2017, 2017.

[187] P. S. R. Murty, “Power Flow Studies,” in *Power Systems Analysis*, 2nd Ed., Elsevier, 2017, pp. 205–276.

[188] A. Bemporad, F. Borrelli, and M. Morari, “Model predictive control based on linear programming - the explicit solution,” *IEEE Trans. Automat. Contr.*, vol. 47, no. 12, pp. 1974–1985, Dec. 2002, doi: 10.1109/TAC.2002.805688.

Appendix I Load Flow

In this appendix, the derivation of the load flow problem is detailed. This material has been condensed from power system analysis textbooks, e.g., [136], [152]. First, the load flow equations for a two-bus system are determined. Then, these equations are extended to a system with more than two components, that is, determination of the nodal equations and matrix representation for any system. Then, the general load problem is presented. This problem is analysed for the two types of systems, alternating current (AC) and direct current (DC) systems.

System's representation for the load flow

There are two representations for the interconnection characteristics in the network matrix, i.e., steady state electrical model of components and connections. The current that flows through a component can be related to the voltage drop (between its input and output terminals) by *admittance* or *impedance* parameters. Both representations are equivalent because they have the same components' information consolidated as a network matrix, an *admittance matrix* or an *impedance matrix*. However, different mathematical steps are required for recalculating the parameters on both matrices once a change in the system is exercised, e.g., topology change (disconnection between two buses that were previously connected), set a component to raise its output's voltage by 20%, etc. In the load flow studies, the admittance matrix is most utilized because the power flow equations (nodal equations) of the load flow problem are amenable for dropping or adding terms when connections and disconnections occur. This is essential for topology reconfiguration and efficiency maximization. For instance, power distribution among generators might require that some connections are disconnected while others are connected, i.e., change the topology of the system to achieve generators' maximum efficiency.

Load Flow Equations for a two-bus system

Consider a system with two buses (or nodes), i and j, where there is a current flow from bus i to j, i.e., there is power flowing from i to j as shown in **Figure *1***. There is a component connecting both buses through which the power is being transmitted. The component's admittance $Y_{i,j}$ is related to the voltages at buses i and j and the current flowing from i to j, as in the following expression,

$$I_{i,j} = Y_{i,j}(V_i - V_j) \tag{a}$$

The admittance $Y_{i,j}$ for connection ij in (77) (Section 5.3 on component location and cable selection) is the same admittance as calculated in (*a*). If bus j were the reference bus (EPS ground), j voltage is 0, then (*a*) is simply $I_i = Y_i V_i$. On the other hand, buses i, j can be referenced to a *third* bus assumed to be ground or 0. Thus, there can also be additional components connected from each bus to ground that generate or consume current. In fact, this is the convention that is commonly used in power system analysis. Following the notation in (*a*), a component that is connected from bus to ground is represented by an admittance $Y_{i,i}$ and it known as a *bus self-admittance*. This admittance models a power source, load, or other sink/source device, e.g., compensator, supercapacitor, etc. When generating or consuming, there is a current I_i being injected or dropped at the bus i in addition to the currents $I_{i,j}$ that are simply distributed to other buses in the EPS through the interconnecting components and distribution lines.

In addition to $I_{i,j}$ defined in (*a*), currents can be defined for power source at bus i, and load at receiving bus j. There is an admittance modelling a power source in bus i and another admittance modelling a load in bus j. These currents can be written as,

$$\begin{aligned} I_i &= V_i Y_{i,i} && \text{For bus } i \\ I_j &= V_j Y_{j,j} && \text{For bus } j \end{aligned} \tag{b}$$

In this system, the same current flows from generator to load, so the current flow balance on each bus is,

$$I_i = I_{i,j} \quad \text{For bus } i$$
$$I_{i,j} = I_j \quad \text{For bus } j \qquad \text{(c)}$$

Therefore, $I_i = I_j = I_{i,j}$. Now, the power values can be written as,

$$P_i = V_i I_i = V_i V_i Y_{i,i} = V_i Y_{i,j}(V_i - V_j) \quad \text{For bus } i$$
$$P_{i,j} = (V_i - V_j) I_{i,j} = Y_{i,j}(V_i - V_j)^2 \quad \text{For component between } i,j \qquad \text{(d)}$$
$$P_j = V_j I_j = V_j V_j Y_{j,j} = V_j Y_{i,j}(V_i - V_j) \quad \text{For bus } j$$

By simple inspection of (d):

$$P_i = P_{i,j} + P_j \qquad \text{(e)}$$

In (e), the receiving power P_j is not the same as the sending power P_i by a quantity $P_{i,j}$, which means that a certain amount of power is lost in the component due to the voltage drop between buses. In fact, no power transference is possible if the voltage in both buses were equal. Equations (d), (e) represents the power balance equations (considering now the relationships between voltages and currents). A conceptual summary of the two-bus system is illustrated in **Figure *1***.

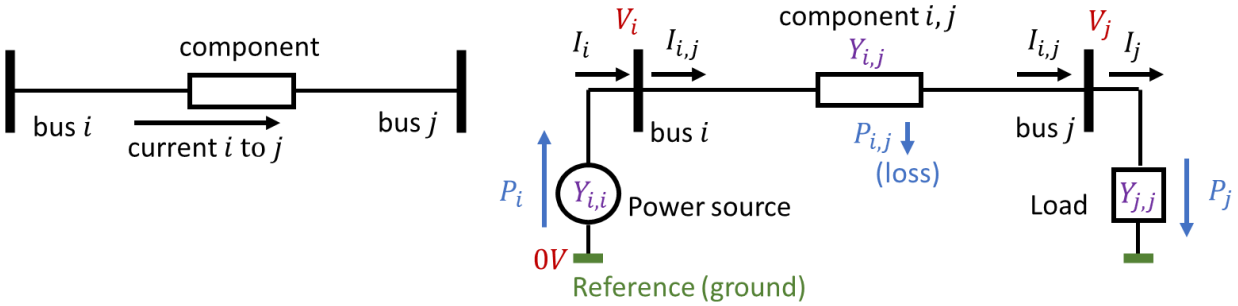

Figure 1. Two-bus system example with current flows, power flows, bus voltages, and admittances.

Power balance in (e) is equivalent to (5) in **O.P. 2** (Section 3.3 on general mathematical formulations for the design of an EPS), where $P_{GENERATORS}$ is P_i (sending end), P_{LOADS} is P_j (receiving end), and P_{LOSSES} is $P_{i,j}$; power source is at bus i, and load is supplied at bus j.

Nodal equations and Matrix representation

When defining an optimization formulation for the PDD problem, (31) has been presented as the power balance expression for every component i in a distribution system (see Section 4.3.2 on power distribution design). This equation also represents a nodal flow balance for every bus in the EPS. Then, for the two-bus system example:

$$\begin{aligned} -P_{i,i} - P_{i,j} &= d^{GEN} && \text{For bus } i \\ P_{j,i} + P_{j,j} &= -d^{LOAD} && \text{For bus } j \end{aligned} \tag{f}$$

Now, expanding the power equations in (d) for buses i, j and rearranging the terms,

$$\begin{aligned} V_i V_i Y_{i,i} - V_i V_j Y_{i,j} &= P_i && \text{For bus } i \\ V_j V_i Y_{j,i} - V_j V_j Y_{j,j} &= P_j && \text{For bus } j \end{aligned} \tag{g}$$

Where $Y_{i,j} = Y_{j,i}$. There are ± signs differences between (f) and (g) because of the chosen conventions. However, there is an equivalence of terms between (g) and (d), i.e., $V_i V_i Y_{i,i} = P_{i,i}$ and $V_i V_j Y_{i,j} = P_{i,j}$ for bus i, and also $V_j V_i Y_{j,i} = P_{j,i}$ and $V_j V_j Y_{j,j} = P_{j,j}$ for bus j, where $P_i = d^{GEN}$ and $P_j = d^{LOAD}$. Therefore, both (f) and (g) are equivalent. There are five parameters in (g): V_i, V_j, $Y_{i,j}$, P_i, and P_j.

One can solve the two-equation system in (g) by finding two unknowns, i.e., there are three parameters that must be known beforehand. Usually, load power P_j, each component's admittance $Y_{i,j}$, and voltage at each power source's terminals V_i are known, then (g) is solved for V_j and P_i. If all voltages in the system

were known in advance, the powers in (g) can be solved straightforwardly. The matrix representation of the power equations in (g) can be written as,

$$\begin{bmatrix} V_i Y_{i,i} & -V_i Y_{i,j} \\ -V_j Y_{j,i} & V_j Y_{j,j} \end{bmatrix} \begin{bmatrix} V_i \\ V_j \end{bmatrix} = \begin{bmatrix} I_i & -I_{i,j} \\ -I_{j,i} & I_j \end{bmatrix} \begin{bmatrix} V_i \\ V_j \end{bmatrix} = \begin{bmatrix} P_i \\ -P_j \end{bmatrix} \quad \text{(h)}$$

Dividing (h) by the corresponding voltages on each bus,

$$\begin{bmatrix} Y_{i,i} & -Y_{i,j} \\ -Y_{j,i} & Y_{j,j} \end{bmatrix} \begin{bmatrix} V_i \\ V_j \end{bmatrix} = \begin{bmatrix} I_i \\ -I_j \end{bmatrix} \quad \text{(i)}$$

There are two equations in (i), one for bus i and one for bus j. These equations, in addition to (h), represent the nodal flow balance (power balance) in both buses when there is a power flow between connection i, j across them. When these equations are extended to every bus in the EPS, it is said that there is a load flow problem. Any distribution component in the EPS has its terminals connected to buses, that is, any component can be included in the admittance matrix of (i). Having determined the load flow equations, it is possible to compactly write the load flow problem.

General Load Flow problem

In compact notation, (h) and (i) can be written as,

$$[\mathbf{Y}]\boldsymbol{V} = \boldsymbol{I} \quad \wedge \quad \text{diag}(\boldsymbol{V})[\mathbf{Y}]\boldsymbol{V} = \boldsymbol{P} \quad \text{(j)}$$

Where $\boldsymbol{V} = \{V_1, V_2, \dots, V_i, \dots\}$, $\boldsymbol{I} = \{I_1, I_2, \dots, I_i, \dots\}$, and $\boldsymbol{P} = \{P_1, P_2, \dots, P_i, \dots\}$. The $\mathbf{Y}$ matrix (left-hand side of (j)) is known as the admittance matrix and it contains the interconnection characteristics of the EPS that relates voltages, currents, and powers in steady state. The compact notation in (j) can be extended to systems with any number of buses. The number of unknowns must be at most equal to the number of equations, then the general load flow problem is,

$$\text{Find unknowns given a set of specified } V \text{ and } P\text{, such that: } \text{diag}(\boldsymbol{V})[\mathbf{Y}]\boldsymbol{V} = \boldsymbol{P} \quad \text{(k)}$$

In the load flow problem of (k), the EPS's components and connections are modelled as a square admittance matrix $\mathbf{Y}$. This matrix is relatively simple to build when modelling existing systems, and it is amenable for reconfiguration algorithms because changes in the system's topology requires few additions or subtractions in few elements. On the other hand, if an impedance matrix model were used, matrix reductions, complex mathematical simplifications, and other successive row and column operations are required to update the EPS upon a change in topology. The load flow is used to solve for the steady state of AC, DC, and hybrid systems (AC/DC).

Load Flow in AC systems

In alternating current (AC) systems, power has two components, one that is completely transformed in the load into actual work (active power P), and other that keep circulating in the system but cannot be transformed into usable work (reactive power Q). Voltage and current are assumed sinusoidal signals that are represented by complex numbers and phasors, e.g., $V = |V|\angle\delta$. The admittances also have the form $Y = |Y|\angle\theta$ because components use active and reactive powers. Extending (*a*) for buses with more connections, the total current that is injected at any bus i is,

$$I_i = Y_{i1}V_1 + Y_{i2}V_2 + \cdots Y_{iN}V_N = \sum_{n=1}^{N} Y_{in}V_n \tag{l}$$

The active and reactive power of a bus i can be written as,

$$P_i - jQ_i = V_i^* \sum_{n=1}^{N} Y_{in}V_n = \sum_{n=1}^{N} |Y_{in}V_iV_n|\angle\big(\theta_{in} + (\delta_n - \delta_i)\big) \tag{m}$$

Where V_i^* is the complex conjugate of V_i, θ_{in} is the admittance angle of component between buses i, n, and δ_n and δ_i are the voltages' angles of buses n and i respectively. By expanding (m), the AC load flow problem can be written as,

Find unknowns given a set of specified V, P, and δ, such that:

$$P_i = \sum_{n=1}^{N} |Y_{in} V_i V_n| \cos\left(\theta_{in} + (\delta_n - \delta_i)\right) \qquad \forall i \in N \qquad \text{(n)}$$

$$Q_i = -\sum_{n=1}^{N} |Y_{in} V_i V_n| \sin\left(\theta_{in} + (\delta_n - \delta_i)\right)$$

Current aircraft have AC electrical systems working at frequencies in the range 400-800 Hz produced at electrical machines driven by high-speed engines [163]. The higher the speed, the smaller the generators are, this being the reason for which higher frequencies are attractive to reduce weight in EPS components. However, the existence of reactive power Q increases the size of cabling and some distribution components because of several reasons: skin effect of cables, additional power loss dissipation payload, larger hardware controllers and devices, etc. On the other hand, DC systems' lack of reactive power is attractive because some weight saving is possible, and controllers can be less complex.

Load Flow in DC systems

In direct current (DC) systems, there is no reactive power Q, only active power is transmitted and transformed into actual work at the loads, so voltages and currents are constant[5] and represented by real numbers only. The load flow problem in (k) can be directly used in a DC system. The admittance Y_{ij} is replaced by the conductance G_{ij} because components only use/transform active power, so that a *conductance matrix* $\mathbf{G}$ models the EPS. Then,

Find unknowns given a set of specified V and P, such that: $\text{diag}(\boldsymbol{V})[\mathbf{G}]\boldsymbol{V} = \boldsymbol{P}$

$$[\mathbf{G}]\boldsymbol{V} = \boldsymbol{I} \qquad \text{(o)}$$

[5] Unlike AC systems where the signals oscillate sinusoidally between a maximum positive and maximum negative values, DC systems signals are constant, that is, the signals' levels are kept unchanged throughout time.

For any bus i, the total current is $I_i = \sum_{n=1}^{N} G_{in} V_n$. It has been said that any bus can have a power injecting or consuming device connected to it, e.g., power source, load, supercapacitor, etc. This device can be modelled as a constant conductance g^0, constant current i^0, constant power p^0, or a combination of all of these (the knot superscript denotes a connection between bus and reference bus or ground). In most cases, powers are known at almost all of the buses (loads consumption, fixed generation, etc.), voltages are known for only a few buses (main power sources), and the system's currents are unknown (unless current sources are present) [187]. Considering that a bus can have a g^0, i^0, p^0 component, the current can be written as,

$$[\mathbf{G}]\boldsymbol{V} = \mathrm{diag}(\boldsymbol{G^0})\boldsymbol{V} + (\boldsymbol{P}^0 \oslash \boldsymbol{V}) + \boldsymbol{I}^0 \tag{p}$$

Where $\oslash$ is the element-wise division between vectors $\boldsymbol{P}^0$ and $\boldsymbol{V}$. For a particular bus,

$$\sum_{n=1}^{N} G_{in} V_n = g_i^0 V_i + \frac{p_i^0}{V_i} + i_i^0 \tag{q}$$

Three bus types are allowed:

- Step-bus: there is no component between bus and ground, so $g_i^0 = 0$, $p_i^0 = 0$, and $i_i^0 = 0$
- Power-bus: power source/load component is injecting/consuming power, p_i^0 or i_i^0 are positive for generation, or negative for loads.
- Voltage-bus: voltage is known and constant, irrespective of having a power source or load.

When both sides of (q) are multiplied by V_i, the following power expression applies,

$$V_i \sum_{n=1}^{N} G_{in} V_n = g_i^0 V_i V_i + p_i^0 + i_i^0 V_i \tag{r}$$

Following the power balance notation in (31) (see Section 4.3.2 on power distribution design), and similarly to (f), (r) can be written as,

$$\sum_{n=1}^{N} P_{in} = \sum_{n=1}^{N} P_{in} - \sum_{n=1}^{N} P_{ni} = P_i \quad \text{(s)}$$

Where $P_{in} = G_{in}V_iV_n$ and $P_i = g_i^0 V_i V_i + p_i^0 + i_i^0 V_i$ according to (r). The left-hand side of (s) is divided into incoming ($i \rightarrow$ other buses n) and outgoing (other buses $n \rightarrow i$) power flows in the middle equivalence of (s). Also, P_i is equivalent to $d^{GEN} - d^{LOAD}$ as bus i can be injecting/consuming power via connected devices. Still, power balance is preserved and the expressions (31), (r) and (s) are equivalent.